Imperial College London

PhD Thesis

The Roles of Tumour Necrosis Factor and its Receptors in the Injury, Inflammation and Resolution of Acute Lung Injury

Dr Brijesh Vipinchandra Patel

Supervisors:
Professor Masao Takata
Magill Professor of Anaesthesia

Dr Michael Wilson
Senior Lecturer

Section of Anaesthetics, Pain Medicine and Intensive Care

Department of Surgery and Cancer

Imperial College London

Funded by the Wellcome Trust and the National Institute of Academic Anaesthesia

Abstract

The acute respiratory distress syndrome (ARDS) remains a major cause of morbidity and mortality in the intensive care. Despite improvements in intensive care and advances in respiratory support, mortality remains high with no active treatments. Tumour necrosis factor (TNF) is a cytokine that has been implicated in ARDS for over 30 years but its precise roles remain elusive. It signals through two main receptors – the p55 TNF receptor and p75 TNF receptor.

The first aspect of this thesis investigated the roles of TNF receptors (TNFR) in the early phase of acute acid-induced lung injury. Using genetically modified mice we discovered that alveolar oedema, as a result of acid aspiration, was specifically mediated through the p55-TNFR, whereas, the p75-TNFR promoted a protective effect. Alveolar oedema formation occurred through an effect independent to the downstream inflammatory events, but instead through the activation of TNF/p55-TNFR/caspase-8 death signalling specifically in the alveolar epithelium. Furthermore, this death-signalling axis led to a reduced alveolar epithelial fluid clearance rate. Epithelial dysfunction occurred prior to epithelial cell death and pharmacological blockade of caspase-8 rescued epithelial function with improvements in gas exchange, suggesting that the activation of caspase-8 per se induced this functional deficit in the alveolar epithelium.

The second part of the thesis describes the development of a longer-term model of acid aspiration aimed at extending investigation into the later, arguably more clinically relevant, phases of lung injury (0-10 days). Mice showed respiratory physiology that reached clinical ARDS criteria with significant inflammation and epithelial/endothelial injury, which importantly, resolved facilitating investigation into reparative processes. This model was further characterised using novel flow cytometry protocols to examine the compartmental location of leukocytes during the various phases of ARDS. This model provides a translational platform to allow investigation into the injurious, inflammatory, and resolution mechanisms of ARDS.

Table of Contents

Abstract **3**

Table of Contents **5**

Dedication **11**

Acknowledgements **12**

Statement of Originality **13**

Statement of Copyright **13**

Index of Figures **14**

Index of Tables **16**

Abbreviations **17**

1 Introduction **21**

1.1 The lung in normal physiology **21**

1.1.1 The lung in a constant state of alert 21

1.1.2 The alveolar-capillary unit – the site of action… 22

1.1.3 The pulmonary capillary endothelium – a silk lining 24

1.1.4 The pulmonary epithelium – the dam and the pump 25

1.1.5 The resident alveolar macrophage – the gate keeper 26

1.2 The acute respiratory distress syndrome **30**

1.2.1 Epidemiology. 31

1.2.2 Aetiology. 31

1.2.3 Outcomes. 32

1.3 Injury and inflammation in ARDS **34**

1.3.1 Diffuse alveolar damage is the cardinal histopathological feature of ARDS 34

1.3.2 DAD is characterised by two overlapping phases 34

1.3.3 Alveolar-capillary barrier dysfunction in ARDS 35

1.3.4 Inflammatory mechanisms of endothelial injury in ARDS 37

1.3.5 Apoptosis as a mechanism of epithelial injury in ARDS 39

1.3.6 Alveolar fluid clearance as an index of epithelial function 44

1.3.7 Pulmonary inflammation in ARDS 45

1.4 Resolution of injury and inflammation in ARDS **48**

1.4.1 Phase 1: “The stop signal” 48

1.4.2 Phase 2: “Clearing up the mess” 50

1.4.3 Phase 3 – “Re-establishing order and function” 51

1.4.4 Translational therapies promoting resolution in critical care 54

1.5 Tumour necrosis factor biology **57**

1.5.1 The discovery of TNF 57

1.5.2 TNF ligand and its receptors 58

1.5.3 Molecular mechanisms and functional consequences of TNF receptor signalling 59

1.6 TNF and critical illness **64**

1.6.1 TNF – elusive in clinical ARDS 64

1.6.2 TNF in sepsis – ‘clinical trials and tribulations…’ 65

1.7 Mechanisms of TNF in ARDS pathobiology **68**

1.7.1 TNF and acid aspiration 68

1.7.2 TNF and alveolar-capillary permeability 70

1.7.3 TNF and alveolar fluid clearance – the ups and downs 71

1.7.4 Differential effects of TNF receptors 73
1.7.5 TNF and the Takata lab 74
1.8 Pre-clinical modelling of ARDS: Mice treatments work; human treatments fail… 50 years of frustration. 75
1.8.1 The ideal model of ARDS – the experts' opinion 78
1.8.2 Histological evidence of injury 80
1.8.3 Altered alveolar capillary barrier function 81
1.8.4 Inflammatory responses 81
1.8.5 Physiological derangement 82
1.9 Hypotheses and Aims 84
1.10 Overview of thesis 84

2 Materials, Methods and Protocols 87
2.1 Materials 87
2.1.1 Reagents 87
2.1.2 Commercial detection assays 89
2.1.3 Pharmacological agents 90
2.1.4 Instruments, equipment, and software 90
2.1.5 Flow cytometry antibodies 92
2.2 Animals 93
2.3 In vivo models of acid-induced lung injury 93
2.3.1 In vivo mechanical ventilation 94
2.3.2 Acute acid aspiration: 0-3 hours (relevance to chapters 3/4/5) 95
2.3.3 Resolution phase acid aspiration: 0-10 days (relevance to chapters 6/7) 96
2.3.4 In vivo labelling of lung compartments (relevance to chapter 7) 97
2.4 Harvesting of experimental samples 98
2.4.1 Bronchoalveolar lavage 98
2.4.2 Blood/plasma 98
2.4.3 Lung tissue preparation 99
2.5 Physiological measurements 99
2.5.1 Respiratory mechanics 99
2.5.2 Arterial blood gas analysis 100
2.5.3 Wet/Dry weight assessment 100
2.5.4 Protein Assay 101
2.5.5 Lung permeability index 101
2.6 Inflammatory measurements 101
2.6.1 ELISA 101
2.6.2 Lung cytology 102
2.6.3 Lung leukocyte quantification using flow cytometry 102
2.7 In situ measurement of alveolar fluid clearance 103
2.7.1 Overview 103
2.7.2 Surgical Preparation 104
2.7.3 Measurement protocol 104
2.8 Tissue imaging 105
2.8.1 Background 105
2.8.2 Preparation of lungs 105
2.8.3 Haematoxylin and Eosin staining. 106
2.8.4 Masson's Trichrome staining. 106
2.8.5 Histological lung injury scoring 107
2.9 Apoptosis detection 107
2.9.1 TUNEL assay 107
2.9.2 Caspase-8/-9 activity assay 109

2.9.3 Flow cytometric localisation of caspase-8 activity 110
2.10 Interventional studies 111
2.10.1 Caspase-8 inhibition 111
2.10.2 Alveolar macrophage depletion 111
2.11 Statistical analysis 111

3 Differential roles for TNF receptors in acid-induced lung injury 113
3.1 Introduction 114
3.2 Aims 116
3.3 Experimental design 116
3.3.1 Animals 116
3.3.2 In vivo model 116
3.3.3 Respiratory physiology 117
3.3.4 Analysis of inflammation 117
3.3.5 Histological preparation 117
3.4 Results 117
3.4.1 Acute acid aspiration model optimisation 117
3.4.2 Alveolar oedema is mediated specifically through the p55 TNF receptor in acid-induced lung injury. 120
3.4.3 Respiratory Mechanics 120
3.4.4 Arterial blood gas analysis 124
3.4.5 Lung water content 125
3.4.6 Alveolar capillary barrier permeability 125
3.4.7 Inflammatory consequences of TNF receptor signalling in acid aspiration. 127
3.4.8 Histology 130
3.4.9 TNF receptor shedding and expression in blood monocytes and neutrophils 131
3.5 Discussion 134
3.5.1 Mechanisms of oedema formation after acid aspiration 134
3.5.2 The TNF double edged sword – p55 versus p75 signalling 135
3.5.3 TNF receptor expression in lung cells 138
3.5.4 Oedema formation occurs through the p55 TNF receptor and independent of pro-inflammatory effects 139
3.5.5 The p75 TNF receptor – a potential alveolar inflammatory rheostat 140
3.6 Concluding remarks 142

4 Activation of alveolar epithelial p55 TNF receptor death signalling in acid-induced lung injury 145
4.1 Introduction 147
4.2 Aims 149
4.3 Experimental design 149
4.3.1 In vivo model 149
4.3.2 Analysis of alveolar mediators 149
4.3.3 TUNEL analysis 149
4.3.4 Measurement of apoptosis signalling 150
4.4 Results 151
4.4.1 Acid aspiration induces epithelial injury. 151
4.4.2 Lung oedema formation is not explained by completed apoptosis of alveolar cells 152
4.4.3 TNF p55 receptor activates caspase-8 'death signalling' in lungs after acid aspiration 154
4.4.4 Caspase-8 activation occurs early in experimental lung injury 154
4.4.5 Localisation of caspase-8 activity 157
4.5 Discussion 160

4.5.1 Epithelial caspase-8 activation dominates in acid aspiration 160
4.5.2 The amount of completed 'cell death' in clinical and experimental ARDS does not correlate with physiological derangements 162
4.5.3 Pro-apoptotic "death" versus inflammatory "survival" signaling 164
4.5.4 Introducing the concept of "apoptotic limbo" 165
4.6 Concluding remarks 166

5 TNF-induced death signalling triggers alveolar epithelial dysfunction in acid-induced lung injury 167
5.1 Introduction 168
5.2 Aims 169
5.3 Experimental design 169
5.3.1 In situ measurement of alveolar fluid clearance 169
5.3.2 Caspase-8 inhibition experiments 170
5.3.3 Alveolar macrophage depletion 170
5.4 Results 170
5.4.1 Validation of in situ alveolar fluid clearance measurement 170
5.4.2 Measurement of in situ AFC during injury. 174
5.4.3 AFC deteriorates acutely after acid aspiration and correlates with markers of alveolar epithelial injury. 175
5.4.4 The p55 TNF receptor triggers the early disturbance of alveolar fluid clearance in experimental ARDS 176
5.4.5 Caspase-8 activity leads to epithelial dysfunction. 178
5.4.6 Early epithelial death signalling is dependant on resident alveolar macrophage derived TNF 180
5.4.7 Alternative mechanisms of caspase-8 activation 185
5.5 Discussion 189
5.5.1 Alveolar fluid clearance – conceptual discussions 189
5.5.2 RAGE, the epithelium, and apoptosis 190
5.5.3 TNF, the epithelium and apoptosis 190
5.5.4 Caspase-8, the epithelium, and "apoptotic limbo" 192
5.5.5 Alveolar epithelial bioenergetics failure 193
5.5.6 Alveolar epithelial cytoskeletal dysregulation 195
5.5.7 The epithelial death signal is initiated by alveolar macrophages… 195
5.5.8 The epithelial death signal may be perpetuated by neutrophils… 197
5.6 Concluding remarks 199

6 Animal modelling of resolution in lung injury and inflammation 201
6.1 Introduction 202
6.2 Aims 204
6.3 Experimental Design 204
6.3.1 Intra-tracheal instillation technique 204
6.3.2 Provision of high dependency care 205
6.3.3 Measurement of physiology changes 205
6.3.4 Assessment of pulmonary inflammation 206
6.3.5 Histological lung injury assessment 206
6.3.6 Quantification of alveolar epithelial dysfunction 206
6.4 Results 207
6.4.1 Physiological injury induced by acid aspiration 207
6.4.2 Weight loss. 208
6.4.3 Respiratory mechanics. 210
6.4.4 Oxygenation. 210
6.4.5 Indices of lung oedema – permeability and clearance 212

6.4.6 Epithelial injury and recovery. 215
6.4.7 Characterisation of alveolar inflammation and resolution 217
6.4.8 Lung injury scoring 221
6.4.9 Resolution through fibrosis 223
6.5 Discussion 225
6.5.1 Pitfalls in animal models of ARDS 225
6.5.2 Acid aspiration – a truly translational model 226
6.5.3 Respiratory physiology attains ARDS criteria 227
6.5.4 Alveolar epithelial dysfunction and recovery in later phases of ARDS 228
6.5.5 DAMPen the RAGE 229
6.5.6 Resolution of inflammation is integral to physiological resolution 231
6.5.7 Resolution through pulmonary fibrosis 233
6.6 Concluding remarks 234

7 Compartmental analysis of leukocytes in healthy and injured mouse lungs 235
7.1 Introduction 236
7.2 Aims 238
7.3 Experimental Design 238
7.3.1 In vivo protocols 238
7.3.2 Flow cytometric processing. 239
7.4 Results 239
7.4.1 Characterisation of myeloid populations in the uninjured mouse lung using standard in vitro antibody incubation 239
7.4.2 Validation of in vivo staining of alveolar and vascular compartments 242
7.4.3 Resident alveolar macrophage and dendritic cell populations validate the distinction between the alveolar and interstitial compartments of the lung 245
7.4.4 MHCII expression on interstitial and vascular monocyte populations validates the distinction between interstitial and vascular compartments of the lung 248
7.4.5 Phenotypic and compartmental characterisation of myeloid subsets in the naïve mouse lung 250
7.4.6 A preliminary examination of leukocyte kinetics during experimental acid-induced lung injury 250
7.4.7 Changes in resident alveolar macrophages during the acute phase of lung injury 252
7.4.8 Reductions in dendritic cell numbers from the onset of lung injury 253
7.4.9 The pulmonary sequestration of blood derived myeloid cells 255
7.4.10 CD4 T-cell infiltration during resolution of lung injury 261
7.5 Discussion 264
7.5.1 Rationale for compartmental evaluation 265
7.5.2 Confounding factors to in vivo labelling strategies 266
7.5.3 Resident alveolar macrophages populations during lung injury 268
7.5.4 Resident interstitial monocyte populations 270
7.5.5 Resident interstitial dendritic cell populations 271
7.5.6 Two phases of myeloid infiltration 272
7.5.7 Neutrophil apoptosis may promote a resolving second phase 276
7.5.8 Myeloid and T-cell interactions may enable healing and resolution 277
7.6 Concluding remarks 277

8 Final thoughts – where to now in ARDS research… 279
8.1 The translation of p55 blockade to the ICU bedside 279
8.2 The p55 DAb in acute ARDS 280
8.3 The p55 DAb - epithelial rescue versus non-resolution of inflammation in ARDS 282
8.4 Translating therapies to ARDS 283

8.5 Limitations of work in this thesis 284
8.6 Future work 285
1. How does apoptosis signaling promote epithelial injury? 285
2. What is the role of the p75 TNF receptor? 286
3. What is the best model of ARDS and how does one compare against the other? 287
4. What is the impact of co-morbidities in the pathobiology of ARDS? 287

9 Publications and awards arising from work 289
9.1 Journal publications 289
9.2 Abstract publications 289
9.3 Awards 290

10 References 291

Dedication

This thesis is dedicated to my wife, children, and parents. Firstly, to my wife Hetal for not only enduring the pain of completing her own thesis but also supporting me through mine. You have been my third supervisor and are my supervisor in life. Through the past five years since embarking on this work, we were blessed by the arrival of our two beautiful daughters, Vaishvi and Anjali, both of whom continue to keep life in perspective. In particular, the games of hide and seek whilst writing this thesis. I thank Peppa Pig and her friends who distracted them to allow me to find some extra time to write in the evenings after busy clinical shifts in the ICU. Finally, I thank my parents, Vipin and Saroj, as well as my sister Sneha. You have worked so hard to support and educate me as well as inspire me to achieve and seize every day with passion. Your continued support has enabled me to embark on a research track.

Any thesis cannot be complete without dedicating the efforts to the patients and families who have suffered from critical illness. Additionally, to all the dedicated staff that I have had the pleasure to work with. I hope that this research contributes to ICU knowledge and practice and helps anyone that has to go through an intensive care unit.

Acknowledgements

I would like to acknowledge my supervisors, Professor Masao Takata and Dr Michael Wilson, for their fantastic supervision and support. My first meeting with Masao in 2006 changed the way I saw clinical medicine. Everyday clinical practice is important as it influences individual patients, but clinical academic practice has the potential to change thousands of lives, of patients and students. I thank him for mentoring and supervising me throughout this thesis, and for always having an 'open door' policy. I thank Mike for having an exceptional ability to look at data and point out directions that were over looked and for the hours of debate over these issues, in particular, in the Sporting Page pub. Additionally, I thank Dr Kieran O'Dea for the many discussions concerning science as well as life, and also for helping me to unblock the flow cytometer.

I would like to thanks Professor Charles Pusey and his team on the Imperial College Wellcome Trust Clinical PhD scheme. Financial support from The Wellcome Trust has been integral to allowing me to experience science in a truly inspirational way. I also thank the clinical committee at the Wellcome Trust for initially turning me down after interview. Their advice to reapply with a project with greater depth and ambition has enabled me to truly gain momentum in my research experience.

Finally, thanks go out to the critical care group and staff at APMIC. In particular, I thank Mr Faruq Noormohamed who managed the lab throughout my time. Every student and staff member has helped me achieve this body of work and it was a delight undertaking a PhD with you all.

Statement of Originality

No part of this thesis has previously been submitted for a degree in any university and to the best of my knowledge contains no material previously published or written by another person except where due acknowledgment is made in the thesis itself. All work contained within the thesis was performed by myself or in collaboration with members of the laboratory or Imperial College.

Statement of Copyright

The copyright of this thesis rests with the author and is made available under a Creative Commons Attribution Non-Commercial No Derivatives licence. Researchers are free to copy, distribute or transmit the thesis on the condition that they attribute it, that they do not use it for commercial purposes and that they do not alter, transform or build upon it. For any reuse or redistribution, researchers must make clear to others the licence terms of this work.

2 Index of Figures

Figure 1.1. The alveolus 23
Figure 1.2. Components of the alveolar-capillary barrier 29
Figure 1.3. Apoptosis signalling pathways 43
Figure 1.4. The phases of resolution in lung inflammation 52
Figure 1.5. The interactions and plasticity of macrophages 53
Figure 1.6. Survival versus death signalling through the p55 TNF receptor 63
Figure 2.1. Set up for mouse cardiorespiratory monitoring and mechanical ventilation 95
Figure 2.2. Set up for orotracheal instillation of substances 97
Figure 2.3. Mouse recovery unit 97
Figure 2.4. Measurement and calculation of respiratory mechanics 100
Figure 3.1. Development of acute acid aspiration lung injury model 119
Figure 3.2. Ventilation settings between mouse strains 121
Figure 3.3. Differences in respiratory mechanics between strains after acid aspiration 123
Figure 3.4. Differences in gas exchange between strains after acid aspiration 124
Figure 3.5. Differences in alveolar-capillary barrier permeability between strains after acid aspiration 126
Figure 3.6. Differences in alveolar cytokines/chemokines between strains after acid aspiration 128
Figure 3.7. Differences in lung leukocyte numbers between strains after acid aspiration 130
Figure 3.8. Lung histology after acid aspiration 131
Figure 3.9. Soluble TNF receptor levels in alveolar lavage after acid aspiration 132
Figure 3.10. Cell surface TNF receptor expression on neutrophils and monocytes in all knockout strains 133
Figure 4.1. Epithelial and endothelial markers of injury in WT and p55KO strains .. 151
Figure 4.2. TUNEL staining at 3 hours after acid aspiration 153
Figure 4.3. Caspase-8 and -9 activity in lung homogenates after acid aspiration 156
Figure 4.4. Flow cytometric analysis of cell specific caspase-8 activity after acid aspiration 159
Figure 5.1. Development and validation of in situ measurement of alveolar fluid clearance 172
Figure 5.2. Animal size and strain differences in AFC measurement 173
Figure 5.3. Correlations between AFC and other markers of epithelial dysfunction 175
Figure 5.4. Differences in AFC between WT and TNFR knockout strains after acid aspiration 177
Figure 5.5. Protective effect on respiratory physiology by caspase-8 inhibition 179
Figure 5.6. Flow cytometric evaluation of resident alveolar macrophage depletion by intratracheal clodronate administration 181
Figure 5.7. Protective effects on respiratory physiology through alveolar macrophage depletion 182
Figure 5.8. The protective effects of alveolar macrophage depletion are mediated through a reduction in TNF-induced epithelial dysfunction 184

Figure 5.9. Cell surface expression of death ligands TNF and FasL on alveolar macrophages, neutrophils and inflammatory monocytes in naïve and injured animals 187
Figure 5.10. Correlations in alveolar FasL levels with leukocyte sequestration to the lung 188
Figure 6.1. Development and refinement of the resolving model of acid aspiration 209
Figure 6.2. Changes in respiratory mechanics and oxygenation during resolving acid aspiration 211
Figure 6.3. Changes in alveolar capillary barrier dysfunction during resolving acid aspiration 213
Figure 6.4. Changes in macroscopic appearance of lungs during resolving acid aspiration 214
Figure 6.5. Changes in epithelial dysfunction and injury during resolving acid aspiration 216
Figure 6.6. Changes in alveolar leukocyte types and numbers during resolving acid aspiration 218
Figure 6.7. Changes in alveolar cytology during resolving acid aspiration 219
Figure 6.8. Changes in alveolar cytokines/chemokines during resolving acid aspiration 220
Figure 6.9. Histological analysis of resolving acid aspiration 222
Figure 6.10. Analysis of fibrosis during resolution of acid aspiration 224
Figure 7.1. Flow cytometric analysis of naïve mouse lungs (without in vivo labelling) 241
Figure 7.2. Development of in vivo labelling protocol 244
Figure 7.3. In vivo labelling protocol enables separation of alveolar and interstitial compartments of the naïve mouse lung 247
Figure 7.4. In vivo labelling enables separation of the interstitial and vascular compartments of the naïve mouse lung 249
Figure 7.5. Changes in myeloid cell type in lung compartments after acid aspiration 252
Figure 7.6. Changes in resident alveolar macrophage and dendritic cell numbers during lung injury 254
Figure 7.7. Changes in neutrophil and monocytes numbers in lung compartments and blood during lung injury 258
Figure 7.8. A preliminary analysis of neutrophil apoptosis during lung injury 259
Figure 7.9. Kinetics of CD11b positive events during lung injury 260
Figure 7.10. Increasing expression of cell surface CD11c and MHCII during monocyte transmigration 261
Figure 7.11. Interstitial T-cell infiltration during lung injury resolution 263
Figure 8.1. Domain antibody (DAb) fragment in comparison to an IgG molecule 280

3 Index of Tables

Table 1.1. The 1994 AECC definition of ALI/ARDS 30
Table 1.2. The 2012 Berlin definition of ALI/ARDS 31
Table 1.3. The clinical associations with ARDS 32
Table 1.4. Lung injury scoring system 80
Table 2.1. In vivo reagents 87
Table 2.2. Enzyme-linked immunosorbant assay (ELISA) reagents 87
Table 2.3. Flow Cytometry reagents 88
Table 2.4. Cytology/histology reagents 88
Table 2.5. Commercial detection and quantification kits 89
Table 2.6. Agonists, antagonists, inhibitors and depletion agents 90
Table 2.7. In vivo protocols 90
Table 2.8. Enzyme-linked immunosorbant assay (ELISA) protocols 90
Table 2.9. Flow cytometry protocols 91
Table 2.10. Miscellaneous equipment 91
Table 2.11. Software packages 91
Table 2.12. Flow cytometry antibodies 92
Table 2.13. Histological lung injury scoring method 107
Table 3.1. Baseline respiratory mechanics and blood gas measurements in all mouse strains 120
Table 6.1. Pathophysiological features of human ALI 204
Table 7.1. The phenotypic characteristics of myeloid cell populations in the naïve mouse lung 250

Abbreviations

ABG	Arterial Blood Gas
AEC	Alveolar Epithelial Cell
AECC	American-European Consensus Conference
AFC	Alveolar Fluid Clearance
ALI	Acute Lung Injury
APAF	Apoptotic Protease Activating Factor
ARDS	Acute Respiratory Distress Syndrome
BALF	Bronchoalveolar Lavage Fluid
BSA	Bovine Serum Albumin
CAM	Cell Adhesion Molecule
cFLIP	Cellular FLICE-inhibitory protein
CFTR	Cystic Fibrosis Transmembrane Regulator
cIAP	Cellular Inhibitor of Apoptosis
CPAP	Continuous Positive Airway Pressure
DAb	Domain Antibody
DAB	Diaminobenzidine
DAD	Diffuse Alveolar Damage
DAMP	Damage-associated Molecular Pattern
cDC/pDC	Conventional/Plasmacytoid Dendritic Cell
DD	Death Domain
DISC	Death-inducing Signalling Complex
DKO	Double TNF receptor knockout
DR	Death Receptor
EJV	External Jugular vein
ELISA	Enzyme-Linked Immunosorbent Assay
EMT	Epithelial-Mesenchymal Transition
ENaC	Epithelial Sodium Channel
EPCAM	Epithelial cell adhesion molecule
Ers	Respiratory System Elastance
FADD	Fas-associated Death Domain

Fas	Fas Receptor
FasL	Fas Ligand
FiO_2	Fractional Inspired Oxygen
FLICE	FADD-like IL-1β-converting enzyme
FWB	Flow cytometry Wash Buffer
GM-CSF	Granulocyte-Macrophage Colony-Stimulating Factor
HCl	Hydrochloric Acid
ICAM	Intercellular cell adhesion molecule
IL	Interleukin
KC	Keratinocyte-derived Chemokine
LPS	Lipopolysaccharide
LUBAC	Linear Ubiquitin chain assembly complex
MAPK	Mitogen-activated Protein Kinase
MHC	Major Histocompatibility Complex
MIP-2	Macrophage Inflammatory Protein 2
MLC	Myosin Light Chain
MOMP	Mitochondrial outer membrane permeabilisation
MPO	Myeloperoxidase
MPT	Mitochondrial Permeability Transition
MSC	Mesenchymal Stem Cells
NaCl	Sodium Chloride
Na^+/K^+ ATPase	Sodium Potassium ATPase Transporter
NEMO	NF-kappa-B essential modulator
NFκB	Nuclear-Factor kappa B
PAMP	Pathogen-associated Molecular Pattern
PaO_2	Arterial Partial Pressure of Oxygen
PECAM	Platelet-Endothelial Cell Adhesion Molecule
PEEP	Positive End-Expiratory Pressure
PFR	PaO_2/FiO_2 Ratio
PIP	Peak Inspiratory Pressure
p55KO	p55 TNF receptor knockout
p75KO	p75 TNF receptor knockout

RAGE	Receptor for Advanced Glycation End-products
RIP	Receptor Interacting Protein kinase
ROS/RNS	Reactive Oxygen/Nitrogen Species
Rrs	Respiratory System Resistance
T1-alpha	Type 1 cell alpha Protein
TACE	TNF Alpha-Converting Enzyme
TdT	Terminal deoxynucleotidyl Transferase
TGFβ	Transforming Growth Factor beta
TLR	Toll-like Receptor
TNF	Tumour Necrosis Factor
TNFR	Tumour Necrosis Factor Receptor
TRADD	TNF Receptor Associated Death Domain
TRAF	TNF Receptor Associated Factor
TRAIL	TNF-related Apoptosis-inducing Ligand
TUNEL	Terminal deoxynucleotidyl transferase dUTP nick end labeling
Ub	Ubiquitin
UIP	Usual Interstitial Pneumonia
VALI	Ventilator Associated Lung Injury
VCAM	Vascular Cell Adhesion Molecule
VILI	Ventilator Induced Lung Injury
V/Q	Ventilation/Perfusion
VT	Tidal Volume
WT	Wild Type

1 Introduction

1.1 The lung in normal physiology

The human respiratory system consists of upper (the nasal and oral cavities, pharynx, larynx and trachea) and lower airways (the bronchi, bronchioles and terminal bronchioles), and terminate in a vast air-blood interface provided by millions of alveolar-capillary units (1). The process of respiration involves a coordinated neuronal activity producing an inspiratory and expiratory cycle facilitating the movement of gas into and out of the lung delivering oxygen to, and removing carbon dioxide, the end product of cellular metabolism, from these alveolar-capillary units. This interface between the outside environment and the circulating blood provide a surface area of over 70m^2 across which gas exchange can occur (2). Unlike any other tissue bed the lung is exposed to the entire cardiac output and hence, the lung has the potential to not only be affected by, but also have significant influence upon, the rest of the body. Indeed, it is now well established that the lung is able to modulate multiple endocrine factors and also influence injury and inflammation at remote sites.

1.1.1 The lung in a constant state of alert

It is this direct exposure of the alveolus to the external environment, which necessitates the lung to develop mechanisms whereby any harmful particles that enter can be extruded or eliminated in a timely manner, without causing collateral tissue damage. With each breath the respiratory system is bombarded with particles. These range from pollutants in the air, to oropharyngeal contents that have been aspirated, to infectious agents such as bacteria, fungi, or viruses. The upper respiratory system has developed physical mechanisms to prevent this entry. For instance, the epiglottis prevents food from entering the trachea during swallowing; the cough reflex extrudes particles that may have bypassed this epiglottic defence; a ‘sticky’ mucus layer on the inner surface of the trachea and major bronchi prevents particles accessing the lung parenchyma; and cilia on the bronchial epithelium waft these trapped particles up and out of the respiratory tract (1).

However, inevitably some particles do get through these physical defences and access the distal pulmonary tree. Here, within the distal bronchioles and alveoli, there is a cellular and molecular defence system, which wages war against this resilient unwanted matter. In health, these mainly comprise alveolar macrophages, floating in a sea of surfactant within the alveolus; and dendritic cells, located just beneath the alveolar/bronchial epithelium, protruding dendrites into the alveolar/bronchial lumen actively looking for foreign antigen. This surfactant is a phospholipid layer lining the inside of the alveoli, primarily preventing their collapse inwards by maintaining a reduced surface tension. However, surfactant also serves a defensive purpose as it contains numerous molecules that bind a diverse array of foreign molecular patterns facilitating presentation to immune cells for their clearance. If these defences are breached there is a cavalry recruited from the blood to fight these invaders on the battlefield that is the alveolar space. Inevitably, in such circumstances, there is collateral damage to the alveolar space. If the battle ends through clearance or tolerance of the invading matter, there begins a clear up and reparative process, to restore the lung to working order, in preparation for the next battle. Unfortunately, when clearance, tolerance, and resolution do not occur after an acute insult, the collateral damage to the lung can lead to acutely devastating and life-threatening forms of lung injury.

1.1.2 The alveolar-capillary unit – the site of action…

The alveolar-capillary interface (figure 1.1 and 1.2) is a unique tissue interface and can be likened to a large dam with air on one side (the alveolus) and water (blood) on the other. Efficient gas exchange relies on a combination of factors including a large surface area, a concentration gradient and a small thickness for diffusion. The alveolar-capillary unit is designed to maximise the efficiency through which this process occurs. Firstly, as mentioned the lung consists of millions of alveoli which are maintained in an open state by surfactant lining their inner surface. Alveolar walls are lined by two types of alveolar epithelial cell (AEC) - type I and type II. These are closely apposed to the pulmonary capillary endothelium. An interstitial layer containing a basement membrane aids this close apposition. This interstitial layer

also harbours numerous immune cells including interstitial macrophages, fibroblasts, myofibroblasts and dendritic cells. There are also, resident within the alveoli, sentinel cells called alveolar macrophages, and these present an important first line of defence. These alveolar and interstitial leukocytes are exposed to the outside world, and hence survey and sample the alveolar space and additionally have close physical and molecular interactions with the alveolar epithelium and endothelium.

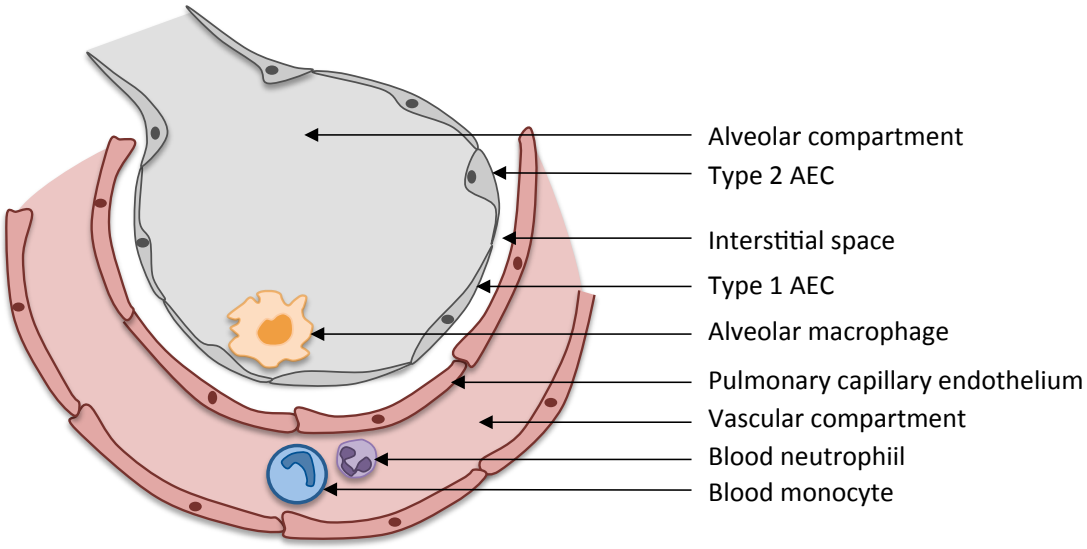

Figure 1.1. The alveolus

The terminal alveolar ducts ends in a number of air sacs called alveoli. Each alveoli has walls comprised of alveolar epithelial cells (AEC) and is lined by a phospholipid layer of surfactant. This layer reduces the surface tension within the alveolus preventing its collapse. Furthermore, the surfactant layer consists of proteins that facilitate protection from foreign material including bacteria. This aids resident alveolar macrophages to respond in an appropriate manner to the constant exposure to the outside world. The interstitial space also contains a vast array of resident cells including dendritic cells and interstitial macrophages. Such resident leukocytes detect and engulf any foreign materials that enter the alveolus. Overwhelming activation leads to significant exudation and inflammation within the lung. This occurs through activation of the epithelial and endothelial cells and the release of chemokines and cytokines. Endothelial and epithelial cells subsequently upregulate cell adhesion molecules on their cell surface attracting leukocytes such as neutrophils and monocytes from the vasculature into the interstitial and subsequently the alveolar space.

1.1.3 The pulmonary capillary endothelium – a silk lining

The lung endothelium produces a continuous monolayer providing an intimal lining of pulmonary blood vessels separating blood components from interstitial tissue layers. This layer provides a large surface area ($120m^2$) with the main function of gas exchange, as well as host defence, surveillance, and homeostasis (2). The lung endothelium is in contact with the entire cardiac output and this unique feature places it in a position to control systemic physiology. The pulmonary circulation is a low pressure, high flow system enabling small changes in vascular tone to have significant impact upon cardiovascular physiology as well as gas exchange. For instance, hypoxic vasoconstriction in response to local alveolar hypoxia leads to only those alveoli that are ventilated being perfused improving ventilation perfusion matching (V/Q) and ultimately making gas exchange as efficient as possible. During states of injury where there is damage to the alveolar structure and damage to the underlying pulmonary microvasculature, there is remodelling and scarring which ultimately disrupts this efficiency of the pulmonary vasculature to maintain V/Q as 1. This leads to ventilated lung areas not being perfused (i.e. increasing dead space; $V/Q=\infty$) and non-ventilated areas being perfused (i.e. shunt; $V/Q=0$). Overall, this significantly disables the lung from performing its primary function, namely gas exchange.

The endothelium also functions to keep plasma and cellular constituents within the circulation. This is crucial in the pulmonary circulation as a unique feature is the presence of a dry alveolar space and a thin alveolar-capillary barrier to facilitate gas exchange. When the endothelium is disrupted there is a leak of plasma into the interstitial space, and eventually into the alveolar space, leading to impaired gas exchange ability of the lungs. The endothelium is the first barrier that has to be overcome to produce alveolar oedema. Endothelial cells are able to prevent large plasma proteins (such as albumin) from entering the interstitial space whilst enabling small molecules to move across and this process is called protein sieving (3). This results in a higher plasma protein concentration and hence a higher plasma oncotic pressure in comparison to respective tissue pressures enabling retention of water within the vasculature. Failure of the endothelium to prevent large proteins crossing

the barrier leads to a reversal of oncotic gradients with subsequent vascular hyper-permeability and filtration.

Another major role of the endothelium is to facilitate the recruitment of the 'cavalry' – blood derived leukocytes. This is achieved through signals emanating from the alveolus causing the endothelium to upregulate cell adhesion molecules enabling the adhesion, rolling and transmigration of 'circulating' leukocytes into the interstitial and alveolar space. Unlike other vascular beds, the pulmonary circulation is different in that there is an unusually large amount of physiological sequestration of leukocytes from the systemic circulation. This is secondary to the significant deformation required of leukocytes, for them to migrate through the pulmonary microcirculation (4, 5). Although this close leukocyte/endothelial interaction is regarded as an important process within the lung, the exact mechanisms of this so-called 'margination' are still unclear and under immense scrutiny by lung researchers worldwide. However, it is well established that the lung endothelium has a constitutive expression of some cell adhesion molecules such as ICAM-1 and PECAM, as well as, an inducible expression of others such as E-, P-selectin and VCAM (6). It is important to appreciate that this 'marginated' pool of leukocytes is in dynamic equilibrium with the non-marginated 'circulating' pool, which in turn is in dynamic equilibrium with the 'bone-marrow' pool. This is discussed later but it is clearer that the lung endothelium has the potential to dramatically influence the state of these leukocytes as they 'marginate' or 'circulate' through the pulmonary microvasculature.

1.1.4 The pulmonary epithelium – the dam and the pump

The alveolar epithelium is composed of an equal number of two cell types – alveolar epithelial type I (AEC I) and type II (AEC II) cells. They have distinct structures with AEC I cells having a flattened structure and covering 95% of the alveolar septal surface. Functionally, AEC I cell morphology is specialised for gas exchange. AEC II cells have a cuboidal structure covering the rest of the septal surface and are located near the corners where alveoli meet. Both contain vesicles that can transport substances in each direction across the air-blood interface.

The cytoplasm of AEC II cells have prominent amounts of endoplasmic reticulum and Golgi complexes which aid the production of vesicles containing surfactant proteins which prevent alveolar collapse. In addition, both types of epithelium are involved in the prevention of alveolar flooding through the promotion of a tight intercellular barrier. Alveolar epithelial cells are joined to each other by tight junctions and provide a barrier to diffusion of fluid into the alveolar space. The tight junctions can be described as the "cement", binding the epithelial cells, the "bricks", forming a dam with air on one side and fluid on the other. This "cement" is linked closely with the actin-myosin cytoskeleton (figure 1.2). In addition to this barrier function, which prevents flooding of the alveoli, both cell types express pumps and channels to transport ions and solutes allowing the control of the constitution of the alveolar lining fluid (or hypophase). The predominant active mechanism is that of sodium transport by Na^+/K^+ ATPase transporters located on the basal surface of the epithelium thereby creating an electrochemical gradient allowing movement of Na^+ though apical epithelial Na^+ channels (ENaC). This gradient drives the movement of water out of the alveolus through paracellular and transcellular (aquaporins) routes, a process called alveolar fluid clearance (7).

Surfactant mostly consists of 90% phospholipids, however, approximately 10% of its constitution is protein, mainly four surfactant proteins – A to D. Type 2 AECs produce all four surfactant proteins. Surfactant protein B and C are hydrophobic, with the former playing a significant role in reducing alveolar surface tension, and the latter has been found to bind endotoxin. SP-A and -D are part of the collectin family of molecules and help in host defence by acting as opsonins facilitating enhanced uptake of foreign matter (e.g. bacteria) or debris (e.g. apoptotic cells) by phagocytes, such as alveolar macrophages (8).

1.1.5 The resident alveolar macrophage – the gate keeper

Resident alveolar macrophages within the alveolus provide surveillance against invading foreign material (infectious and non-infectious), and are at centre-stage of any acute immune response within the lung. They comprise 95% of all immune cells within the airspace in the healthy lung. They express a number of receptors allowing

them to sense the nearby environment as well as interact with the lung epithelium and other immune cells. These include scavenger receptors, integrins, immunoglobulin superfamily receptors (Fc receptor; Triggering receptor expressed on myeloid cells (TREM)) and toll-like receptors (TLR) (9). These interactions are crucial for not only for the recognition of infectious agents through the presentation of pathogen associated molecular patterns (PAMPs, such as endotoxin, lipoteichoic acid, and zymogen) (10), but also for clearance of tissue debris consisting of apoptotic/necrotic cells (11), and recognition of sterile injury through the recognition of damage associated molecular patterns (DAMPs, such as ATP, DNA and formyl peptides) (12, 13). The ligation and signalling through PAMP receptors (TLR-2, -3, -4, -6, -9) and the increasing variety of DAMP receptors (TLRs, RAGE, Dectin-1, P2Y P2X, CD14, CD44) leads to the elaboration of pre-made and the transcriptional upregulation of pro-inflammatory cytokines (e.g. TNF and IL-6) and chemokines (e.g. CCL-2, IL-8), expression of cell adhesion molecules on the lung endothelium, and subsequent recruitment of blood derived leucocytes such as neutrophils and inflammatory monocytes. In contrast, the recognition of apoptotic cells is a crucial switch to promote anti-inflammatory mechanisms and the eventual resolution of the inflammatory response (14, 15). This plasticity in macrophage phenotype is crucial in determining the alveolar milieu throughout the course of any injurious response.

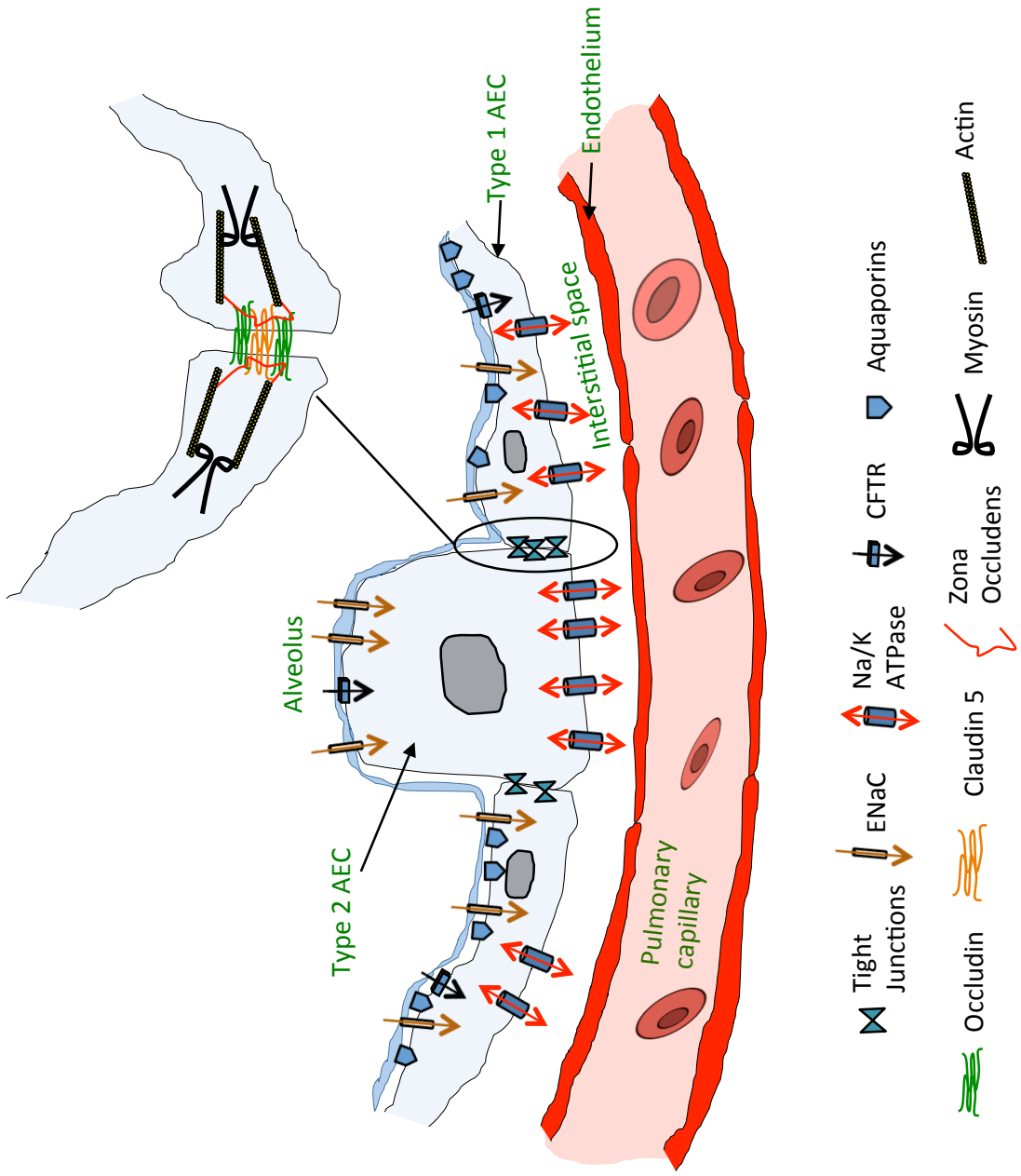
Endothelium
Type 1 AEC
Interstitial space
Alveolus
Type 2 AEC
Pulmonary capillary
Aquaporins
CFTR
Na/K ATPase
ENaC
Tight Junctions
Actin
Myosin
Zona Occludens
Claudin 5
Occludin

Figure 1.2. Components of the alveolar-capillary barrier
The alveolus is formed of type 1 and type 2 alveolar epithelial cells (AECs). Cuboidal type 2 AECs, found on the corners of adjoining alveoli, produce terminally differentiated type 1 AECs that take on a thin stretched appearance forming over 95% of the wall of the alveolus. The epithelium is bound tightly together by multiple transmembrane (occludins, claudins, cadherins) and cytoplasmic protein (zona occludens) that are cross linked together and bound to the intracellular actin-myosin cytoskeletal scaffold. This actin myosin scaffold is controlled through multiple cytoplasmic signalling pathways. Myosin light chain (MLC) is the principal regulatory component of actomyosin condensation and contraction, and hence, cell shape and permeability. Multiple mediators (most notably TNF) induce activation of MLC kinase leading to phosphorylation of MLC and subsequent increases in paracellular permeability. Such adhesion molecules also exist between endothelial cells but do not show as tight a regulation as the epithelium. The basal cell membrane (vascular facing) of the epithelium also contains a significant number of Na^+/K^+ ATPase transporters that actively transport 3 Na^+ out of the cell and 2 K^+ ions into the cells creating a concentration gradient for Na^+. This facilitates entry of Na^+ from apical sodium channels (ENaC) and drives an osmotic gradient for the transport of water out of the alveolus into the interstitium. This process is called alveolar fluid clearance and can occur through transcellular (aquaporin channels) or paracellular routes. Cystic fibrosis transmembrane regulator (CFTR) is located on the apical surface (alveolar facing) and channels chloride ions into cells to ensure electroneutrality.

1.2 The acute respiratory distress syndrome

The acute respiratory distress syndrome (ARDS) was first described in 1967 by Ashbaugh et al (16) who described 12 patients exhibiting "…severe dyspnoea, tachypnoea, cyanosis that is refractory to oxygen therapy, loss of lung compliance, and diffuse, bilateral alveolar infiltrates seen on chest X-ray". Since these initial descriptions there have been multiple attempts to classify this heterogeneous syndrome. In 1994 an American-European Consensus Conference (AECC) defined ARDS as acute onset hypoxaemia ($PaO_2/FiO_2 \leq 200$mmHg) with bilateral diffuse infiltrates on chest radiograph, in the absence of left atrial hypertension. At this time, a less severe form of ARDS was described as acute lung injury (ALI), which had the same characteristics except for a $PaO_2/FiO_2 \leq 300$mmHg and hence, also, by definition included all ARDS cases (table 1.1) (17). In 2012, the definition has been revised in an attempt to improve the criterion up on which future clinical care and research could be conducted (18, 19). This was described as "the Berlin definition of ARDS" (table 1.2) and has been shown to correlate well with the classic histopathological findings, i.e. diffuse alveolar damage (DAD), which characterise ARDS (20).

	Timing	Oxygenation	Chest Radiograph	Pulmonary Artery Wedge Pressure
ALI	Acute Onset	$PaO_2/FiO_2 \leq 300$ mmHg	Bilateral Pulmonary Infiltrates	≤18 mmHg No evidence of left atrial hypertension
ARDS	Acute Onset	$PaO_2/FiO_2 \leq 200$ mmHg	Bilateral Pulmonary Infiltrates	≤18 mmHg No evidence of left atrial hypertension

Table 1.1. The 1994 AECC definition of ALI/ARDS

	MILD	MODERATE	SEVERE
Timing	Acute onset within 1 week of a known clinical insult or new/worsening respiratory symptoms		
Hypoxaemia	PaO_2/FiO_2: 201-300 PEEP ≤ 5 cmH_20	$PaO_2/FiO_2 \leq 200$ PEEP: 5-10 cmH_20	$PaO_2/FiO_2 \leq 100$ PEEP ≥ 10 cmH_20
Origin of Edema	Respiratory failure not fully explained by cardiac failure or fluid overload		
Radiological Abnormalities	Bilateral opacities—not fully explained by effusions, lobar/lung collapse, or nodules		
Additional physiological derangement	N/A	N/A	VE Corr > 10L/min Crs < 40ml/cmH_20

Table 1.2. The 2012 Berlin definition of ALI/ARDS
V_E Corr - corrected minute ventilation = V_E x $PaCO_2/40$
Crs - respiratory system compliance

1.2.1 Epidemiology.

ARDS continues to be a significant cause of morbidity and mortality and has an incidence of 75/100,000 and effects over 190,000 patients in the US (21), which extrapolates to an annual UK incidence of 33,000 occupying 450,000 ICU days (ARDS Foundation (USA)). This implicates a massive health economic burden to NHS UK in terms of ICU bed occupancy (costing on average £1300-1500 per day). Hence, the discovery of new innovations and therapies to reduce this impact, in an era when health budgets are reducing in real terms, is an absolute necessity.

1.2.2 Aetiology.

ARDS can be caused by a number of insults (table 1.3), each of which culminates in a syndrome presenting with severe non-cardiogenic pulmonary oedema causing life-threatening hypoxaemia often necessitating the implementation of mechanical ventilatory support. Aetiologies are broadly classified into pulmonary (or direct) and extra-pulmonary (or indirect) insults. This is related to the direction of the insult, with pulmonary insults arising from the alveolar space (e.g. pneumonia, aspiration) and extra-pulmonary insults being derived from systemic injury (e.g. non-pulmonary sepsis, trauma, pancreatitis, cardiopulmonary bypass). It is important to appreciate that the direction through which any insult mediates lung injury, that is, alveolar to

systemic (pulmonary) and systemic to alveolar (extra-pulmonary) will have markedly different underlying pathophysiological mechanisms, although certain aetiologies may share final common pathways. Importantly, this heterogeneity of mechanisms will certainly have been a major reason as to why no effective pharmacological therapy has to date been delivered. This is compounded by the neglect of clinical research to investigate the separate diseases leading to ARDS in combination with a lack of mechanistic research to define the distinct differences between these 'directions'. This is exemplified by the testing of compounds on non-clinically relevant animal models, and the reliance on data derived from single models, as opposed to, testing any intervention on multiple models. In particular, the recruitment of patients into clinical trials of ARDS in the absence of true disease or biomarker-based stratification may be flawed. Indeed, certain sub-groups may benefit but further investigation is often not pursued.

Pulmonary (Direct)	**Extra-pulmonary (Indirect)**
Common Pneumonia Gastric aspiration	**Common** Systemic non-pulmonary sepsis Severe Trauma
Less Common Pulmonary contusion Near-drowning Inhalational/Burn injury Reperfusion pulmonary oedema One-lung ventilation Fat emboli	**Less Common** Cardiopulmonary bypass Drug overdose Acute pancreatitis Transfusion of blood products

Table 1.3. The clinical associations with ARDS

1.2.3 Outcomes.

Mortality significantly increases after 2 weeks of the syndrome and is mainly a consequence of non-respiratory causes i.e. sepsis and multi-organ dysfunction syndrome. Early mortality (within 72 hours of onset) is attributed to the underlying illness or injury. Respiratory failure per se is a contributing factor to the death of 24% of patients and the primary cause of death in only 9-16% of patients (22-24). Furthermore, prognosis is better if recovery occurs within 2 weeks (21).

Phua et al performed a systematic review of 89 studies and concluded that baseline mortality risk was 40-45% in observational studies and 35-40% in randomised control trials (25). It was also shown in this study that mortality had not decreased since 1994. Assuming an incidence of 33,000 in the UK and a mortality rate of 40%, ARDS carries a high attributable mortality of 13,200 deaths per year. To place this in context, data from the Office of National Statistics placed the number of deaths per year from acute myocardial infarction, lung cancer, and breast cancer at 23,704, 31,089, and 10,397, respectively (Office of National Statistics (UK)).

There are no active therapies other than supportive organ support. For decades, this therapy consisted of ventilatory support in combination with diuretic therapy. Ironically, the only positive clinical study that has shown a proven mortality benefit was a trial that showed us that mechanical ventilation itself produces a form of lung injury known as ventilator-induced lung injury (VILI) which exacerbates the underlying syndrome. This clinical study compared ventilation with 6ml/kg versus 12ml/kg and showcased that limiting the stretch imposed by the ventilator reduced mortality by 7% (26). Despite this landmark study, the systematic review by Phua et al also found that mortality remained unchanged (25), highlighting a number of problems in implementing research findings to the bedside. Currently, novel and sophisticated improvements of old technologies such as veno-venous extracorporeal membrane oxygenation (VV-ECMO) may enable severe forms of ARDS to be successfully supported such that iatrogenic injury from the ventilator can be minimised. This seemed a successful strategy in recent flu pandemics in the UK (27) and Australasia (28). Further analysis of mortality once these techniques have embedded themselves into routine clinical practice may show improvements in survival.

An alternative explanation for this unchanged mortality is that despite improved ventilator strategies and general delivery of intensive care, ARDS is a changing phenomenon occurring in sicker and more elderly patients. This is particularly relevant in view of the fact that one of the predictors of poor prognosis is age over 55 (29) and that those between 60 and 69 years of age have a three times higher risk

for developing ARDS (30), and those over 70 have a higher risk of death (hazard ratio 2.5) (31). Hence, with an aging global population, and given that intensive care units are admitting older patients with more complex disease interactions, the projected burden and health economic impact of critical illness, and more specifically ARDS, is predicted to increase. These factors highlight the urgent requirement for effective therapies to target the underlying pathobiology of this devastating condition.

1.3 Injury and inflammation in ARDS

1.3.1 Diffuse alveolar damage is the cardinal histopathological feature of ARDS

The characteristic histological feature of ARDS is diffuse alveolar damage (DAD). This histological description was first noted by Hamman and Rich in association with "usual" interstitial pneumonia (UIP) (32). Katzenstein reviewed associations of DAD with oxygen therapy, shock, and other related factors. Many of these related factors are now the well-known clinical associations of ARDS as shown in table 1.3. This important review connecting the pathological findings to the current clinical entity known as ARDS also points out, quite correctly, that 1) the "recognition of DAD should stimulate a thorough search for and subsequent eradication of the underlying cause", and 2) that "DAD is not a diagnosis; it is a concept which is useful in understanding the pathogenesis of a group of similar pulmonary lesions which result from numerous and dissimilar agents" (33). Current clinical research strategies do not often appreciate these two statements and often amalgamate aetiologies, recruiting all ARDS patients into clinical trials, as opposed to those specific groups with distinct diagnoses. More sophisticated trial designs are an absolute necessity to improve the translation of therapies to the bedside.

1.3.2 DAD is characterised by two overlapping phases

Exudative phase

The insult leads to a marked increase in alveolar capillary barrier permeability leading to the flooding of the alveolar space with a proteinaceous fluid containing immunoglobulin, fibrin and complement. The fluid organises around alveolar walls leading to the formation of hyaline membranes. There is also translocation of blood-

derived leukocytes from the pulmonary microvasculature through the interstitium into the alveolar space. Overall, the alveolus is consumed by fluid, leukocytes, cellular debris and fibrin clots, dissipating the available space and worsening the diffusion barrier for gas exchange to occur.

Fibro-proliferative phase

Quite early on in the progression of ARDS there is epithelial mesenchymal transformation (EMT) leading to the infiltration of myofibroblasts which start laying a collagen scaffold for proliferation and repair. Hence, there is focal interstitial fibrosis and hyperplasia of the alveolar lining. Unlike UIP, DAD associated with ARDS does not always enter a fibrotic phase. Most ARDS recovers without fibrosis but this can be quite variable. This phase, if it occurs in ARDS, tends to show significant interstitial and alveolar fibrosis with vascular myointimal thickening. The amount of total lung collagen can double (34).

Interestingly, there is considerable overlap between these phases of DAD in ARDS. However, the clinical picture is often blurred by superimposed ventilator-associated pneumonia and sepsis; the major causes of morbidity and mortality during the later stages of ARDS.

1.3.3 Alveolar-capillary barrier dysfunction in ARDS

The first and primary physiological deterioration in ARDS is the development of non-cardiogenic alveolar oedema as a result of alveolar capillary barrier dysfunction. ARDS is the most rapidly deteriorating state of respiratory pathophysiology with alveolar oedema sometimes occurring within minutes to hours of the antecedent insult. This oedema formation and subsequent V/Q mismatch (with significantly increased intrapulmonary shunt) determines the deteriorations in arterial oxygenation necessitating mechanical ventilation to ensure survival. Mechanical ventilatory support with general anaesthesia and other organ support introduce further deleterious impacts, such as shock, VILI, and ventilator associated pneumonia, upon an already injured lung. The mechanisms of oedema formation are still poorly understood. Certainly, the exclusion of a raised pulmonary capillary pressure as a result of cardiogenic insults is important to subsequently direct the

underlying injury at the pulmonary capillary endothelium and/or the alveolar epithelium. This is often difficult to entirely exclude given that sepsis can lead to myocardial depression and diastolic dysfunction (35). Hence, the Berlin definition takes this into account by stating that the hypoxaemia not fully explained by cardiac failure or fluid overload should also constitute the definition of ARDS.

Depending on the insult, either or both of these layers comprising the air-fluid interface are 'hit'. Very recent data from Ware and colleagues suggests that intrapulmonary insults lead to higher biomarkers of epithelial injury (surfactant protein D and RAGE) and extrapulmonary insults induce greater levels of endothelial biomarkers (Ang2) in the plasma of ARDS patients (36). The alveolar epithelium is immediately exposed to intrapulmonary insults and hence there is often an immediate increase in epithelial permeability. This is also usually associated with concomitant increases in endothelial permeability due to the proximity of these two layers. This loss of epithelial mucosal protection promotes fluid leak into the alveolar space. In contrast, pre-clinical studies have shown that endothelial injury occurs in nearly all models of extra-pulmonary ARDS but that epithelial injury may not necessarily occur (37). Furthermore, indirect insults do not always generate alveolar oedema and hence, endothelial injury alone may be insufficient to induce the extensive alveolar oedema generated in ARDS.

There is several data as to why epithelial dysfunction leads to a state of rapidly progressive alveolar oedema formation. Firstly, the epithelial layer provides over 92% of the resistance to albumin flux during normal physiology (38). Intrapulmonary insults induce significant damage to the alveolar epithelium and this damage is easily transmitted to the endothelium, either directly by the insult itself (due to loss of mucosal barrier defences) or through signalling from the alveolar space (39-42). In comparison, extra-pulmonary forms of lung injury may show a maintained alveolar epithelial tight junction integrity and/or sufficient alveolar epithelial fluid clearance (in combination with interstitial lymphatic clearance) to prevent the flooding of alveolar airspace. It is only when interstitial lymphatic clearance is overwhelmed and/or alveolar fluid clearance is reduced that indirect causes may induce leak into

the alveolar space. This was corroborated by two studies in which sheep were exposed to intravenous endotoxin (43) and septic shock (44). In the latter, Pittet et al infused live P. *aeroginasa* into the lung perfusate of a sheep isolated perfused lung preparation and found that there were significant increases in lung endothelial permeability with an increased interstitial oedema, however, there was no impact upon the lung epithelial permeability. They surmised from this that the epithelial barrier was more resistant than the endothelium to gram-negative shock.

Overall, in ARDS the endothelium and epithelial barriers lose their ability to control protein and fluid influx (45) which may be dependant on the type, intensity, and 'direction' of insult. Epithelial injury and dysfunction seem to be an absolute necessity for the development of alveolar oedema through not only increased permeability but also reduced resolution of alveolar oedema through active clearance mechanisms (46).

1.3.4 Inflammatory mechanisms of endothelial injury in ARDS

Endothelial activation and dysfunction remains integral to the development of ARDS, in that, it not only promotes interstitial oedema formation, but also, is necessary for leukocyte migration into the interstitial and alveolar spaces of the lung. However, the aetiology and direction of lung injury is likely to significantly influence the manner in which the endothelium is activated.

The first pathophysiological impact on the lung during systemic, non-pulmonary aetiologies of ARDS is likely to be pulmonary capillary endothelial activation, given the exposure of this layer to molecular and cellular constituents within the circulation. This may occur through the interaction of molecular mediators released from the site of injury/infection acting directly on corresponding receptors on the pulmonary capillary endothelium. Alternatively, this may occur through leukocytes that have been primed/activated at a distant site of injury which subsequently migrate or are trap in the pulmonary vasculature, thereby, inducing pulmonary capillary endothelial activation through cell-cell interactions (47). Indeed, there is a

school of thought that the lung actively sequesters activated neutrophils from the circulation in an attempt to “de-prime” them (48).

In the case of direct injury, although there is significant epithelial injury, the proximity of the endothelia makes endothelial dysfunction inevitable. Whether this is a direct consequence of the pulmonary injury/infection or a signalling cascade from injured epithelium is still under investigation. For instance, Kuebler et al showed that intra-alveolar microinjection of TNF-alpha induces epithelial phospholipase-A2 activation leading to release of calcium and activation of endothelial pro-inflammatory responses (P-selectin expression) within minutes of delivery (39), suggesting a signalling communication between epithelial and endothelial layers. Westphalen et al also found in a rat model of acid-induced lung injury that a direct impact upon the alveolar epithelial cell membrane initiates endothelial cell pro-inflammatory signalling through reactive oxygen species (42).

It seems that regardless of pulmonary or systemic ‘direction’ of aetiology, the response of the pulmonary capillary endothelium includes activation of intracellular signalling cascades such as mitogen-activated protein (MAP) kinases, phosphokinase-C, and intracellular calcium. This pro-inflammatory phenotype possesses an upregulated surface expression of leukocyte adhesion molecules (such as E- and P-selectin), an increased production of reactive oxygen/nitrogen species (ROS/RNS), and an increased secretion of chemokines (such as IL-8). The intimate proximity of the endothelium surface to circulating mediators is enhanced by the acute degradation of an endothelial surface layer called the glycocalyx. This degradation has been shown in intravenous endotoxin model of sepsis to increase the availability of ICAM-1 and VCAM on the endothelial surface thus facilitating the tethering and firm adhesion of neutrophils to the endothelial surface (49). Subsequently, the local secretion of proteases (e.g. elastin) by leukocytes breaks down intercellular bonds between endothelial cells facilitating their transmigration into the alveolar-capillary interstitial space. The interactions between neutrophils, monocytes, platelets and endothelial cells leads to the release of more toxic mediators such as ROS/RNS (e.g. peroxide; peroxynitrite), cytokines (e.g. TNF), proteases, and procoagulant molecules

(e.g. thrombin), thereby amplifying this pro-inflammatory and injurious response. These toxic cellular and molecular mediators enhance vascular permeability through further disruption of intercellular adhesion molecules and the intracellular actin-myosin cytoskeleton (50), thereby promoting intercellular gaps. Intercellular adherens junctions consisting of molecules such as VE-cadherin maintain tight cell-cell adhesion between endothelial cells, and maintain endothelial barrier integrity. A number of investigations have found that the loss of intercellular junctions such as cadherins leads to the formation of intercellular gaps that lead to a failure in endothelial protein sieving and increased microvascular permeability and hyperfiltration, allowing plasma constituents into the interstitial space (3, 51). Furthermore, stretch of endothelial cells through mechanical ventilation can also enhance vascular permeability adding further insult to injury (52, 53).

1.3.5 Apoptosis as a mechanism of epithelial injury in ARDS

Experimental models utilising direct insults seem to produce greater alveolar oedema than indirect insults suggesting a larger impact to the alveolar epithelium. In addition to barrier function, the alveolar epithelium is essential in clearing alveolar oedema and maintaining homeostasis of the alveolar lining fluid. The mechanisms that lead to injury to the alveolar epithelium have received less attention than the endothelium, partly due to difficulties in harvesting and maintaining the phenotype of primary type 1 AEC cell cultures.

The discovery that apoptosis (programmed cell death) of alveolar epithelial cells occurs in ARDS has been a pivotal finding. Historically, the pathways for cell death have been placed into the distinct categories of apoptosis or necrosis. Apoptosis is a controlled form of cell death leading to a staged cellular demise avoiding the release of toxic intracellular debris, which contains numerous DAMPs. Necrosis on the other hand is associated with cell swelling, cell membrane rupture and release of intracellular contents to the outside with toxic inflammatory consequences. However, this concept of apoptosis versus necrosis is too simplistic and it is now fair to say that there are much more complicated aspects to cellular death. Not only has apoptosis been implicated in the development of injury but also it is crucial in the

resolution and repair processes of ARDS. In normal physiology, a balanced tissue homeostasis and cellular turnover determines growth through the number of cells scheduled for 'death' and the number to be 'born' through mitosis. Thus removal of cells through apoptosis is integral to whole body homeostasis which is why cell death pathways are "programmed" into each and every cell. Disturbances in this balance lead to dangerous consequence through the formation of cancers and organ dysfunction. To understand the implications of alveolar apoptosis, we need initially to have an appreciation of the signalling cascades and organelles involved during cellular death.

Apoptosis can be initiated through either extrinsic or intrinsic mechanisms (figure 1.3). The intrinsic pathway involves the release of mitochondrial products, including cytochrome c, in response to various forms of cellular stress such as DNA damage, heat, reactive oxygen species, radiation, and viral proteins. The released cytochrome c binds to apoptotic protease activating factor 1 (APAF-1), leading to the recruitment of caspase-9 forming the 'apoptosome' complex. Caspase-9 propagates the caspase cascade through activation of the effector caspases (-3, -7, and -10), which in turn, activate the machinery required for cellular demise.

The extrinsic pathway involves the activation of one or more members of the death receptor family on the cell surface that includes the p55 TNF receptor, Fas, DR4 (TRAIL-R1), DR5 (TRAIL-R2) and DR6. These receptors all possess an intracellular death domain, which on ligand-receptor interaction leads to the recruitment of intracellular adaptor molecules, forming the 'death-inducing signalling complex' (DISC), which in turn, activates caspase-8. The activation of caspase-8 is a critical juncture, as from here on, depending on the cell type, there are two pathways through which the extrinsic death signal can be propagated, dependent upon the extent to which procaspase-3 is converted to caspase-3. In type A cells, there is sufficient activation of caspase-3 in order to proceed to the final pathways of cell death. By contrast, type B cells require additional help to activate caspase-3. This additional help comes through caspase-8 activating pro-apoptotic molecules Bid, Bad and Bax, on the mitochondrial outer membrane to activate apoptosome formation.

The finding that type 2 AECs expressed Fas (54), a member of the death receptor superfamily, sparked the first thoughts as to the involvement of epithelial apoptosis in ARDS pathobiology. Subsequently, Hagimoto and colleagues showed not only was Fas/Fas ligand mRNA upregulated in the lungs of mice exposed to bleomycin (55), but also that inhalation of a Fas activating antibody led to increased epithelial apoptosis and alveolar inflammation. Matute-Bello subsequently showed that biologically active soluble Fas ligand (FasL) is found in the alveolar space of ARDS patients and induces the apoptosis of distal lung epithelial cells, which could be blocked by anti-Fas and anti-FasL antibodies (56). Furthermore, the instillation of recombinant human FasL into rabbit lungs induces ARDS through alveolar epithelial apoptosis (57). Albertine and co-workers found 10% of alveolar lining cells were apoptotic in post-mortem investigation of patients who died with ARDS (58). They found that pulmonary oedema fluid from ARDS patients had increased concentrations of Fas and FasL compared to the hydrostatic oedema controls. Additionally, both epithelial and inflammatory cells within the alveolar space expressed both Fas and FasL. Hence, the last decade of investigations into the mechanisms through which FasL/Fas lead to lung injury remain quite primitive with a significant lack mechanistic approaches. This has recently been addressed in a study performed by Herrero et al that found that the human FasL was prone to modulation by oxidants and proteases within the alveolar microenvironment (59). This modulation included the cleavage of stalk regions of FasL (required for its bioactivity) by matrix metalloproteinase (MMP)-7, as well as, the oxidation of FasL leading to the multimerisation of FasL. Of note, cleavage reduced activity of FasL and oxidation/multimerisation enhanced it, and this study found that human ARDS BAL contained a significant quantity of non-cleaved (i.e. with stalk region), methionine oxidised and aggregated FasL.

Other death receptors in the extrinsic pathway (including TNF (60-65) and TRAIL (66, 67)) and proteins in the intrinsic apoptotic pathway (68) have been implicated in development of epithelial cell death in various models of lung injury. However, overall, investigations into the role of cell death in ARDS are still in their infancy. In

particular very few have localised signalling pathways to the actual cell type and furthermore there is little mechanistic insight into how epithelial apoptosis may induce the important pathophysiological manifestations observed in lung injury, such as increased permeability and reduced alveolar fluid clearance.

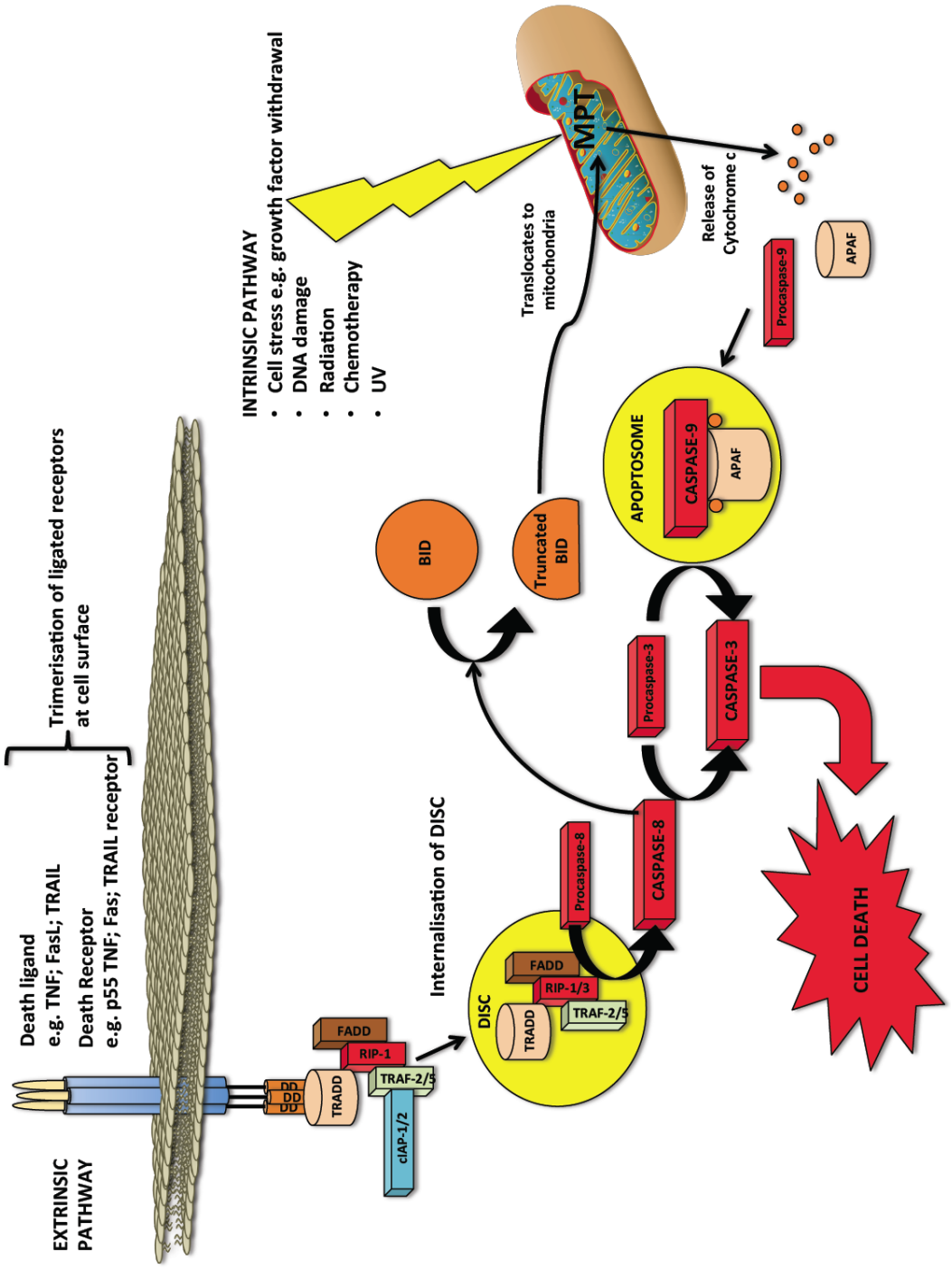

Figure 1.3. Apoptosis signalling pathways

Apoptosis or programmed cell death can be activated through two main pathways – the intrinsic and extrinsic. The intrinsic pathway is activated by multiple distinct intracellular conditions and is regulated by mitochondria. In response to these stressors there is activation of pro-apoptotic mediators including Bid, BAK and BAX within the mitochondria inducing permeabilisation of the mitochondrial membranes (via the mitochondrial permeability transition, or MPT). This leads to mitochondrial swelling and release of cytochrome c into the cytoplasm. In combination with dATP and APAF, cytochrome c forms the apoptosome leading to activated caspase-9, which subsequently activates caspase-3. The extrinsic pathway is initiated by death receptor activation (p55 TNF receptor, Fas, DR3/4/5/6). This leads to the formation of the death inducing signalling complex (DISC) that activates caspase-8. Caspase-8 is a crucial checkpoint in apoptosis progression. If sufficient caspase-3 activation occurs then apoptosis proceeds through this route. If insufficient caspase-3 activation occurs, then caspase-8 can lead to cleavage of Bid. Truncated Bid translocates onto the inner mitochondrial membrane where it activates BAK activation, induces MPT, with the subsequent release of cytochrome c and activation of the intrinsic pathway.

(APAF, apoptotic protease activating factor; BAK, BH antagonist or killer; BID, BH3-interacting domain death agonist; cIAP, cellular inhibitor of apoptosis; dATP, deoxyadenosine triphosphate; *DD, death domain; DISC, death inducing signalling complex; FADD, Fas associated death domain; MPT, mitochondrial permeability transition; RIP, receptor interacting protein kinase; TRADD, TNF receptor associated death domain; TRAF, TNF receptor associated factor; TRAIL, TNF related apoptosis inducing ligand)*

1.3.6 Alveolar fluid clearance as an index of epithelial function

Alveolar fluid clearance is driven through the vectorial transport of sodium from the alveolar space into the interstitial space thereby creating an electrochemical gradient for the transport of water (figure 1.2). This sodium gradient is formed by the presence of Na^+/K^+ ATPase channels in the basal surface of the alveolar epithelium. Hence, the alveolar epithelium is a highly energy consuming layer. Sodium enters the epithelium from the alveolar lining fluid through epithelial Na^+ channels (ENaC) located in the apical surface.

The first evidence in humans to suggest that active transport of ions facilitated the clearance of oedema from the alveoli was found by Matthay and Wiener-Kronish in 1990. This study found that alveolar fluid clearance is better in patients who resolve clinically from ARDS, and in those who have low fluid clearance in the first 12 hours post-intubation showed a poor prognosis (46). Ware and Matthay obtained serial samples of lavage from a larger cohort of patients with ALI/ARDS and calculated AFC through the increase in protein concentration over time (69). They found that AFC was impaired in 56% of patients with ARDS with maximal clearance only occurring in 13% of patients. In particular, those with higher levels of AFC showed significantly improved hospital mortality, and reduced number of ventilator days, with a trend to improved oxygenation.

There has been significant investigation into strategies that may stimulate the resolution of pulmonary oedema through augmenting intrinsic mechanisms of alveolar fluid clearance. The compounds that have received the most interest include beta-adrenergic agonists (e.g. salbutamol, albuterol) and have been shown to augment AFC in preclinical (70-73) as well as ex vivo human lung studies (74). The BALTI study showed, as proof of concept, some improvement in extravascular lung water in ARDS patients treated with intravenous salbutamol (75). The larger multicentre, randomised controlled follow-up study, the BALTI-2, showed no improvement in outcomes and was stopped early as the salbutamol arm showed greater harm (76). Additionally, a recent study led by the ARDS Clinical Trials Network showed no benefit with aerosolised albuterol (77). Hence, this has left

many investigators to contemplate reasons for these failures and think of new directions and mechanisms to enhance AFC. One of the major issues has always been whether the injured alveolar epithelium is able to increase its activity and whether driving an injured cell to increase its activity would actually be beneficial or harmful. Furthermore, before the implementation of clinical trials such as these, we should have a better idea as to the mechanisms that drive epithelial injury and dysfunction in ARDS. For instance, there are no studies investigating links between epithelial apoptosis and alveolar fluid clearance in ARDS. If the majority of the epithelium is compromised then enhancing AFC may be futile. Rather a more sophisticated approach to rescue the epithelium may be more applicable.

1.3.7 Pulmonary inflammation in ARDS

A hallmark observation of ARDS is the accumulation of inflammatory leukocytes and leukocyte-derived mediators, in particular neutrophils, within the alveolar space (78-80). The oedema fluid within the alveolar space has a vast array of cellular and molecular mediators, some of which are locally produced, but many have translocated from the plasma compartment. The kinetics of cellular recruitment is difficult to investigate in clinical ARDS and hence extrapolation has to be made from experimental models. However, the question of 'what is (are) the initiating factor(s) leading to ARDS and how do the pathways initiated by direct or indirect insults converge to induce alveolar capillary barrier dysfunction?' remains unanswered. It is hypothesised that direct insults induce the activation of resident alveolar macrophages and epithelial damage, whereas, circulating factors (cellular and molecular) and endothelial dysfunction may be integral to indirect causes such as pancreatitis. However, the final common pathways involve damage to both epithelial and endothelial barriers and hence, promoting alveolar oedema.

Depletion of alveolar macrophages has been shown to attenuate intra-tracheal endotoxin- (81), ventilator- (82), and acid- (83) induced lung injury, suggesting a pivotal role to initiate alveolar inflammatory cascades. It is likely that once parenchymal injury has occurred, regardless of route, there is an influx of blood-derived leukocytes that either aggravate the injury or promote resolution/repair.

Elucidating this 'resolution switch' is the 'holy grail' of inflammation research. Transcription of more downstream inflammatory mediators such as IL-6, IL-8 from lung parenchyma, in addition to alveolar macrophages, also upregulates leukocyte adhesion molecules on the endothelial surface activating leukocytes which eventually transmigrate into the alveolar space, further amplifying inflammatory cascades (84, 85). It has been shown that persistently increased levels of cytokines (TNF, IL-1β, IL-6, and IL-8) in the lungs correlate with a poor outcome in ARDS (86). Whether this is cause or effect remains undetermined. Regardless of the initial driver, neutrophils and monocytes have been shown to be important components of the inflammatory response that characterises ARDS. Other studies investigating indirect aetiologies have shown that the activation of complement protein C5a (a circulating complement mediator) induces neutrophil activation in the blood and sequestration into the pulmonary vasculature (87). Additionally, experimental studies of lung injury have shown that neutrophil depletion is protective (88) and that monocyte depletion attenuates injury (89).

In contrast, it has also been shown that leukocytes do not contribute significantly to barrier dysfunction. Wiener-Kronish et al (43) and Martin et al (90) showed large numbers of neutrophils crossing into the alveolar space in sheep and man, respectively, with endothelial permeability changes in the absence of epithelial changes in permeability. In addition, ARDS also occurs in neutropenic patients and those with bone marrow failure, which supports the view that leukocytes, whilst integral in some aspects of ARDS, may not be absolutely necessary in its pathobiology (91-94). Although neutropenic recovery has also been associated with a near 5-fold increased risk of ARDS development, this risk is only apparent if complicated by pneumonia (95). Hence, it is crucial to appreciate the context in which leukocytes are recruited to the lung parenchyma as they may play quite divergent roles depending on the phase and type of lung injury - injurious/inflammatory/infectious versus reparative/resolving. For instance, neutrophil mediated responses are crucial to fight bacterial infection in the context of pneumonia whereas collateral damage to self may ensue in sterile lung injury. Interestingly, not all pneumonias develop into ARDS and, in the majority of patients,

neutrophils are present in the alveolar space to perform their duties, that is, fight microbial infection without causing significant self- or collateral harm. In addition, neutrophil transmigration has also been recently shown to promote epithelial repair in an intratracheal model of lung inflammation through beta-catenin signalling (96). Additionally, as we shall see, leukocytes (predominantly monocytes and lymphocytes) continue to migrate into the alveolar space and depending on the situation can, with one hand, promote inflammatory consequences during the acute phase (97), and with the other, direct repair and resolution (98-100), or even potentiate lung fibrosis (101).

Importantly, syndromes such as ARDS and sepsis characterised by perpetuating inflammation, are associated with an increased neutrophil lifespan (102). Studies have shown that the alveolar microenvironment in ARDS patients can prolong the survival of neutrophils. For instance, Matute-Bello incubated normal human neutrophils with ARDS BAL and found an anti-apoptotic effect that could be ameliorated through the immunodepletion of G-CSF and GM-CSF (103). It is also well established that the apoptosis of leukocytes is crucial to initiate resolution and repair processes by limiting inflammation and the degree of tissue injury (14).

Leukocytes can take on different roles depending on their interactions with nearby molecular and cellular mediators. Hence, leukocytes can adopt different phenotypes at different stages of inflammation and resolution. This ability of leukocytes to control and switch their responsiveness is integral for resolution and recovery and it is this dysregulated control switch that may be at the centre stage of ARDS pathogenesis. Hence, understanding the context in which a leukocyte has been called to the lung is an important concept to investigate and appreciate clinically. Furthermore, most research in lung leukocyte recruitment utilises endotoxin administration and hence, produce significant levels of alveolar inflammation but in the context of sustained and overwhelming activation of one initial pathway, that of TLR-4 activation. Many of these endotoxin models also lack the physiological indices which define ARDS e.g. hypoxaemia (37). The exact inflammatory mechanisms that trigger these early inflammatory events in more clinically relevant forms of lung

injury (such as acid aspiration, pneumonia, or trauma) have received relatively little attention. The key question of how inflammation produces physiological injury and dysfunction surmounting to the high morbidity and mortality seen in ARDS remains unanswered.

It is unlikely that all the cellular and molecular mediators implicated in lung injury are amenable to blockade, and even more unlikely that research will unravel the intricate nature of their relationships, particularly in such a heterogeneous syndrome. What seems more sensible is the blockade of either more proximal inflammatory paradigms that set downstream inflammatory cascades into motion (prophylactic/ early phase strategies), or to target and investigate paradigms that promote resolution and repair once dysregulated inflammation is established (late phase strategies).

1.4 Resolution of injury and inflammation in ARDS

The ideal response to injury should ensure removal of any harmful stimuli, followed by a decline in the inflammatory response limiting damage to self. There should be in parallel successful repair of tissue enabling it to return to normal structure and function. There is now convincing evidence that inflammation does not just simply 'fizzle out'. In contrast, resolution of inflammation, repair and recovery, involves a highly coordinated and actively controlled series of events. ARDS shows overwhelming inflammation due to disturbed mechanisms that control resolution of oedema and inflammation. The hallmarks for tissue recovery and resolution of inflammation can be described in three overlapping phases (figure 1.4).

1.4.1 Phase 1: "The stop signal"

Firstly, the early phase of resolution removes the inciting stimulus, ceases further proinflammatory leukocyte recruitment, and promotes catabolism of pro-inflammatory mediators with a controlled anti-inflammatory response. There is now more evidence that this phase of resolution is triggered even earlier than previously thought. Within hours of the initial stimulus there is a switch between the formation of pro-inflammatory eicosanoids (e.g. prostaglandins, leukotrienes and platelet

activating factor) to the anti-inflammatory eicosanoids (including lipoxins, resolvins and protectins) (104). This switch is triggered by the neutrophils themselves (via neutrophil-platelet interactions) in an attempt to limit the inflammatory response (105, 106). More importantly, these mediators also prevent further neutrophil trafficking, reduce vascular permeability, promote exudative monocyte entry,as well as, the ingestion/clearance of debris and apoptotic neutrophils, which are integral to later stages of resolution (107).

The ability to initiate this shut down of proinflammatory leukocyte activity is an important checkpoint for resolution of inflammation. Indeed, the resolution interval is an experimental index defined by the time taken for numbers of infiltrated neutrophils in the inflamed tissue to decline from their peak by 50% (104). This decline is dependent on constitutive apoptosis programme of neutrophils that consequently imparts a limited life span of 24 hours or less. Perpetuated neutrophil mediated inflammation as a result of abnormal (delayed) apoptosis can indeed be detrimental in the overzealous inflammatory processes that occur in ARDS. For example, studies have shown that bronchoalveolar lavage fluid from patients with established ARDS prolongs the survival of neutrophils through disrupted apoptosis (103).

A variety of cytokines (including IL-1 receptor antagonist, IL-4, IL-10, and IL-13) as well as the soluble forms of their receptors (including soluble TNF receptors, IL-6 receptors) are also implicated in this phase. One of the most studied, IL-10, has been shown to block the synthesis of a number of pro-inflammatory cytokines (including IFN-γ, IL-1, TNF, IL-12), chemokines (such as IL-8, and CCL2) and, is often released from macrophages that have changed their phenotype response having ingested debris and apoptotic neutrophils. IL-4 and IL-13 also influence monocyte/macrophage phenotype by increased endocytic activity through increased expression of scavenger receptors to recognise and increase parasite killing; stimulation of mRNA of proteins such as matrix metalloproteinases and collagen types, all of which are crucial in enhancing tissue repair and fibrosis. IL-10 and TGFβ

on the other hand can deactivate monocytes and reduce expression of MHC class II molecules used for antigen presentation to cytotoxic T-cells.

1.4.2 Phase 2: "Clearing up the mess"

Secondly, a clearance phase of resolution is initiated. A short time after neutrophil infiltration into damaged/infected tissue the adaptive system is activated with T-cell infiltration into the tissue. Cell-cell interactions with resident macrophages, exudative monocytes and dendritic cells (DC) leads to the release of mediators such as TGFβ and IL-10 promoting apoptosis of neutrophils and their uptake by macrophages.

Cell death can proceed through a spectrum, which ranges from the programmed form termed apoptosis, or a less ordered process termed necrosis. As discussed with the epithelium, apoptosis is the ideal way for cells in the body to die as it prevents the activation of proinflammatory responses against intracellular molecular patterns, which are released with necrotic cell death. Neutrophil apoptosis can be modulated by a number of agents, including GM-CSF, which delays apoptosis, and endotoxin, FasL, TRAIL and TNF, all of which promote neutrophil apoptosis.

More importantly, apoptotic cells upregulate recognition signals facilitating their uptake by macrophages. These include thrombospondin-1, annexin-1, phosphatidylserine and lysophosphatidylcholine. The mechanisms that dictate neutrophil apoptosis are beyond the scope of this section but it is important to appreciate that apoptotic neutrophils are non-functional but retain their histotoxic cellular constituents, and hence, delayed uptake by macrophages will lead to secondary necrosis, amplifying inflammatory responses through release of intracellular DAMPs. Indeed, the mechanisms through which apoptotic cells signal their own disposal is crucial for the macrophage switch from pro-inflammatory to pro-resolving phenotypes (14, 108). This plasticity to their environment makes macrophages vital regulators and effectors of local immune responses (figure 1.5). Influx of blood-derived monocytes increases total tissue macrophage numbers (109,

110) to help initially fight the inflammatory battle but then to subsequently switch phenotype to clear debris and efferocytose apoptotic neutrophils.

After clearance of neutrophils and debris, T-cells continue to be present producing TH_2 cytokines, such as IL-4 and IL-13, which regulate resident tissue macrophages. As a consequence, these resident macrophages take on a wound healing phenotype leading to myofibroblast proliferation and collagen deposition. The extent of which is most likely dependent on the severity of epithelial damage in ARDS (111). The fate of these exudative macrophages are still uncertain but there is evidence suggesting that they too undergo constitutive apoptosis and that this may occur either locally (112) or after emigration to local lymph nodes (113).

1.4.3 Phase 3 – "Re-establishing order and function"

So, once the battlefield has been cleared, we return to the overall goal, that is, functional recovery and catabasis, which requires recovery of cellular structure and function at a microscopic and macroscopic level, improvement in cellular bio-energetics, as well as, controlled apoptosis and replacement of damaged parenchymal cells. It remains unclear as to why certain patients heal whilst others repair through fibrosis. For instance, ARDS can lead to a protracted fibrotic phase. It is also clear that fibrosis occurs much earlier at the onset of inflammation and, factors (such as TGFβ), which regulate resolution, also influence fibrosis. Increasing evidence suggests that parenchymal cell death may dictate acute and chronic fibrotic responses (114). For instance, Sisson et al showed that targeted injury to the type II alveolar epithelium induces collagen deposition and lung scarring (115). This may be due to an inability to produce type 1 AECs, or that epithelial death leads to a reduction in signals, such as prostaglandin E2 (116), that are important in suppressing protein production by lung fibroblasts. In addition, damaged epithelium may be promoting pro-fibrotic factors to activate local fibrosis.

Hence, although it would be attractive to promote timely apoptosis of leukocytes thereby switching on resolution mechanisms, a potential side effect of this approach may be tissue scarring if parenchymal apoptosis is inadvertently activated. There lies

the double-edged sword in any strategy targeting apoptosis and hence, investigations to clarify specific targeting of cells within the lung may lead to novel treatment strategies.

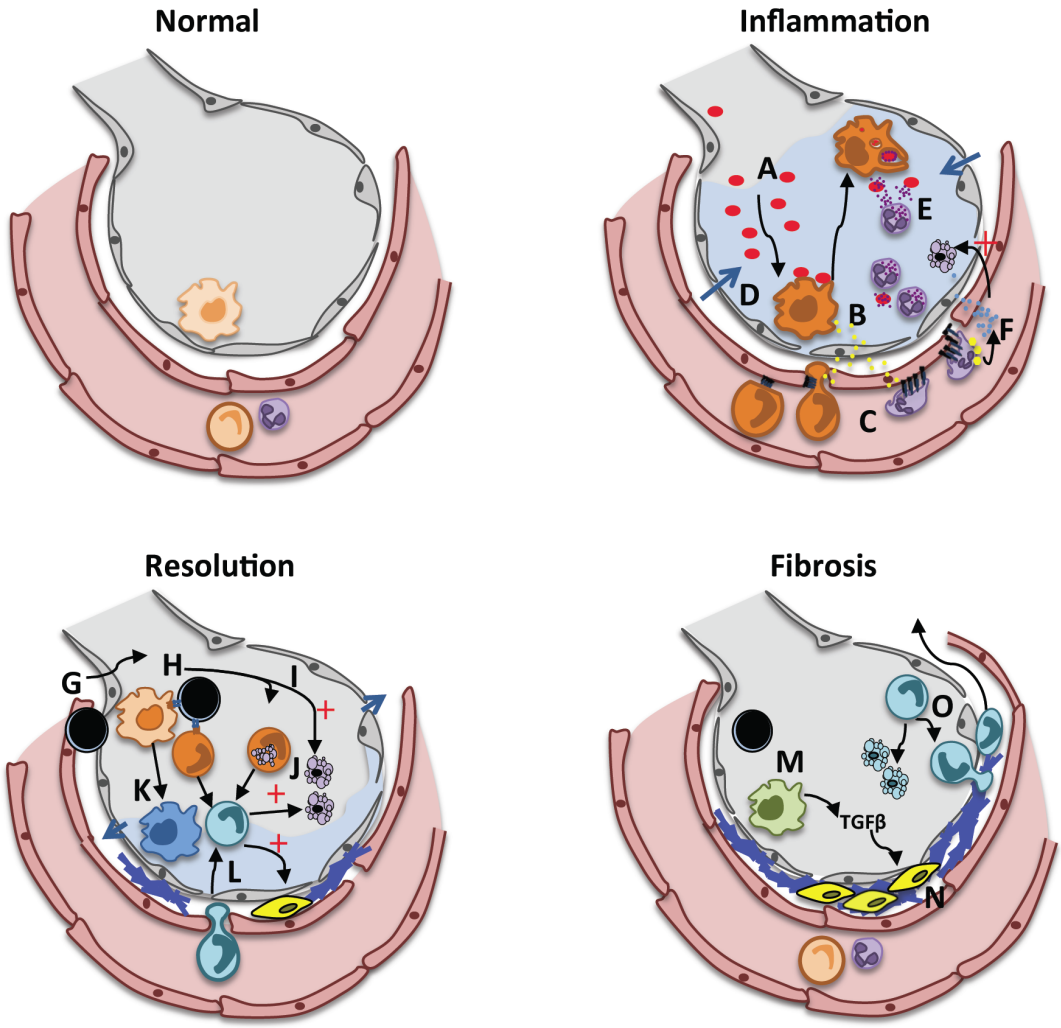

Figure 1.4. The phases of resolution in lung inflammation
The mechanisms portrayed here are separated to aid description but actually occur simultaneously. The dysregulation of these phases likely lead to continual inflammation and malresolution. A) Injurious insult induces classical activation of resident tissue macrophages. B) Activated macrophages release reactive oxygen species, cytokines and chemokines. C) Molecular mediators released from macrophages leads to epithelial and endothelial activation with recruitment of early phase neutrophils and monocytes. D) Barrier dysfunction leads to oedema formation. E) Migrated leukocytes release opsonins (e.g. complement) to facilitate removal of insult. F) Early resolution mediators (e.g. lipoxins, resolvins, protectins) are released as a consequence of neutrophil platelet interactions, limiting

overzealous inflammatory actions. G) Activation of T-cell responses. H) Interactions with T-cells induces a phenotype change in macrophages, monocytes and dendritic cells. I) At the same time neutrophils undergo apoptosis heralding the initiation and amplification of the resolution process. J) Apoptotic neutrophils are taken up by alveolar macrophages inducing further phenotypic class switching. K) This involves a macrophage switch from pro-inflammatory to pro-resolving phenotypes. (L) There is an influx of blood-derived cells to help clear the debris including dead tissue and apoptotic leukocytes. M) T-cells continue to be present and release IL-4/-13 regulating tissue macrophages inducing a wound healing phenotype. N) These macrophages induce myofibroblast proliferation and collagen deposition through further release of TGFβ. O) The fate of exudative leukocytes after restoration of tissue function may occur locally through apoptosis or at draining lymph nodes.

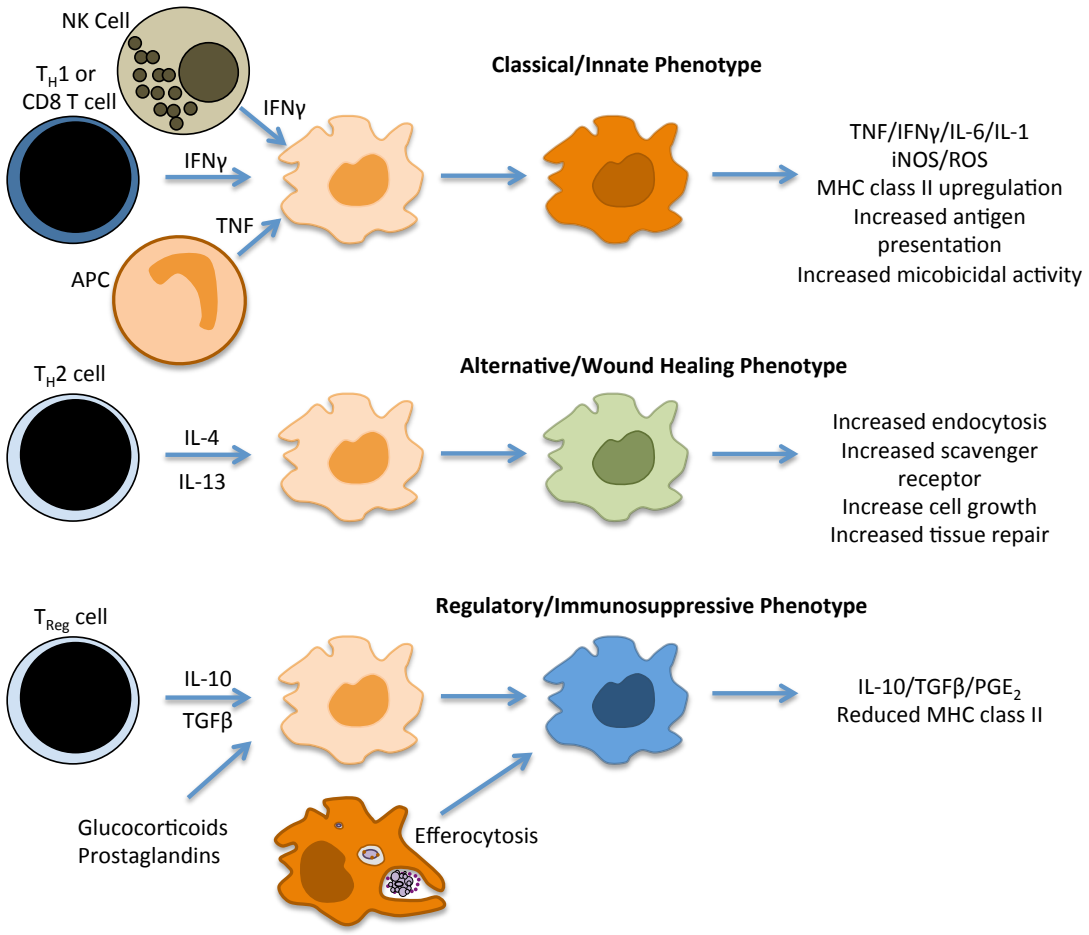

Figure 1.5. The interactions and plasticity of macrophages

1.4.4 Translational therapies promoting resolution in critical care

It is unclear as to why an initial focused inflammatory response becomes maladaptive in critical illness. There are significant challenges to bedside translation of biological therapies to treat conditions such as sepsis and ARDS. A major hurdle is that patients do not present at time zero and often have overwhelming inflammation on presentation.

Prevention is better than cure

Much of the recent improvement in mortality is a result of improved delivery of care attenuating perpetual inflammation as result of iatrogenic insults such as ventilation, invasive monitoring, and nosocomial infection. The first significant breakthrough was the use of low tidal volumes to prevent iatrogenic ventilator induced lung injury (26). However, simple measures such as 30^{o} head up tilt to reduce gastric aspiration; venous thromboembolic prophylaxis; regular turning to prevent pressure ulcers; closed loop suctioning to prevent nosocomial infection; stress ulcer protection have dramatically reduced the incidence of iatrogenic insults during the critical care stay of many patients.

Anti-inflammatory strategies

A major focus of research over the past few decades has been to elucidate anti-inflammatory strategies. These strategies are fraught with difficulty as they may promote an immune compromised state with the augmentation of uncontrolled 'compensatory anti-inflammatory response syndrome'. For instance, low levels of pro-inflammatory mediators, such as nitric oxide, TNF-α and IL-6, have been shown to be both pro-resolving and reparative (117, 118). This may explain why the bench to bedside translation of cytokine-based blocking therapies in the absence of mechanistic insights has increased mortality in some studies of sepsis. The temporal relationship between this initial anti-inflammatory response and the progression of the first and second phases of resolution (as described earlier) may determine the susceptibility to nosocomial infection – a major cause of morbidity and mortality in intensive care.

Enhancing active resolution phase mediators

The notion of active resolution mechanisms is so recent that well-known agents such as glucocorticoids and aspirin have been labelled as anti-inflammatory whereas in actual fact they are significantly pro-resolving in nature. For instance, glucocorticoids have been shown to enhance (119) and inhibit neutrophil apoptosis (120, 121) but a major influence on macrophage phenotype imparts vital resolving effects through induction of annexin A1 (122) and increased neutrophil efferocytosis (123). Overall, glucocorticoids have been shown to reduce pro-inflammatory cytokine release, reduce neutrophil trafficking, increase neutrophil apoptosis and efferocytosis, and reparative macrophage phenotype switching – all key steps in inflammatory resolution.

More recent advances have discovered the lipoxin, resolvin and protectin classes of the eicosanoid family, which serve to actively promote homeostasis and resolution of inflammation (124, 125). For instance, lipoxin A2 has been shown to reinstitute epithelial barrier function in experimental ALI (126) and resolvin D2 improved survival in a model of microbial sepsis induced by caecal ligation and puncture (127). Hence, enhancing the effects of endogenous pro-resolving mediators may prove a better therapeutic option. Interestingly, aspirin influences resolution within hours of the onset of inflammation through the production of lipoxin A4 precursors (128).

In addition to molecular mediators, cellular mediators also direct the path through which inflammation may proceed. This involves a concerted crosstalk between the acute innate and the regulatory adaptive arms of the immune system. Recruitment of exudative macrophages is an important phase, in particular, once these early phase monocyte derived myeloid cells ingest apoptotic cells, the resolution phase is well underway (129, 130). More recently a certain subset of T-cells called regulatory T-cells, which are identified by the cell surface markers CD4, CD25 and the transcription factor FoxP3, have been shown to reduce proinflammatory cytokine production, increase TGFβ levels and increase neutrophil apoptosis in experimental ALI and were found to be present in humans with ARDS (98).

Further insights into the mechanisms through which infiltrating cells die may improve our understanding as to how we may be able to manipulate leukocyte apoptosis to help promote resolution, especially in states of critical illness in which leukocyte apoptosis is delayed. There is potential scope for manipulating neutrophil apoptosis and enhancing their uptake by macrophages, thus promoting pro-resolving reparative macrophage phenotypes. Additionally, the diagnostic evaluation of macrophage phenotype in intensive care may give insights into the immune status of patients allowing the implementation of personalised therapies to promote resolution.

Most excitingly, the future role of cell therapy has been significantly fuelled by the application of mesenchymal stem cells (MSCs) in experimental models of critical illness. The heterogeneous and plastic nature of these cells allowing them to adapt and respond appropriately to various inflammatory milieus in a reparative fashion has shown significant therapeutic potential. MSCs have been shown to improve experimental ALI, bacterial pneumonia, and gram-negative sepsis. Unfortunately, the application of MSCs in critical illness is still relatively devoid of mechanisms. However, there is emerging evidence that these may include paracrine effects such as secretion of growth factors such as KGF and anti-bacterial proteins; and immunomodulatory effects on circulating monocytes, tissue macrophages and T-cells (131).

Aiming for full functional recovery

Mitochondrial abnormalities and dysfunction have now been shown to be integral in the pathogenesis of sepsis and multi-organ failure and can be induced by a variety of soluble mediators including nitric oxide and reactive oxygen species, as well as, through the activation of apoptosis signalling. Mitochondrial biogenesis most likely occurs at a transcriptional level involving nuclear regulators such as PGC-1α (132), which integrates multiple external signals including ROS/RNS. Furthermore, endocrine factors such as thyroid hormones also influence mitochondrial recovery. Hence, strategies aimed at ‘jump starting’ mitochondria are attractive as repair and recovery would undoubtedly require energy (133). Another approach involves

mesenchymal stem cells which have more recently been visually captured to adopt a 'trojan horse' strategy to deliver mitochondria, packaged in microvesicles, to injured alveolar epithelial cells improving tissue bioenergetics and thereby preventing injury and promoting recovery (134).

1.5 Tumour necrosis factor biology

1.5.1 The discovery of TNF

The events that culminated in the discovery of TNF can only be described as a remarkable series of landmark investigations that have changed the face of medicine. In 1888, Bruns described the treatment of sarcoma with the injection of streptococcus erysipelatis leading to regression and cure of tumour in 3 out of 5 patients. In 1891, William B. Coley extended this observation further in 9 more patients to produce Coley's toxin, a mixture of a Streptococcus and Serratia organisms, with the theory that a stimulation of the immune system can cure cancer (135). Shear showed that endotoxin from bacteria was responsible for tumour regression (136) and Algire showed endotoxin induced haemorrhagic necrosis in tumour (137). Finally, TNF was first named in 1975 by Carswell and colleagues as a substance released by macrophages in response to endotoxin leading to the haemorrhagic necrosis of tumours (138). It was subsequently found to have the same molecular structure as cachectin as discovered by Beutler and Cerami in 1985 (139, 140). TNF has mainly been regarded as a pleiotropic cytokine strongly implicated in inflammation, but there still remains considerable controversy as to its precise roles, due to the complex nature of TNF signalling (141). Indeed, an editorial in Nature in 1987, in connection with the publication for the role of TNF in septic shock, stated that the "anti-tumour action, role in inflammation and immunity, and toxicity…" are precisely why TNF has gained so much interest (142).

TNF was found to be a member of a much larger family with homology to other mediators being investigated at the time. For instance, Granger et al discovered lymphotoxin, which was a lymphocyte-derived mediator that caused tumour regression (143). Agarwal and colleagues initially purified lymphotoxin protein and

found a 30% homology in protein sequence between lymphotoxin and TNF. In particular, with the view that they also had common cell surface receptors, TNF and lymphotoxin were subsequently named TNF-α and TNF-β, respectively. This heralded the discovery of multiple ligands and receptors, which are now part of the extended TNF superfamily (141). For consistency, TNF-α will be referred as TNF for the remainder of the thesis.

1.5.2 TNF ligand and its receptors

TNF is the quintessential proinflammatory cytokine and a central proximal controller in the production of proinflammatory consequences. Hence, its role in the pathobiology of many diseases and syndromes has mainly focussed on this inflammatory aspect. Myeloid cells such as monocytes and macrophages secrete TNF in large quantities in response to TLR-4 signalling and NFκB activation, and hence, TNF is highly abundant in inflamed tissue.

TNF is initially formed as a 26 kDa transmembrane protein which is expressed on the cell surface as a stable homotrimer. It is present in two forms – a membrane bound and a soluble form. TNF-alpha converting enzyme (TACE or ADAM17), a metalloproteinase enzyme, cleaves the transmembrane TNF homotrimer thereby releasing a bioactive 51 kDa soluble TNF homotrimer (144). This soluble homotrimer dissociates below the nanomolar range rendering it inactive.

Over the decade following the discovery of TNF ligand, two distinct receptors for TNF were characterised (145, 146), and called TNF receptor 1 (TNFR1, p55, CD120a) and TNF receptor 2 (TNFR2, p75, CD120b). Whilst both receptors are able to bind the membrane bound, as well as, the soluble form of TNF, the p55 TNF receptor was found to have greater affinity for the soluble form and the p75 TNF receptor to the membrane expressed form (147, 148). Furthermore, the complexity of TNF biology increased further by the discovery that TACE could also cleave the cell surface expressed receptors to produce soluble forms (149-151). The shedding of TNF and its receptors has dramatic effects on its biology. Firstly, not only are soluble receptors

unable to mediate intracellular signals (as compared to their non-shed surface expressed counterparts), but secondly, the soluble receptors also bind to free soluble TNF and hence, quench its ability to activate cell surface expressed receptors that have not been shed. This complex dynamic regulation of TNF and its receptors at the cell surface is seldom appreciated.

1.5.3 Molecular mechanisms and functional consequences of TNF receptor signalling

The p55 TNF receptor (TNFR) is constitutively expressed on most cells and tissues. In contrast, the expression of the p75 TNFR is more regulated with high expression found on leukocytes, myocytes, endothelial cells, and human mesenchymal stem cells. Historically, p55 TNFR signalling has been thought to be the predominant pathway through which the cellular effects of TNF occur. In view of the profound cytotoxic effects, the p55 TNFR pathway has been well characterised. The p75 TNFR pathway has been thought to play predominantly modulatory roles of either "ligand passing" (enhancing p55 TNFR signalling) or sequestering excess TNF through its soluble receptor form (152). However, it is now more apparent that both TNF receptors initiate distinct signalling pathways and different cellular responses (153).

p55 TNFR signalling

The ligation of the p55 TNFR leads to two distinct consequences – 1) cell survival through pro-inflammatory gene transcription, and 2) cell death through pro-apoptotic cascades. At the molecular level, the binding of TNF to the p55 TNFR leads to an immediate conformational change in the intracellular component of the receptor allowing the recruitment of TNF receptor associated death domain (TRADD). TRADD acts as a docking protein allowing multiple mediators, including receptor interacting protein kinase-1 (RIP1), TNF receptor associated factor (TRAF-2) and cellular inhibitors of apoptosis protein (cIAP) -1 and -2, to attach to this intracellular TNFR1 signalling complex. The attachment of RIP1 occurs within minutes of p55 TNFR ligation. This undergoes ubiquitination by TRAF2 and cIAP1/2, leading to the formation of polyubiquitin chains that act as a scaffold for the attachment of multiple subunits to the initial p55 TNFR intracellular death domain. For instance, NFκB essential modulator (NEMO) is an adaptor protein that binds to

ubiquitinated RIP1. This mediates the first of two pro-inflammatory signalling cascades, that of classical NFκB activation (through IκB recruitment). The second pro-inflammatory survival signal occurs through the MAPK pathway – leading to p38 MAPK, c-Jun N-terminal kinase (JNK) and activator protein-1 (AP-1) activation. The alternative route of p55 TNFR activation is the recruitment of procaspase-8, instead of NEMO, to RIP1 and its subsequent conversion to caspase-8. This caspase-8 signal leads to the activation of caspase-3, which executes cell death. If this caspase-8 signal is inhibited, a new signalling complex (the necroptosome) is formed, which leads to cell death through a caspase independent pathway called necroptosis.

Interestingly, most cells do not die when treated with TNF and only do so when exposed to protein synthesis inhibitors such as cyclophosphamide suggesting that a) TNF activates the expression of survival genes to block cell death; and b) the proteins required to execute cell death are pre-made and independent of protein synthesis. It is now established that NFκB activation supresses the TNF-induced cell death programme (154-156). The serine proteases comprising the caspase family are pre-made within the cell whereas the anti-apoptotic NFκB pathway requires the synthesis of new proteins suggests cell death to be the default pathway after p55 TNFR ligation. However, given that the time required for gene transcription is likely to be much slower than the time taken for caspase-3 activation and that cells do not die immediately, suggests that a more proximal switch should exist in the decision of whether a cell lives or dies.

In fact, this initial interaction of RIP1 with either NEMO or procaspase-8 appears to be the first of two control points that determine whether a cell survives or dies from p55 TNFR ligation. This switch is determined by the ubiqitination of RIP1, which is essential for the binding of NEMO and the subsequent activation of IκB and NFκB. RIP1 polyubiquitination, forming a linear ubiquitin chain assembly complex (LUBAC) off of RIP1, is performed by TRAF2 in collaboration with ubiquitin conjugating enzyme E2 (also known as UBC13) (157, 158). Non-ubiquitinated RIP1 is a non-essential enhancer of caspase-8 activation. Hence, p55 TNFR activation immediately represents an important rheostat that determines whether a cell is destined to

survive or die (159). This first "live/die" switch is independent of new protein synthesis. If this first switch fails (i.e. the ubiquitination of RIP1, attachment of NEMO and hence inaccessibility of procaspase-8 to RIP1) as a result of degradation of E3 ligases (which are responsible for ubiquitination), then there is a second control point at the level of NFκB transcription. This second controller provides a later, but more protracted cell survival signal, and is dependant on the NFκB mediated transcription of an anti-apoptotic protein called cFLIP. Most importantly, this NFκB transcription can occur through a variety of pathways e.g. p75 TNFR activation.

p75 TNFR signalling

The p75 TNFR, on the other hand, has no death domain and has been shown to have distinctive cell signalling pathways. TNF binding induces the trimerisation of the p75 TNFR leading to the recruitment of TRAF2. The binding of TRAF2 leads to the binding of TRAF3 and cIAP-1 and -2 to the signalling complex. It has been shown that the activation of NF-κB element correlates with TRAF2 protein levels (155, 160). Hence, p75 TNFR signalling can promote cell survival (161) through this NF-κB activation as well as the induction of anti-apoptotic pathways including the Protein kinase B (PkB)/AKT pathways (162). However, in some circumstances certain residues of p75 TNFR can also degrade TRAF2 negatively regulating the NF-κB response. In addition, there is crosstalk between both TNFRs where TRAF2 degradation and lack of NF-κB transcription (by p75 TNFR) augments p55 TNFR induced cytotoxicity (163). There is controversy as to whether the p75 TNFR complex has any intrinsic enzyme activity. The majority of literature suggests it does not but there is some evidence to suggest it can, independent to TRAF2, recruit Etk/Bmx protein kinase pathway (164).

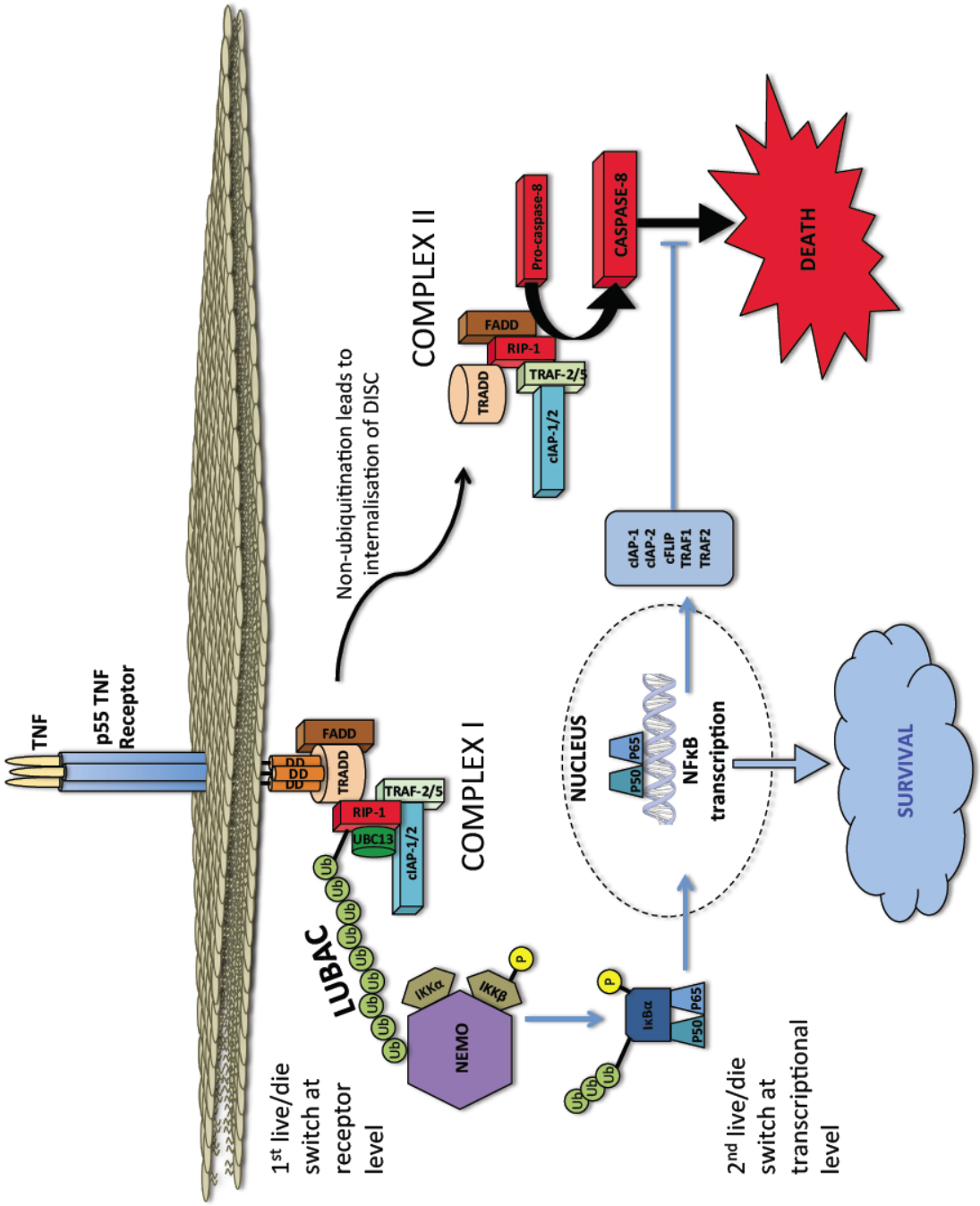
TNF
p55 TNF Receptor
FADD
TRADD
DD
DD
DD
TRAF-2/5
RIP-1
UBC13
cIAP-1/2
Ub
LUBAC
IKKα
IKKβ
P
NEMO
COMPLEX I
1st live/die switch at receptor level
Non-ubiquitination leads to internalisation of DISC
COMPLEX II
FADD
RIP-1
TRAF-2/5
TRADD
cIAP-1/2
Pro-caspase-8
CASPASE-8
DEATH
cIAP-1
cIAP-2
cFLIP
TRAF1
TRAF2
NUCLEUS
P50
P65
NFκB transcription
IκBα
SURVIVAL
2nd live/die switch at transcriptional level

Figure 1.6. Survival versus death signalling through the p55 TNF receptor
Within minutes of ligation of the p55 TNF receptor by TNF there is recruitment of RIP1 to the intracellular receptor complex. If RIP1 is ubiquitinated by TRAF2, cIAP-1/2 in collaboration with UBC13 a linear ubiquitin chain assembly complex is formed allowing proteins such as NEMO to dock to RIP-1 inducing IKK and IκBα assembly and activation of the NFκB transcription factor. If RIP-1 ubiquitination is blocked, for instance through a degradation in the enzymes responsible e.g. UBC13 and E3 ligases, then there is a switch to the formation of a death inducing signalling complex (DISC). Furthermore, RIP-1 is a non-essential enhancer of caspase-8 leading to its activation and subsequent death signalling. This represents the first live/die switch at the receptor level. If this switch is activated there is a back-up switch through NFκB transcription, which leads to the transcription of anti-apoptotic proteins cIAP-1/2, cFLIP and TRAF-1/2. These proteins prevent the activation of effector caspases and the final stages of cell death. Importantly other receptors/signalling pathways that activate NFκB transcription can contribute through this survival pathway.

(cIAP, cellular inhibitor of apoptosis; cFLIP, Cellular FLICE (FADD-like IL-1β-converting enzyme)-inhibitory protein; DD, death domain; DISC, death inducing signalling complex; FADD, Fas associated death domain; IKK, I kappa kinase; LUBAC, linear ubiquitin chain assembly complex; NEMO, NF-κB essential modulator; P, phosphate; RIP, receptor interacting protein kinase; TRADD, TNF receptor associated death domain; TRAF, TNF receptor associated factor; TRAIL, TNF related apoptosis inducing ligand; Ub, ubiquitin; UBC13, ubiquitin-conjugating enzyme-13)

1.6 TNF and critical illness

1.6.1 TNF – elusive in clinical ARDS

Since the discovery that TNF and cachectin were one and the same, the role of TNF in ARDS has been heavily investigated. Millar and colleagues found a significant upregulation in all 5 patients analysed with ARDS compared to non-ARDS control patients (165). Marks and colleagues performed measurements of serial plasma samples for TNF on 86 patients (166). They found that over a third of patients with septic shock showed the presence of TNF in plasma, and that these levels peaked on admission and reduced over the first 12-24 hours thereafter. Patients with septic shock showed increased levels compared to patients in shock from non-septic causes. Importantly, this study found that those patients in septic shock with detectable TNF levels showed a significantly higher propensity to develop ARDS compared to those in septic shock without measureable TNF in their plasma (55% versus 26%, respectively). Furthermore, those with measureable TNF showed a higher parenchymal lung injury score with a doubling in mortality (81% versus 43%). Hyers et al corroborated these results, also showing that septic shock led to significantly higher serum levels of TNF compared to non-septic patients. Importantly, this study analysed the alveolar levels of TNF and found that these were higher in ARDS patients than normal subjects. These levels were highest in the first 24 hours (167). The most common causes of ARDS in this study were sepsis and aspiration of gastric contents. Gastric aspiration led to a significantly higher BAL level of TNF compared to the non-aspirated ARDS group.

Hence, TNF is upregulated early within the first day in the BALF of ARDS patients (167) and sustained release of TNF is not required for lung injury development in sepsis (168). In addition to the acute kinetics of TNF upregulation, the role of TNF has been further confused by the inconsistencies in measurement of TNF which has been shown to be heavily dependant on the experimental assays utilised (169). Furthermore, there is suggestion that TNF may indeed mediate its effects through cell-cell contact mechanisms through the membrane expressed TNF as opposed to

its soluble form (170). In view of all of these factors, it is not surprising that the role of TNF in the pathogenesis of ALI/ARDS has remained elusive and controversial.

1.6.2 TNF in sepsis – 'clinical trials and tribulations…'

In the 80's and 90's, there was considerable evidence from animal and human studies that TNF played a significant role in sepsis and ARDS. However, the mechanisms through which TNF functions, in particular, the receptors through which its actions were mediated had not been investigated and despite the paucity of mechanistic detail, clinical trials applying anti-TNF agents to sepsis were performed. One of the first studies was conducted by Fisher et al and showed that although the anti-TNF monoclonal antibody did not demonstrate a survival benefit in all study patients, those with elevated TNF plasma levels showed improved survival with a higher dose of intravenously administered antibody (86% versus 50%, respectively) (171). All other studies have to date failed to show benefit with global TNF blockade in sepsis (172-174). When we analyse the evidence for ARDS, again, animal studies show significant improvements but there is a lack of clinical data to support TNF blockade in ARDS.

There are multiple reasons for these failures.

1. **Sepsis and ARDS are not diseases but heterogeneous syndromes caused by varying aetiologies.** Many clinical trials group meningococcal and peritoneal sepsis as one entity, or group pulmonary oedema induced by Streptococcal *pneumoniae* with that induced by pancreatitis. This may be very inappropriate given the potentially varying mechanisms of injury. Furthermore, different aetiologies may have a variable dependence on TNF mediated pathways. Hence, it is no surprise that beneficial effects are absent when such patients are grouped together in a clinical trial – regardless of power.

2. **The underlying scientific rationale is flawed.** An example of this is the recently published ACCESS trial investigating the MD2-TLR-4 antagonist Eritoran (175). This double blind, large multicentre study administered this

drug to all septic patients. However, the baseline infectious characteristics of patients recruited within this trial showed that only 32% of patients had confirmed gram-negative septicaemia. Nearly 30% had gram-positive sepsis, 10% had mixed positive and negative sepsis; 23% of unknown sepsis; 3% with fungal sepsis; and 4% showed no evidence of infection at all! Gram-negative infections mediate their effects through TLR-4 (176) whereas gram-positive infections predominantly through TLR-2 pathways (177, 178). Hence, a trial investigating the effect of this drug solely on gram-negative infections would seem scientifically valid whereas the ACCESS study recruitment criteria seemed irrational (179). Furthermore, the multiple positive results in animal studies, which are often conducted with a single insult/model, corroborate this view that more homogenous populations need to be studied. Clinically, for example, patients with higher serum TNF levels seem to benefit from TNF blockade (171). Furthermore, although alveolar TNF levels in human ARDS are greater than in normal controls, it is significantly higher in those with ARDS secondary to gastric aspiration compared to non-aspiration causes of ARDS (167). Hence, recruiting those patients with elevated TNF levels to receive anti-TNF strategies, or those patients with detectable endotoxin to receive a drug such as Eritoran may lead to better trial designs leading to personalised targeted therapies/studies in the intensive care. Hence, biomarker based recruitment to clinical trials may improve translation, as has occurred in other medical specialties such as cardiology e.g. troponin directed therapies. A thorn in the side of TNF based therapy to this is that plasma measurements of TNF do not reflect the amount of bioactive TNF at a tissue level, and hence, more sophisticated strategies may be required to correctly decide who may benefit from TNF blocking strategies.

3. **The timing of administration is often quite variable.** We have already discussed that TNF is upregulated very acutely in response to stimuli such as endotoxin and hence, early drug administration to block TNF is likely to be more beneficial than late. This is exemplified in the study by Abraham et al that used a p55-IgG fusion protein to block TNF mediated effects in sepsis. It

was found that this compound led to better outcomes when administered to those with early severe sepsis as opposed to those established septic shock (173). Total TNF blocking agents varying from mouse/humanised anti-TNF polyclonal/monoclonal antibodies to p55/p75 receptors and fusion proteins have been investigated in clinical trials. None have shown significant benefit and some have shown a worsened survival, in particular, the p75 receptor fusion proteins (174). These have been prematurely applied to clinical studies in the absence of true mechanistic insights as to how TNF functions during the various stages of critical illness. The strategy to produce total blockade of TNF signalling may be very wrong. TNF has a role in normal physiology and also signals through two receptors, which have distinct signalling pathways (153). Furthermore, the shedding of the TNF receptors also impacts upon their ability to signal the effects of TNF ligand. Hence, in view of the complicated biology of TNF ligand and receptors, reducing the downstream effects of TNF ligand may be a rather naïve approach and a targeted strategy of the consequences of specific receptor signalling in specific cell types may be better. Furthermore, research into the precise mechanisms and under which circumstances, TNF and its receptors mediate physiologically relevant deterioration is an absolute necessity.

4. **There is a lack of translational animal models of critical illness that truly mimic the clinical situation.** Recently for sepsis, there has been significant controversy with respect to the extent to which models such as intravenous endotoxin and caecal ligation and puncture mimic the clinical situation (180). This is particularly relevant in view of the failure to see benefit from Xigris, or activated protein C, for the treatment of severe sepsis (181, 182) leading to the subsequent withdrawal of the drug. This fundamental translational gap is also present in ARDS research, but the ARDS research community has published multiple recent reports on how best to model this devastating condition in animals (37, 183-191). One of the most valuable has been a workshop report by the American Thoracic Society and this is summarised later in this chapter (192).

Fundamentally, the application of anti-TNF therapeutics in the absence of clear mechanisms has been premature and detrimental to the translation of biologics in critical illness. This thesis concentrates on the pre-clinical end of the spectrum as defined by the points 3 and 4 above. It aims to identify the roles and mechanisms of each TNF receptor in mediating physiologically and pathologically relevant effects of TNF in experimental ARDS and attempts to address the translational gap that exists between the pre-clinical and clinical elements of ARDS.

1.7 Mechanisms of TNF in ARDS pathobiology

Just as it is easier to reach a destination if you know the route and have a map, mechanistic insights into how TNF may mediate its effects in ARDS will better enable TNF-based therapeutics to be successfully translated and applied at the bedside. This section describes the experimental studies that have so far discovered various roles of TNF in ARDS. Unsurprisingly, TNF has been found to have quite divergent effects on the development of lung injury. It promotes endothelial and epithelial permeability leading to the formation of pulmonary oedema, but in contrast has been found to enhance alveolar fluid clearance mechanisms mediating the resolution of pulmonary oedema (193). Its classical role as a pro-inflammatory cytokine is also well established and these aspects and the experiments that led to their discovery will be explored further within this section.

1.7.1 TNF and acid aspiration

In 1946 Curtis Mendelson first described the aspiration of stomach contents leading to acute pneumonitis in 66 women undergoing obstetric anaesthesia. Within this landmark observation he described the development of two syndromes that resulted from the aspiration of gastric contents. The first syndrome involved complete or partial laryngeal/bronchial obstruction leading to atelectasis and was responsive to bronchial toilet and external stimulation. However, the second syndrome was one akin to ARDS and occurred as a result of the aspiration of liquid material into the distal airspaces. This led to an “asthmatic-like syndrome” which progressed to cyanosis, tachycardia and dyspnoea, and was associated with X-ray

changes consistent with alveolar consolidation, and has been misdiagnosed as bronchopneumonia or primary cardiac failure (despite the "previous normal condition of the heart"). He went onto to perform animal experiments and found that within this condition hydrochloric acid was responsible for this pulmonary congestion, and was similar to chlorine and phosgene induced lung pathology following war gas injury (194). Most interestingly, the description of aspiration pneumonitis by Mendelson preceded Ashbaugh's seminal description of ARDS (16). Ever since, aspiration pneumonitis has become a well-recognised complication resulting from any cause of unconsciousness, for instance, trauma, general anaesthesia, drug overdose etc.… Hence, numerous animal models of acid aspiration have been established to investigate this phenomenon. One of the first rodent models was developed and characterised by Kennedy and colleagues in rats. This found experimental acid aspiration to follow a biphasic pathogenesis showing an acute physicochemical phase (<1 hour) and a second neutrophil mediated phase occurring between 2-4 hours (195).

Of particular importance to the work presented in this thesis, it was found that this experimental acid-induced lung injury seemed to be an excellent translational model to investigate the role of TNF, corroborating clinical studies showing that alveolar TNF is upregulated early in ARDS caused by clinical gastric aspiration (167). Goldman and colleagues were the first to apply TNF antisera intravenously in experimental acid aspiration and showed that local and systemic leukocyte sequestration was mediated through a TNF-induced increase in endothelial cell adhesion molecule expression (196). However, this study also suggested that the early mechanisms (<1 hour) through which TNF mediated barrier dysfunction after acid aspiration was independent of neutrophils, which were recruited at 2-3 hours post-insult. Furthermore, only a modest reduction in leukocyte sequestration (30%) could not account for the significant physiological protection (60% reduction in oedema) seen with TNF-alpha anti-sera. Davidson et al also found that intratracheal anti-TNF-alpha antisera led to significant reductions in lung injury indices (protein permeability and wet/dry weight ratio) as well as neutrophil infiltration. This study also showed that inhibition of intra-alveolar TNF also led to an improved oxygenation (197). Overall,

these data show that TNF is important in acid-induced ALI/ARDS but that total blockade does not completely ameliorate lung injury and that alveolar targeting may be more beneficial in that some relevant physiological protection is accrued.

1.7.2 TNF and alveolar-capillary permeability

TNF promotes neutrophil-endothelial interactions through a variety of mechanisms including complement activation and cell adhesion molecule upregulation in septic shock. As a result of this data from experimental and clinical sepsis, most subsequent research focussed on the impact of circulating TNF on endothelial permeability. Stephens et al performed one of first studies linking TNF to sepsis-induced ARDS in 1988 (198). Within this study, five groups of guinea pigs were studied with the separate groups receiving an inoculum of E. coli, LPS or saline and two further groups receiving a low and high dose of recombinant human TNF. The high dose of TNF led to similar levels of permeablility and oedema as seen in the E. coli group and also led to a worsening arterial oxygenation and alveolar neutrophilia. This provided the first notion that TNF could contribute to alveolar-capillary permeability in ARDS. This was supported by a study by Horvath et al which found intravenous TNF to produce pulmonary endothelial dysfunction and microvascular permeability in sheep made neutropenic through exposure to hydroxyurea, and hence, this effect seemed to be neutrophil independent (199). Goldblum and colleagues also found that the intravenous administration of recombinant human TNF to rabbits increased pulmonary microvascular permeability in vivo with increases in lung wet/dry weight ratios and alveolar protein levels (200). The same study reported an increased albumin transfer in pulmonary artery endothelial cell monolayers suggesting a direct effect of TNF on the endothelium. However, it is uncertain in these studies if this effect of TNF was a result of direct impact on the lung or an indirect one through the induction of circulatory collapse. Work within our group confirmed a direct effect of TNF on the endothelium by showing that the upregulation of cell adhesion molecules on pulmonary endothelial cells is predominantly mediated by the p55 TNF receptor, with p75 mediating a minor role (201). It is now thought that the impact on endothelial permeability by TNF is mediated through changes in microtubule

arrangements within endothelial cells leading to shape changes and loss of tight junction regulation (50).

Whilst the mechanisms of TNF-induced microvascular permeability are well investigated, the effects on alveolar epithelium are less established. The first investigation found TNF to increase epithelial permeability in a model of Corynebacterium *parvum* induced alveolitis (202). This study found epithelial permeability peaking at 8 hours with an associated increase in TNF within the alveolar space. Furthermore, the TNF was produced by macrophages, rather than neutrophils, and an anti-TNF antibody attenuated the epithelial permeability. Hence, the authors concluded that macrophage derived TNF played a major role in the epithelial permeability induced in this model of acute alveolitis.

1.7.3 TNF and alveolar fluid clearance – the ups and downs

TNF has been shown to have quite divergent roles in alveolar fluid clearance. A number of investigators have shown alveolar fluid clearance (AFC) to be increased through TNF-dependent mechanisms. Rezaiguia et al showed in a model of Pseudomonas *aeroginosa* pneumonia that AFC was enhanced through a TNF dependant enhancement of epithelial sodium transport (193). Furthermore, TNF has been shown to enhance AFC in a model of ischaemia-reperfusion injury (203) and chronic bronchial inflammation induced by ovalbumin (204). In addition, endotoxin, a potent stimulator of TNF production, has also been shown to enhance AFC (205).

These experiments showing that TNF could actually reduce alveolar oedema through promoting AFC surprised many and led to an extensive search for mechanisms to explain these observations. A major breakthrough was the discovery of a lectin-like domain on the TNF molecule (206), a site on the molecule not associated with the receptor binding domains, and implicated in the direct trypanocidal activity of TNF through lectin-carbohydrate interactions (207, 208). This effect was independent to the regions that associate with receptor binding (206). Initially it was postulated that this trypanosomal lysing activity of the TNF could be due to an ability of the TNF trimer to penetrate cell membranes in a pH and temperature dependent manner

(208, 209), forming pores potentially allowing itself to act as a sodium channel (210, 211), leading to influx of sodium with subsequent lysis. Later, it was found that TNF through its lectin-like domain promotes membrane conductance activities in endothelia and peritoneal macrophages (212) by interacting with endogenous ion channels (213). Subsequently, Fukuda and colleagues linked this lectin-like domain activation of ion channels to the positive effect of TNF on alveolar fluid clearance (214). This study found that recombinant TNF upregulated AFC independent of beta-agonist mediated effects but dependant on amiloride sensitive sodium currents. A triple TNF mutant (lacking the lectin-domain activity) did not simulate alveolar sodium and fluid transport, as was induced by wild-type TNF. Elia et al found that the instillation of TNF in mice lacking both TNF receptors induced a similar increase in AFC as compared to WT animals, suggesting that TNF receptor-independent effects were predominant in uninjured mouse lungs. Furthermore, the intratracheal instillation of an Ltip peptide (which mimics the activity of the lectin-like domain of TNF and does not activate either TNF receptors) even further enhanced AFC rate (215).

Given that TNF-receptor mediated signalling can enhance oedema formation, Braun et al attempted to dissect the pathways that lead to TNF's opposing role in lung oedema formation and liquid clearance (216). They utilised various pharmacological compounds to differentially inhibit either or both of 1) the lectin-like domain and 2) the receptor binding sites of TNF. Indeed, they found that these two distinct areas of the TNF molecule mediate quite differential actions on the ability of the lungs to clear fluid. Firstly, in their setting, TNF alone was unable to enhance AFC, and only did so when the TNFR1 binding site was blocked using a soluble p55 TNFR construct. They found N,N'-diacetylchitobiose, a carbohydrate epitope which inhibits the lectin-like domain, to subsequently inhibit this increase in AFC. Furthermore, TNF through its p55 TNFR receptor-binding site showed deleterious effects on lung mechanics and inhibition of AFC, suggesting opposing roles for TNF receptor dependant and independent activities on AFC.

To summarise the involvement of TNF in AFC it can be said that TNF promotes receptor independent and dependent effects on alveolar fluid clearance. The mechanisms for the former are mediated through this lectin-like domain of the TNF trimer enhancing sodium and water transport. The Ltip compound (based on the lectin-like domain) is currently undergoing pre-clinical studies to look at the impact of this (217-219). In contrast, the mechanisms for the TNF-receptor dependent effects that lead to a negative impact on alveolar fluid clearance are still unknown. In particular, the roles of the receptor dependant downregulation of AFC in clinically relevant models of lung injury has not been discerned. This requires careful investigation and interpretation given the complex nature of TNF ligand and TNF receptor biology during injury (shedding, internalisation, decoy effects) during tissue injury.

1.7.4 Differential effects of TNF receptors

The functional relevance of the majority of TNF (soluble or membrane) mediated effects is meaningless without an appreciation as to how these are transduced by the receptors. This aspect has been ignored in investigations looking at the role of TNF. As both receptors are also amenable to shedding through TACE, the physiological impacts are often difficult to discern. However, over the past decade, the development of mice deficient in either or both of the TNF receptors has facilitated a more in depth analysis of TNF receptor mediated effects in multiple disease models. Peschon and colleagues developed single and double TNF receptor knockout mice and subjected them to pulmonary and systemic endotoxin administration with variable doses (220). This study found that the systemic administration of endotoxin (in mice sensitised by D-gal) produced 100% lethality in WT strain whereas p55 deficient strain showed no mortality. In contrast when the endotoxin dose was reduced slightly to produce a lower level of mortality in WT animals the p75 deficient animals tended to a slightly elevated mortality. When endotoxin was administered intranasally, the p75 deficient animals showed increased neutrophil influx. Hence, this suggested that endotoxin mediated shock requires p55 and not p75 TNFR signalling, but also that p75 TNFR may confer some protection through reduced inflammation.

Fontaine et al, found that the two TNF receptors showed antagonistic functions in a model of retinal ischaemia. This study showed that neurodegeneration was mediated through the p55 TNFR whereas the p75 TNFR mediated protection and that this protective effect correlated with the activation of the Akt/PKB pathway (162). Ebach et al found that the two receptors showed opposing effects in a model of sepsis induced by caecal ligation and puncture (221). Al-Lamki showed differential regulation and function of the TNF receptors in a murine heart organ culture model (222). They showed that whilst signalling through the p55 TNFR induces apoptosis and mediates cell death; signalling through the p75 TNFR signals cell cycle entry and proliferation and subsequently, activates repair mechanisms. Monden and colleagues examined the roles of TNF receptors in a model of myocardial infarction and found that ventricular dysfunction was mediated through p55 TNFR pathways, whereas, p75 TNFR deletion led to exacerbated injury and inflammation (223). Finally, data from our laboratory examined the roles of these receptors in a model of alveolar oedema formation induced by high stretch mechanical ventilation. This study again found divergent roles for the two receptors, with p55 TNFR mediating injury and the p75 TNFR conferring protection (224).

These set of data examining the roles for these receptors during models of acute inflammation question the original notion of the p75 TNFR simply playing an auxiliary role in TNF signalling through the 'ligand passing' of TNF to its p55 counterpart (152). They suggest that not only is injury mediated specifically through the p55 TNFR but also that the p75 TNFR has distinct signalling pathways that confer protection. Hence, overall these data support the therapeutic paradigm of specific blockade at the p55 TNFR and activation of p75 TNFR signalling, as opposed to global TNF/TNFR blocking strategies.

1.7.5 TNF and the Takata lab

To summarise, studies in the late 1980's and early 1990's by Goldblum (200) and Goldman (196) implicated a role for TNF in the formation of pulmonary oedema. However, since these investigations there have been very few studies that dissected

these roles further. A surge in the investigation of ventilator induced lung injury in the 1990's suggested a role for TNF in this form of lung injury, although studies were performed using conventional ventilation in rabbit models of saline lung lavage. Takata et al found the upregulation of intra-alveolar TNF gene expression in rabbits ventilated with conventional ventilation after surfactant depletion (through saline lavage) (225). Imai et al showed that the intra-tracheal application of an anti-TNF antibody attenuated deteriorations in oxygenation and respiratory mechanics in a similar rabbit model (226). Our group went onto show that TNF was upregulated in the alveolar space in a mouse model of stretch induced lung injury (227, 228) and, as discussed, induced this oedema formation in this model specifically through its p55 TNFR (224). This brings us to the current state of play within our group.

The aim of this thesis was to ascertain if this differential receptor signalling was also true in other models of ARDS, and determine the exact mechanisms though which TNF influenced oedema. Given the large translational gap that exists between pre-clinical and clinical studies in ARDS it was important to replicate such a phenomenon in a more clinically relevant model of ARDS. This brings us onto the next section of ARDS and how to develop a truly translational model with clinically relevant end-points.

1.8 Pre-clinical modelling of ARDS: Mice treatments work; human treatments fail… 50 years of frustration.

The manifestations of ARDS have been well characterised in humans - an acute onset of refractory hypoxaemia secondary to increased permeability pulmonary oedema. This often necessitates mechanical ventilation and organ support. Currently, there is no pharmacological therapy for ARDS despite multiple studies showcasing positive therapeutic effects in animals. This deficit in bench to bedside translation can only be addressed through the examination of the translational pathway. Is the answer as simple as 'humans are more complex then animals'? This may be the major dilemma that is currently limiting bench to bedside translation of therapeutics within critical care. As a clinician performing basic science research, certain questions have to be

addressed to sensibly set out a bench to bedside strategy in critical care. Are the complexities of ARDS not very well reproduced in pre-clinical models? Is this leading to a lack of understanding in the pathophysiology of ARDS deterring research in non-meaningful directions? Are we targeting the wrong molecules? Are potential therapeutics applied to clinical studies prematurely without an understanding of the mechanism through which they may benefit patients? Is the patient population in critical care too heterogeneous such that a single therapeutic intervention would not lead to a clinically relevant benefit?

In order to improve our understanding into the circumstances in which a drug would be expected to work (or more importantly, not work), compounds need to be tested in more than one pre-clinical model and one, which ideally recapitulates all of the relevant features of clinical ARDS. The investigation of TNF mediated oedema formation in a pre-clinical model of ARDS that shows all the characteristics of the human condition is crucial to determine which patients may benefit from manipulation of a specific aspect of a pathway. The determination of a cell specific mechanism would also allow application to a more homogenous patient population. However, this requires the development of robust pre-clinical models to deliver reliable and reproducible data.

It is important to appreciate that animal models can and will never reproduce the complexities of the human condition. Examples of such complexities include the heterogeneous causality of ARDS; the host susceptibilities and co-morbidities (e.g. age and chronic illness); the kinetics of human ARDS; and the iatrogenic influences of critical care (e.g. general anaesthesia, mechanical ventilation, and nosocomial infections). Animal experiments often mainly investigate only specific aspects and targets of ARDS pathogenesis (e.g. endotoxin and leukocyte mediated mechanisms; bleomycin and mechanisms leading to fibrosis). Furthermore, only certain end-points are measured (e.g. neutrophil sequestration and permeability) and these often have very little direct relevance to the human condition given that patients are intubated and admitted to ICU on merit of their clinical deterioration (mainly based on the extent to which gas exchange and circulation is compromised). Hence for ARDS,

more emphasis on respiratory physiological parameters such as gas exchange would certainly be more clinically applicable and may improve experimental relevance. Reiss et al have recently published an excellent review supporting the inclusion of gas exchange measurements in experimental studies of ARDS (188). Hence, many targets have been shown to ameliorate indices of ALI in animals that are often irrelevant to the human setting. The reproducibility of mechanisms in multiple animal models, at various stages (early and late; injury and resolution), focussed on clinically relevant end-points of ARDS would surely improve the robustness for any scientific translation to the human condition.

Nevertheless, animal models provide an important intermediary step in the translational pathway to understand the pathobiology of ALI, discover novel targets, investigate the mechanisms of action, and test novel therapeutic compounds prior to their application in humans. One major hurdle is that most preclinical models do not reproduce the severity and temporal profile of the human ARDS. For instance, most models only enable investigation into the acute phase of ARDS (within 48 hours) but not into the later phases, arguably the phase in which most patients present to (and die in) the ICU. Investigation of early phases will help deliver prophylactic/preventative therapies in patients with a high likelihood in developing ARDS e.g. post one-lung ventilation; witnessed aspiration etc…. However, much more investment is required to investigate mechanisms and drug effects in established ARDS, in particular, its resolution/repair; and this may allow more therapeutic windows to be available during these complex later phases of the syndrome.

Currently, the only models that enable investigation into such later time-points are the inhaled/intratracheal endotoxin, pneumonia, and inhaled bleomycin model. The endotoxin model utilises single receptor over-activation, that of TLR-4, and hence may bias many conclusions. Indeed, TLR-4 ligation within this model leads to significant neutrophilic infiltration with minimal increases in lung water content and unsatisfactory deteriorations in respiratory mechanics or arterial oxygenation. In our hands, high dose intratracheal LPS (20μg) led to minimal changes in peak inspiratory

pressure and arterial oxygenation over 3 hours, but induced significant neutrophil infiltration (229). Most pneumonia models also lead to a similar pattern of injury but have an added complication in that bacterial susceptibilities differ significantly between man and mouse (230, 231). With this in mind, these first two models of injury, albeit having high aetiological relevance, have questionable physiological translation to ARDS given that alveolar oedema and arterial hypoxaemia is mild. They may be more appropriate models for the investigation of lung infections that do not progress to ARDS. In contrast, the bleomycin model develops significant hypoxaemia but its translatability is hindered by the severe fibrotic reaction and the significant variability within the model (232). Additionally, the bleomycin model does not induce injury if the preparation is above a pH of 5.0 (personal correspondence with Professor Rachel Chambers, Rayne Institute, University College London).

1.8.1 The ideal model of ARDS – the experts' opinion

Observational clinical studies allow the development of paradigms and hypotheses with regards to the pathogenesis of ARDS. However, since the first description of ARDS by Ashbaugh in 1967 (16), in which the majority of the observations still remain valid and are used to some degree in the most recent Berlin definition, there has been relatively little advance in therapy. Animal models allow a bridge between the bedside and the bench, in particular, as sampling (such as lung biopsy) is fraught with difficulty in patients already at the extremes of respiratory physiology. Recent developments using ex vivo and in vivo human models will strengthen this divide (74, 187). Ex vivo models utilising rejected transplant lungs to perform ex vivo lung perfusion are facilitating the step from animal to human experimentation. However, given these organs have already been rejected for transplantation there is significant uncertainty as to the heterogenous nature of injury and care of organs prior to experimentation. Furthermore, limited procurement may reduce the extent to which experiments can be performed. Although they also prove very expensive, these models have a definite role in the translational pathway between mouse and man. In vivo human models of lung injury (such as inhaled endotoxin and one lung ventilation) may also provide a step between phase 1 studies in normal volunteers to phase 2 studies in patients. These in vivo models are conceptual models that may

allow investigation of distinct pathways in a homogenous population with minor injury (as in the case of inhaled endotoxin) or subclinical injury (given that the incidence of ARDS is only 2-4% and 8% in patients undergoing one-lung ventilation for lobectomy and pneumonectomy, respectively) (187).

Regardless, correctly performed experimentation in robust animal models continue to provide the cleanest experimental set-ups to investigate mechanisms of disease. Hence, given the expense of human in vivo and ex vivo models, experiments performed in animal models should be used to deliver more mechanistic insights into the pathobiology and mechanisms of action of novel compounds prior to human application (ex vivo, in vivo, or patient-based studies). Importantly, the expanding potential for the development of novel genetic backgrounds in mice to elucidate important mechanisms in disease pathogenesis, makes the development of an optimal mouse ARDS model even more valuable. Unfortunately, there is no single mouse model that recapitulates all of the features of clinical ARDS with many only allowing focussed research on particular aspects e.g. endotoxin and neutrophil mediated mechanisms or TLR-4 mediated inflammation; bleomycin and fibrosis. An overview of every model of ARDS is beyond the scope of this thesis but please refer to an excellent and thorough review article by Matute-Bello et al, which provides an excellent update of animal models in ARDS (37).

A major step to inform the research community as to what constitutes ARDS in an experimental setting was the production of guidelines by an ATS workshop (192). This workshop report sent questionnaires to 22 international experts to establish opinions on:

1. Which features constitute ARDS in animal models?
2. Which measurements should be used to define these features?

They suggested that the main features required of an animal model should be a rapid onset within 24 hours of:

1. Histological tissue injury
2. Altered alveolar capillary barrier function

3. Inflammatory response
4. Physiological derangement

1.8.2 Histological evidence of injury

Experimental models often show a patchy distribution of lung damage as compared to the classic DAD found in human ARDS, as discussed previously. However, it can be said that ARDS in humans often results from unilateral consolidation with increased extravascular lung water in one lung that spreads to the other. No animal model reproduces the features and kinetics of DAD. However, it is also well known that histological scoring systems vary considerably and hence, the requirement of standardised blinded scoring enabling comparisons of injury between experiments, as well as, between groups of investigators. The histological features depend very much on the model being utilised, as a model producing only neutrophil infiltration with no oedema formation or hypoxaemia should preclude it from representing a model of ARDS (188). The report suggested a strict morphometric scoring system shown in table 1.4. The exact details of the score are described in the methods section. It is import to appreciate the propensity for this scoring system to over evaluate the lung injury scoring in models that induce a high level of neutrophil recruitment. However, the use of a consistent scoring system may enable valid inter-experimental and inter-laboratory comparisons to be made.

Parameter	Score per field		
	0	**1**	**2**
i. Neutrophils in the alveolar space	None	1-5	>5
ii. Neutrophils in the interstitial space	None	1-5	>5
iii. Hyaline membranes	None	1	>1
iv. Proteinaceous debris filling the airspaces	None	1	>1
v. Alveolar septal thickening	None	2x-4x	>4x
Score = [20*(i) + 14*(ii) + 7*(iii) + 7*(iv) + 2*(v)] / (number of fields * 100)			

Table 1.4. Lung injury scoring system
(adapted from Matute-bello et al (192))

1.8.3 Altered alveolar capillary barrier function

Hypoxaemia is always present in ARDS (by definition) and is mediated by 1) an increased permeability pulmonary oedema (as opposed to increased pulmonary capillary pressure seen in cardiogenic causes) and 2) ventilation/perfusion mismatch leading to increased intrapulmonary shunt. Dysfunction of the alveolar capillary barrier occurs early in its pathogenesis and leads to leakage of plasma proteins into the alveolar space. There are a variety of methodologies used to measure alveolar capillary barrier dysfunction. The most common is the measurement of alveolar protein content or other high molecular weight proteins such as IgM. This measurement is suitable for early measurements as later measurements may be influenced by alveolar fluid clearance and or protein clearance leading to erroneous readings. An alternative method is the use of a labelled protein injected intravenously and its measurement in the alveolar space after a defined period of time. The ratio of alveolar to plasma label allows a calculation of a permeability index. Another approach is the measurement of increased lung water content through wet:dry weight ratio.

1.8.4 Inflammatory responses

Inflammation is also a key feature of ARDS, although whether an inflammatory response is responsible for, or a response to, an ARDS insult remains unknown. A neutrophil response is found in most patients with ARDS and there are increased concentrations of pro-inflammatory mediators during the injurious phase of ARDS. Hence, BAL counts through differential cytology is the easiest route for quantification of inflammatory cell numbers. Additionally, through a morphological analysis most cell types can be generally distinguished. Another method of measuring cellular inflammatory activity is an assessment of myeloperoxidase (MPO) activity. MPO is a glycoprotein expressed in myeloid cells and most abundantly in the azurophilic granules of activated neutrophils. Hence, the measurement can give a surrogate marker for neutrophilic inflammation. Finally, the analysis of BAL for soluble mediators using ELISA also allows a quantitation of the pro-inflammatory versus anti-inflammatory milieu of the alveolar space.

These are very basic methodologies that should form the minimum of any inflammatory assessment. However, although BAL provides alveolar localisation, activated leukocytes are often more adherent and hence may not be recoverable through any lavage procedure. This so-called 'disappearance reaction' may mislead the interpretation of many inflammatory measurements. Furthermore, the cellular source of many molecular mediators cannot be completely apparent. Finally, the role of cells not within the alveolar compartment (i.e. within the interstitium and vascular space) cannot be measured using the lavage technique and more sophisticated techniques, such as isolated perfused apparatus (217, 233-237) and intravital microscopy (238), are now revolutionising inflammation research. The combination with immunohistochemical or flow cytometric techniques further enables the phenotypic characterisation of various cell types but also the cellular expression (whole cell and cell surface) of a variety of chemical and molecular mediators e.g. cell adhesion molecules, cytokines, reactive oxygen species etc.….

1.8.5 Physiological derangement

The primary derangement seen in clinical ARDS is a life threatening deterioration in gaseous exchange. Hence, the measurement of an increased alveolar-arterial oxygen difference is extremely relevant. However, the measurement of oxygenation can be inconsistent, particularly in rodent lungs because of their propensity to collapse. Hence, rigorous standardisation is crucial and should include standardised lung volume history (i.e. recruitment), PEEP, FiO_2, and anaesthesia/surgical preparation. The measurement of respiratory mechanics also requires significant standardisation to robustly produce consistency between experiments, models, and time-points. Once achieved, however, these can provide very relevant indicators of oedema development and/or resolution. The translation of physiological measurements needs to appreciate differences between mouse and human lung physiology. In particular, differences in lung and chest wall compliance between humans and mice have major impacts upon the development of lung injury. This was apparent in a recent publication from our group by Wilson et al, which showed that tidal volumes shown to be injurious in human ARDS do not necessarily induce injury in mice (239). Furthermore, the effects of mechanical ventilation of mice at different tidal volumes

with different recruitment strategies induces different types of injury i.e. ventilator-induced versus atelectasis-induced lung injury. Furthermore, a recent study from our laboratory examined differences in injury between mice exposed to high tidal volume ventilation (30mls/kg) with PEEP (3cmH_2O) and regular recruitment (volutrauma) with mice receiving low tidal volume (7mls/kg) without PEEP and regular recruitment (atelectrauma). Interestingly, these two groups show similar degrees of pulmonary oedema as measured by BALF protein, but show significantly different measurements of respiratory system elastance (237). Hence, the standardisation of mechanical ventilation and volume history before basing interpretations on respiratory mechanics data is crucial and often under appreciated.

This workshop report provided a base for the development of a mouse model of ARDS (as shown in chapters 6 and 7) that incorporated all of these measurements and one that should provide a translational platform for the investigation of various components of injury, inflammation, resolution, and repair. In particular, linking these components to clinically relevant physiological indices seen in patients suffering from this devastating disorder.

1.9 Hypotheses and Aims

The principal aims of this work were two-fold:

1. Determine the mechanism by which TNF and its receptors induce pulmonary oedema during the acute phase of a more clinically relevant experimental model of ARDS.
2. Develop translational mouse models of ARDS that reproduce all of the features of the clinical condition but importantly allowing investigation of TNF receptor based therapeutics in the later phases of ARDS, in particular resolution and recovery.

1.10 Overview of thesis

The data presented in this thesis is a continuation of on going work within the laboratory to elucidate the roles of TNF and its receptors in lung injury. I hope this introductory chapter has delivered a rationale as to how we got to where we currently are in ARDS research, in particular, with respect to TNF, and the many mistakes and breakthroughs that have been made to unravel this devastating condition. The five main aspects covered in the introduction (the lung in normal physiology; the acute respiratory distress syndrome; TNF biology; TNF and critical illness; and pre-clinical modelling of ARDS) sets the scene for the aims and experiments presented in the following chapters.

Chapter 2 describes the methods and materials utilised to explore these roles. Methodological enhancements included the in vivo models of acid-induced lung injury, the development of a protocol to measure alveolar fluid clearance, and novel flow cytometric protocols to measure the activity of cellular death signalling and compartmental localisation of leukocytes.

The investigation of aim 1 is described in Chapters 3, 4, and 5. Chapter 3 describes the development of an acid aspiration model to facilitate the investigation for the roles of TNF and its receptors during the acute phase of oedema formation (0-3 hours). This chapter confirms that differential TNF receptor signalling also occurs in

acid-induced lung injury with the p55 TNFR playing an injurious role and the p75 TNFR potentially attenuating injury and inflammation.

Chapter 4 discusses the novel finding that p55 TNFR activation promotes oedema formation through the activation of death signalling, as opposed to the well-investigated classic pro-inflammatory pathways. The activity of caspase-8 in whole lung homogenates increases dramatically within 90 minutes of acid aspiration in WT animals but is attenuated in p55 TNFR deficient animals. Furthermore, using a novel flow cytometric protocol utilising a fluorescent caspase-8 probe, this chapter shows that this early caspase-8 activity is confined to the type 1 alveolar epithelium.

Chapter 5 links the TNF/p55-TNFR/caspase-8 axis to alveolar epithelial function through the measurement of alveolar fluid clearance (AFC). This chapter, for the first time, describes how activation of death signalling per se influences AFC. Furthermore, using a pharmacological approach to inhibit caspase-8 activation we show that the degree to which caspase-8 is activated determines the level of deterioration in AFC. Finally, to confirm alveolar macrophages as the source of TNF, we depleted macrophages using intra-tracheal clodronate liposome instillation and found a protective effect through a reduced upregulation of alveolar TNF, reduced caspase-8 activation, and improved AFC and arterial oxygenation. The early time-points and lack of significant apoptosis display a novel paradigm that caspase-8 signalling may itself determine epithelial dysfunction in ARDS, as opposed to completed cell death per se.

The investigation of aim 2 is described in chapters 6 and 7. Chapter 6 describes the development of a model of acid-induced lung injury allowing the investigation of not only the injurious/inflammatory phases but also the resolving/reparative phases of ARDS. Given our initial findings involved a very early time point (90 minutes) which, was prior to significant neutrophil infiltration into the lungs, it was important to facilitate the investigation into more later phases of ARDS, arguably, more clinically relevant phases. Furthermore, it was important to investigate the role of inflammation during later phases in determining epithelial death signalling, in

particular, given that many patients present after 2-3 days as opposed to 90 minutes. This model provides an excellent translational platform to base such mechanistic studies and evaluate the effects of potential TNF based pharmacological strategies in the pre-clinical arena. Given the importance of resolution and repair within lung injury, chapter 7 describes a through cellular characterisation of this model so as to determine the leukocytes present within the lung. Excitingly, this chapter describes a novel flow cytometry protocol to evaluate the presence of leukocytes in all three compartments of the lung – alveolar, interstitial, and vascular. I hope this model will be of substantial value for many investigators in this field given that it encompasses virtually all of the recommended measurements described in the ATS workshop discussed earlier.

As a clinician in the intensive care I feel it is crucial to investigate clinically relevant indices within animal models and hence, the breadth of the work presented within this thesis. Although, experiments defining the role of TNF are still on going by others within the laboratory and not presented herein, I hope this is the beginning of my journey within basic translational research in ARDS. Hence, I include Chapter 8 to develop a final overarching discussion of the thesis, speculating on potential paradigms, and elaborating on the future experimental and translation approaches that may be pursued as a result of this thesis, in particular, the prospects of pharmacological blockade of the p55 TNFR in clinical ARDS.

2 Materials, Methods and Protocols

2.1 Materials

The following tables describe the materials (reagents and equipment) utilised within this thesis, as well as their application and from where they were obtained.

2.1.1 Reagents

Table 2.1. In vivo reagents

Reagent	Constituents	Application	Source
Ketamine	-	In vivo	Imperial CBS
Xylazine	-	In vivo	Imperial CBS
Oxygen gas (cylinder)	-	In vivo	BOC
Air (piped)	-	In vivo	BOC
Normal Saline	-	In vivo	NHS supplies
Sterile water	-	In vivo	NHS supplies
Heparin	-	In vivo	Imperial CBS
Hydrochloric acid 1M	-	In vivo	VWR International
Bovine serum albumin (BSA) – Low endotoxin	-	Alveolar fluid clearance	Sigma Aldrich
AlexaFluor 594-conjugated BSA	-	Alveolar fluid clearance	Invitrogen
AlexaFluor 488-conjugated BSA	-	Alveolar fluid clearance validation	Invitrogen

Table 2.2. Enzyme-linked immunosorbant assay (ELISA) reagents

Reagent	Constituents	Application	Source
ELISA assay buffer	1 x PBS 0.5 % BSA (w/v) 0.05 % Tween-20 (v/v)	ELISA	Gibco Sigma Aldrich Invitrogen
ELISA substrate reagent	3,3’,5,5’-Tetramethylbenzidine	ELISA	Invitrogen
ELISA stop reagent	Sulphuric acid	ELISA	Gibco

Table 2.3. Flow Cytometry reagents

Reagent	Constituents	Application	Source
Cell fixative	Intracellular (IC) fixative	Leukocyte counting	eBioscience
Flow cytometry buffer	PBS with 2% FCS 0.1% sodium azide 5 mM EDTA	All flow cytometry (except during caspase-8 localisation)	Invitrogen Invitrogen Invitrogen
Dispase enzyme	-	Caspase-8 localisation	Invitrogen
DMEM/F12	-	Caspase-8 localisation	Invitrogen
HEPES	-	Caspase-8 localisation	Invitrogen
DNAse I	-	Caspase-8 localisation	Roche Diagnostics
AccuCheck counting beads	-	Leukocyte quantification	Invitrogen

Table 2.4. Cytology/histology reagents

Reagent	Constituents	Application	Source
Turk's nuclear stain	Gentian violet 6% acetic acid	Cytology	Fisher Scientific
4% paraformaldehyde	-	Fixative	VWR International
Ethanol	-	Re-/De-hydrant	VWR International
Xylene	-	Re-/De-hydrant	VWR International
Nuclease free water	-	TUNEL assay	Invitrogen
Hydrogen peroxide	-	TUNEL assay	Invitrogen
Permount	-	Mounting medium	Fisher Scientific

2.1.2 Commercial detection assays

Table 2.5. Commercial detection and quantification kits

Kit	Constituents	Source
TNF Duoset	Capture Antibody Conjugated Detection Antibody Calibrated Immunoassay Standard Streptavidin-HRP	R&D systems
IL-6 Duoset		
MIP-2 Duoset		
KC Duoset		
MCP-1 Duoset		
RAGE Duoset		
Endocam Duoset		
Fas Ligand Duoset		
Bradford protein assay	450 ml dye reagent (Coomassie Brilliant Blue G-250) BSA standard	Bio-Rad
DiffQuik	Diff-Quik Stain I: Eosin Y Diff-Quik Stain II: Thiazine Dye Diff-Quik Fix: Fast Green	Medion Diagnostics AG
TACS.XL diaminobenzidine (DAB) in situ apoptosis detection set	Proteinase K Solution Terminal deoxynucleotidyl transferase enzyme (TdT) Labeling Buffer TdT Stop Buffer B-dNTP reaction Mix TdT Enzyme Strep-HRP DAB Solution DAB Enhancer Anti-BrdU antibody Strep-Diluent TACS-Nuclease TACS-Nuclease Buffer Methyl Green Counterstain	Trevigen
Haemoatoxylin & Eosin	Mayer's haematoxylin Eosin A Y solution	Sigma Aldrich
Masson's Trichrome	Biebrich Scarlet-Acid Fuchsin Solution Phosphomolybdic Acid Solution Phosphotungstic Acid Solution Aniline Blue Solution Weigert's haematoxylin	Sigma Aldrich
Caspase-8/ -9 Fluorometric Assay Kit	Cell Lysis Buffer 2X Reaction Buffer IETD-AFC (caspase-8) LEHD-AFC (caspase-9) Dithithreitol (DTT)	Biovision

2.1.3 Pharmacological agents

Table 2.6. Agonists, antagonists, inhibitors and depletion agents

Reagent	Application	Source
Heparin	In vivo	Imperial CBS
Amiloride	Alveolar fluid clearance	Sigma Aldrich
Isoproterenol	Alveolar fluid clearance	Sigma Aldrich
FAM-IETD-FMK caspase-8 reagent	Flow cytometry	Immunochemistry
Z-VAD-IETD	Caspase-8 inhibition	BD Biosciences
Clodronate/PBS liposomes	Macrophage depletion	Encapsula NanoSciences

2.1.4 Instruments, equipment, and software

Table 2.7. In vivo protocols

Equipment	Application	Source
Ventilator-pulmonary function testing system	In vivo ventilation	Harvard Apparatus GmbH
Infusion pump	In vivo fluid administration	Harvard Apparatus
PowerLab data acquisition system	Physiology data	AD Instruments
Chart software	Physiology data	AD Instruments
RapidLab 248 blood gas machine	In vivo blood gas analyser	Siemens healthcare

Table 2.8. Enzyme-linked immunosorbant assay (ELISA) protocols

Enzyme-linked immunosorbant assay (ELISA) protocols		
Equipment	**Application**	**Source**
ELISA washer	Plate washer	Dynex Technologies
MRX II absorbance reader	ELISA colorimetric plate reader	Dynex Technologies

Table 2.9. Flow cytometry protocols

Flow cytometry protocols		
Equipment	**Application**	**Source**
GentleMACS tissue dissociator	Tissue homogenisation	Miltenyi Biotec Ltd
Cell strainer	Single cell suspension	BD Biosciences
Centrifuge	-	Kendro Lab Products
CyAn ADP analyser	Flow cytometer	Beckman Coulter

Table 2.10. Miscellaneous equipment

Equipment	Application	Source
Cytospin	Differential cytology	Shandon
FLx800 fluorescence microplate reader	Fluorescence plate readings	BioTek
BX-60 light microscope and a digital AxioCam camera	Light microscopy	Zeiss Olympus

Table 2.11. Software packages

Software	Application	Source
SPSS	Statistical analysis	IBM
Prism v6	Statistical analysis	GraphPad
KS300 v3.0 software	Histology	Zeiss
FlowJo v9.6.6	Flow cytometry	Tree Star Inc

2.1.5 Flow cytometry antibodies

Table 2.12. Flow cytometry antibodies

Epitope	Fluorophore	Clone	Final concentration	Source
CD45	PE	30-F11	1/400	BioLegend
	PerCP	30-F11	1/400	BioLegend
	PE-Cy7	30-F11	1/400	BioLegend
CD11b	PE	M1/70	1/400	BioLegend
	PE-CF594	M1/70	1/400	BD Biosciences
	PerCP	M1/70	1/400	BioLegend
	Alexafluor 647	M1/70	1/800	BioLegend
	APC-eFluor 780	M1/70	1/800	eBioscience
CD11c	PE-Cy7	N418	1/400	eBioscience
	Alexa Fluor 647	N418	1/800	BioLegend
	APC-eFluor 780	N418	1/800	eBioscience
F4/80	Alexa Fluor 488	CI:A3-1	1/400	BioLegend
NK1.1	PE-Cy7	PK136	1/400	BioLegend
Ly-6C	FITC	AL-21	1/400	BD Biosciences
Gr-1 (Ly-6G/Ly6C)	PerCP	RB6-8C5	1/400	BioLegend
CD103	Alexa Fluor 647	2E7	1/400	BioLegend
I-A/I-E (MHC II)	PerCP	M5/114.15.2	1/400	BioLegend
CD4	Alexa Fluor 488	L3T4	1/400	BioLegend
CD8a	PerCP	53-6.7	1/400	BioLegend
CD25	APC-eFluor 780	PC61.5	1/400	eBioscience
TNFR1	APC	55R-286	1/25	AbD Serotec
TNFR2	APC	TR75- 89	1/25	AbD Serotec
CD176 (Fas Ligand)	APC	MFL3	1/25	eBioscience
TNFR1/2/Fas	APC	Armenian	1/25	eBioscience

ligand Isotype		hamster IgG		
CD31 (PECAM)	Alexa Fluor 647	MEC 13.3	1/1000	BioLegend
EpCAM	PE	G8.8	1/400	eBioscience
T1-alpha	PE-Cy7	8.1.1	1/1000	eBioscience

2.2 Animals

All protocols were approved by the Ethical Review Board of Imperial College London and the United Kingdom Home Office in accordance with the Animals (Scientific Procedures) Act 1986, United Kingdom. The project utilizes C57BL6 wild type (WT, Charles River, Margate, UK), p55 TNF receptor knockout (p55KO, Jackson Laboratories, USA), p75 TNF receptor knockout (p75KO, Jackson Laboratories, USA), or TNF receptor double knockout (DKO, Jackson Laboratories, USA) mice (220). All mice were bred in house to between 8 and 18 weeks old and weighed between 20-30g. Animals had free access to food and water. Genetically deficient animals underwent genotyping at the start of the work. Given that surface expression of TNF receptors were easily detectable using flow cytometry, animals also underwent more frequent phenotyping (6-monthly) to measure cell surface TNFR expression/non-expression.

2.3 In vivo models of acid-induced lung injury

Two models of acid aspiration-induced lung injury were developed for this project. The first involved acid aspiration followed by mechanical ventilation and was primarily to investigate the acute phase of the injury (0-3 hours). The second model was designed to allow investigation into later phases (0-10 days) after acid aspiration. Both models involved mechanical ventilation to varying degrees for measurement of respiratory mechanics.

2.3.1 In vivo mechanical ventilation

Surgical preparation

Mice were anaesthetised using intraperitoneal ketamine (80mg/kg) and xylazine (8mg/kg). Mice underwent tracheostomy and were ventilated with non-injurious 8ml/kg tidal volume (VT), 2.5-3.0 cmH_2O positive end-expiratory pressure (PEEP), and respiratory rate (RR) of 120 breaths/minute using a custom-made mouse ventilator-pulmonary function testing system with FiO_2 of 1.0. In some experiments the left carotid artery was cannulated for monitoring arterial blood pressure (BP) and blood gases (ABG), and for saline infusion (0.4ml/hr).

Ventilator system

A flow-controlled, time-cycled jet ventilation system (photo 2.1) was used to give a predefined VT. In this custom-made system, flow is generated from a high-pressure gas cylinder through the high resistance flow regulator. Thus, contact flow is delivered when the inspiratory valve opens, regardless to the stiffness of the lung connected to the ventilator. The inspiratory flow is measured by a pneumotache (placed just before the tracheal tube), and adjusted by the flow regulator. A time-cycling ventilator controls inspiratory and expiratory solenoid valves and provides an inspiratory:expiratory ratio of 1:2. An end-inspiratory occlusion technique is used to measure respiratory mechanics (see section 2.5.1).

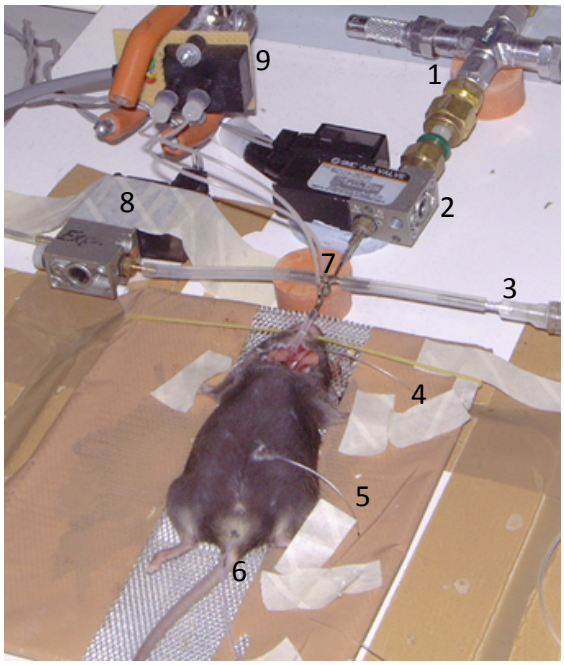

1. Flow regulator
2. Inspiratory solenoid
3. Airway pressure transducer
4. Carotid arterial line
5. Intraperitoneal line
6. Temperature probe
7. Pneumotach
8. Expiratory solenoid
9. Flow transducer

Figure 2.1. Set up for mouse cardiorespiratory monitoring and mechanical ventilation

2.3.2 Acute acid aspiration: 0-3 hours (relevance to chapters 3/4/5)

After surgical preparation mice were ventilated as described above. Once instrumentation was complete, baseline blood gases, peak inspiratory pressure (PIP) and respiratory mechanics were recorded. Subsequently, 50µl of 0.15M HCl (pH<1.5) or 0.9% NaCl was instilled via the endotracheal tube using an intra-tracheal catheter. This was immediately followed by 5 sustained inflations of 30cmH_2O to ensure distal pulmonary distribution of the acid. Subsequently ventilation was continued until the specified time-point for the experiment (no more than 3 hours). The volume and molarity of the acid was initially determined by dose titration experiments (see figure 3.1) to attain a 100% increase in respiratory elastance. Airway pressure, gas flow, and mean BP were continuously monitored throughout the experimental protocol, while respiratory mechanics and ABGs were assessed at pre-determined intervals. Sustained inflation of 30cmH_2O for 5 seconds was performed every 30 minutes to maintain alveolar recruitment.

2.3.3 Resolution phase acid aspiration: 0-10 days (relevance to chapters 6/7)

WT male C57BL6 mice aged 10–12 weeks were anaesthetised by intraperitoneal injection of xylazine (6mg/kg) and ketamine (60mg/kg). At this point, a 20µl/g intraperitoneal fluid bolus of normal saline was administered.

Injury Induction

Anaesthetised mice were then vertically suspended on a custom made mount from their incisors using a 2/0 suture (photo 2.2). A non-thermal light source was used to transilluminate the trachea. Careful retraction of the tongue and laryngoscopy using blunt curved forceps allowed a grade 1-2 view of the vocal cords (photo 2.2). A fine catheter was subsequently guided 1cm below the vocal cords and 75µl of an isoosmolar (to mouse plasma - 322mosmol/L) 0.1M hydrochloric acid (pH 1.0) solution was instilled. Animals were left suspended for one minute and placed in a custom-made murine high dependency recovery area (photo 2.3). During this recovery period they were actively warmed and given humidified gases with reducing FiO_2 from 1.0 to 0.21 over 4 hours. To ensure even distribution of the instillate mice were rotated every 5 minutes until spontaneously moving. After this recovery period they were placed in isolated ventilated cages with air and free access to food and water. After predefined time-points (days after acid instillation) some animals underwent anaesthesia and instrumentation (as described) to measure respiratory mechanics and arterial oxygenation. In animals where no respiratory physiology measurements were performed then animals were sacrificed under terminal anaesthesia.

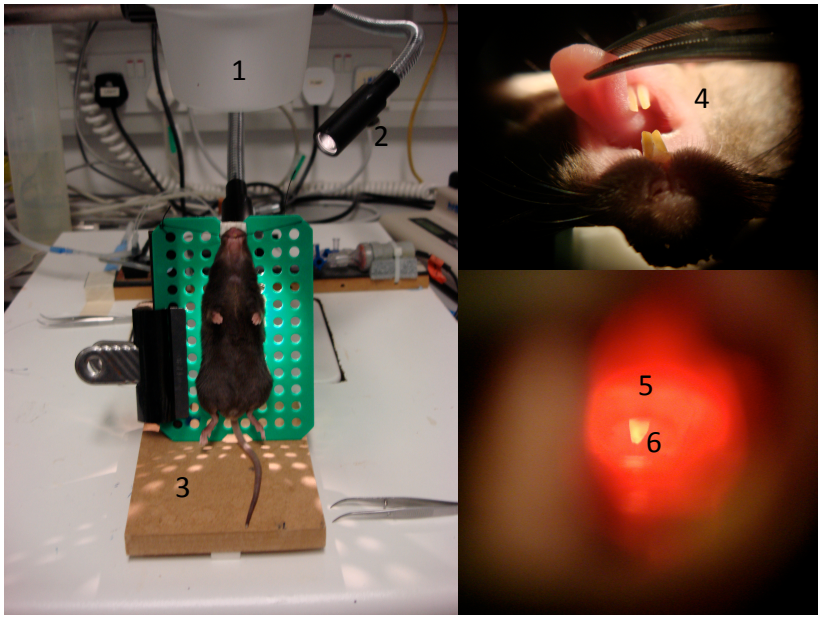

1. Microscope
2. Lamp
3. Vertical stand
4. Curved forceps
5. Epiglottis
6. Vocal cords

Figure 2.2. Set up for orotracheal instillation of substances

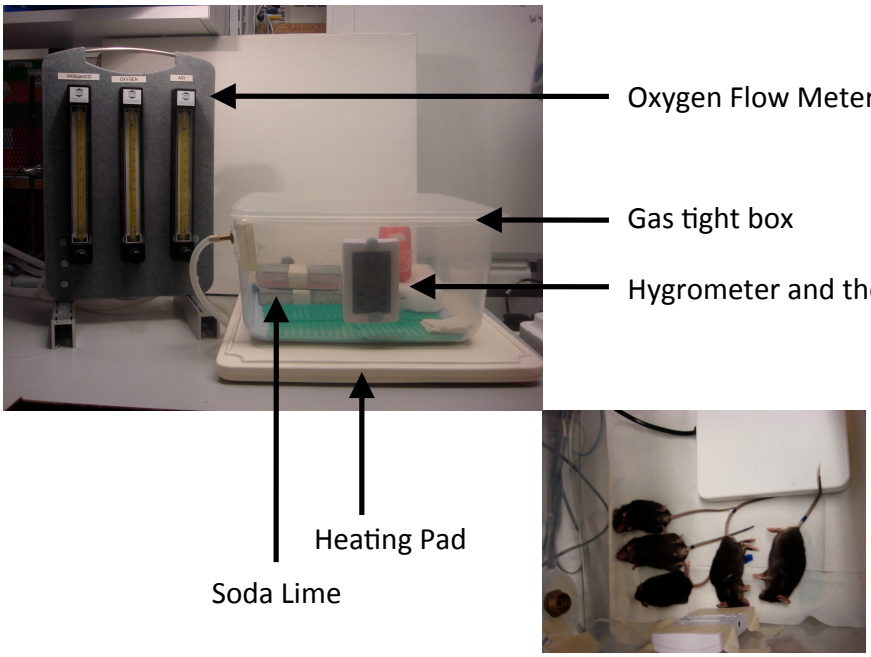

Figure 2.3. Mouse recovery unit

2.3.4 In vivo labelling of lung compartments (relevance to chapter 7)

Chapter 7 describes an in vivo labelling approach to identify leukocyte subsets in the various compartments of the lung to investigate the number, localisation, phenotype and function of leukocytes in healthy and injured mouse lungs. Anaesthetised WT mice underwent instillation of hydrochloric acid as described in the resolution phase model. At various time-points after injury, animals underwent tracheostomy and

right external jugular vein cannulation through which 2µg of a PE anti-CD45 antibody (diluted in 100µl sterile PBS) was injected. At the same time, animals underwent systemic anticoagulation and five minutes after injection of the antibody animals were exsanguinated under terminal anaesthesia. The thoracic cavity was exposed through a midline sternotomy and the lungs gently teased from their pleural adhesions. Subsequently, 5-0 silk sutures was placed carefully around the right and left main bronchi. One or both lungs underwent instillation with 0.5ml or 1ml sterile PBS containing 2µg of a PE-Cy7 anti-CD45 antibody and removed from the thoracic cavity. Lungs remained exposed to the intratracheal antibody for 5 minutes. Whole blood was also attained for analysis via the external jugular venous cannula and/or cardiac puncture. Lungs were processed using the flow cytometry protocol as described later in section 2.6.3. The precise gating and identification strategies used to determine the specific cell types and their compartmental localisation are described in detail in chapter 7.

2.4 Harvesting of experimental samples

2.4.1 Bronchoalveolar lavage

At the end of each protocol, mice were sacrificed via intra-arterial anaesthetic overdose. BALF was sampled with 750µl of normal saline if both lungs were lavaged or 400µl if unilateral lavage was being performed. During unilateral lavage, a thoracotomy was performed and the left main bronchus identified and tied off. The recovered BAL was transferred to an Eppendorf and centrifuged at 1500rpm for 5 minutes at 4^{o}C. The supernatant was pipetted off and aliquots stored at -80^{o}C. Cells in BALF were counted by haemocytometer, and differential cytology was performed on DiffQuik-stained samples prepared by cytospin (Shandon Runcorn, UK).

2.4.2 Blood/plasma

Blood was sampled using a syringe containing 10 international units (iu) of heparin by either cardiac puncture or through any external jugular or carotid arterial lines that had been inserted during the protocol. This was placed into Eppendorfs for

centrifugation at 4000rpm for 5 minutes at 4^{o}C. The supernatant was pipetted off and aliquots stored at -80^{o}C.

2.4.3 Lung tissue preparation

Lungs were carefully dissected to ensure minimal trauma. They were detached from their surrounding ligatures and removed by identifying the respective bronchi supplying each lobe, ligating as close as possible to the lung tissue, thus, ensuring the removal of all peri-bronchial lymphoid tissue. Furthermore, to standardise (as much as possible) the influence of blood within the pulmonary vasculature, animals were systemically anti-coagulated (20iu heparin) and exsanguinated through the transection of major vessels leading to and arising from the heart (internal and external jugular veins, internal carotid, inferior vena cava, and aorta). Three recruitment manoeuvres led to the release of blood from the transected vessels and hence, ensured the emptying of pulmonary vessels present in West's zone 2 and 3. Retrieved lungs underwent a number of analyses including assessment of wet/dry weight, flow cytometric and some lungs were snap frozen in liquid nitrogen and stored at -80^{o}C for later analysis.

2.5 Physiological measurements

2.5.1 Respiratory mechanics

The mechanical properties of the lung can be described in terms of its resistive and elastic properties. Respiratory mechanics were measured using the end-inspiratory occlusion technique, as described by Ewart et al (240), which allows differentiation between these elements of the lungs. This involves both solenoid valves being closed and producing zero flow at the end of inspiration. This allows calculation of the elastic and resistive components of the respiratory system through measurement of airway pressure and gas flow (figure 2.4). This was of particular importance, as the intratracheal instillation of fluid will affect both components and, both influence peak inspiratory pressure readings. Preliminary experiments in both models showed increases in respiratory system elastance (Ers) with increasing acid molarity

suggesting that indeed Ers was a robust marker of alveolar injury (see figure 3.1 and 6.1).

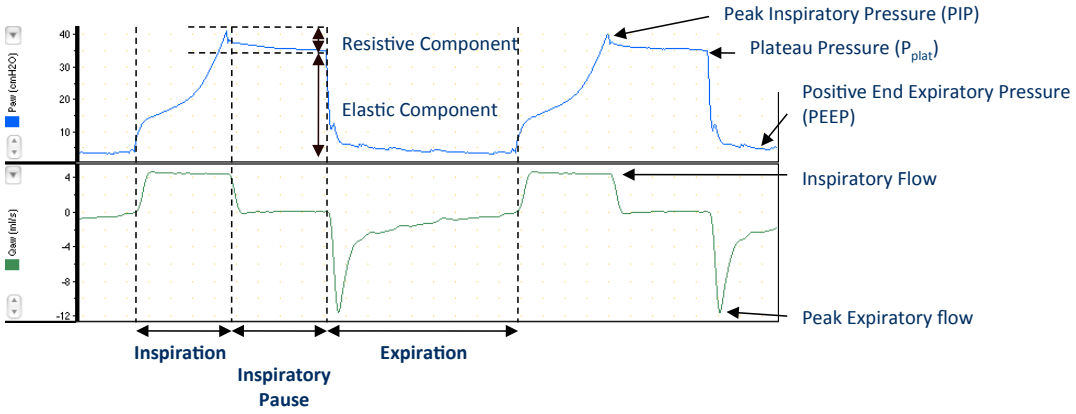

Compliance = Tidal Volume/(P_{plat} – PEEP)

Elastance = 1/Compliance = (P_{plat} – PEEP)/Tidal Volume

Resistance = (PIP-P_{plat})/Flow

Figure 2.4. Measurement and calculation of respiratory mechanics

2.5.2 Arterial blood gas analysis

After tracheostomy and low tidal volume ventilation, the left internal carotid was exposed and cannulated. This was attached to a pressure transducer and a syringe pump, through which an infusion of heparinised saline was continuously administered (0.4ml/hr). This enabled measurement of blood pressure as well as arterial blood gas analysis. Blood (approx. 70µl) was sampled using a heparinised capillary tube and analysed with a RapidLab 248 blood gas analyser. After blood sampling a 75µl bolus of heparinised saline was administered through the carotid line.

2.5.3 Wet/Dry weight assessment

Left lungs were removed and briefly rinsed in saline and blotted. They were immediately weighed and subsequently dried at 60^{o}C for 24 hours, after which they were reweighed for wet/dry weight analysis.

2.5.4 Protein Assay

BALF protein measurement was performed using the Bradford method as per the BioRad protein assay kit. The kit utilises the shift in absorption of light, which is proportional to the extent to which the dye Coomassie Brilliant Blue G-250 binds to protein. Standards of BSA were prepared through serial dilution and both samples and standards were analysed in triplicate. The dye reagent was added to each well and plates analysed after 10 minutes using a colorimetric plate reader.

2.5.5 Lung permeability index

Some animals underwent insertion of a right external jugular line for administration of 100µl of AlexaFluor 594-conjugated albumin (Invitrogen). This was administered at 30 minutes before the end of the experiment. After termination of the experiment, blood and BALF were sampled as described above. Neat supernatants (50µl) (and saline for blank control wells) were pipetted into a black 96-well plate in triplicate. Alveolar-capillary barrier permeability index was calculated by the ratio of spectroscopic analysis (Biotek) of BALF:plasma fluorescence.

2.6 Inflammatory measurements

2.6.1 ELISA

BALF levels of soluble mediators (TNF, IL-6, MIP-2, KC, MCP-1, RAGE, FasL) were measured with sandwich ELISA. All measurements were performed using a validated Duoset ELISA (R&D). 96-well plates were coated overnight with respective anti-mouse capture antibody diluted in PBS. After blocking and washing, 50µl of standards and samples were added in duplicate and incubated at room temperature for 2 hours. Respective biotinylated detection antibodies were added after washing and again incubated at room temperature for 2 hours. Horseradish peroxidase (HRP) was added after washing and incubated for 20 minutes. After a final wash cycle, a substrate mixture (3,3’,5,5’-Tetramethylbenzidine (TMB) – Sigma Aldrich) was added for colour development over 20-30 minutes at which point 2N sulphuric acid was used as a stop solution. The plate was then read at 450nm in a MRX II absorbance colorimetric plate reader.

2.6.2 Lung cytology

BAL was centrifuged as described above to attain BALF supernatant. The cell pellet was resuspended in 500µl of 0.9% NaCl, of which 120µl was used for cytospin preparation and 50µl was stained with 10µl of Turk's nuclear stain for haemocytometer counts. Differential cytology was performed on DiffQuik stained cytospin slides and proportions of leukocytes were attained with counts up to a total of 300 cells per slide. The total BAL cell count was attained through haemocytometric analysis allowing the calculation of numbers of individual leukocyte populations based on cellular morphology.

2.6.3 Lung leukocyte quantification using flow cytometry

Flow cytometry was utilised to determine leukocyte numbers and phenotype in whole lung single cell suspension.

Preparation of single cell suspension

Lungs underwent mechanical disruption using a GentleMacs tissue dissociator (Miltenyi Biotec) for 1 minute in 2mls of intracellular (IC) fixative. This technique allows immediate fixation and dissociation enabling the best stability of epitopes. The fixation reaction was stopped through the addition of 20mls of ice-cold flow cytometry wash buffer (FWB - PBS with 2% FCS, 0.1% sodium azide, and 5mM EDTA). The suspension was subsequently sieved through a 40µm filter and washed again with ice-cold 20mls FWB. The lung cell suspension was subsequently centrifuged at 4^{o}C at 200rpm. The cell pellet was resuspended in 1ml of FWB and placed on ice.

Staining protocols

Extracellular staining was performed by incubation of single cell suspension with fluorochrome-conjugated antibodies for 30 minutes in the dark at room temperature or 4^{o}C, dependant on experimental protocol. Antibody stocks were prepared in FWB to attain the final concentrations stated in table 2.12. After incubation 4mls of FWB was added to stop the antibody reaction and samples centrifuged at 2000rpm at 4^{o}C for 5 minutes. Cells were resuspended in FWB and kept on ice until analysed using a 7-channel CyAn ADP flow cytometer (Beckton

Coulter). Prior to analysis the addition of AccuCheck counting beads (Invitrogen) enabled cell counts to be calculated.

Cell identification

The leukocytes analysed during the acute phase acid aspiration included resident alveolar macrophages, neutrophils and monocytes. Resident alveolar macrophages were identified as $CD45^{+}F4/80^{+}CD11c^{+}CD11b^{-}$ population with high auto-fluorescence. Neutrophils and monocytes were gated using $CD45^{+}CD11b^{+}NK1.1^{-}$ events with subsequent gates separating these two cell types. Both neutrophils and monocytes express the marker Gr-1 and this consists of two main fragments – Ly-6C and Ly-6G. Both fragments are required for the recognition by the Gr-1 antibody used in these experiments (clone RB6-8C5). Mouse monocytes are classified into 2 types: inflammatory (Ly-$6C^{hi}$, Gr-1^{hi}, $CCR2^{hi}$, $CX3CR1^{lo}$) and non-inflammatory (Ly-$6C^{lo}$, Gr-1^{lo}, $CCR2^{lo}$, $CX3CR1^{hi}$) subsets. Our group has previously found that the cell-fixation procedure used to prepare the lung cell suspension leads to a denaturation of the Gr-1 epitope specifically on monocytes. Hence, this leads to the loss of recognition of the Ly-6G fragment by the anti-Gr-1 antibody on monocytes. Hence, Gr-1 could not be used to distinguish between these two monocyte subsets (241). In effect, the Gr-1 antibody functioned as a "Ly-6G antibody" which could only be used to recognize the Ly-6G epitope on neutrophils, and not monocytes. To overcome this technical issue, the addition of an antibody specifically against Ly-6C enabled the distinction between the two monocyte populations. Thus, events showing positive staining with this Ly-6C antibody were defined as Ly-$6C^{hi}$. For ease of explanation, the Gr-1 antibody will now be referred to as a "Ly-6G antibody". To summarise, neutrophiils were gated as Ly-$6C^{inter}$Ly-$6G^{hi;}$ and monocytes were separated into their two subsets – inflammatory (Ly-$6C^{hi}$ Ly-$6G^{lo}$) and non-inflammatory (Ly-$6C^{lo}$ Ly-$6G^{lo}$).

2.7 In situ measurement of alveolar fluid clearance

2.7.1 Overview

To gain a quantification of alveolar epithelial function we examined the rate at which the lungs clear fluid (alveolar fluid clearance - AFC) over a defined period of time. AFC was ascertained by the increase in concentration of a tracheally instilled non-

permeable tracer (AlexaFluor 594-conjugated BSA) within the BALF over a 30-minute period using an adaptation of a published in situ model (242).

2.7.2 Surgical Preparation

Animals underwent anaesthesia, tracheostomy and low tidal volume ventilation for a brief period on FiO_2 of 1.0 (in total less than 15 minutes) and maintained at a temp of 36.5-38^{o}C. Animals were given 20iu heparin intravenously through an external jugular vein cannulation and after 3 minutes, an arterial blood sample was taken for blood gas analysis. Animals were exsanguinated under anaesthetic overdose (through transection of the carotid artery, internal and external jugular veins, inferior vena cava and aorta) to reduce the impact of pulmonary vascular pressure on alveolar fluid clearance. Each animal then underwent 3 further recruitment manoeuvres to standardise lung recruitment between animals and time points and empty pulmonary vessels present in West's zone 2 and 3.

2.7.3 Measurement protocol

Mice underwent intratracheal instillation with 700µl of isoosmolar 5% low endotoxin BSA (Sigma-Aldrich) containing 50µg/ml of AlexaFluor 594-conjugated (AF594) BSA (Invitrogen). Without disconnecting the instillation syringe, the plunger was withdrawn to 400µl and reinstilled, and immediately after this "flush" manoeuvre a first aliquot of 200µl was removed as a t=0 reference sample. This ensured adequate mixing of instillate with alveolar contents and a homogenous distribution of the instillation. The tracheostomy was clamped to prevent any loss of instillate, whilst the instillation syringe was disconnected to immediately place mice on a custom-made continuous-positive-airway pressure (CPAP) system delivering a FiO_2 1.0 at 8cmH_2O. On connection of the tracheal tube to the CPAP system the clamp was removed such that the positive pressure and a 30^{o} head up tilt ensured delivery of the instillate into the distal airspaces. A heating pad and overhead warming light source was used to maintain intra-thoracic temperature (measured through an intra-oesophageal probe) at 36.5-38^{o}C throughout the protocol. These measures are aimed to maintain stable alveolar epithelial function throughout the period of measurement in this in situ model.

At the end of the 30 minutes, the tracheal tube was again clamped to prevent loss of instillate whilst animals were removed from the CPAP system. The instillate was withdrawn gently by attaching a new syringe onto the tracheal tube. A surgical pneumothorax was induced through blunt dissection of the diaphragm to facilitate maximum recovery of remaining instillate. BALF samples were then centrifuged at 3000*g* for 5 minutes and the supernatant analysed immediately for fluorescence using a FLx800 fluorescence microplate reader (Biotek). The fluorescence of the original instillate (Fi), the t=0 (F0) and the t=30 (F30) sample was measured in triplicate. The distal airways fluid clearance over 30 minutes was determined by the equation: [1-(F0/F30)] x100 where F0 is the fluorescence of the t=0 reference sample and F30 is the fluorescence of the 30-minute sample. Pharmacological intervention using amiloride (2mM) and isoproterenol (2mM) (added to the instillate) to respectively inhibit and augment AFC was used to ensure that measurements accurately reflected AFC.

2.8 Tissue imaging

2.8.1 Background

The practicalities to attain a standardised measurement of lung injury through histological assessment require considerable attention to detail. Unlike solid organs, sectioning of the lung can be fraught with difficulty with significant potential for artefacts. The standardisation of lung inflation (using a specified transpulmonary pressure) prior to fixation is crucial to allow consistencies between experimental groups.

2.8.2 Preparation of lungs

Animals were systemically heparinised and euthanised through exsanguination under terminal anaesthesia, as already described. They were tracheostomised and a careful thoracotomy was performed avoiding damage to the lungs. Sutures were placed behind the main bronchi of the lung to be used for histological assessment. The open chest enabled transpulmonary pressure to be zero prior to inflation. A fine catheter was placed in the tracheostomy and lungs inflated to 15cm pressure of 4%

paraformaldehyde solution (the relative density of water and parafmormaldehyde are likely to be similar given the latter is dissolved in water). The sutures were subsequently tied and the lungs removed and placed in a bijou containing 4% paraformaldehyde overnight. Lungs were subsequently placed in a tissue processor for dehydration and rehydration prior to paraffin embedding. The lungs were mounted in wax and 5µm sections were obtained using a sledge microtome. Sections were floated on a 37^{o}C water bath and collected on glass microscope slides and allowed to dry at room temperature prior to histological staining.

2.8.3 Haematoxylin and Eosin staining.

Lung sections were placed in a 65^{o}C oven for 15 minutes to melt the paraffin wax. The sections were de-waxed by placing them in a xylene bath for 10 minutes. Sections were rehydrated through a graded immersion in alcohols (absolute to 90% to 70% alcohol) for 30 seconds each and then in distilled water for 5 minutes. They were stained with Mayer's haematoxylin for 10 minutes followed by washing in tap water for 5 minutes. The slides were dipped in 1% hydrochloric acid in 70% ethanol and washed again for 5 minutes. They were counterstained with 1% eosin for 10 minutes and dipped in water to remove any excess eosin. They underwent dehydration in 100% ethanol followed placement in a bath of xylene overnight prior to mounting with DePex plus coverslip.

2.8.4 Masson's Trichrome staining.

Paraffin embedded slides underwent deparaffinisation and rehydration in xylene and graded ethanol. The slides were placed overnight in Bouin's mordant solution. The slides were washed in tap water for 5 minutes and then stained for 5 minutes in working Weigert's iron haematoxylin Solution (made fresh through the mixing of equal volumes of solution A (1% Haematoxylin in 95% ethanol) with solution B (1.2% ferric chloride and 1% Acetic acid in distilled water). Haematoxylin stained the nuclei black. Slides were subsequently washed in running tap water for a further five minutes. And rinsed in deionised water. Slides were then placed in Biebrich Scarlet-acid fuchsin for 5 minutes to stain cytoplasm and muscle red. This was rinsed in deionised water. Slides were exposed to phosphomolybdic/phosphotungstic acid solution for 5-10 minutes. This enables the uptake of the next dye, aniline blue, in

which the slides were placed for 5 minutes to stain the collagen blue. Slides were rinsed again and differentiated in 1% acetic acid for 1 minute. Finally, slides underwent dehydration in 100% ethanol and placed in xylene overnight prior to mounting as previously described.

2.8.5 Histological lung injury scoring

A variety of scoring systems are available to quantify lung injury. A recent ATS workshop proposed a histological system that incorporated simple graded scores for a number of separate morphometric criteria (192). Lung injury scores were quantified in a blinded manner in 20 random high-power fields (x400 original magnification) according to the table 2.13. Of note each field analysed had at the minimum 50% occupation by lung alveoli. The final injury score was derived from the following calculation: Score = (20*A + 14*B + 7*C + 7*D + 2*E) / (number of fields) * 100.

Parameter	Score per field		
	0	1	2
A. Neutrophils in the alveolar space	None	1-5	>5
B. Neutrophils in the interstitial space	None	1-5	>5
C. Hyaline membranes	None	1	>1
D. Proteinaceous debris filling the airspaces	None	1	>1
E. Alveolar septal thickening	None	2x-4x	>4x

Table 2.13. Histological lung injury scoring method
(adapted from Matute-bello *et al* (192))

2.9 Apoptosis detection

2.9.1 TUNEL assay

The Terminal UTP Nick End-Labilling (TUNEL) assay was developed in 1992 by Gavrieli et al (243) and is a method for detecting cells that show DNA fragmentation. It involves the use of the enzyme terminal deoxynucleotidyl transferase to attach biotin-conjugated dUTP onto the broken ends of the double stranded DNA. The

TACS.XL diaminobenzidine in situ Apoptosis Detection Kit (Trevigen Ltd) was used to detect the extent of morphological TUNEL positive staining in lung sections. Tissues are first fixed in 4% paraformaldehyde overnight to prevent the loss of low molecular weight DNA fragments. Sections prepared from paraffin blocks of fixed lungs were warmed to 57^{o}C for 5 minutes. They were subsequently immersed in 2 changes of xylene, 5 minutes each, followed by graded immersion in 100%, 95% then 70% ethanol, 5 minutes each. Slides were placed in PBS for 10 minutes at room temperature and carefully dried around the sample. The sample was covered with 50µl of proteinase K Solution and incubated for 15 minutes at room temperature, to permeabilise the tissue making the DNA accessible to the labeling enzyme, prior to in situ detection of apoptosis. The sections were washed twice in DNAse free (Roche) deionised water for 2 minutes each. Endogenous peroxidase activity was quenched using methanol (45mls 100%)/hydrogen peroxide (5mls 30%) quenching solution for 5 minutes with a further wash step in PBS for 1 minute. The slide was immersed in the terminal deoxynucleotidyl transferase enzyme (TdT) labeling buffer for 5 minutes and then covered with 50µl of labelling reaction mix to incorporate biotinylated nucleotides into the 3-OH ends of the DNA fragments by the TdT enzyme. Slides were incubated for 60 minutes at 37^{o}C in a humidity chamber. To generate a positive control using TACS-Nuclease, 1µl of TACS-Nuclease was added to 50µl of labelling reaction mixture. A hydrophobic cover slip was used to facilitate homogenous distribution of labelling solution over the section. After 60 minutes the TdT stop buffer was added to the slide for 5 minutes and washed twice with deionised H_2O for 5 minutes each to remove unbound conjugate. The sample was covered with 50µl of streptavadin-HRP solution, and incubated for 10 minutes at 37^{o}C in a humidity chamber. After washing twice in PBS for 2 minutes each, slides were immersed in diaminobenzamine (DAB) solution for 5 minutes. Slides underwent a further two washes in deionised water and were background stained with 1% methyl green for 2 minutes. Slides were dipped ten times each in 2 changes of deionised H_2O, 95%, and 100% ethanol and finally in xylene prior to mounting with DePex and glass coverslips. The enzyme reaction generates an insoluble coloured precipitate where DNA fragmentation has occurred.

By principal TUNEL can label any 3' hydroxyl end of DNA and hence, has also been shown to produce false positives in cells undergoing necrosis and in the S-phase of the mitotic cell cycle (the phase in which DNA is replicated) (244). A recent classification of cell death by a nomenclature committee on cell death (245) discussed the controversies in defining cell death. They suggested that apoptosis involves the:

1. Rounding-up of the cell
2. Retraction of pseudopodes
3. Reduction of cellular and nuclear volume (pyknosis)
4. Nuclear fragmentation (karyorrhexis)
5. Minor modification of cytoplasmic organelles
6. Plasma membrane blebbing
7. Engulfment by resident phagocytes

Some investigators view TUNEL as an inadequate technique given its propensity to overestimate the number of apoptotic cells. Hence, our counting of cells undergoing apoptosis also included only those cells that matched strict morphological criteria for apoptosis (i.e. condensed DAB staining in the nucleus i.e. pyknosis) to count the number of cells per high power field that were TUNEL positive.

2.9.2 Caspase-8/-9 activity assay

The caspase-8/-9 fluorometric activity assay Kit (Biovision) is based on detection of cleavage of substrate IETD-AFC (for caspase-8) and LEHD-AFC (for caspase-9) (AFC: 7-amino-4-trifluoromethyl coumarin). The IETD-AFC/LEHD-AFC emits blue light (λmax = 400 nm); upon cleavage of the substrate by caspase-8, free AFC emits a yellow-green fluorescence (λmax = 505nm), which can be quantified using a fluorescence plate reader. Hence, snap frozen left lungs were defrosted and homogenised (using a hand-held homogeniser) for 30 seconds in the cell lysis buffer supplied and placed on ice until incubation. Subsequently, 50µl of homogenate, substrate, and reaction buffer are incubated at 37^{o}C in black 96-well plates for fluorescence to be measured after 60 minutes using a fluorescence microplate reader.

2.9.3 Flow cytometric localisation of caspase-8 activity

The whole lung caspase-8 assay described above does not allow localization of caspase-8 activity to specific cell types. Hence, a flow cytometry method was developed to specifically localise and measure the activity of caspase-8 within the major cell types of the uninjured and injured lungs of WT mice. In contrast to the previous flow cytometry protocols (section 2.6.3), this assay required the preparation of live lung single-cell suspensions given that formaldehyde fixation quenches caspase activity. Hence, a previously published tissue-digestion protocol used to recover endothelial cells was modified to efficiently retrieve epithelial and endothelial cells in an unfixed state into single cell suspension (66, 246, 247). One or both lungs were instilled (through the tracheostomy), respectively, with 0.5 or 1 ml DMEM containing 1 mg/ml sterile filtered dispase enzyme (Invitrogen). Lungs were tied at the bronchus and removed as previously stated and placed in the same dispase solution for 30 minutes at room temperature. Lung parenchyma was gently separated from the bronchial tree and minced in ice-cold sterile DMEM/2.5% HEPES with 0.01% DNase (Roche). This distal lung cell suspension was passed through a 40µm filter, washed with, and reconstituted in ice-cold DMEM/2.5% HEPES. The lung cell suspension was centrifuged at 2000rpm at 4^{o}C. Subsequently, cell suspension was incubated with a FAM-IETD-FMK caspase-8 reagent (Immunochemistry) for 60 min at 37^{o}C in the dark, per the manufacturer's instructions. This reagent is a fluorochrome-conjugated caspase-8 inhibitor–based compound that freely permeates cells and binds specifically and covalently to activated intracellular caspase-8, and can be detected by flow cytometry (in the FITC channel). This was followed by a 15-minute passive wash step where cells were washed, resuspended and incubated in 2mls DMEM/2.5% HEPES, for 15 minutes at 37^{o}C to allow any unbound caspase-8 reagent to diffuse out of the cells. Cells were washed in 4mls of DMEM/2.5% HEPES and resuspended in 500µl of DMEM/2.5% HEPES. Subsequently, 50µl of cell suspension were incubated on ice with antibody stock containing fluorophore-conjugated anti-mouse antibodies to pan-endothelial marker CD31, the pan-leukocyte marker CD45, the pan-epithelial marker epithelial cell adhesion molecule (EpCAM), and the type 1 alveolar epithelial cell (AEC) marker - type 1 cell alpha protein (t1α). After a final wash and reconstitution in ice-cold DMEM/1%

HEPES the samples were analysed by flow cytometry, as described above. Importantly given that the lung cell suspensions were unfixed they were kept on ice throughout the protocol, except during the incubation/wash steps for the FAM-IETD-FMK caspase-8 reagent binding, to minimize changes to intracellular reactions. Furthermore, a buffered cell culture media was used in all steps in order to allow the optimal physiological environment as possible throughout the ex-vivo processing.

2.10 Interventional studies

2.10.1 Caspase-8 inhibition

Animals were anaesthetised and ventilated as per the acute acid model. To ascertain the impact of caspase-8 inhibition on acid-induced lung injury, 4 mg/kg of a selective caspase-8 inhibitor Z-VAD-IETD (Becton Dickinson Biosciences), or DMSO as the vehicle, was administered intravenously (via the external jugular) to WT mice 5 minutes before intra-tracheal acid instillation.

2.10.2 Alveolar macrophage depletion

WT mice underwent anaesthesia 48 hours before acid instillation for the orotracheal instillation of 75µl of clodronate or PBS containing liposomes (Encapsula NanoSciences) to deplete the resident alveolar macrophage population. We have previously found that 48 hours leads to a significant reduction in the alveolar macrophage population (248). Animals subsequently underwent the acute acid instillation protocol to determine the impact of alveolar macrophages on acid aspiration. We confirmed a 90% reduction in the resident alveolar macrophage population ($CD45^{+}F4/80^{+}CD11c^{+}CD11b^{-}$) through flow cytometric quantification of lung single cell suspension.

2.11 Statistical analysis

Data are expressed/presented as means±SD/column graphs (if parametric) or median±interquartile range/box and whisker plots (if nonparametric). The model assumption of normality of residuals was assessed by QQ plot and the Shapiro–Wilk test. Statistical analyses of data were made using either a two-tailed Student t test or

one-way ANOVA with Bonferroni tests for multiple comparisons (if parametric) and Mann–Whitney/Kruskal–Wallis tests (if nonparametric). Time courses were analyzed using a two-way ANOVA or a t-test of final end point values. We used Pearson's product-moment correlation coefficients to test the relationships between continuous variables. Analyses of normal distribution were performed using SPSS version 20 (IBM) and statistical comparisons used GraphPad Prism version 6. A p-value of less than 0.05 was considered significant.

3 Differential roles for TNF receptors in acid-induced lung injury

Abstract

Tumour necrosis factor has been heavily implicated in the pathogenesis of ARDS in pre-clinical and clinical investigations. However, despite this intensive investigation there has been no translation of anti-TNF therapies into ARDS. One possibility for this failure may be that therapies have targeted total blockade of TNF signalling. Indeed, TNF signals through two receptors, the p55 and p75 TNF receptors, which have been recently found to signal through quite distinct pathways.

Within this chapter an acute phase model of acid-induced lung injury has been developed. Using wild type (WT) C57BL6 mice and knockout mouse strains for p55 only (p55KO), p75 only (p75KO), and both p55 and p75 (DKO), we showed that the development of acute pulmonary oedema during the first three hours after intra-tracheal instillation of hydrochloric acid was specifically promoted through p55 TNFR activation. Genetic deletion of p55 TNFR led to a protective effect with animals showing improved respiratory mechanics, improved gas exchange, and reduced lung oedema (as measured by protein permeability and wet/dry weight ratio). Interestingly, p75KO and DKO animals showed either a similar or worse injury to WT animals.

Given that TNF is an important pro-inflammatory cytokine we hypothesised that injurious pro-inflammatory signalling through p55 TNFR induced the pathophysiological derangements seen after acid aspiration. Interestingly, no differences were found in the concentrations of inflammatory mediators in bronchoalveolar lavage (e.g. interleukin-6) and lung leukocytes (neutrophils and monocytes, as evaluated using flow cytometry).

3.1 Introduction

TNF is important in the pathogenesis of lung injury, but despite significant research the precise molecular and cellular pathways that mediate these effects remain unclear. Therapeutic blockade of TNF has been performed through either monoclonal antibodies against TNF or through the development of p55 or p75-IgG fusion proteins with an aim to 'mop up' circulating TNF (173, 249-251). As discussed in the introduction, there are several potential considerations as to why these trials have failed but one important aspect that has been completely ignored is that TNF signals through two receptors which show distinct signalling pathways and hence, potentially different cellular responses (153). TNF is simply the messenger whereas the receptors are the effectors. Furthermore, the precise downstream biological mechanisms of how TNF induces organ dysfunction in sepsis/ARDS are not investigated in many experimental studies.

Historically, p55 TNFR signalling has been thought to be the predominant pathway through which the cellular actions of TNF occur. It has been shown that the two cell surface receptors for TNF may have divergent and sometimes opposing roles in a number of models of acute inflammation including myocardial infarction, sepsis and pneumonia (220-223). Using genetic and pharmacological approaches, our laboratory showed that pulmonary oedema formation is specifically mediated through the p55 TNFR, and that genetic deletion of the p75 TNFR opposed alveolar oedema formation during the early phases of ventilator-induced lung injury (VILI) (224, 252). In these studies, mice deficient in the p55 TNFR or mice treated with a domain antibody against the p55 TNFR were exposed to high stretch ventilation and showed significant attenuation in injury as shown by respiratory mechanics, arterial blood gases, and markers of endothelial-epithelial permeability, in addition to, improved survival. In view of this protection, we wished to investigate whether this would also be true for other aetiologies of alveolar oedema in lung injury and determine the mechanisms through which this injury (or protection when blocked) was conveyed.

The acid aspiration model was chosen as it is regarded as one of the most clinically relevant models of experimental ARDS (253). It accounts for 11% of all cases of ARDS (21) and a number of clinical and experimental studies have demonstrated a significant involvement of TNF in mediating ARDS resulting from gastric aspiration (167, 197). Hyers showed that clinical ARDS induced by gastric aspiration had a significantly greater level of TNF in bronchoalveolar lavage fluid than the non-aspirated ARDS group (167). Acid aspiration produces overwhelming lung injury over a very short dose range and hence often requires mechanical ventilation in rodents, limiting the time period for investigation to hours. Early injury progresses through two phases - the first phase involves a direct physicochemical reaction with acid (the nature of which remains unknown) leading to increased permeability, and the second phase occurs at 2-4 hours and is thought to involve neutrophils (195). A number of other inflammatory mediators have also been implicated including IL-6 (254), IL-8 (88, 255), complement (256), and reactive oxygen species (257, 258). Imai and colleagues showed that acid aspiration lung injury involves the activation of Toll-like receptor 4 (TLR-4) on lung macrophages and mice deficient in TLR-4 showed a reduced cytokine storm and alveolar oedema (254). Modelska and colleagues showed that blockade of IL-8 could ameliorate barrier dysfunction after acid aspiration in rabbits (255). TNF is released early after experimental (196, 197) and clinical (166, 167) acid aspiration and has been shown to be a proximal regulator of many of the aforementioned mediators. However, despite the evident importance of TNF in acid aspiration, total blockade does not completely ameliorate lung injury (197) and, the exact roles of each TNF receptor remains unknown. Hence, we sought to examine if the differential effects of its two receptors would explain some of the inconsistencies found in investigating TNF in this very relevant model of experimental lung injury.

3.2 Aims

The work within this chapter focuses on the investigation of the effects of TNF receptor signalling on acid-induced lung injury. The aims included:

1. The development of a reproducible model of experimental lung injury induced by intra-tracheal acid instillation to facilitate the measurement of clinically relevant respiratory physiological parameters.
2. To investigate a) the physiological impact and b) the inflammatory consequences of each TNF receptor in this model of experimental lung injury.

3.3 Experimental design

3.3.1 Animals

This part of the project used a genetic approach using wild-type (WT) male C57BL6 mice (Charles River, Margate, UK), and p55KO, p75KO, and DKO mice (all from The Jackson Laboratory, USA) to ascertain the acute roles for these receptors in lung injury induced by acid aspiration.

3.3.2 In vivo model

The previous work by Wilson et al in the mouse VILI model (224) highlighted an early impact of TNF signalling upon the development of pulmonary oedema. Hence, an acute model of acid aspiration was developed to investigate the formation of oedema within a similar time frame. In brief, WT, p55KO, p75KO and DKO mice were anaesthetised and tracheotomised for mechanical ventilation (FiO_2 1.0; VT: 8-9 mls/kg; PEEP: 2.5-3.0 cmH_2O; RR: 120 bpm) and underwent carotid cannulation. After an initial recruitment manoeuvre (30 cmH_2O; 5 seconds) to standardise the volume history of the lungs for the effects of surgery and anaesthesia, baseline readings were taken. Subsequently, 50µl of HCl or saline was administered via the tracheal tube. Animals underwent 5 further pulmonary recruitment manoeuvres immediately after acid instillation, and then every 30 minutes up to the termination of the protocol. Subsequent physiological readings were taken prior to recruitment manoeuvres.

3.3.3 Respiratory physiology

At specified intervals indices of respiratory physiology were taken as previously described. These included respiratory mechanics measurements, arterial blood gas analysis, lung wet/dry weight ratio, alveolar protein, and permeability index.

3.3.4 Analysis of inflammation

At the end of the three-hour protocol animals underwent unilateral bronchoalveolar lavage for analysis of soluble mediators and cell counts. Right lungs were processed for flow cytometric counting to quantify neutrophil and inflammatory monocyte sequestration to the lung at 3 hours. Blood from WT and the three knockout strains were analysed for TNF receptor expression on monocytes and neutrophils to ensure phenotype.

3.3.5 Histological preparation

In another set of experiments, lungs of animals were also inflated at a transpulmonary pressure of 15cm height of 4% paraformaldehyde. Lungs were subsequently processed for paraffin embedding and sections attained for H&E staining.

3.4 Results

3.4.1 Acute acid aspiration model optimisation

The majority of previous reports have instilled 50µl 0.1M hydrochloric acid with subsequent mechanical ventilation for a variable period of time (72, 259-261). The tracheal instillation of 50µl of Evan's blue dye (via a catheter fed into the tracheal tube) confirmed that the instillation technique produced an even bilateral distal pulmonary distribution of the instilled fluid – bilateral injury being a prerequisite for ARDS. Immediately after intratracheal instillation the fluid was driven distally into the respiratory tract through the application of 5 deep inflations at 30 cmH_2O. It is well established that recruitment manoeuvres are required at regular intervals to prevent atelectasis of mouse lungs (239, 262, 263). Deep inflations (again to 30 cmH_2O) were applied at intervals of 30 minutes in order to recruit for any atelectasis component inevitable after instillation of fluid into the airways, prolonged

mechanical ventilation, and injury progression (264). Respiratory mechanics (end-inspiratory occlusion technique) were measured before each recruitment manoeuvre.

A dose titration (keeping a fixed volume of 50µl) was performed to ascertain a clinically relevant degree of injury using two clinically relevant parameters – respiratory mechanics (elastance) and arterial oxygenation (figure 3.1). There was an increasing elastance and worsening oxygenation as the number of protons instilled into the lungs increased. The use of 0.1M HCl, although producing a 50% increase in elastance did not produce significant changes in arterial oxygenation at three hours. In contrast, 0.25M HCl produced overwhelming injury with the loss of two animals (severe hypotension with a blood pressure below 50mmHg) by 60 minutes. A concentration of 0.15M was chosen, for subsequent studies, as it produced a 100% increase in elastance, a 2.5 fold reduction in arterial oxygenation (reaching moderate/severe ARDS levels according to the revised Berlin criteria), and a 100% survival (no blood pressure below 50 mmHg) by the end of a three-hour protocol.

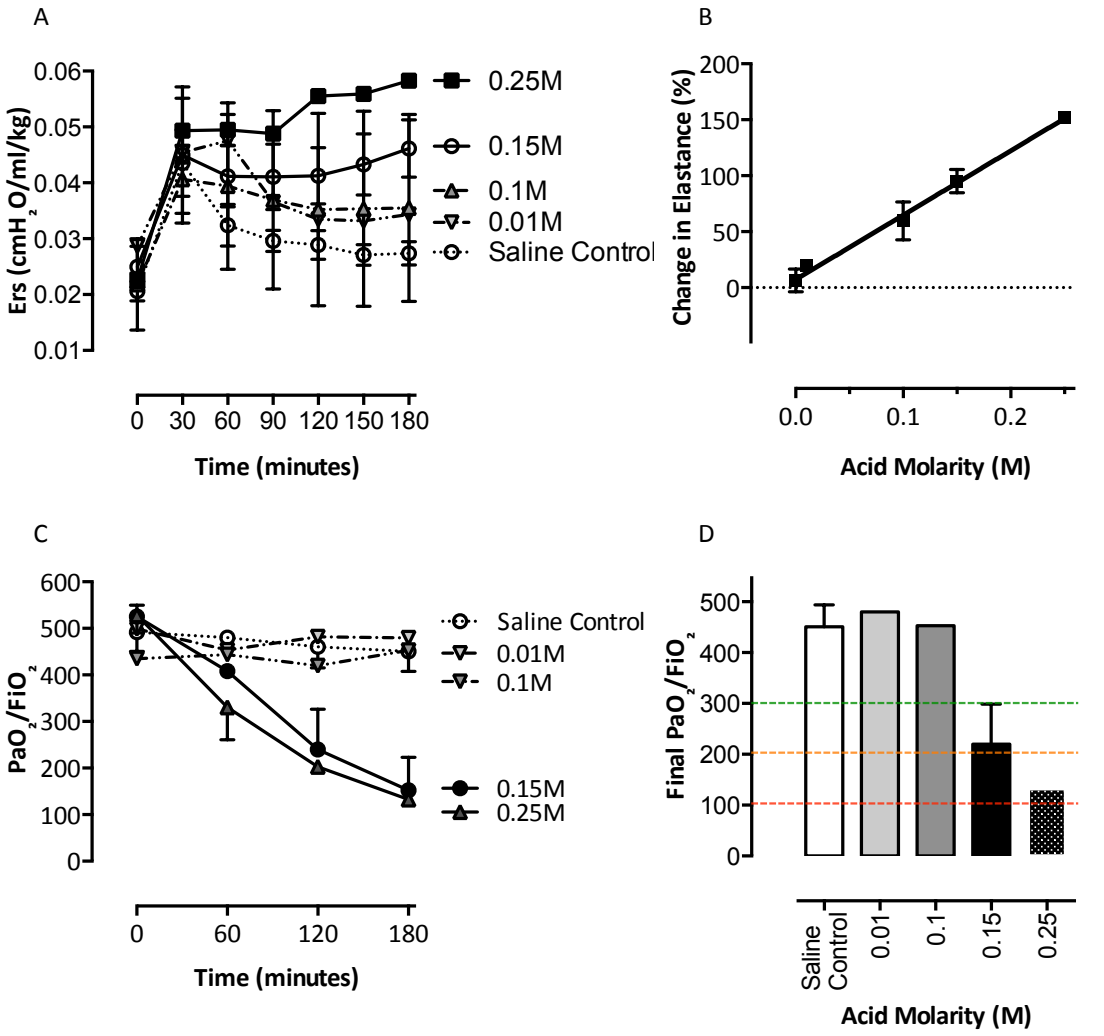

Figure 3.1. Development of acute acid aspiration lung injury model

A) Initial dose titration showed that fluid instillation caused an immediate increase in elastance (Ers) due to fluid in the airway. During the instillation of saline or low concentration of acid Ers returned back to near baseline. As dose of protons (i.e. the pH of the acid was reduced, keeping volume constant), there was no recovery of Ers from a dose of 0.15M upwards. This dose of 0.15M produced a sustained increase in Ers after 90 minutes leading to an increase from baseline Ers of 100% at 3 hours. The 0.25M acid dose led to a high mortality rate. B) There was a strong correlation with proton dose and change in Ers over 90 minutes (Pearson r = 0.995, P<0.0001). C) Only acid doses above 0.15M produced changes to oxygenation. D) 0.15M acid concentration produced deteriorations in oxygenation equivalent to ARDS levels with a PaO_2/FiO_2 of less than 300. Green, amber and red lines demarcate mild, moderate, and severe ARDS as stratified clinically by the Berlin definition. (N=2-5 per group).

3.4.2 Alveolar oedema is mediated specifically through the p55 TNF receptor in acid-induced lung injury.

There were no differences in baseline tidal volume (VT), respiratory system elastance (Ers), resistance (Rrs), peak inspiratory pressures (PIP), and arterial blood gases between the animal groups (table 3.1), indicating that respiratory mechanics and functions were similar between WT and knockout mice in the absence of injurious challenge.

	WT	**p55KO**	**p75KO**	**DKO**
VT (ml/kg)	8.7±0.9	8.7±0.4	8.6±0.5	8.9±0.7
PIP (cmH_2O)	10.7±0.7	10.1±0.5	9.9±0.6	10.2±0.1
Ers (cmH_2O/ml/kg)	0.022±0.003	0.021±0.002	0.023±0.002	0.021±0.001
Rrs (cmH_2O/ml/s)	1.8±0.3	1.6±0.4	1.6±0.1	1.7±0.2
PaO_2/FiO_2	456±37	476±35	453±30	486±27
$PaCO_2$ (mmHg)	43±7	41±4	43±4	42±4

Table 3.1. Baseline respiratory mechanics and blood gas measurements in all mouse strains
Baseline respiratory mechanics and blood gases before saline or acid instillation showed no differences between groups. Note that RR (120bpm) and VT (minute ventilation) were similar between groups leading to a similar $PaCO_2$, confirming that the same ventilatory strategy was applied to all strains of mice at the beginning of the protocol. (N=6-12 per group; no statistical differences found between groups)

3.4.3 Respiratory Mechanics

The measurement of respiratory mechanics is dynamic and Ers (calculated by [Pplat-PEEP]/VT) is dependant on the tidal volume delivered and the set PEEP. Hence, it was important to standardise PEEP and VT throughout the course of injury. As can be seen from figure 3.2 there were no changes in VT (over time) within the groups and no differences in VT between groups throughout the 3-hour protocol, suggesting

that the measurements represent changing respiratory physiology and that the instillation of fluid and development of oedema had no effect on the VT delivered by the ventilator.

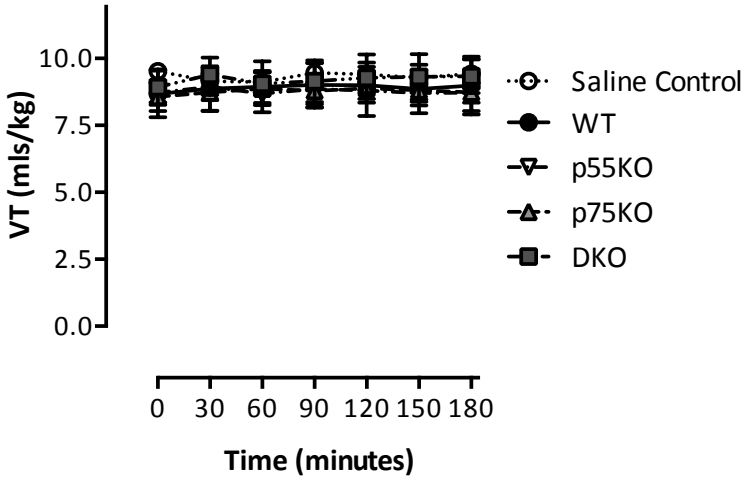

Figure 3.2. Ventilation settings between mouse strains
All strains were ventilated between 8-9mls/kg with no intra- or inter-strain differences over the 3 hours protocol. A volume and flow controlled ventilation system was used and hence this confirms that the observed changes in respiratory mechanics reflects alterations to respiratory physiology. Furthermore, this confirms that instillation of fluid into the alveolar space had no impact upon the tidal volume delivered by the ventilator. (N=6-12 per group; no statistical differences found between groups)

The instillation of fluid into the tracheal tube led to an immediate worsening of respiratory mechanics in all strains (figure 3.3). This was entirely due to the presence of fluid within the airways as saline instillation induced a similar increase to acid instillation. After this immediate increase in Ers, acid aspiration in WT animals showed a sustained increase, which further increased in the final 60 minutes, and led to a significant 1.8 fold increase by the end of the three-hour protocol. In contrast, saline instillation led to a gradual reduction in Ers, presumably as fluid was cleared or distributed from the lungs.

The p75KO and DKO strains showed greater immediate increases in Ers (at 30 minutes) but showed a similar gradient of increase to WT animals for the remainder of the protocol. However, these strains ended with a significantly higher final Ers

compared to WT animals, possibly due to this higher initial increase. In contrast, animals deficient in the p55 TNFR showed a similar trend to saline instilled sham controls and showed a statistically significant improvement as early as 90 minutes. Similar changes were also reflected by changes in the peak inspiratory pressure (PIP) where p75KO and DKO animals showed greater increases by 3 hours; and p55KO animals showed near complete protection. Interestingly, there was very little difference in respiratory system resistance (Rrs) between the p55KO and WT groups, whereas, the p75KO group showed a statistically significant increase in final Rrs by 3 hours.

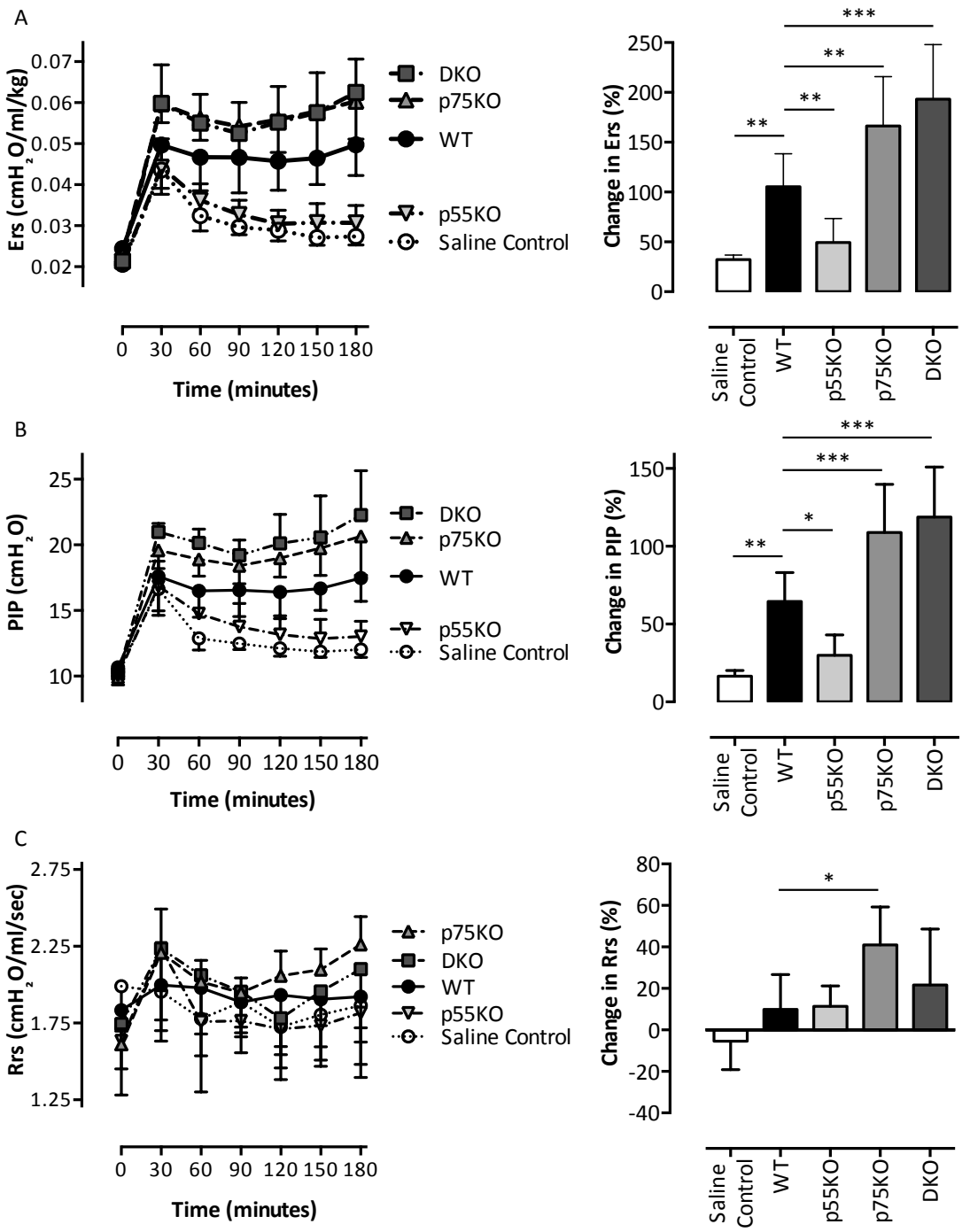

Figure 3.3. Differences in respiratory mechanics between strains after acid aspiration

The time course of respiratory mechanics: A) respiratory system elastance (Ers); B) Peak inspiratory pressure (PIP) and C) respiratory system resistance (Rrs) over 3 hours in WT and TNF receptor knockout strains exposed to acid-induced lung injury. (N=6-12 per group; ***P<0.001 **P<0.01 *P<0.05)

3.4.4 Arterial blood gas analysis

Mice were ventilated with a FiO_2 of 1.0 and PEEP of 2.5-3.0cmH_2O, and underwent hourly arterial blood gas analysis. The WT, p75KO and DKO strains showed significant and immediate deteriorations in arterial oxygenation leading to PaO_2/FiO_2 ratios achieving clinical ARDS criteria of at least moderate severity (i.e. <200) (figure 3.4). In contrast, p55KO strains maintained arterial oxygenation at levels similar to saline instilled sham controls. A statistically significant difference between WT and p55KO strains was apparent even at 60 minutes after acid aspiration. Gas exchange in terms of $PaCO_2$ showed a similar pattern, i.e. deterioration in WT, p75KO and DKO mice, with significant improvement in p55KO mice.

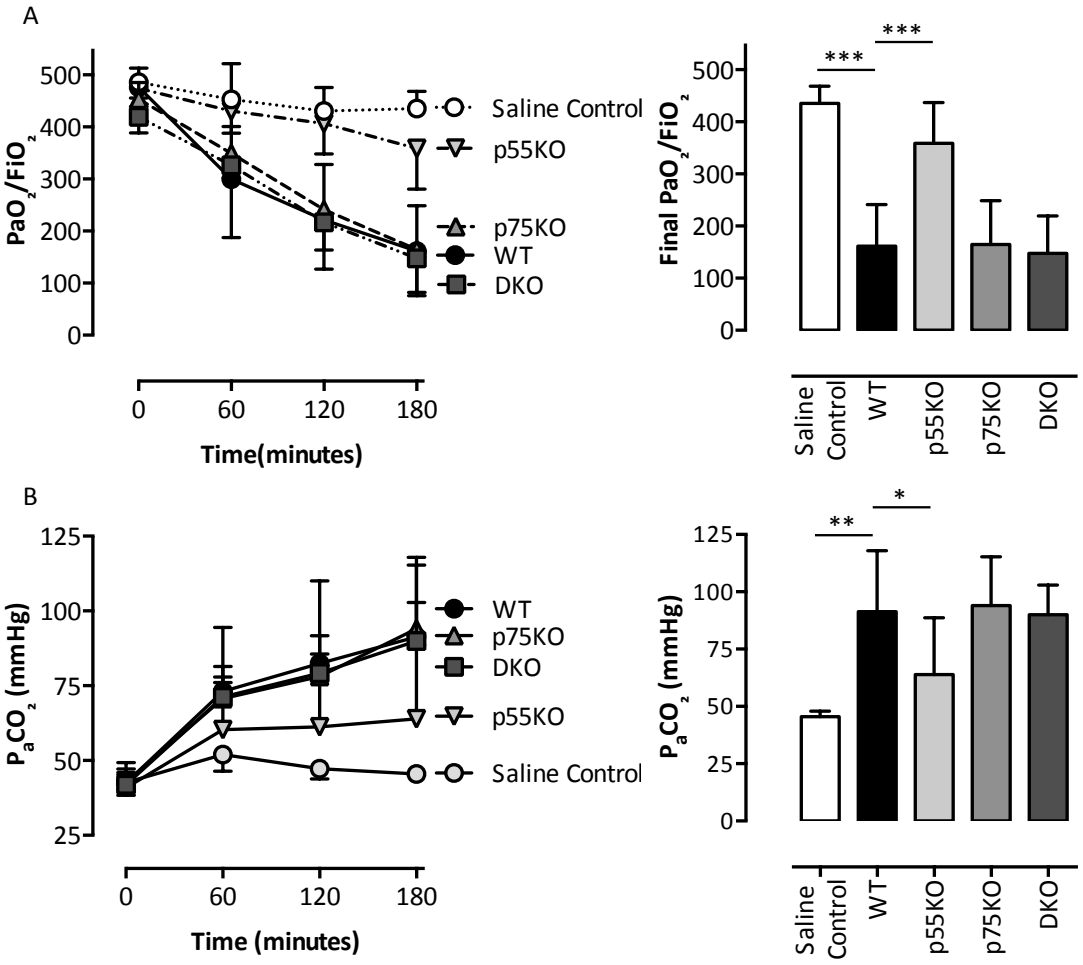

Figure 3.4. Differences in gas exchange between strains after acid aspiration
The time course and final measurements of arterial blood gases A) PaO_2/FiO_2 ratio; B) $PaCO_2$ over 3 hours in WT and TNF receptor knockout strains exposed to acid-induced lung injury. (N=6-12 per group; ***P<0.001 **P<0.01 *P<0.05)

3.4.5 Lung water content

The above alterations in respiratory function most likely represent a combination of pulmonary oedema development inducing intrapulmonary shunt and atelectasis of alveolar units. Pulmonary oedema formation was assessed directly by assessing wet/dry weight ratio (figure 3.5 A) of the lungs at the end of the protocol. As anticipated, acid instillation induced significant pulmonary oedema in WT animals, which was similar in p75KO and DKO mice, but greatly attenuated in p55KO mice.

3.4.6 Alveolar capillary barrier permeability

This was assessed using two methodologies. Firstly, the protein levels within the BALF were determined (figure 3.5 B). This showed a significantly reduced protein content in p55KO animals as compared to the other strains. In view of the significant protection seen in p55KO animals we went on further to measure a more direct parameter of permeability. BALF protein can be influenced by not only the translocation of protein but also the clearance of fluid over the three-hour protocol. Hence, we measured the translocation of fluorescently labelled albumin from the blood compartment to the alveolar space in the final 30 minutes of the 3-hour protocol (figure 3.5 C). Both indices of permeability showed that p55KO animals showed significantly better alveolar capillary barrier function as compared to WT animals. DKO and p75KO animals showed levels of injury similar to the WT group. Given the similar injury pattern to WT animals and in part due to poor breeding of animals no further experiments were performed on DKO animals, and hence their absence from figure 3.5 C onwards.

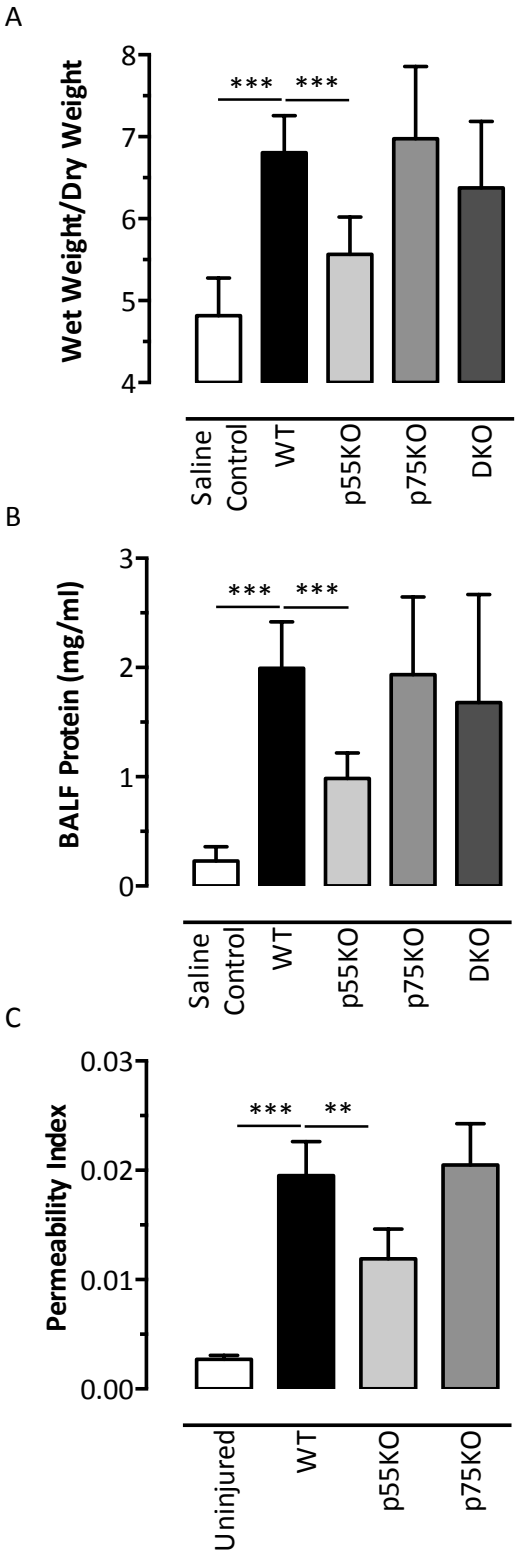

Figure 3.5. Differences in alveolar-capillary barrier permeability between strains after acid aspiration

Measures of lung oedema formation – A) Wet weight/dry weight; B) lavage protein concentration; and C) permeability index show significant attenuation in p55KO animals. (N=4-6 per group; *** P<0.001 ** P<0.01)

3.4.7 Inflammatory consequences of TNF receptor signalling in acid aspiration.

Acid aspiration has been shown to be dependant on IL-8 (88) and neutrophils (260). Given the ability of TNF to induce IL-8 production (265) in the lung and ultimately promoting neutrophil recruitment, it was hypothesised that each TNF receptor induced different degrees of inflammation within the lung. In particular, the protection conferred through p55 TNFR deletion could be secondary to reduced TNF driven inflammatory signalling within the lung. Hence, soluble levels of cytokines/chemokines (figure 3.6) as well as lung leukocytes (figure 3.7) were measured.

Inflammatory cytokines/chemokines.

It was first confirmed that TNF was upregulated within the alveolar space to similar levels between all the strains. The fact that there was TNF present at similar levels supported the view that differences in TNF bioavailability did not account for the physiological differences observed between the groups i.e. lower levels of bioactive TNF accounting for protection in p55KO strains, and vice versa for p75KO/DKO animals. When BALF was analysed at this 3-hour time point for neutrophil/monocyte chemoattractants including MIP-2/KC (mouse IL-8 analogues) and MCP-1, there were no differences found between knockout groups. Interestingly, IL-6 levels were not attenuated in p55KO animals but showed a strong tendency to be higher in p75KO injured animals as compared to WT injured controls ($P=0.068$, Mann-Whitney U-test). There were no differences seen between acid injured p55KO and WT animals.

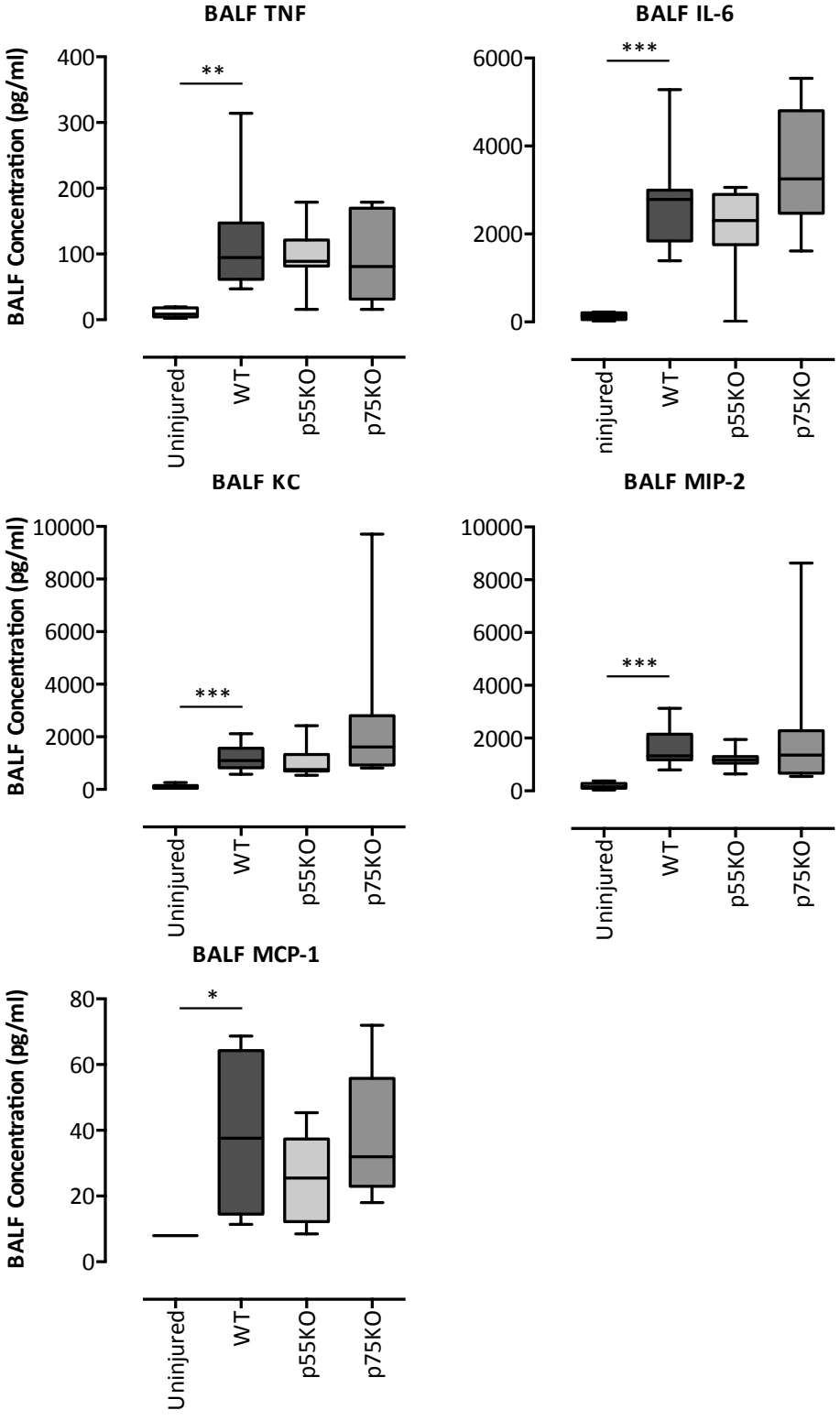

Figure 3.6. Differences in alveolar cytokines/chemokines between strains after acid aspiration

Acid aspiration leads to a significant increase in alveolar levels of cytokines (TNF and IL-6) and chemokines (KC, MIP-2 and MCP-1). This increase occurs in WT, p55KO and p75KO groups to a similar degree. There is a tendency for p75KO group to have a higher level of IL-6. (N=6-10 per group; *** P<0.001 ** P<0.01 * P<0.05)

Pulmonary leukocyte recruitment

Analysis of lavage cell numbers using haemocytometric cell counting at the end of the 3 hour protocol showed no significant neutrophil proportions within the alveolar space in any of the groups tested (% neutrophils among BALF cells - WT Saline 1±0%; WT acid 3.3±1.7%; p55KO 4.1±2.4%; p75KO 0.3±0.4%; DKO 0.3±0.3%).

Hence, it was likely that within this early time-frame leukocytes had not fully migrated into the alveolar space and may have been present either adhered to lung endothelium within the vasculature, or were within the lung interstitium, and hence not retrievable through lung lavage. This prompted the evaluation of analysis of leukocyte sequestration to the whole lung using flow cytometry. Whole lung homogenate was gated using the gating strategy shown in figure 3.7. Neutrophils and monocytes were first gated in lung cell suspensions as $CD45^{+}CD11b^{+}NK1.1^{-}$ events (R1 + R2). Subsequently, neutrophils were identified as $Ly\text{-}6C^{intermediate}Ly\text{-}6G^{hi}$ (R3), whereas inflammatory monocytes were identified as $Ly\text{-}6C^{hi}Ly\text{-}6G^{lo}$ (R4). We have previously showed that following the cell fixation procedure (using IC fixative) that the Gr-1 antibody (clone RB6-8C5) only recognizes the Ly-6G epitope on cells (241). Thus the staining with this antibody here are defined as $Ly\text{-}6G^{hi}$, rather than $Gr\text{-}1^{hi}$. As expected, at three hours there were significant increases in lung-sequestered neutrophils and inflammatory ($Ly\text{-}6C^{hi}$) monocytes in WT animals. However, consistent with the chemokine data, no differences between p55KO and WT strains were seen. Very interestingly the p75KO animals showed significantly more leukocyte infiltration.

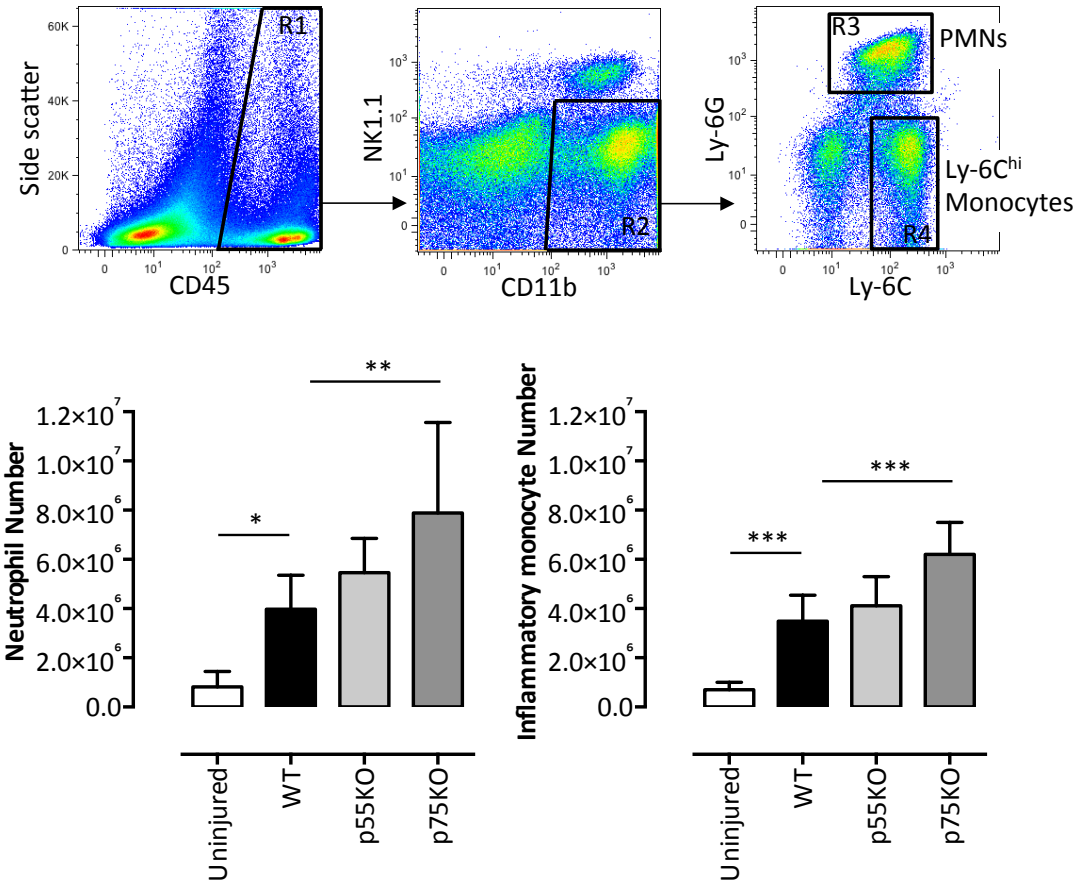

Figure 3.7. Differences in lung leukocyte numbers between strains after acid aspiration

Lung sequestered neutrophils and inflammatory monocytes were counted using flow cytometry on single cell suspension produced by mechanical disruption of the right lung. Leukocytes were gated as CD45 positive (R1). Myeloid cells (R2) were identified as $CD11b^{+}$ and $NK1.1^{-}$ (to exclude NK cell populations). Neutrophils were identified as Ly-$6G^{hi}$ (R3). Inflammatory monocytes were identified as Ly-$6G^{lo}$ and Ly-$6c^{hi}$ subset (R4). Acid aspiration leads to a significant increase in lung sequestered neutrophils and inflammatory monocytes in all groups. The p55KO group shows similar levels to WT animals. In contrast the p75KO group shows significantly higher levels of sequestered leukocytes as compared to WT animals. (N=5-7 per group; *** P<0.001 ** P<0.01 * P<0.05)

3.4.8 Histology

Histological analysis (figure 3.8) supported the flow cytometric evaluation. No differences were present in terms of leukocyte infiltration between WT and p55KO animals. However, p75KO lung sections showed substantial leukocyte infiltration. With respect to other measures of lung injury, p55KO animals seemed to have a

lower extent of alveolar wall thickening, intra-alveolar proteinaceous material, and alveolar oedema as compared with WT animals.

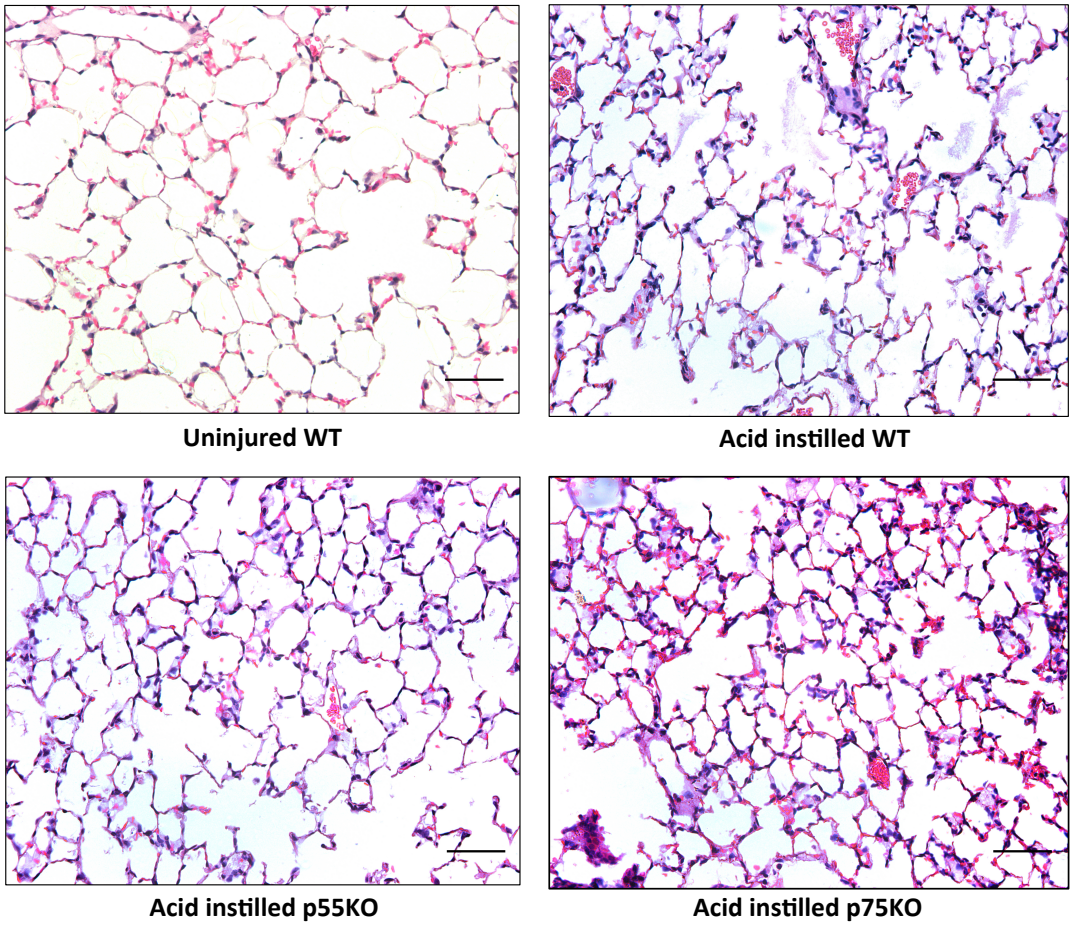

Figure 3.8. Lung histology after acid aspiration
H&E-stained sections (original magnification x200) of WT and p55KO animals at 3 hours after acid instillation. Acid instillation induces significant increases in alveolar wall thickening, intra-alveolar proteinaceous material, and alveolar oedema in WT animals. These parameters representing alveolar capillary barrier breakdown are reduced in p55KO animals, whereas leukocyte infiltration is present in all strains and to a greater extent in p75KO animals. Scale bar represents 50μm.

3.4.9 TNF receptor shedding and expression in blood monocytes and neutrophils

Acid aspiration led to a significant increase in soluble TNF receptor levels in the alveolar space as compared to saline controls (Figure 3.9 A). Consistent with previous data from our laboratory, the levels of soluble TNF receptors correlated well with alveolar protein concentration suggesting leak into the alveolar space from

the vascular compartment (Figure 3.9 B). Hence, TNF receptor expression was analysed on blood monocytes and neutrophils (potential sources of these receptors) to ensure a) that the phenotype of the strains matched their respective genotype, and b) that levels of expression of the non-deleted TNF receptor in the p55KO and p75KO strains were equivocal to WT animals expressing both receptors. Figure 3.10 confirms the strain phenotypes match the genotypes. It also shows that the cell surface expressions of the non-depleted TNF receptors in the genetically modified strains are similar to WT animals. Hence, differences in the levels of shed soluble TNF receptor and/or increased compensatory TNF signalling through an overexpressed non-depleted receptor do not explain the physiological effects seen.

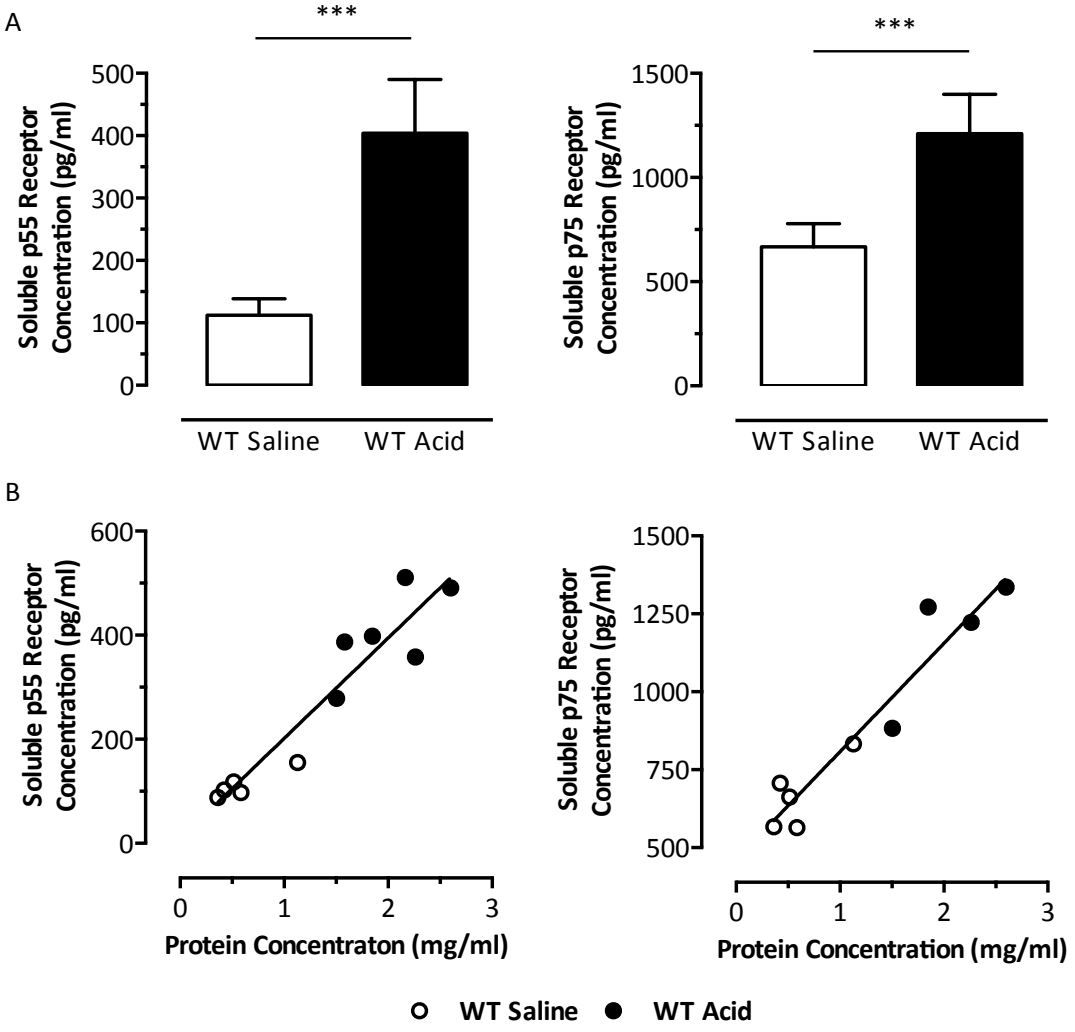

Figure 3.9. Soluble TNF receptor levels in alveolar lavage after acid aspiration
A) Acid-induced the production of the soluble forms for both p55 and p75 TNF receptors. (N=5-6 per group; *** P<0.001). B) The sources for these receptors are

predominantly from the plasma compartment as their levels shows strong significant correlations with the extent of protein leak (Pearson R = 0.995; P<0.0001).

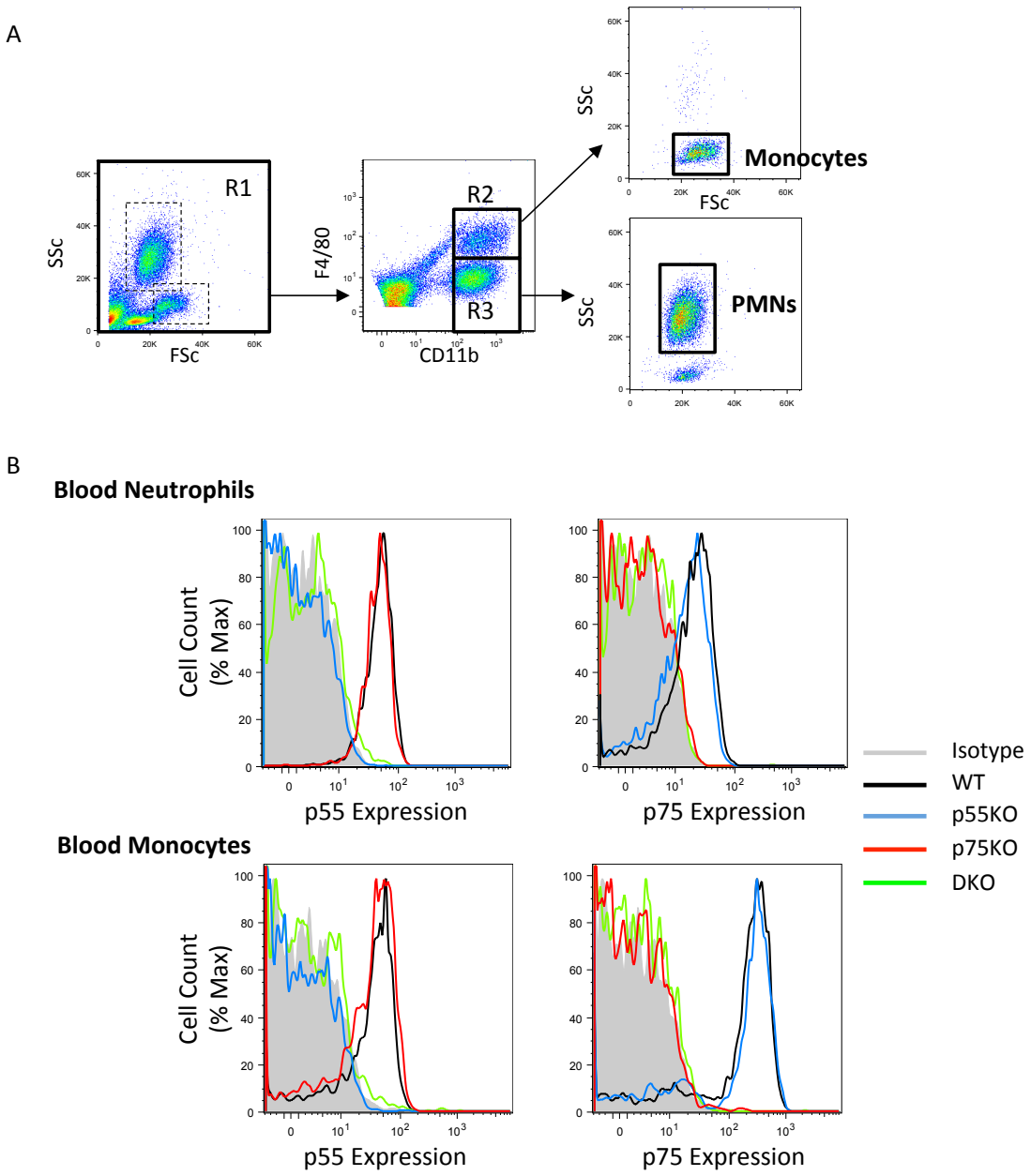

Figure 3.10. Cell surface TNF receptor expression on neutrophils and monocytes in all knockout strains

Given that the likely sources for the soluble TNF receptors in the lavage are vascular, TNF receptor expression was measured on blood leukocytes. A) Whole blood (R1) was processed for flow cytometric assessment. First CD11b positive cells were divided into F4/80 positive (R2 - monocytes) and negative (R3 - neutrophils). Neutrophils show a high side scatter as a consequence of their granular composition whereas monocytes are slightly larger (higher forward scatter) and less granular. B) WT animals had expression of both receptors with DKO animals having no receptors.

The levels of expression of p75 on p55KO and vice versa for p75KO are similar to WT animals. Monocytes showed a higher level of expression of cell surface p75 receptors as compared to neutrophils.

3.5 Discussion

There are some important observations and discussion points that arise from these physiology data with respect to the way in which oedema formation occurs immediately following acid aspiration:

1 The p55 TNFR has an impact on indices of alveolar-capillary barrier function.

2 The p55 TNFR mediates injury independent of downstream pro-inflammatory events.

3 The p75 TNFR impacts upon alveolar inflammation and lung leukocyte sequestration.

4 Finally, physiological disturbance occurs well before leukocyte infiltration into the alveolar space.

3.5.1 Mechanisms of oedema formation after acid aspiration

ARDS shows sudden deteriorations in gas exchange as a result of acute onset alveolar oedema. This is particularly true in the case of ARDS caused by gastric aspiration in which oedema can develop within hours in relation to the acidic nature of these contents. Although the signalling from within the alveolar space to the peri-capillary compartment is fast (39, 42, 85), leukocyte transmigration from the pulmonary microcirculation into the alveolar space occurs from 4 hours after acid aspiration (195). Kennedy and colleagues showed in a non-ventilated rat model of acid aspiration that the injury was of a biphasic pattern of injury. They hypothesised that the initial phase (1-2 hours) was a consequence of a direct physicochemical process and that the second phase (2-4 hours) was a consequence of an acute inflammatory response (195). The majority of studies utilising the acid aspiration paradigm of lung injury have investigated the second stage of early acid aspiration events (i.e. after 3 hours of insult).

However, the data presented in figure 3.1 shows that acid produces an immediate and sustained deterioration in respiratory mechanics in WT animals from 30 minutes, and at 90 minutes there is a worsening of the Ers, which likely represents the true development of alveolar oedema. Saline instillation, on the other hand, produces the same initial increase (at 30 minutes) but leads to immediate improvements by 60 minutes. The cause and nature of this immediate and sustained increase in Ers (0-90 minutes) after acid remains unknown and has received little attention. However, it is imaginable that the alveolar instillation of acid induces immediate contraction of smooth muscle within the conducting airways. Mitzner showed a significant contribution of airways calibre to changes in compliance (1/Ers) by adding methacholine to rabbit bronchial circulation (266) and Ewart showed a similar response to acetylcholine infusion in mouse lungs (240). An alternative explanation for the sudden change in elastance could be an early surfactant dysfunction causing increased alveolar recoil. However, this is unlikely as the instilled fluid is unlikely to be immediately delivered to the alveoli lining fluid, making a chemical reaction with surfactant leading to its dysfunction within 30 minutes unlikely. A further possibility could be alveolar fluid clearance with sustained AFC resulting in improvements of respiratory mechanics after saline instillation. Alveolar fluid clearance is performed by the epithelium of the distal conducting airways as well as the alveolus. Acid aspiration has been shown to impact upon alveolar fluid clearance but this has often only been measured at much later time-points i.e. after 4 hours (71, 255).

3.5.2 The TNF double edged sword – p55 versus p75 signalling

TNF has been implicated in sepsis induced ARDS since it was first discovered to have the same molecular structure as cachectin by Beutler and Cerami in 1985 (140). A number of studies have demonstrated an involvement of TNF in mediating acid aspiration-induced lung injury. Davidson et al (197) showed decreased albumin permeability index, lung myeloperoxidase activity (leukocyte infiltration) and improved PaO_2/FiO_2 after treatment with intra-tracheal anti-TNF antisera, in a rat model of acid aspiration. Other groups have identified a role for TNF in mediating

systemic injury following acid (196). However, in these model systems simply blocking the activity of TNF does not fully prevent the lung injury.

In contrast, in our experiments, animals with the specific deletion of the p55 receptor showed near complete abrogation of lung injury in oxygenation and respiratory mechanics. Additionally, animals with no TNF/TNF receptor signalling (i.e. DKO) have a similar, if not greater injury (with respect to respiratory mechanics) than WT animals. The physiological data support previous data from our laboratory showing protection (in respiratory mechanics, lung wet/dry weights, alveolar-capillary barrier permeability, and survival) with p55 TNFR blockade through genetic and pharmacological approaches in mice exposed to ventilator induced lung injury (224, 252).

The protective effect of p55 deletion in acid aspiration could not be explained by differences in available soluble TNF. Any difference in TNF bioavailability was important to exclude for two reasons. Firstly, p55 TNFR activation can induce NFκB transcription and induce TNF production and therefore its absence could reduce TNF upregulation in the alveolar space. Secondly, soluble TNF receptors are found in the alveolar space after acid aspiration and hence, could quench TNF, inducing significant alterations in TNF bioavailability between the experimental groups (150, 267). Soluble receptor levels were not measured in the lavage of knockout animals as the roles and relative contributions of each soluble TNF receptor (soluble p55 versus soluble 75) is uncertain and not within the scope of this work. Indeed, our laboratory has shown that pulmonary inflammation induces the release of soluble p75 TNFR from alveolar macrophages, whereas models showing significant alveolar epithelial permeability and pulmonary oedema lead to the upregulation of both soluble p55 and soluble p75 TNFRs in the alveolar space, as a consequence of leakage from the plasma (248). The correlation between protein and receptor levels in WT animals exposed to acid aspiration confirms the latter and hence, makes interpretation of alveolar soluble receptor levels difficult. Importantly, no differences between soluble TNF levels existed between experimental groups.

By contrast, the p75 TNFR seems to have a minimal role in oedema formation given that the p75KO strain showed similar degrees of alveolar capillary barrier dysfunction (wet/dry weight and permeability) to WT animals. Within these experiments in acid aspiration (as well as those from the VILI model above (224)), the conclusion that p75 TNFR signalling may be protective is based substantially on the significant exacerbation of respiratory mechanics in p75KO mice over WT. However, as the model was designed to induce a substantial amount of injury in WT mice, it was inherently easier to detect attenuation of injury than exacerbation of injury in most parameters. Hence, it remained uncertain as to how p75 TNFR deletion transduces changes in physiological responses such as Ers, PIP and Rrs. One possible explanation may come from the p75KO group having greater inflammatory responses with respect to the macrophage-derived cytokine IL-6 and neutrophil/monocyte recruitment.

Peschon and colleagues developed the genetic strains used in our work by inserting neomycin cassettes within the encoding genetic sequence of the TNF receptors (220). Using these knockout strains, Peschon et al was the first to suggest divergent physiological roles for the TNF receptors in models of sepsis and lung inflammation. Their data showed that p75KO mice continued to be susceptible to septic shock whereas p55KO mice showed protection. It was not until the development of these knockout strains that the precise effects of TNF signalling through its receptors could be elucidated. Studies prior to this utilised agonist and antagonist antibodies with variable affinities and effects. More recent studies utilising these strains have found divergent roles for the TNF receptors in a variety of models including myocardial infarction (223), septic shock (221), retinal ischaemia (162), cardiac transplantation (222), acute kidney rejection (268), and VILI (224). However, the mechanisms remain obscure. Interestingly, all these studies describing such opposing effects of the individual TNF receptors, irrespective of the model being tested, draw the same inference regarding their relative roles (i.e. p55 TNFR is injurious, p75 TNFR is protective).

3.5.3 TNF receptor expression in lung cells

To begin to dissect this differential effect of the two receptors for TNF, it is important to discuss the receptor expression on different cells within the lung. There is continuing debate as to the cell specific expression of TNF receptors within the lung. Liu et al used flow cytometry to show that epithelial cells (MLE-Kd) and rat primary type 2 AECs express both p55 and p75 TNFRs and that cell surface expression of the p75 TNFR is lower than p55 TNFR (269). Ermert and colleagues showed using immunolocalisation that alveolar septa have undetectable p55 TNFR and weak p75 TNFR expression in rat and human lungs (270). This study also found moderate localisation of both receptors on alveolar macrophages. It has been recently shown by our laboratory using flow cytometry that pulmonary endothelial cells have greater expression of the p55 TNFR compared to the p75 TNFR and that the p55 TNFR plays a dominant role in TNF-mediated pulmonary microvascular dysfunction (201). Dorr et al showed that alveolar macrophages have higher p75 TNFR surface expression than p55 TNFR expression. Of note, this study showed that in direct inflammatory insults, depletion of alveolar macrophages leads to a reduced amount of alveolar soluble p75 TNFR, suggesting this cell type contributes significantly to the effects mediated by soluble p75 TNFR (248). The evidence thus far is weighted towards ubiquitous expression of TNF receptors in the pulmonary endothelium, alveolar epithelium and alveolar macrophages but with p55 TNFR being highly expressed on lung parenchyma and p75 TNFR being highly expressed on leukocytes.

These data are most easily explained by oedema formation occurring specifically through signalling via the p55 TNFR. Furthermore, in light of the possible opposing protective effect conveyed by the p75 TNFR, it was important to confirm that no differences existed in surface expression of TNF receptors between uninjured knockout and WT strains (i.e. p75 receptor expression in p55KO animals; and p55 receptor expression in p75KO animals are the same as expression of both receptors in WT animals). To do so, TNF receptor expression in blood neutrophils and monocytes was measured. Although this expression was not comprehensively examined in all cell types, the data suggests that overexpression of the undeleted

receptor does not account for any physiological differences observed. In summary, precisely which TNF receptor signalling predominates in any given scenario is likely to be a complicated situation governed by the tissue specific expression level of each receptor (as previously discussed), which may be upregulated at the transcriptional/translational level, or downregulated by the action of sheddases (271, 272).

3.5.4 Oedema formation occurs through the p55 TNF receptor and independent of pro-inflammatory effects

Ligation of the p55 TNFR by TNF has two broad consequences with respect to signalling events. The first is the formation of complex I on the cell surface leading to the activation of MAPK-induced gene transcription through the activation of the transcription factor NFκB. These signalling pathways drive the 'pro-inflammatory' consequences of TNF ligand leading to cytokine/chemokine upregulation, endothelial cell adhesion molecule expression, and leukocyte transmigration. The alternative event that can occur as a consequence of TNF binding to the p55 TNFR is the activation of 'death-signalling' through the formation of complex II. The physiology data show that the p55 TNFR plays an important direct role, 'independent' of downstream inflammatory consequences, in mediating the injurious effects of TNF on the alveolar-capillary barrier.

Given this overwhelming evidence for the role of p55 TNFR signalling in leukocyte recruitment it was surprising that there was no reduction in inflammation within the p55KO group, albeit at very early stages of lung injury. Furthermore, a multitude of experimental studies have investigated the roles of neutrophils and mononuclear cells in mediating alveolar capillary barrier dysfunction in acid aspiration (260, 273). The importance of p55 TNFR signalling in early leukocyte sequestration has also been suggested (39, 85).

Flow cytometric analysis of lungs found significant numbers of inflammatory leukocytes sequestered within the lung after acid aspiration but these had not transmigrated into the alveolar space. Most interestingly, the p55KO animals

showed significant physiological protection but had comparable leukocyte numbers within the lung. This is consistent with the study by our laboratory looking at the role of TNF receptors in VILI (224). At 2 hours after onset of high stretch ventilation, Wilson et al found minimal alveolar neutrophilia and no difference in lung myeloperoxidase activity between WT and p55KO strains exposed to high stretch ventilation, despite the p55KO group showing profound physiological protection. Finally, WT animals died from 90 minutes producing a 25% survival rate at 2 hours, whereas p55KO mice showed 100% survival by the end of the protocol. Such profound differences in respiratory physiology further question the role and implication of neutrophil mediated inflammation driving the pathogenesis of alveolar oedema early in ARDS.

Additionally, many studies also show that physiological deterioration occurs prior to significant neutrophil infiltration within the lung suggesting that the neutrophilic infiltration may be a consequence of, as opposed to, the mechanism for injury. For instance, Matt and colleagues showed significant elevations in BALF total protein levels at 4 hours in a model of acid aspiration but minimal neutrophil infiltration into the alveolar space (274). Additionally, oedema can form in the absence of neutrophils, for instance, in neutropenic patients (94, 275).

One explanation for the equivalent amounts of 'inflammation' between genetically modified animals could be explained by chronic compensation and this may account for the non-dependence on the p55 TNFR in leukocyte sequestration in p55KO animals. Indeed, acute blockade of p55, by Bertok et al (252), using a domain antibody shows attenuation in oedema as well as inflammation in a two-hit mouse model of endotoxin plus VILI.

3.5.5 The p75 TNF receptor – a potential alveolar inflammatory rheostat

The p75KO animals show worse respiratory mechanics and increased leukocyte recruitment to the lung. Very little is known about the downstream intracellular signalling and functional consequences of p75 TNFR ligation (in comparison to p55 TNFR ligation). The p75 TNFR pathway has been thought to play the role of "ligand

passing" exacerbating p55 TNFR signalling (152). If this were the case in these data one would expect a protective effect in the p75KO group. Additionally, as discussed, the p75 TNFR plays a role in sequestering excess TNF through its soluble receptor form. A significant proportion of alveolar soluble p75 TNFR comes from shedding from the cell surface of alveolar macrophages given that their depletion (by clodronate liposomes) significantly attenuates soluble p75 levels in endotoxin induced lung inflammation (248). While one explanation for this protective role of p75 TNFR could be that this 'quenching' effect on TNF ligand is important to limit signalling through the 'injurious' p55 TNFR, this does not adequately explain these data. If the p75 TNFR simply had such a modulating role, then the 'double knockout' (DKO) animals should show some protection, which was not the case. In contrast, the increased injury in DKO animals suggests that p75 TNFR signalling per se likely induces some protective effect.

Interestingly, the study performed by Peschon and colleagues also showed that neutrophil trafficking into the lung was increased in p75KO animals. Increased activation of the lung endothelium in p75KO strains does not explain the increased recruitment of leukocytes. Bertok et al that showed that lung endothelial cell adhesion molecule (CAM) upregulation (VCAM-1, E-selectin, ICAM-1) during intravenous TNF injection was dependant predominantly on the p55 TNFR. Furthermore, Bertok showed that the lung endothelium has a higher expression of the p55 TNFR versus the p75 TNFR and, within 2 hours of intravenous LPS challenge, the p55 TNFR is shed whereas the p75 TNFR remains stable (201).

In addition, the consequences of p75 TNFR activation may be different depending on the specific cell type on which it is activated and hence, its role within the alveolar space may be very different to that on the endothelium. In direct forms of lung injury, alveolar macrophages have been shown to release TNF and induce the intrapulmonary activation of NFκB, leading to cytokine/chemokine elaboration, with subsequent leukocyte recruitment into the lung (81, 276, 277). The p75 TNFR is highly expressed on alveolar macrophages (248, 278). TGFβ has been shown to upregulate p75 TNFR expression on peritoneal macrophages and TNF signalling

through the p75 TNFR has been shown to induce tolerogenic anti-inflammatory properties in these macrophages (279). Hence, It is possible that the p75 TNFR inhibits the release of pro-inflammatory mediators from alveolar macrophages. This would explain the tendency for increased IL-6 production in p75KO as compared with WT animals (figure 3.6). It is possible that the p75 TNFR makes alveolar macrophages tolerant to any overwhelming insult, such as acid aspiration, delivered to the alveolar space.

Furthermore, the proliferation and function of $CD4^{+}CD25^{+}$ T-regulatory cells, that have recently been shown to promote resolution of lung injury (98), is mediated by p75 TNFR ligation (280). This receptor has been shown to induce maximally anti-inflammatory suppressive effect of this subset of regulatory T-cells (281). Finally, p75 TNFR mediated gene transcription leads to the expression of genes coding for anti-inflammatory molecules such as adrenomedullin, GM-CSF and IL-10 in brain microglia in response to various inflammatory stimuli (282).

Intratracheal instillation of TNF has been shown to induce airway hyperresponsiveness through a receptor dependant manner. A possible explanation between the increased respiratory resistance and inflammation seen in p75KO animals may be provided by a study investigating airway hyperresponsiveness to methacholine in mouse model of airway inflammation (283). This study by Kanehiro et al showed that TNF is upregulated in an ovalbumin model of allergy and signals specifically through the p75 TNFR on γδ T-cells to downregulate airway inflammation and hyperresponsiveness. Hence, investigation into p75 TNFR activation within the bronchial walls and alveolar spaces in direct forms of ARDS could be a potential important therapeutic strategy to prevent the overzealous inflammation, and reduce the derangements in respiratory mechanics that occurs in ARDS.

3.6 Concluding remarks

Despite extensive research over the span of what is now nearly 30 years, no TNF based biological therapies have been found to treat ARDS whereas chronic

conditions such as rheumatoid arthritis and Crohn's disease have found successful clinical translation. Unfortunately, therapeutic strategies in critical illness to target the deleterious effects of TNF have been non-specific and prematurely conducted with the absence of mechanistic insights. For instance, many compounds targeting TNF quench the total activity of TNF – 'good and bad' – as opposed to the specific signalling pathways that lead to its 'toxic' effects. The possibility that the two receptors for TNF could have very different functionalities remained ignored until very recently. Overall, the physiological data in this clinically relevant experimental model of ARDS suggests that global blockade is unlikely to have a positive therapeutic effect (as DKO strains remained injured), whereas more sophisticated therapeutic blockade of the p55 TNFR at the endothelial/epithelial junction and/or enhancement of the p75 TNFR (possibly on alveolar macrophages/monocytes) may prove beneficial.

In view of the significant protection conveyed by p55 TNFR deletion the remainder of this thesis now focuses on this receptor. Furthermore, this receptor is potentially amenable to therapeutic blockade using a novel p55 targeted domain antibody as has been recently published by Bertok et al (252).

4 Activation of alveolar epithelial p55 TNF receptor death signalling in acid-induced lung injury

Abstract

TNF has consistently been implicated as the quintessential pro-inflammatory cytokine. However, chapter 3 showed that the effects of p55 and p75 TNFR signalling seem very diverse, even opposing. Furthermore, downstream, cellular or molecular inflammatory events could not explain the protection observed from acid aspiration in p55KO animals. Hence, I hypothesised that an alternative p55 TNFR signalling pathway may explain how it mediates pulmonary oedema formation.

The major difference between the p55 and p75 TNFRs is the ability of the p55 TNFR to signal through its intra-cytoplasmic death domain, and hence this extrinsic 'death signalling' pathway was investigated. The activity of a cysteine protease (caspase-8) involved in activation of the death domain (and formation of the death signalling inducing signalling complex) was measured as an index of p55 TNFR death domain activation. Indeed, lungs from p55KO animals were found to have significantly lower levels of caspase-8 activation and in WT animals this activation occurred within 90 minutes of acid instillation. Interestingly, in injured WT animals only 1-2% of alveolar cells showed signs of late stage apoptosis (positive TUNEL staining) after 3 hours, despite significant caspase-8 activation and in the presence of severe physiological dysfunction.

A soluble marker of epithelial injury called receptor for advanced glycation end-products (RAGE) was measured and found to be reduced in p55KO animals, implicating an injurious effect of the p55 TNFR on the alveolar epithelium. A novel flow cytometry based caspase-8 assay was developed to determine that p55 TNFR mediated caspase-8 activation occurred specifically in type 1 AECs.

Multiple studies have implicated the importance of the alveolar epithelium as an integral layer preventing the formation of pulmonary oedema. Data in this chapter shows that p55 TNFR mediated caspase-8 activation occurs within the type 1 epithelium prior to completed cell death. This implicates the activation of the p55 TNFR death domain and signalling through caspase-8 as the mechanism by which this receptor mediates oedema formation.

4.1 Introduction

ARDS is primarily characterised by a disruption in alveolar-capillary barrier function with increased endothelial and epithelial permeability, ultimately leading to flooding of the alveolar space. Although the capillary endothelium prevents high molecular weight proteins and plasma to leak into the interstitium, the alveolar epithelium is an essential layer that has to be breached for alveolar oedema to develop. In the 1970's, Schneeberger et al showed that bidirectional movement of low molecular weight proteins (such as HRP) is restricted by the zona occludens junctions found between alveolar epithelial cells (284-286). Gorin and Stewart showed in a seminal study that the alveolar epithelial layer provides the greatest resistance (greater than 92%) to the flux of proteins from the circulation to the alveolar space (38). The lung epithelium also has a dual role in not only preventing oedema formation but also actively clearing it from the alveolar space. Firstly, the tight junctions that bind epithelial cells together prevent fluid from entering the alveolar space. Secondly, the alveolar epithelium is a crucial controller of the water content and constitution of alveolar lining fluid. This function is performed through the net active transport of sodium out of the alveolar space into the interstitial space and hence creating an electrochemical gradient for water absorption. This specific function of the alveolar epithelium known as alveolar fluid clearance (AFC) is crucial for the resolution of alveolar oedema during lung injury states (69).

Chapter 3 showed that pulmonary oedema development during the early phase of acid aspiration was mediated specifically through the p55 TNFR, and not the p75 TNFR. Surprisingly, there remained significantly high levels of lung inflammation (to a similar level as WT animals) in p55KO animals. Hence, the data shows two fundamental aspects of TNF-induced alveolar-capillary barrier dysfunction. Firstly, it is independent of p55 TNFR pro-inflammatory signalling, and secondly, that it occurs through non-neutrophil mediated mechanisms (given that injury occurred early when no alveolar neutrophilia was present). In addition, the significant maintenance of barrier function in p55KO animals turned the attention for subsequent

experiments towards the alveolar epithelium, which as discussed has been suggested to be the most important defence against the exudative phase of lung injury (43, 44, 46, 287).

The mechanism through which epithelial injury is induced in ARDS remains obscure although more recently has been shown to occur through apoptosis mechanisms (288). However, the majority of these studies have focussed at much later time-points (>6 hours) compared to the physiological dysfunction seen in our model of acid aspiration (60-120 minutes). Unlike the p75 TNFR, the p55 TNFR has an intracytoplasmic death domain and is a member of the death receptor family along with 5 other receptors including Fas receptor (Fas), TNF-related apoptosis inducing ligand (TRAIL) -1 and -2, death receptor (DR) -5, and -6. Much of the literature has focussed on mechanisms through which the Fas ligand/Fas interactions have contributed to epithelial injury (56, 57, 59, 289-295) and TRAIL has also been associated in influenza virus induced lung inflammation (66).

Ligation of the p55 TNFR leads to the recruitment of a number of death domain proteins with the activation of caspase-8 through the formation of a cytoplasmic death inducing signalling complex (DISC). Importantly, the p75 TNFR has no capability of directly activating caspase-8, as it does not possess a death domain. There is a paucity of literature investigating TNF-induced apoptosis in lung injury in comparison to the pro-inflammatory effects of the cytokine, namely, pulmonary capillary endothelial activation with subsequent recruitment and activation of blood-derived leucocytes (201, 252, 296-303). The p55 TNFR has been shown very recently to mediate injury through apoptosis in radiation-induced lung toxicity (62), chest trauma-induced lung injury (65), renal ischaemia induced lung injury (64), and febrile endotoxin-induced lung injury (63, 304). Over the period of this thesis, Maniatis et al showed that p55 TNFR can induce caspase-3 activation in acid aspiration at 24 hours in addition to pro-inflammatory signalling (305). Hence, in view of increasing evidence for TNF-induced apoptosis in various lung injury models, and that specific signalling through the p75 TNFR had no impact upon the physiological consequences of acid-induced lung injury, all subsequent experiments were focussed to examine

whether the injurious mechanism of p55 TNFR signalling within this model was mediated through the activation of the extrinsic apoptotic pathway, and how this induced the significant physiological dysfunction observed.

4.2 Aims

The significant role of the p55 TNFR pathway in promoting alveolar oedema seemed independent to its downstream inflammatory consequences. Hence, the alternative p55 TNFR 'death' signalling pathway was hypothesised to induce oedema formation. Hence, this chapter seeks to determine 1) the extent, and 2) the localisation of apoptotic cell signalling and death after acid aspiration and determine if this is dependant upon the activation of the p55 TNFR.

4.3 Experimental design

4.3.1 In vivo model

WT and p55KO underwent aspiration of 50µl of 0.15M HCl followed by mechanical ventilation for 90 or 180 minutes. The same experimental set-up was used, as described in chapter 3.

4.3.2 Analysis of alveolar mediators

At the end of the protocol right lungs either underwent unilateral lavage to attain BALF, and left lungs of animals were snap frozen in liquid nitrogen and stored at -80^{o}C for caspase analysis. Markers of epithelial and endothelial injury were measured in BALF by ELISA.

4.3.3 TUNEL analysis

In some experiments, left lungs of some animals were also inflated at a transpulmonary pressure of 15cm height of 4% paraformaldehyde. Lungs were subsequently processed for paraffin embedding and sections attained for terminal deoxynucleotidyl transferase–mediated dUTP nick end-labeling (TUNEL) assay using the TACS in situ Apoptosis Detection Kit, in accordance with manufacturers instructions.

4.3.4 Measurement of apoptosis signalling

Measurement of caspase activity in lung homogenate

Caspase activity was measured in lung homogenates through the detection of the cleavage of a specific substrate: IETD-AFC for caspase-8, and LEHD-AFC for caspase-9. Whilst the conjugated 7-amino-4-trifluoromethyl coumarin (-AFC component) emits blue light (λmax = 400nm), upon cleavage by the relevant caspase, the free -AFC emits yellow-green light (λmax = 505nm) and hence, activity of caspases can be quantified using a fluorescent plate reader. The left lung was snap frozen and homogenised in the cell lysis buffer provided. During the homogenisation process and until the point of incubation with the substrate all samples were kept on ice to minimise any changes to caspase-8 activity. The homogenate, substrate, and reaction buffer were incubated at 37^{o}C and then the fluorescence read after a 60-minute incubation.

Flow cytometric localisation of caspase-8 activity.

In another series of experiments, lungs were instilled and incubated with dispase for 30 minutes at room temperature, after which they were minced gently and washed. They were subsequently incubated for 60 minutes with a cell permeable caspase-8 probe: FAM-IETD-FMK. The probe again utilised the specific caspase-8 substrate sequence - IETD. The unfixed single cell suspension was incubated with this probe for 60 minutes at 37^{o}C with regular 10-minute vortex to facilitate mixing. The IETD sequence is cleaved by active caspase-8 and the probe forms a permanent covalent sulfhydryl bond with the active caspase-8 (using the FMK moiety) and the FAM moiety allows it to be detected in the FITC channel of the flow cytometer. After a wash step the cell mixture was incubated in DMEM/HEPES to allow the unbound probe to freely diffuse out of the cells. After this step, cells were incubated with antibody stock (to identify leukocytes, pulmonary endothelial cells, and type 1 alveolar epithelial cells) to allow cell specific detection of caspase-8 activation within the same sample.

4.4 Results

4.4.1 Acid aspiration induces epithelial injury.

Acid aspiration leads to significant barrier disruption through a predominant impact on epithelial function (37, 42, 306, 307). The type 1 AEC determines 95% of the alveolar cell surface area. The receptor for advanced glycation end-products (RAGE) has been shown to be a specific marker for type 1 AECs (308). Lavage RAGE levels were significantly increased at 3 hours in WT animals after acid aspiration (figure 4.1 A). In contrast levels were significantly lower in the p55KO strain, confirming that injury to type 1 AECs was mediated through activation of the p55 TNFR death signalling. Furthermore, an endothelial marker, endocan (309), was also found to be upregulated after acid aspiration in lavage fluid, but no such reductions were seen in p55KO animals, suggesting that the p55 TNFR is mediating injury specifically through an impact upon the alveolar epithelium (figure 4.1 B). We hypothesised that this epithelial injury was mediated through the activation of p55 TNFR dependant apoptosis pathways.

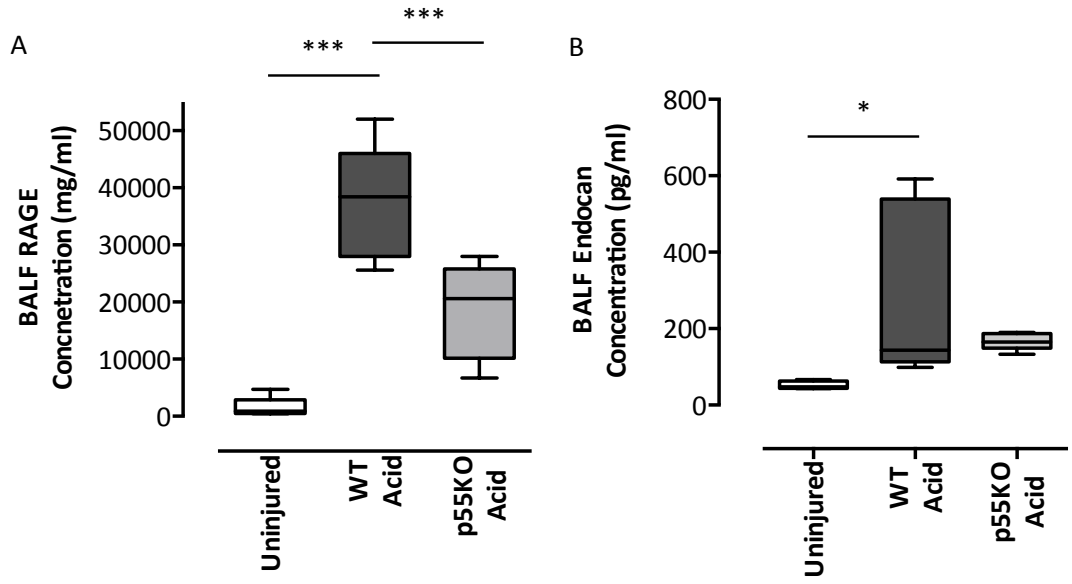

Figure 4.1. Epithelial and endothelial markers of injury in WT and p55KO strains
Levels of receptor for advanced glycation end-products (RAGE), as a specific marker of injury to type 1 AECs, was upregulated at 3 hours, and showed substantial attenuation in p55KO animals, confirming that the p55 TNFR caspase-8 activation induced epithelial injury (A). In contrast, levels of the endothelial marker endocan were upregulated in the alveolar space but showed no difference with p55 deletion (B). (N=6-10; *P<0.05; ***P<0.001).

4.4.2 Lung oedema formation is not explained by completed apoptosis of alveolar cells

One of the most commonly utilised assays for detecting apoptosis is the terminal deoxynucleotidyl transferase–mediated dUTP nick end-labelling (TUNEL) assay. A histological based TUNEL assay was used to detect any DNA fragmentation and condensation suggestive of end stages of apoptotic cell death. In combination with strict morphological evidence i.e. DNA condensation within the nucleus, reliable detection of apoptosis can be performed. The TACS in situ Apoptosis Detection Kit has been used for histological assessment in paraffin embedded lung sections (310).

Acid aspiration produced a subtle but detectable increase in TUNEL positive cell number at 3 hours, compared to control. However, this was in the order of less than one apoptotic nucleus per high power field, out of an average 80 nuclei that were present per field (figure 4.2). When DNA breaks were induced in uninjured sections through the application of a DNAse enzyme, all nuclei stained DAB positive confirming that the protocol was suitable for nuclear staining and that technical issues were not responsible for the lack of TUNEL staining in injured animals (figure 4.2 B). It was difficult to discern the specific cell types stained positive for TUNEL but one criterion for assessment was that they all be located on the alveolar walls. Interestingly, p55KO animals did show a reduced apoptotic index when compared to WT animals suggesting that this receptor indeed plays a role in the development of cell death during lung injury (figure 4.2 D). However, acid aspiration at 3 hours produced a significant amount of alveolar oedema and physiological dysfunction. These data, showing a very low percentage of TUNEL positive cell death, cannot explain such physiological dysfunction and injury.

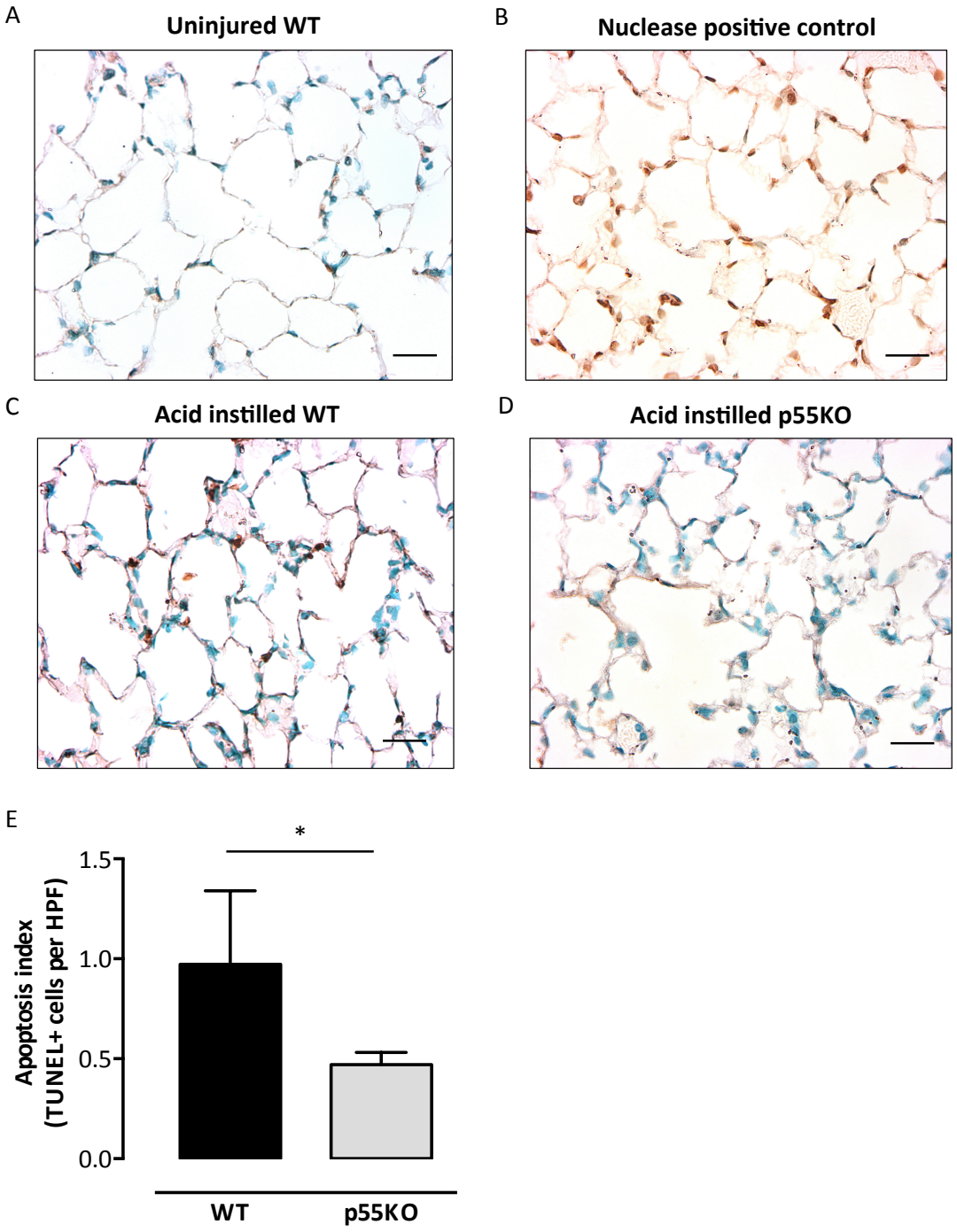

Figure 4.2. TUNEL staining at 3 hours after acid aspiration

(A) TUNEL staining of lung sections showed undetectable staining in uninjured animals. (B) The addition of DNAse to lung sections (to actively induce DNA strand breaks as a positive control) illustrates the maximal number of nuclei that can be stained (≈80 TUNEL positive cells/HPF). (C) TUNEL staining in sections of lungs taken 3 hours after acid aspiration shows some TUNEL positive events which, (D) was partially reduced in p55KO animals. (E) However, although a statistically significant reduction was seen in p55KO strain compared to WT group, the levels of TUNEL

positive nuclei were less than 1 per HPF, implying minimal cell death despite severe physiological injury. (N=5; * P<0.05)

4.4.3 TNF p55 receptor activates caspase-8 'death signalling' in lungs after acid aspiration

The TUNEL data presented a significant disparity between the levels of morphological apoptosis (i.e. 1-2%) and the severity of injury that was apparent in WT animals at this 3-hour time-point. DNA degradation as shown by positive TUNEL stain is the final event of cell death. A number of apoptosis signalling pathways (intrinsic and extrinsic) can lead to the stage of cell death detected by TUNEL. Hence, to determine which pathway of death signalling had been activated, caspase-8 (extrinsic) and caspase-9 activity (intrinsic) were measured in lung homogenates at three hours after acid aspiration. There was a 1.7 fold upregulation in lung caspase-8 activity in the WT group as compared to uninjured animals (figure 4.3 A). Furthermore, this upregulation in caspase-8 activity was significantly reduced by 61% in the p55KO group placing p55 TNFR as the major death receptor responsible for the early activation of caspase-8. The observation that cells did not have to be dead for physiological dysfunction to occur suggested that the p55 TNFR caspase-8 signal itself may have driven the downstream mechanisms leading to the physiological dysfunction.

4.4.4 Caspase-8 activation occurs early in experimental lung injury

Caspases are intracellular serine proteases that are pre-formed. Upon binding of TNF to the p55 TNFR complex it is endocytosed within minutes leading to the recruitment of intracellular adaptor proteins (TRADD and FADD) facilitating the recruitment of caspase-8 (311). Indeed, caspase-8 activity was measured at 90 minutes given that significant separation in oxygenation and respiratory mechanics were already apparent at this time between WT and p55KO groups (figure 3.3). These earlier measurements found caspase-8 activity to be twice as high at 90 minutes in comparison to 3 hours in WT animals (figure 4.3 B). Although not measured there would likely have been an even lower extent of TUNEL positive cells at 90 minutes providing further support that the activation of death signalling per se could have induced the substantial physiological dysfunction observed. There was no

such upregulation in caspase-9 activity (at 3 hours) suggesting the extrinsic pathway (mediated through death receptor activation) and not the intrinsic pathway had been activated after acid aspiration (Figure 4.3 C).

Furthermore, at this earlier time point the levels of neutrophil/monocyte sequestration would be even lower, further substantiating that the signal to activate caspase-8 likely came from the alveolar compartments and that the mechanisms for oedema formation were independent of blood derived leukocytes. The higher caspase-8 signal and the separation in respiratory physiology between WT and p55KO animals prompted all further measurements to be performed at this early time point of 90 minutes.

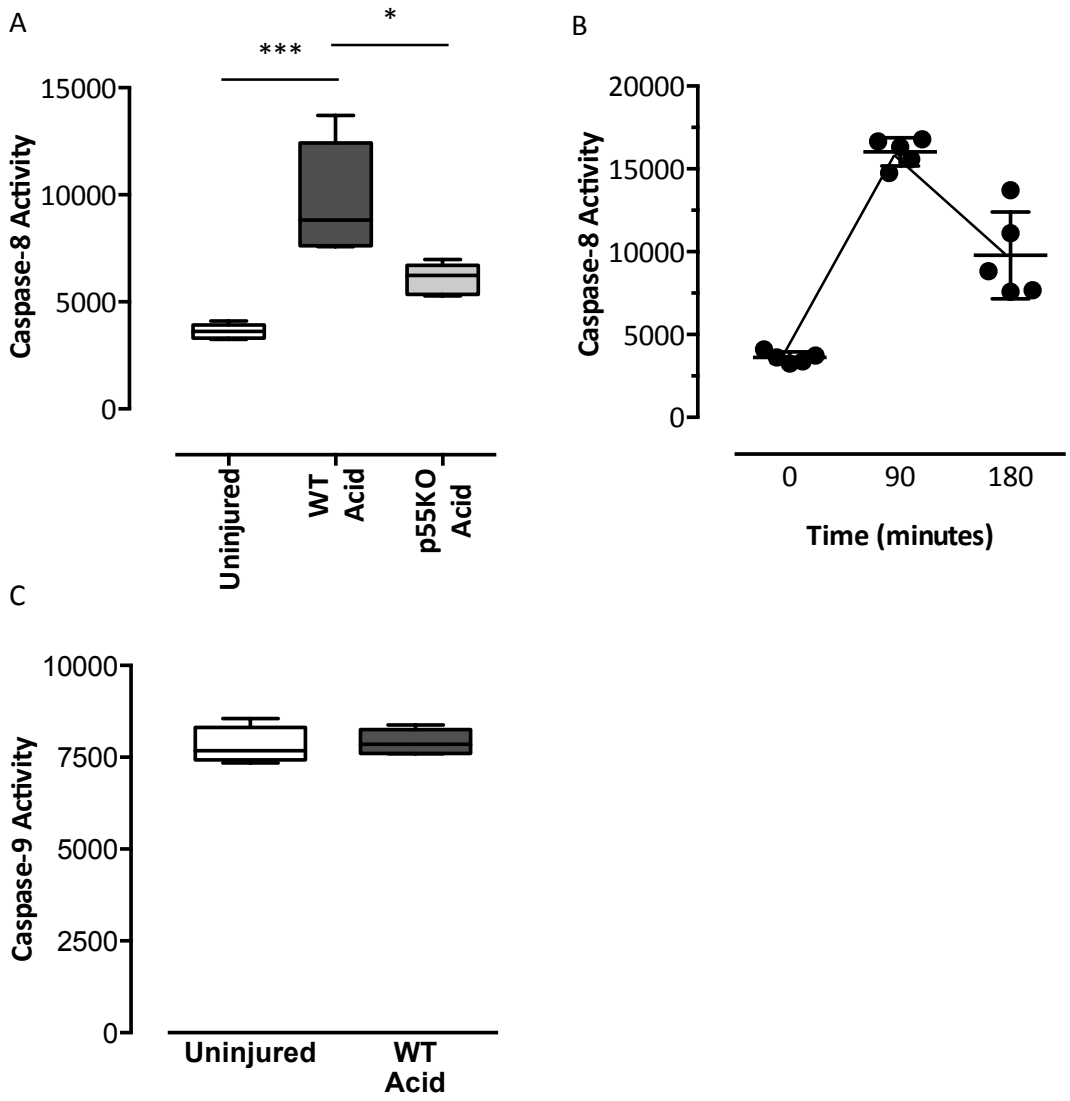

Figure 4.3. Caspase-8 and -9 activity in lung homogenates after acid aspiration
Despite the low numbers of end-stage cell death as assessed by the TUNEL assay, there was a significant activation of the extrinsic death pathway (as measured by caspase-8 activity) in WT injured animals (A). This increase in caspase-8 activation was significantly attenuated (by 61%) in p55KO animals confirming that the p55 TNFR contributes to death signaling activation in acid aspiration. Furthermore, caspase-8 activity in WT animals is higher levels at the earlier time-point of 90 minutes, suggesting that TNF-induced caspase-8 activation is an early phenomenon and may explain the early physiological dysfunction. In contrast, the intrinsic pathway (as measured by caspase-9) remains unaffected by acid aspiration at 3 hours (C). (N=5; * $P<0.05$ *** $P<0.001$)

4.4.5 Localisation of caspase-8 activity

To gain a deeper understanding into how p55 TNFR /caspase-8 signalling mediated oedema formation, it was important to determine the exact cell types in which this caspase-8 signal occurred. A flow cytometric caspase-8 assay was adopted instead of a histological approach for two reasons. Firstly, flow cytometry enables a more quantitative assessment of caspase-8 activity. Secondly, through the use of multiple antibodies (and positive and negative gating strategies) the analysis of caspase-8 activation in various cell types (see below) could be identified in each experiment within the same sample.

Caspase-8 activity in the WT injured lungs was measured using a fluorescent caspase-8 probe (FMK-IETD-FAM). The caspase-8 specific IETD moiety is conjugated to a fluorescent FAM moiety and an FMK moiety. The probe is lipid soluble and freely permeates into and out of cells. Any activated caspase-8 binds and cleaves the IETD sequence and the proximity of the compound leads to the formation of a permanent covalent bond between the active caspase-8 and the FMK moiety. After washing unbound probe out of the cell, flow cytometry was used to quantify the FAM signal (in the FITC channel) of the bound caspase-8-FMK-IETD-FAM complex retained within the cell. This was applied to unfixed cell suspensions from dispase treated lungs to avoid the loss of caspase-8 activity through formaldehyde fixation. Hence, lungs were digested in a standardised fashion through the intra-tracheal instillation of dispase as previously described. Furthermore, as lungs were minced gently the lung parenchyma was teased away from the main bronchi to enable ideal preparation of distal lung cells.

The lung cell suspension was subsequently incubated with the caspase-8 probe. The probe required incubation at 37^{o}C for binding and removal of unbound dye for 60 minutes. Every other stage of the protocol was performed on ice with ice-cold reagents, thereby, minimising alterations in cellular caspase-8 activity. Three main cell types were analysed – alveolar epithelium, pulmonary capillary endothelium, and leukocytes. We focussed our cellular localisation to type 1 AECs as they have distinct membrane bound cellular identification marker (EpCAM and T1-alpha)

whereas type 2 cells require permeabilisation for detection of intracellular molecules such as surfactant protein C. This permeabilisation process could have affected the caspase-8 signal and promoted loss of intracellular molecules as well as bound probe. Leukocytes were identified as $CD31^{-}EpCAM^{-}T1alpha^{-}CD45^{+}$ cells, endothelium as $CD45^{-}Epcam^{-}T1alpha^{-}CD31^{+}$, and type 1 AECs as $CD45^{-}CD31^{-}EpCAM^{+}T1alpha^{+}$ cell populations. The gating strategy is shown in figure 4.4 A.

Caspase-8 activity was localised specifically to type 1 AECs and this activity was 8-fold higher in injured as compared to uninjured animals (figure 4.4 B). In contrast, pulmonary capillary endothelium and leukocytes showed a 10-fold and 40-fold lower level of caspase-8 activity, respectively, and did not show any increase during injury.

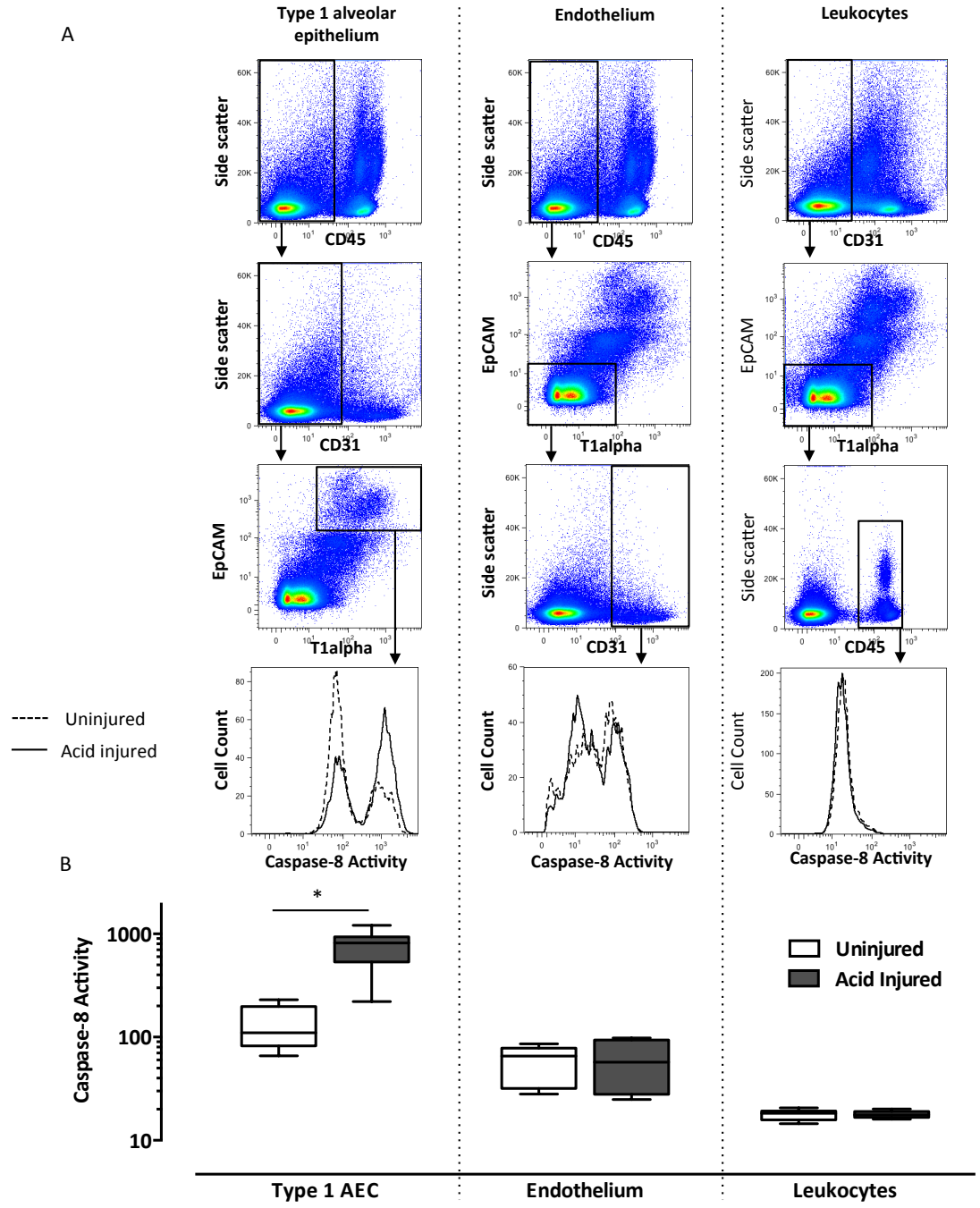

Figure 4.4. Flow cytometric analysis of cell specific caspase-8 activity after acid aspiration

Flow cytometry was used to localise and quantify caspase-8 activation in the lung. After labelling with the FAM-IETD-FMK caspase-8 probe and relevant antibodies, lungs were analysed using the above gating strategies (A). Firstly, debris was excluded using forward and side scatter, and three main cell types were identified – Type 1 AECs as $CD45^{-}CD31^{-}EpCAM^{+}T1alpha^{+}$; endothelial cells as $CD45^{-}Epcam^{-}T1alpha^{-}CD31^{+}$; and leukocytes as $CD31^{-}EpCAM^{-}T1alpha^{-}CD45^{+}$. Caspase-8 activity was localised predominantly to the alveolar epithelium, and this cell type showed a 8-fold increase in activity in injured animals. The epithelium also showed a 10-fold

higher expression than endothelium and leukocytes, neither of which showed any upregulation during injury. (N=6; **P<0.01).

4.5 Discussion

Although, studies have implicated TNF to induce neutrophil sequestration in ARDS and increase the severity of injury (302, 312), others have shown TNF-induced oedema formation to be independent of neutrophils (199). Endothelial activation and subsequent neutrophil recruitment can also increase endothelial/epithelial permeability through the release of mediators such as serine proteases (e.g. elastase), which cleave junctional adhesion molecules such as E-cadherin, found between endothelial cells (313-315). Our work demonstrating that the protection induced through p55 TNFR deletion was seemingly independent to the classical pro-inflammatory effects of TNF signalling, prompted the interrogation of the alternative signalling pathway, that of, p55 TNFR mediated death signalling.

Apoptosis of the endothelium and epithelium has been heavily implicated in the development of barrier dysfunction and pulmonary oedema (56, 290, 316-318). Bachofen and Weibel performed the original studies, which examined epithelial integrity in ARDS, and showed that type 1 AECs of post-mortem ARDS lungs had significant ultrastructural damage (319). In the late nineties, Matute-Bello and colleagues were the first to present data that epithelial apoptosis mechanisms could possibly explain this epithelial injury (56). This study found that increased levels of bioactive Fas ligand in the alveolar space of ARDS patients could induce apoptosis of primary human distal lung epithelial cells. Furthermore, FasL concentration was higher at 24 hours in those patients that died in comparison to survivors.

4.5.1 Epithelial caspase-8 activation dominates in acid aspiration

The localisation of caspase-8 activation was important to truly dissect further the mechanisms through which p55 TNFR ligation mediated injury. There are a variety of methods that could be utilised to ascertain exactly where caspase activation was occurring. A flow cytometry based technique was developed to localise and quantify relative caspase-8 activity in whole lung. Although other publications have localised TNF-induced caspase activation in lung using histology, arguably, this remains a

substandard technique due to the close apposition of the endothelium and epithelium. Indeed, even immunohistochemistry using two/three antibodies staining does not allow complete differentiation within the alveolar wall. In the absence of robust techniques to locate the cell specific activation of death signalling, many studies use in vitro experiments to support their in vivo findings (320). Hence, investigation of cell death signalling using in vitro methods may present large jumps in logic and should be interpreted with caution given that cell culture has significant variability with respect to viability, and is very different from the in vivo situation. The advantage of whole lung flow cytometry through labelling of various epitopes at the same time allows analysis of multiple cell types (from a single sample) through positive and negative gating strategies.

A novel assay was developed using a fluorochrome-conjugated cell-permeable caspase-8-specific inhibitor compound FAM-IETD-FMK. Lungs were dispase digested to prepare single cell suspensions and subsequently incubated with DMEM /2.5% HEPES, as used by a number of investigators, to produce endothelial and epithelial primary cell cultures from lungs (247, 321). This technique enabled the analysis of caspase-8 activity in addition to its localisation, which is significantly quenched by most fixatives including methanol and paraformaldehyde. This advantage of measuring activity (as opposed to presence) is important as caspase-8 can induce its own activation when present in high local concentrations (322).

After the exclusion of debris, and using antibodies to identify the three main cell types in the lungs (endothelia, epithelia, and leukocytes), the caspase-8 signal was specifically localised to within type 1 alveolar epithelial cells (AEC). Type 1 AECs from acid instilled animals showed a 8-fold higher caspase-8 activation as compared to uninjured animals. Furthermore, endothelial cells and leukocytes showed a lower caspase-8 activity and no increase with acid-induced lung injury. The specific localisation and extremely high activity of caspase-8 to type 1 AECs (as opposed to endothelial cells) was supported by the reduction in RAGE (a specific type 1 epithelial marker) and not endocan (an endothelial marker) in p55KO animals.

4.5.2 The amount of completed 'cell death' in clinical and experimental ARDS does not correlate with physiological derangements

The low level of TUNEL staining and the importance of early proximal death signalling per se on physiological outcomes has not really been appreciated in lung injury literature. The TUNEL assay detects cells undergoing apoptosis through DNA fragmentation and involves the labelling of the broken hydroxyl (-OH) ends with a biotin-conjugated dUTP through the terminal deoxynucleatidyl transferase (TdT) enzyme. The specificity of TUNEL as a method for detecting apoptosis has been under debate for some time, due to the fact that necrosis also leads to the development of free DNA ends (323). However, it remains a widespread method amongst most researchers investigating apoptosis. Furthermore, recommendations by the Nomenclature Committee on Cell Death in 2009 suggested that morphological signs of apoptosis, such as classic nuclear condensation into discrete bodies (called 'apoptotic bodies'), in combination with staining for DNA fragmentation should be used to give a more reliable indication of when a cell is actually 'dead' (245). Although positive TUNEL staining was undetectable in uninjured normal lungs, blinded analysis of slides showed only 1-2% of nuclei within injured lungs staining positive for TUNEL. Although this TUNEL index was significantly reduced in p55KO animals, a disparity existed between the extent of injury and low levels of TUNEL positivity in WT animals. Technical reasons could not account for this low incidence as concurrent staining of sections exposed to DNAse to fragment DNA found all nuclei were positively stained (figure 4.2 B).

The finding of such a low incidence of TUNEL positive cells in lungs with significant injury brings into question the role of completed cell death in development of ALI/ARDS. Indeed, post mortem studies of ARDS lungs shows only up to a maximum of 10% of apoptotic TUNEL positive cells (58). The removal of 10% of the total lung capacity of normal lungs should not lead to the severe respiratory compromise found in ARDS. Furthermore, this 10% will likely include many TUNEL positive leukocytes. Hence, an alternative explanation must exist as to how the activation of apoptosis pathways in lung parenchyma would result in the physiological derangements seen in ARDS. Animal investigations of lung injury report similar levels

of TUNEL positive staining to the level we present (68, 317) but at even later time-points of lung injury. Indeed, nearly all animal studies examining the effect of Fas ligation shows low levels of TUNEL positive apoptosis in the presence of greater fold increase in caspase activity. For instance, Bem and colleagues utilised the Fas activating antibody Jo2 to produce a specific intra-alveolar activation of death signalling and showed less than 1 TUNEL positive cell per high power field at 24 hours after Fas ligation despite a much greater upregulation of caspase-3 activity at 24 hours (293). Furthermore, at later stages of injury, there are minimal numbers of TUNEL positive cells, of which the majority are TUNEL positive leukocytes (318). The data presented in this chapter is also consistent with a report by Imai et al looking at acid aspiration with injurious mechanical ventilation where it was found that lungs had minimal TUNEL positive events despite significant injury (53), and increased TUNEL positivity in other organs e.g. kidney. Interestingly, this study showed that acid aspiration with non-injurious ventilation led to more TUNEL positive events than acid aspiration with injurious ventilation, which seems somewhat counter intuitive given the latter showed greater physiological injury. This further confirms a poor correlation between the extent of completed cell death and physiological lung injury.

One explanation for the low level of apoptotic cell numbers (i.e. incidence of TUNEL positivity) detected could be a balance between completed apoptosis and clearance of apoptotic bodies (324). The lack of TUNEL positive cells in our experiments is primarily due to a low level of apoptosis (as opposed to high clearance) for several reasons.

Firstly, if the clearance process by phagocytes occurs very quickly (as has been shown in some studies using intra-tracheally instilled apoptotic thymocytes (324, 325)) not many apoptotic cells will actually be seen. This would therefore underestimate the amount of apoptosis observed. However, the phagocytosis of intratracheally instilled of apoptotic bodies (such as apoptotic thymocytes) (although shown to occur within minutes), does not take into account the time taken for a cell to become apoptotic through condensation of its nucleus. Indeed, induction of apoptosis in vitro of thymocytes can take over 12 hours (325). Of greater relevance,

unpublished in vitro data from within our laboratory (Dr M Fletcher, PhD Thesis) has shown that MLE-12 cells only show significant positive staining for Annexin V at approximately 24 hours after exposure to TNF and cyclohexamide, which can be reversed by a pan-caspase inhibitor. Hence, irreversible apoptosis potentially occurs at much later time-points in epithelial cells in vitro. Our work has examined much earlier time points after injury suggesting that end-stage apoptosis had not yet likely occurred. Indeed, given that caspase-8 activation was still detectable suggests cells were still in the early signalling phases of apoptosis.

Secondly, the removal of apoptotic epithelial cells would require replacement through proliferating type 2 AECs, but histology still suggests the presence of intact alveoli. This is unlikely to occur within such an acute time frame particularly in the presence of an intact alveolar structure. In comparison, chronic lung diseases such as emphysema, where apoptotic bodies are abundant show significant disturbance to alveolar ultrastructure (310).

4.5.3 Pro-apoptotic “death” versus inflammatory “survival” signaling

The important effect of inflammatory signalling through NFκB in reducing cell death could also explain the low levels of cell death in the presence of severe injury. The internalisation of the cell surface TNF/p55 TNFR complex 1 leads to a change in its assembly forming complex 2 and this enables the recruitment of death domain proteins, such as TRADD and FADD, to the internalised complex. This internalised receptor complex also known as the death inducing signalling complex recruits and activates caspase-8. The mechanism behind the switch that determines whether signalling occurs through complex 1 and complex 2 is still unknown and it may be likely that both are activated simultaneously and that the importance is determined through regulatory proteins and ubiquitination. However, it is known that the activation of NFκB promotes the expression of anti-apoptotic proteins such as c-FLIP and c-IAP1 (326, 327). Although the specific activation of NFκB pathways or anti-apoptotic factors are not specifically measured – neutrophil recruitment has been shown to relate to NFκB transcription in acid-induced lung injury (328). Given this, NFκB activation leading to the upregulation of anti-apoptotic factors may explain the

lack of progression to cell death within the three-hour period. Interestingly, preliminary analysis of a longer-term model of acid aspiration (as described in chapter 6) also suggests minimal TUNEL positive staining at 24 and 48 hours. Hence, the potential sustained anti-apoptotic effect of NFκB activation may be an important therapeutic avenue for investigation.

Of note, the p75 TNFR has no death domain and hence, cannot directly activate caspase-8. However, sole signalling through the p75 TNFR in p55KO animals leading to the transcription of NFκB may potentially explain the further reduction in cell death within this strain. Hence, the reduction in apoptosis measurements in p55KO mice may indeed be through various pathways – 1) a reduced p55 TNFR mediated caspase-8 signal; 2) an increase in more downstream inhibitors which mediate a reduced caspase-8 activity; 3) an increase in anti-apoptosis signalling through an intact p75 TNFR. The latter has also been shown to potentially explain the divergent roles for these receptors in retinal ischaemia (162).

4.5.4 Introducing the concept of "apoptotic limbo"

Overall the data suggests a concept whereby death signalling has been initiated, but cellular destruction or entry into the final irreversible pathways of cell death is prevented by pro-survival signals. However, despite minimal cell death and the cell potentially trying to survive, significant physiological dysfunction remains. This concept of a cell, despite receiving overwhelming cell death signals, is prevented from dying as a consequence of organised pro-survival/anti-apoptotic signals has been called "apoptosis interruptus" and has received more interest in cardiology literature. It was first shown in chronic heart failure where activated caspase-3 is prevented from completing cell death through the upregulation of inhibitors of apoptosis such as X-IAP and Smac-L (329). In close similarity to our work, studies performed by Narula et al in acute and chronic heart failure showed that organ function remained compromised during this phase of "apoptosis interruptus" and that apoptotic intermediaries may result in cellular dysfunction (330, 331). Hence, this period of "apoptotic limbo" where the lung is in a state of physiological

dysfunction without cells having died may represent a therapeutic window to reverse and restore cellular function and thereby regain normal physiology.

4.6 Concluding remarks

This chapter advances our knowledge on the specific cell in which p55 TNFR mediated caspase-8 activation is occurring, the alveolar epithelial type 1 cell. This data also reveals an interesting phenomenon where significant physiological dysfunction is seen in the absence of completed apoptosis. Hence, rather than completed cell death, the death signal (i.e. caspase-8) itself or downstream events may have directly promoted oedema formation. The next goal was to ascertain the causal link between p55 TNFR/caspase-8 activation, and epithelial injury. In particular, to determine how "apoptosis limbo" may impact on lung epithelial function, leading to hypoxaemia and changes to respiratory mechanics – both hallmarks of clinical ARDS. The next chapter describes the measurement of alveolar fluid clearance as a clinically relevant and specific index of alveolar epithelial function. This data provides a compelling argument as to how the p55 TNFR death signal manifests as alveolar oedema and may represent an opportunity to inhibit apoptosis signalling, prior to cell death, and restore epithelial function.

5 TNF-induced death signalling triggers alveolar epithelial dysfunction in acid-induced lung injury

Abstract

Maintenance of alveolar epithelial integrity is essential to the prevention of the pulmonary oedema formation in ARDS. Furthermore, not only does the epithelium prevent fluid permeability but it can also clear fluid actively from the alveolar space. This process known as alveolar fluid clearance (AFC) is critically reduced in patients with ARDS. Additionally, those with the lowest AFC show a higher mortality and hence, AFC measurement is a specific marker of alveolar epithelial function and has high clinical relevance. The previous chapter showed that p55 TNFR induced caspase-8 activation was localised to the alveolar type 1 epithelial cell. The data also suggest that physiological disturbance was independent of completed cell death. Hence, we wished to elucidate how caspase-8 activation per se induced epithelial dysfunction. A previously characterised ex vivo model to measure AFC was adapted and validated. Our measurement of AFC rate showed excellent correlations with other markers of epithelial injury, including RAGE and respiratory mechanics. We examined the link between the TNF/p55 TNFR/caspase-8 axis and epithelial dysfunction by using three different experimental approaches (p55 TNFR genetic knockout, pharmacological inhibition of caspase-8, and depletion of resident alveolar macrophages). Collectively, the measurement of AFC in each protocol supported the overall conclusion that TNF-p55 TNFR-caspase-8 axis is a crucial determinant of epithelial function. In particular, the extent to which caspase-8 was activated showed significant correlation with the deterioration in AFC. Importantly, these approaches of p55 TNFR genetic deletion, caspase-8 inhibition, and macrophage depletion all rescued AFC after acid aspiration and showed improved respiratory physiology.

5.1 Introduction

Alveolar fluid clearance (AFC) is a function of the lungs performed specifically by the alveolar and distal bronchial epithelium. Matthay and Wiener-Kronish showed that an intact epithelium was essential to resolve alveolar oedema induced by increased alveolar capillary barrier permeability (46). Ware and Matthay showed AFC is impaired in over 50% of patients with ARDS and those with maintained AFC have better outcomes (69). The ability of the lungs to clear fluid is determined by vectorial transport of sodium and chloride from the alveoli into the lung interstitium. This creates an osmotic gradient for water to be cleared from the airspaces. Epithelial sodium channel (ENaC) are found on the apical surface of the epithelium and transport sodium into the cell through a transcellular gradient created by basal Na^+/K^+ ATPase pumps that actively extrude intracellular sodium from epithelial cells into the interstitium. This process is integral to the maintenance of the lung lining fluid during health, but also the resolution of alveolar oedema in pathological states such as high-altitude pulmonary oedema, cardiogenic oedema and ARDS.

In the previous chapter we showed that pulmonary oedema formation and subsequent physiological deteriorations were mediated through the activation of p55 TNFR signalling. This was found to be an immediate response (within 90 minutes) and independent of the classical pro-inflammatory consequences of p55 TNFR signalling. Instead, p55 TNFR mediated death signalling induced a significant upregulation of caspase-8 that was attenuated in p55KO animals and localised to within the alveolar epithelium. The extent of TUNEL positive cell death seen amounted to 1-2% of all alveolar cells and, although attenuated in p55KO animals, could not fully account for the severity of injury seen in WT animals.

Hence, this chapter elaborates on the trigger and downstream effect of this epithelial p55 TNFR caspase-8 signal and hypothesises that this death signal is triggered by alveolar macrophages and directly impacts upon the epithelial machinery, leading to impaired resolution of alveolar oedema through alveolar fluid clearance. Whilst, apoptosis mechanisms have been shown to mediate injury to the

alveolar epithelium, the relationships between apoptosis and functional measurements of the epithelium (like AFC) remain undetermined. This is link is essential to elucidate, particularly given that alveolar fluid clearance when impaired influences morbidity and mortality in patients with ARDS (69). Determining if, why, when and which precise apoptotic mechanisms impair epithelial function should provide novel links between well-established ARDS paradigms. In particular, if such causal relationships are established, measurement of clinically relevant parameters such as AFC, should improve the translation of compounds targeting apoptosis to the bedside.

5.2 Aims

The aim in this chapter was to determine the causal link between the TNF/p55 TNFR /caspase-8 axis and deteriorations in respiratory physiology with respect to epithelial dysfunction.

5.3 Experimental design

5.3.1 In situ measurement of alveolar fluid clearance

Alveolar fluid clearance (AFC) rate was ascertained by the increase in fluorescence of a tracheally instilled non-permeable tracer (AlexaFluor594-conjugated BSA) within the BALF over a 30-minute period using an adaptation of a published in situ model (242). In brief, animals underwent anaesthesia, tracheostomy and low tidal volume ventilation for a brief period on FiO_2 of 1.0 (in total less than 15 minutes). Animals were given 20 units heparin intravenously, and exsanguinated under terminal anaesthesia. Mice subsequently underwent intra-tracheal instillation with 700µl of isoosmolar 5% BSA (Sigma-Aldrich) containing 50µg/ml of AlexaFluor 594-conjugated (AF594) BSA (Invitrogen). Immediately after instillation a first aliquot of 200µl was removed as a t=0 reference sample. Mice were immediately placed on a custom-made continuous-positive-airway pressure (CPAP) system delivering a FiO_2 1.0 at 8cmH_2O, and they were maintained at 36.5-38^{o}C throughout the protocol. At the end of the 30 minutes, a surgical pneumothorax was induced through blunt

dissection of the diaphragm ensuring full recovery of remaining instillate. The fluorescence of the original instillate (Fi), the t=0 (F0) and the t=30 (F30) sample was measured in triplicate. The distal airways fluid clearance over 30 minutes was determined by the equation: [1-(F0/F30)] x100 where F0 is the fluorescence of the t=0 reference sample and F30 is the fluorescence of the 30-minute sample.

5.3.2 Caspase-8 inhibition experiments

The caspase-8 specific inhibitor (Z-VAD-IETD) again utilising the IETD caspase-8 specific sequence was used. The inhibitor is cleaved by activated caspase-8 and remains bound to the active site preventing further caspase induced caspase activation and hence amplification of the cascade. The caspase-8 specific inhibitor (4mg/kg) was administered through the right external jugular vein 5 minutes prior to acid instillation. The inhibitor is dissolved in DMSO; hence, the same amount and concentration of DMSO was used as the vehicle control. After 90 minutes, AFC was measured, as described earlier. Subsequently, right lungs were used for flow cytometric assessment of leukocyte infiltration and the left lungs for caspase-8 activity assay.

5.3.3 Alveolar macrophage depletion

At 48 hours prior to acid instillation mice underwent laryngoscopy under anaesthesia as previously described. Subsequently, 75ul of clodronate or PBS containing liposomes were instilled to deplete resident alveolar macrophages.

5.4 Results

5.4.1 Validation of in situ alveolar fluid clearance measurement

A number of models have been developed to measure AFC rates in rodents. The most common method utilised has been the in situ method described by Garat and colleagues (242). The majority of clinical and experimental set-ups calculate AFC through the intra-tracheal instillation of a labelled marker in the alveolar space. Ideally this marker should be impermeable and remain in the alveolar space such that as water is absorbed from the instillate through intact AFC mechanisms, the

proportional increase in the alveolar concentration of this marker represents AFC rate.

The Alexafluor594-conjugated BSA was the marker used for these studies as it showed a linear relationship between protein concentration and fluorescence (figure 5.1 A). Hence, over the 30-minute AFC measurement period, as water is absorbed from the lungs, there is an increase in instillate protein concentration from 0 to 30 minutes, which is similarly measured as a proportional increase in fluorescence. Hence, this marker was ideal for the measurement of AFC. The marker concentration chosen was 50μg/ml dissolved in a solution made isotonic to plasma through the addition of BSA at 5% final concentration, and made isoosmotic to mouse plasma at 332mmosol/L (332) through the addition of NaCl.

To ascertain if the measurements derived from this in situ system truly reflected AFC rate, expressed as % AFC over 30 min, a variety of compounds known to enhance and inhibit AFC were introduced into the instillate (242, 333) (figure 5.1 B). In the absence of any compound, basal AFC was 11.5%/30min. When these experiments (figure 5.1 C) were performed with the sodium channel inhibitor amiloride (at 2mM concentration) within the instillate, there was a 47% inhibition of AFC. Conversely, instillation with isoproterenol (at 2mM concentration) produced a 48% enhancement of AFC. Furthermore, isoproterenol continued to augment AFC at 60 minutes suggesting that AFC remained stable in this ex-vivo experimental set-up, reaching a maximal rate of approximately 30%/hour.

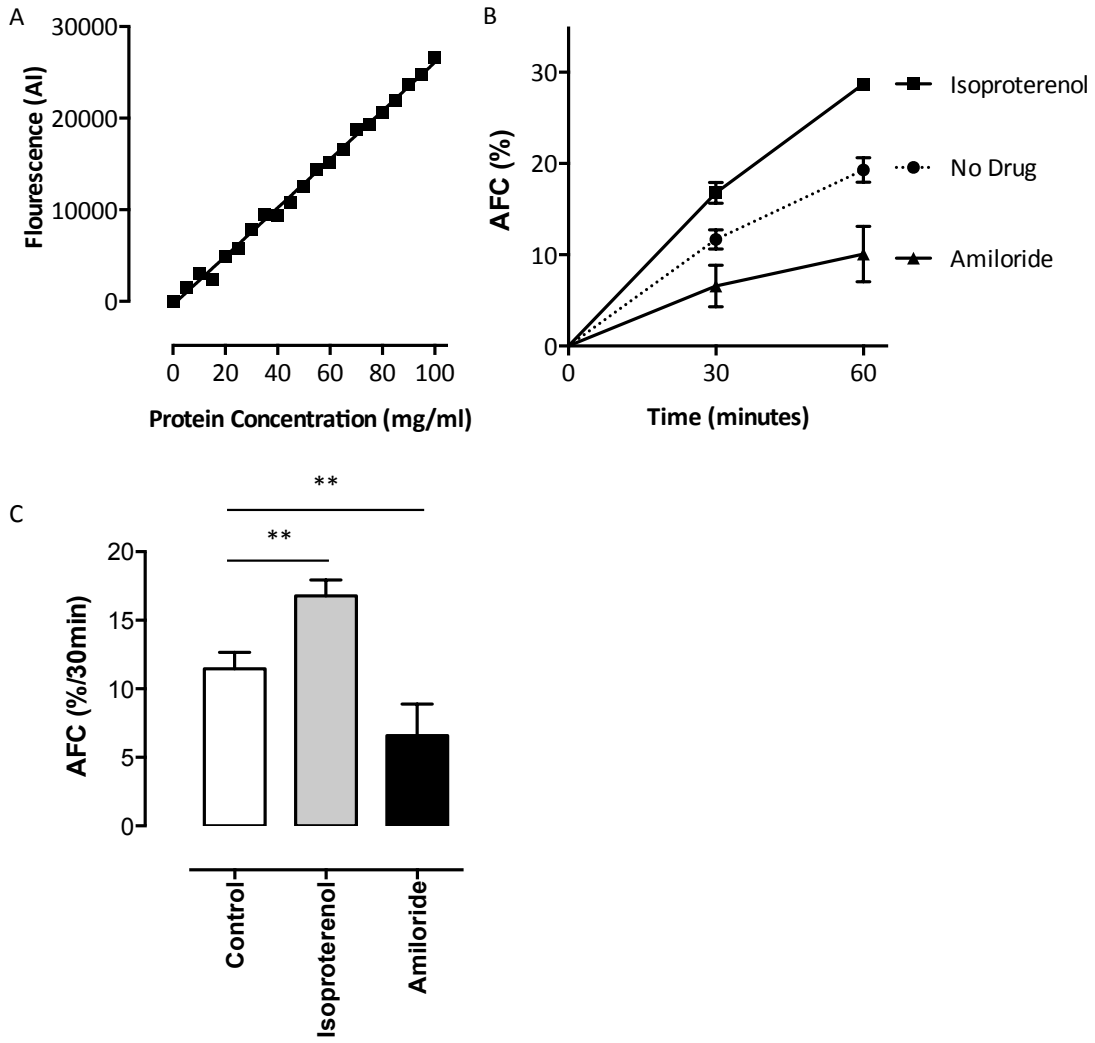

Figure 5.1. Development and validation of in situ measurement of alveolar fluid clearance

AlexaFluor-594 conjugated BSA shows a linear relationship between fluorescence and protein concentration making it ideal for calculating AFC (A). Basal AFC rate is 11.7% in the first 30 minutes and decreases to 7.6% over the following 30 minutes. The maximal augmentation of AFC that could be achieved by isoproterenol (2mM) is approximately 30%/hour (B). Isoproterenol shows a 48% enhancement and amiloride produces a 47% inhibition of AFC at 30 minutes validating the AFC measurement technique (C). (N=4-5 per group; **P<0.01)

We found that there were strong correlations between AFC and mouse body weight as well as lung dry weight. The same volume of instillate was instilled in all animals and hence the larger the animal, the greater the lung size/surface area for fluid reabsorption, the greater proportion of 700µl fluid cleared, and therefore a higher AFC (figure 5.2 A and B). Taking this into account, there were no differences in

uninjured AFC between age and weight matched WT and knockout strains, suggesting baseline differences would not account for any future differences seen (figure 5.2 C). In these validation experiments, we used animals of various different weights/ages. All further measurements of AFC were performed in 10-12 week old mice weighing approximately 25g to minimise this effect of body weight/lung size on AFC.

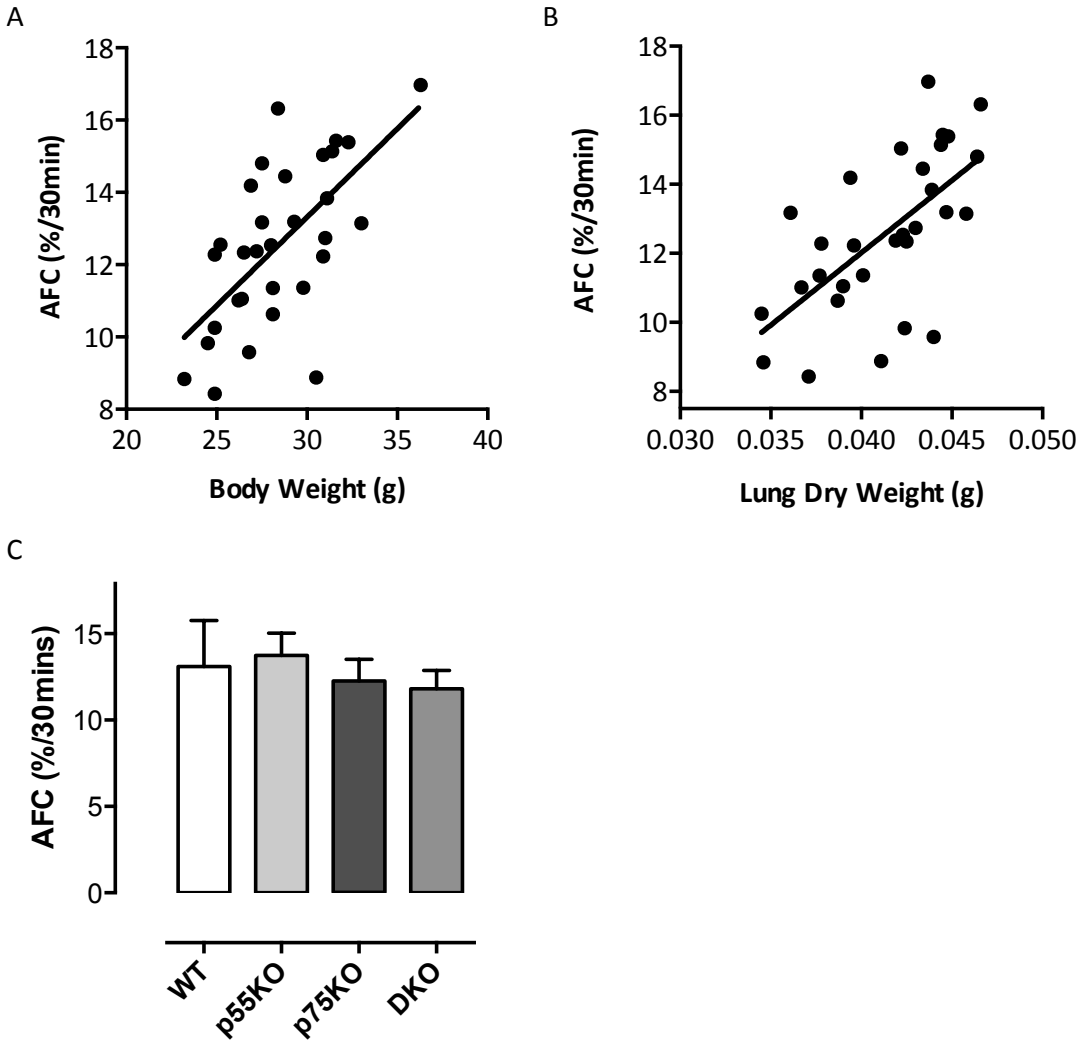

Figure 5.2. Animal size and strain differences in AFC measurement
AFC shows strong correlations with mouse body weight (A - Pearson r = 0.637; P<0.001) and lung dry weight (B - Pearson r = 0.633; P<0.001). There were no differences in baseline AFC measurements between weight matched (30g) WT and p55KO, p75KO or DKO strains (C). N=6-8 per group

5.4.2 Measurement of in situ AFC during injury.

It was important to ensure that loss of alveolar barrier integrity in injured animals did not influence AFC measurements. Firstly, the dilution of the initial instillate by pre-existing alveolar oedema in injured groups would tend to decrease apparent AFC. This was minimised by the initial lavage procedure to retrieve a t=0 sample which had been already mixed with the alveolar milieu.

Secondly, on going fluid leak into the alveolar space (from the vascular compartments) may have diluted the dye in the alveolar compartment. This was minimised through effective exsanguination of the lungs through the transection of the IVC and aorta, followed by the introduction of a pneumothorax and three recruitment manoeuvres of 30cmH_2O to empty West's zone 2 and 3. However, to be certain that these procedures minimised the potential for leak from the remaining blood/plasma into the alveolar space, an AlexaFluor-488 conjugated BSA dye was injected intravenously (5 minutes before the end of the protocol) and the extent of leak into the alveolar space over the 30-minute AFC measurement period was ascertained in uninjured and injured animals (N=2-3). Again minimal leak (of intravenously injected AlexaFluor-488 conjugated BSA) into the alveolar space was observed (less than 0.2% of the plasma fluorescence).

Thirdly, there may have been loss of the intratracheal protein tracer into the interstitial compartment leading to an underestimation of AFC. To ensure that the majority of tracer was indeed recovered, 5 separate alveolar flushes (with 1ml NaCl) were performed. This produced an exponential washout of the intratracheally instilled AlexaFluor594-conjugated BSA and this left less than 1% of total instilled dye in the lung homogenate implying minimal loss of alveolar dye into the alveolar/interstitial space.

5.4.3 AFC deteriorates acutely after acid aspiration and correlates with markers of alveolar epithelial injury.

The above validation confirmed that this method could be applied to the acid aspiration injury model. AFC was measured at 90 minutes after acid aspiration, given that caspase-8 activation was highest and significant differences in the physiology between WT and p55KO animals were already apparent at this early time-point. Acid instillation led to a reduction in AFC from 10.95±0.97% (mean±SD AFC of uninjured group) to 5.55±2.13% (mean±SD AFC of WT acid group). There were strong correlations between AFC and RAGE levels, and AFC and Ers in uninjured animals and WT animals exposed to acid aspiration confirming further that the measurement of AFC gave a true indication of injury to the alveolar epithelium, and that derangements in AFC contributed to the progression of injury after acid aspiration (figure 5.3).

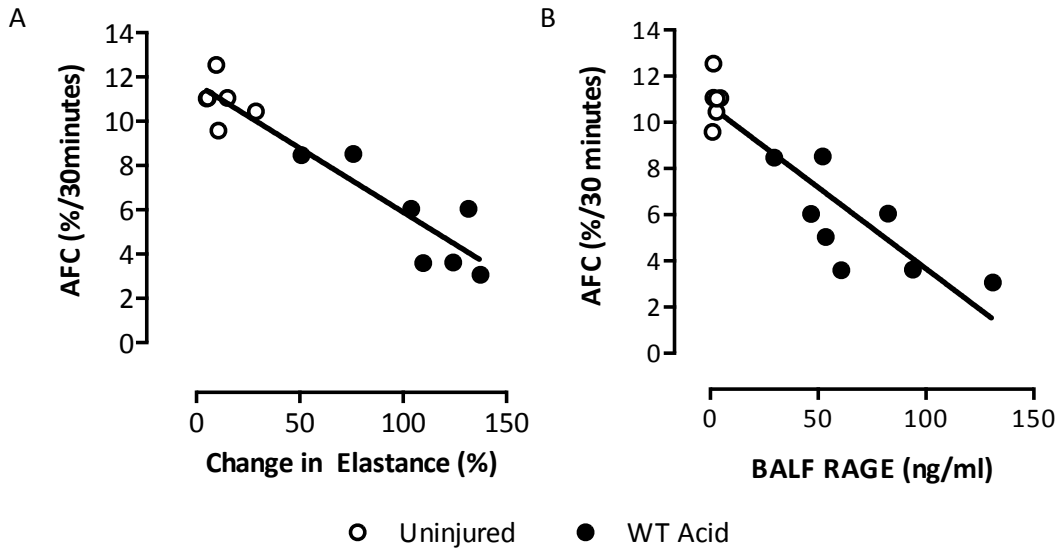

Figure 5.3. Correlations between AFC and other markers of epithelial dysfunction
Deteriorations in AFC induced by acid instillation correlate strongly with measured changes in respiratory system elastance (A - Pearson r = -0.942; P<0.0001) and levels of soluble BALF RAGE (B - Pearson r = -0.901; P <0.0001) confirming robust measurements of AFC.

5.4.4 The p55 TNF receptor triggers the early disturbance of alveolar fluid clearance in experimental ARDS

The work so far showed that the p55 TNFR is activated early at 90 minutes after acid aspiration leading to caspase-8 activation localised to type 1 alveolar epithelial cells. In comparison to the 49% downregulation of AFC in WT animals, the p55KO group showed only a 27% reduction (figure 5.4 A). Furthermore, p55KO animals showed significant reductions in BALF alveolar RAGE level at 90 minutes providing further suggestion that epithelial injury was reduced (figure 5.4 B).

To confirm that this was a p55 TNFR specific phenomenon AFC was also measured in acid instilled p75KO animals. There was substantial epithelial injury in the p75KO strain with increased RAGE and reduced AFC (to similar levels as WT animals). This confirmed our notion that the p55 TNFR was the predominant pathway mediating the TNF signal that leads to epithelial dysfunction. Indeed, when all groups are analysed together, AFC continues to correlate strongly with alveolar RAGE levels and Ers confirming that epithelial dysfunction accounted for differences between p55KO and other groups (figure 5.4 C and D).

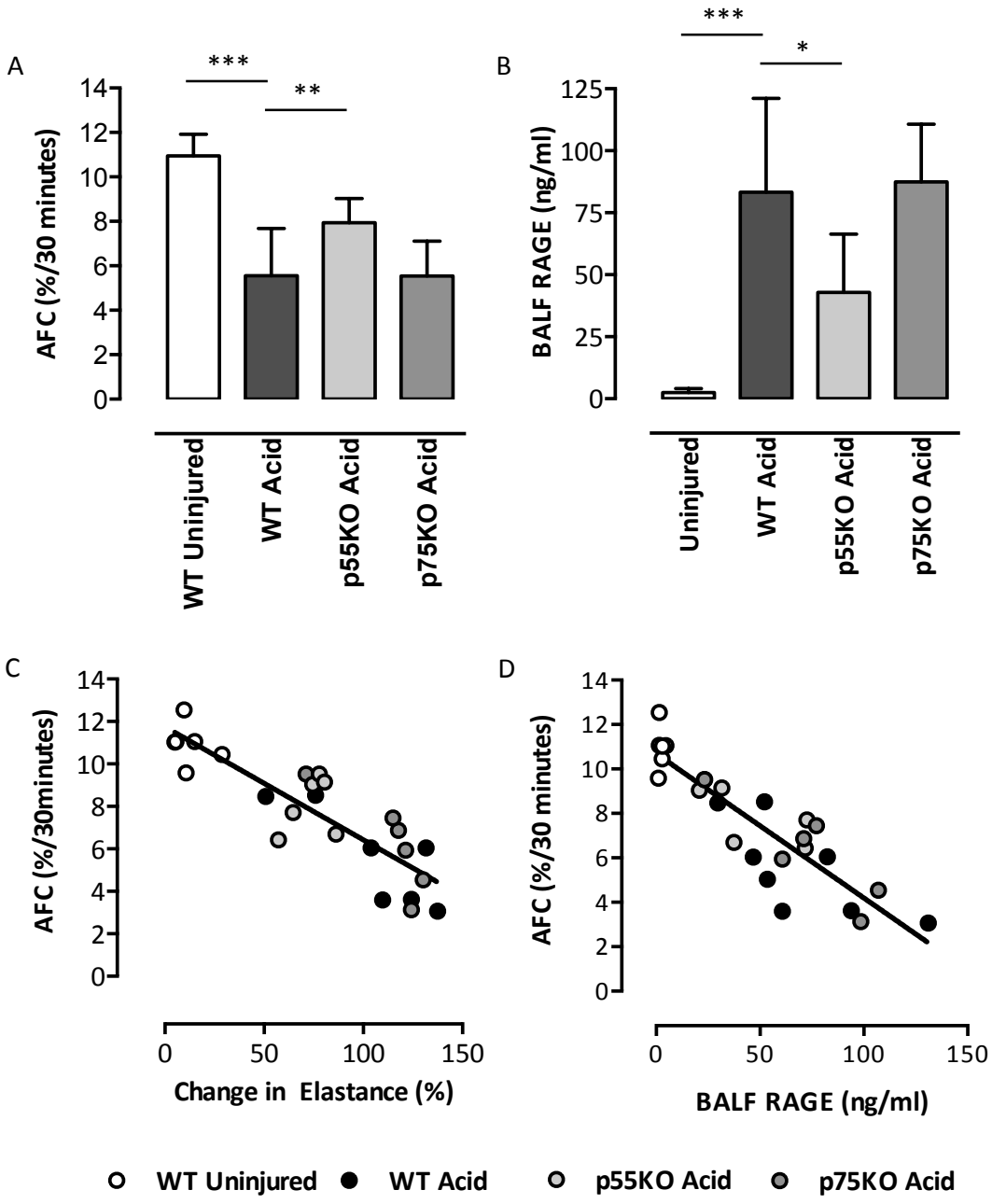

Figure 5.4. Differences in AFC between WT and TNFR knockout strains after acid aspiration

Acid instillation in WT animals induces a significant 49% deterioration in AFC. This deterioration is attenuated in p55KO group implicating TNF death signalling through the p55 TNFR in the development of epithelial dysfunction (A). The p75KO group remains injured confirming TNF mediated effects are independent of this receptor. Levels of BALF RAGE are significantly lower in the p55KO strains further confirming lower epithelial injury (B). The data from the knockout strains follow the previous relationship between AFC and changes in respiratory system elastance (C - Pearson r = -0.871; P<0.0001) and BALF RAGE (D - Pearson r = -0.886; P<0.0001). N=6-8 per group; * P<0.05; ** P<0.01; *** P<0.001

5.4.5 Caspase-8 activity leads to epithelial dysfunction.

To elucidate the causal link between the activation of caspase-8 and alveolar epithelial dysfunction, a cell permeable caspase-8 specific inhibitor compound (Z-VAD-IETD) was administered prior to acid instillation. This was given through the external jugular vein and hence, as directly as possible, into the pulmonary circulation. After 90 minutes we measured parameters of lung injury and alveolar fluid clearance and it was found that the instillation of vehicle produced similar deteriorations in PaO_2/FiO_2 ratio and AFC as compared to WT acid instilled animals (without vehicle). Administration of the caspase-8 inhibitor compound showed a striking improvement in PaO_2/FiO_2 ratio and alveolar fluid clearance measurements (figure 5.5 A and B).

To ensure that the inhibitor did indeed reduce caspase-8 activity we measured it in the lung homogenate and found that the dose administered led to a 26% reduction in activity (figure 5.5 C). Even more interestingly, there was a significant inverse correlation between the extent of caspase-8 activation (or inhibition, as in this case) and alveolar fluid clearance ability within these animals (figure 5.5 D). Hence, these inhibition experiments suggest that the downstream effects of caspase-8 signalling have a specific and direct impact upon the alveolar fluid clearance machinery within the distal lung and alveolar epithelium. This protective effect was seemingly independent to lung leukocyte recruitment (figure 5.5 E).

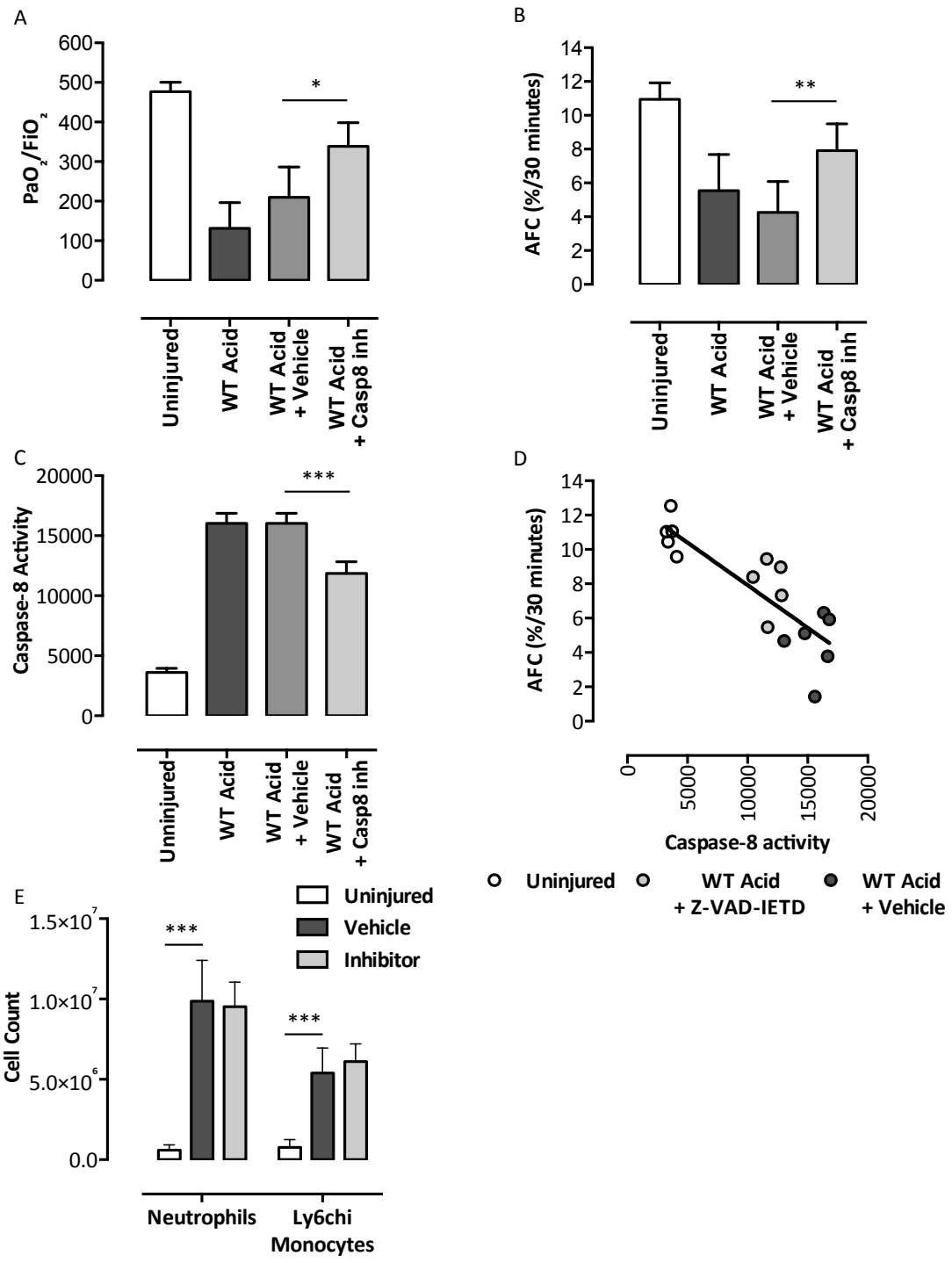

Figure 5.5. Protective effect on respiratory physiology by caspase-8 inhibition
Acid instillation leads to deteriorations in oxygenation (A) and AFC (B) in vehicle treated WT controls, which is rescued by the caspase-8 inhibitor Z-VAD-IETD. Caspase-8 activity is marginally reduced in inhibitor treated animals (C) but the extent of caspase-8 activation (or inhibition) shows strong inverse correlation with AFC (D) (n=16, Pearson r = -0.843; P<0.0001). This protection remains independent of lung sequestered leukocytes as similar levels of lung neutrophil and monocyte

numbers were present between vehicle and inhibitor treated groups (E). N=5-6 per group; * P<0.05; **P<0.01; *** P<0.001

5.4.6 Early epithelial death signalling is dependant on resident alveolar macrophage derived TNF

It has been shown previously that depletion of alveolar macrophages conveyed a protective effect after acid aspiration (83). Hence, resident alveolar macrophages could have been the trigger for the upstream release of TNF leading to the injurious effect through the p55 TNFR. A 90% depletion of the resident alveolar macrophage population was achieved through the intra-tracheal administration of clodronate containing liposomes (48 hours prior to acid instillation). This depletion (figure 5.6) was confirmed by cell counts determined through flow cytometric analysis of whole lung single cell suspensions. Intra-tracheal administration only depleted resident alveolar macrophages, which were defined as $CD45^{+}CD11b^{-}CD11c^{+}F4/80^{+}$ (R3 in figure 5.6). Other cell types such as dendritic cells and systemic leukocyte populations were unaffected (for their specific phenotypes please refer to chapter 7).

Macrophage depletion produced significant improvements in oxygenation as well as respiratory system elastance (Ers) even within 90 minutes of acid aspiration (figure 5.7 A and B). This was also independent of leukocyte infiltration (figure 5.7 C and D). Flow cytometric analysis of right lungs showed significantly increased numbers of neutrophils as a result of clodronate instillation, which increased significantly further on acid aspiration. Despite physiological protection, the clodronate+acid group showed even greater neutrophil infiltration and similar inflammatory monocyte infiltration. This data is consistent with the leukocyte infiltration observed in the genetic knockout animals.

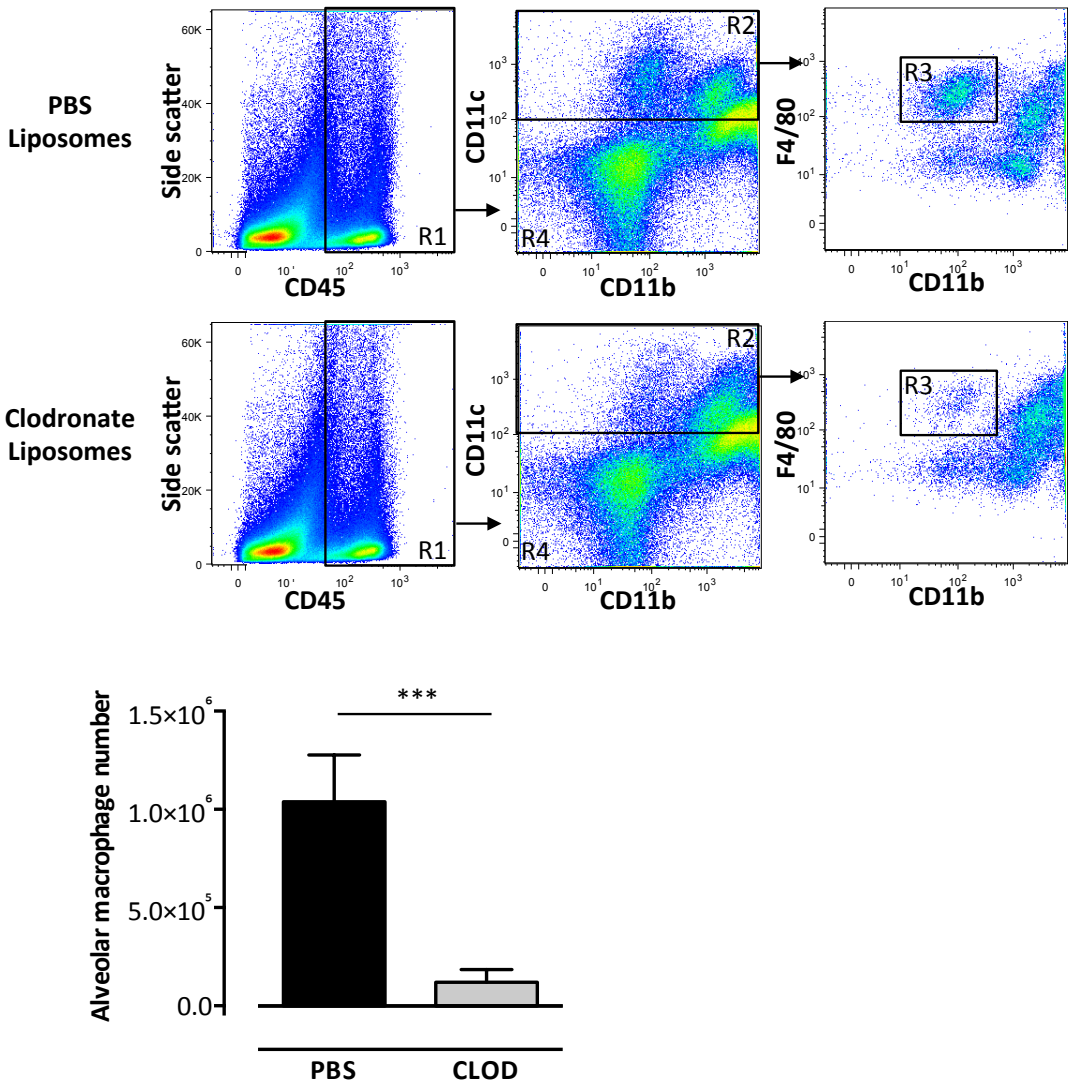

Figure 5.6. Flow cytometric evaluation of resident alveolar macrophage depletion by intratracheal clodronate administration

Resident alveolar macrophages were identified in right lung homogenate as $CD45^{pos}CD11b^{neg}CD11c^{pos}F4/80^{pos}$. Intra-tracheal instillation of clodronate liposomes induced a 90% reduction in the total resident macrophage population without inducing depletion in other lung resident cells such as $CD11b^{pos}$ and $CD11b^{neg}$ dendritic cells, or systemic leukocytes. N=5 per group; *** P<0.001

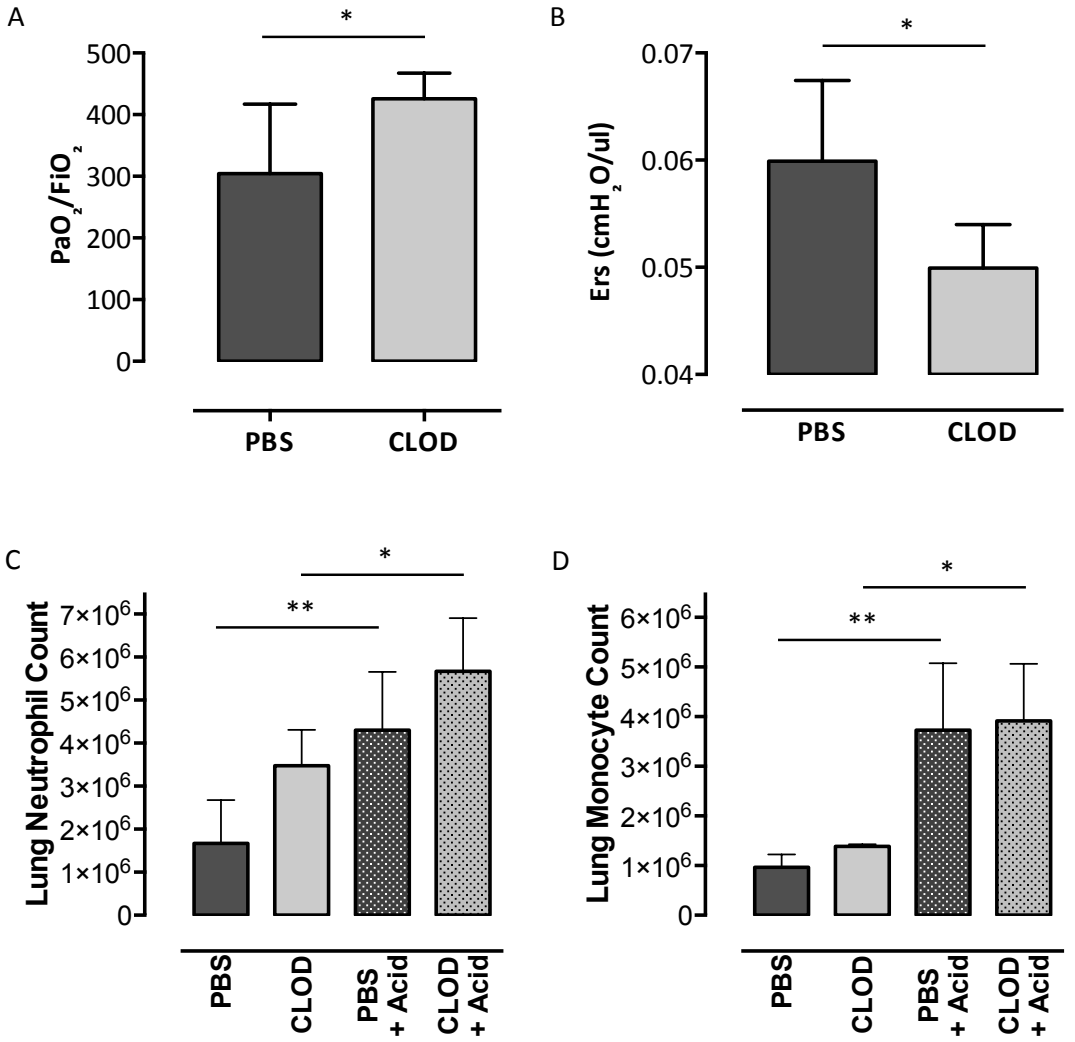

Figure 5.7. Protective effects on respiratory physiology through alveolar macrophage depletion

Depletion of resident alveolar macrophages protected against acid-induced lung injury with improved oxygenation (A) and lower respiratory system elastance (B). Clodronate liposomes alone induced a small increase in lung neutrophil sequestration (C) but overall acid aspiration induced significant numbers of lung neutrophils and monocytes (D) in both PBS and clodronate liposome instilled groups suggesting resident macrophages drive acid-induced lung injury independent to systemic leukocytes during this early phase. N=5-6 per group * P<0.05 ** P<0.01

In view of the apparent dissociation with leukocyte infiltration, it was hypothesised that macrophage depletion seemingly led to a similar impact upon the alveolar epithelium through a reduction in TNF-mediated signalling. Indeed, macrophage depletion led to a significant reduction in alveolar soluble TNF levels at 90 minutes, which corresponded with a reduced caspase-8 activation in the lung homogenate, which as shown previously is confined within alveolar epithelial cells (figure 5.8 A and B). Finally, the reduced activation of TNF-p55 TNFR-caspase-8 signalling resulting from macrophage depletion produced marked improvements in alveolar epithelial injury, as measured by BALF RAGE, as well as function, as measured through AFC (figure 5.8 C and D). The measurement of AFC and RAGE continued to show strong correlations suggesting robust measurement of epithelial function (figure 5.8 E). Once again within this set of experiments, the AFC correlated with lung epithelial caspase-8 activation, confirming that TNF-induced caspase-8 activation determined epithelial injury and function (figure 5.8 F).

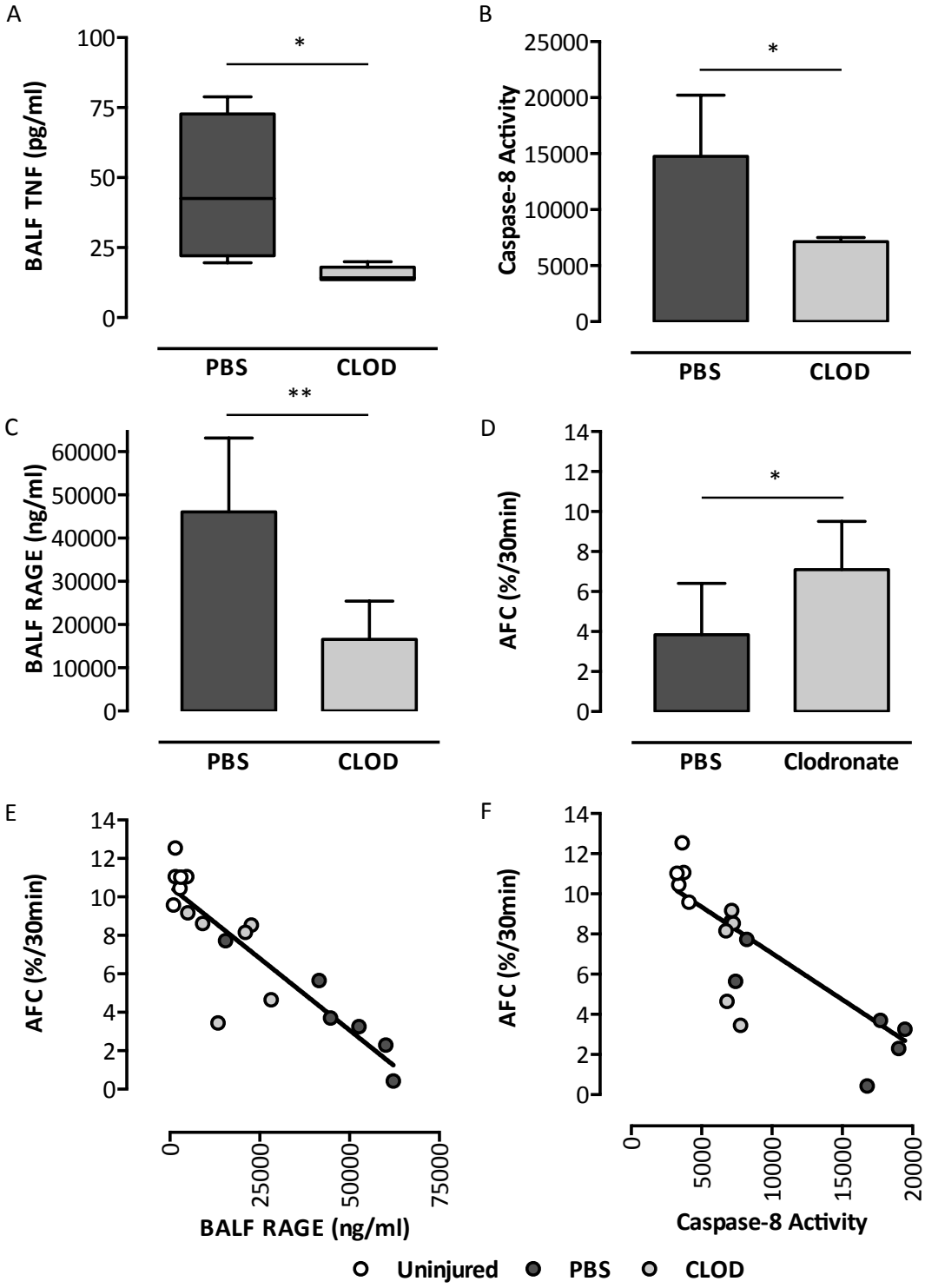

Figure 5.8. The protective effects of alveolar macrophage depletion are mediated through a reduction in TNF-induced epithelial dysfunction

Resident alveolar macrophages were the predominant producers of TNF at 90 minutes after acid aspiration and the reduction in their numbers significantly reduced the alveolar expression of soluble TNF (A). Furthermore, caspase-8 activity was significantly reduced presumably secondary to reduced p55 TNFR induced death signalling (B). This reduction in caspase-8 activation manifest as a reduced alveolar

epithelial injury as measured by BALF RAGE (C) and improved AFC (D). There remained a strong correlation between AFC and BALF RAGE (E; n = 17; Pearson r = -0.845; p<0.0001; uninjured data points are the same as in figures 5.4 and 5.5) confirming a robust measurement of alveolar epithelial injury. Finally, caspase-8 activation showed a strong inverse correlation to AFC (F; n = 17; Pearson r = -0.894; p<0.0001; uninjured data points are the same as in figures 5.4 and 5.5), further corroborating findings from the caspase-8 inhibition studies that caspase-8 is a critical component involved in mediating the early disturbance in AFC. N=5-6 per group *P<0.05; **P<0.01; *** P<0.001

5.4.7 Alternative mechanisms of caspase-8 activation

Although depletion of resident alveolar macrophages led to a significant reduction in soluble TNF levels in BALF (figure 5.8 A), it only induced a 68% reduction in caspase-8 activation at 90 minutes. Furthermore, genetic deletion of the p55 TNFR only conveyed a 61% reduction in caspase-8 activity at 3 hours. This incomplete reduction suggested the presence of alternative mechanisms of death receptor activation. These include mechanisms independent to alveolar macrophages, and soluble TNF/p55 TNFR interactions.

There is substantial evidence implicating the involvement of the FasL/Fas death receptor axis in ARDS and soluble FasL is upregulated in the BALF during experimental and clinical studies (56, 57, 59, 290, 292). At 90 minutes after acid aspiration, unlike soluble TNF (as seen in figure 5.8 A), there was no detectable upregulation of soluble FasL in BALF of WT animals. However, there remained a possibility that those non-depleted alveolar macrophages (approximately 10%) could contribute to death receptor activation through signalling via membrane bound death ligands (mTNF or mFasL), and hence contribute to caspase-8 signalling within the epithelium. Hence, we examined expression of mFasL and mTNF on resident alveolar macrophages. Furthermore other leukocytes such as blood derived neutrophils and inflammatory monocytes could also contribute through membrane ligands or the shedding of soluble ligands. As expected, at 90 minutes, alveolar macrophages expressed mFasL and mTNF on their cell surface (figure 5.9 A). However, lung sequestered neutrophils and inflammatory monocytes also expressed mTNF and mFasL (figure 5.9 B and C). No differences in expression were seen

between uninjured and injured animals. Hence, membrane associated death ligands and other leukocytes such as neutrophils and monocytes could potentially contribute to epithelial death signalling at this time-point. This requires further exploration.

The story becomes more interesting at 3 hours after acid aspiration at which point there is a significant upregulation of BALF soluble FasL (Figure 5.10 A). No differences are seen between WT and p55KO groups. This upregulation of soluble FasL at 3 hours possibly accounts for the incomplete reduction in caspase-8 activation (60%) in p55KO strain at 3 hours. In addition, at three hours, there were strong correlations between soluble FasL in the alveolar space with the amount of neutrophil and monocyte sequestration to the lung. This supports the notion that blood derived leukocytes could act as sources for soluble Fas ligand during later phases of injury (figure 5.10 B and C). The cell surface expression of FasL at 3 hours on these leukocytes remains to be studied and future work investigating the relationship between neutrophils/monocytes and FasL release may shed interesting light into this phenomenon of exudative leukocyte induced epithelial death signalling and how it may influence disturbances in AFC.

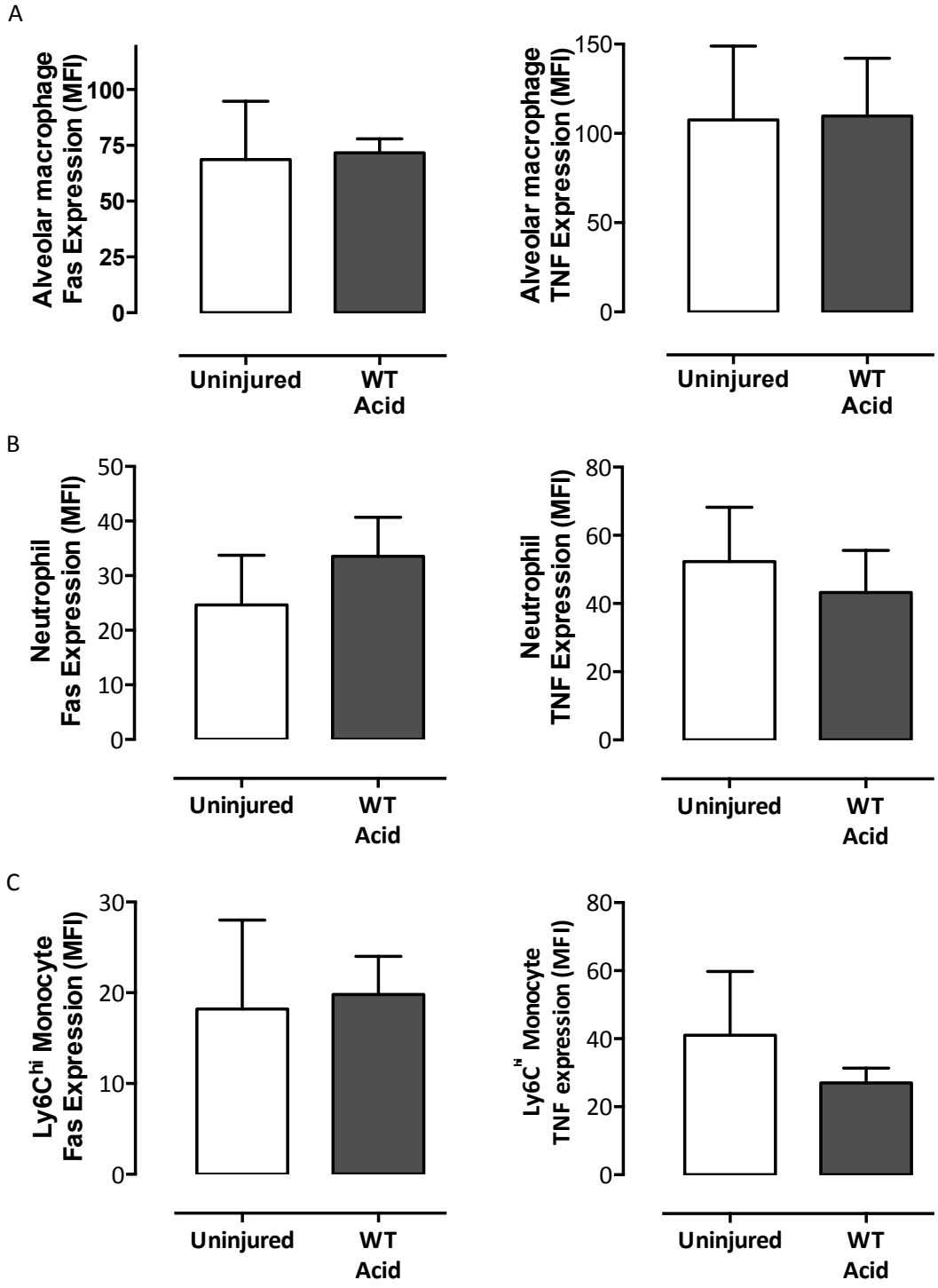

Figure 5.9. Cell surface expression of death ligands TNF and FasL on alveolar macrophages, neutrophils and inflammatory monocytes in naïve and injured animals

TNF and FasL was expressed on the cell surface of lung resident alveolar macrophages (A), lung sequestered neutrophils (B) and lung sequestered Ly6C^{hi} monocytes (C). No statistical differences were found between uninjured and injured

animals. Expression is derived after subtraction of isotype control expression values. N=6 per group

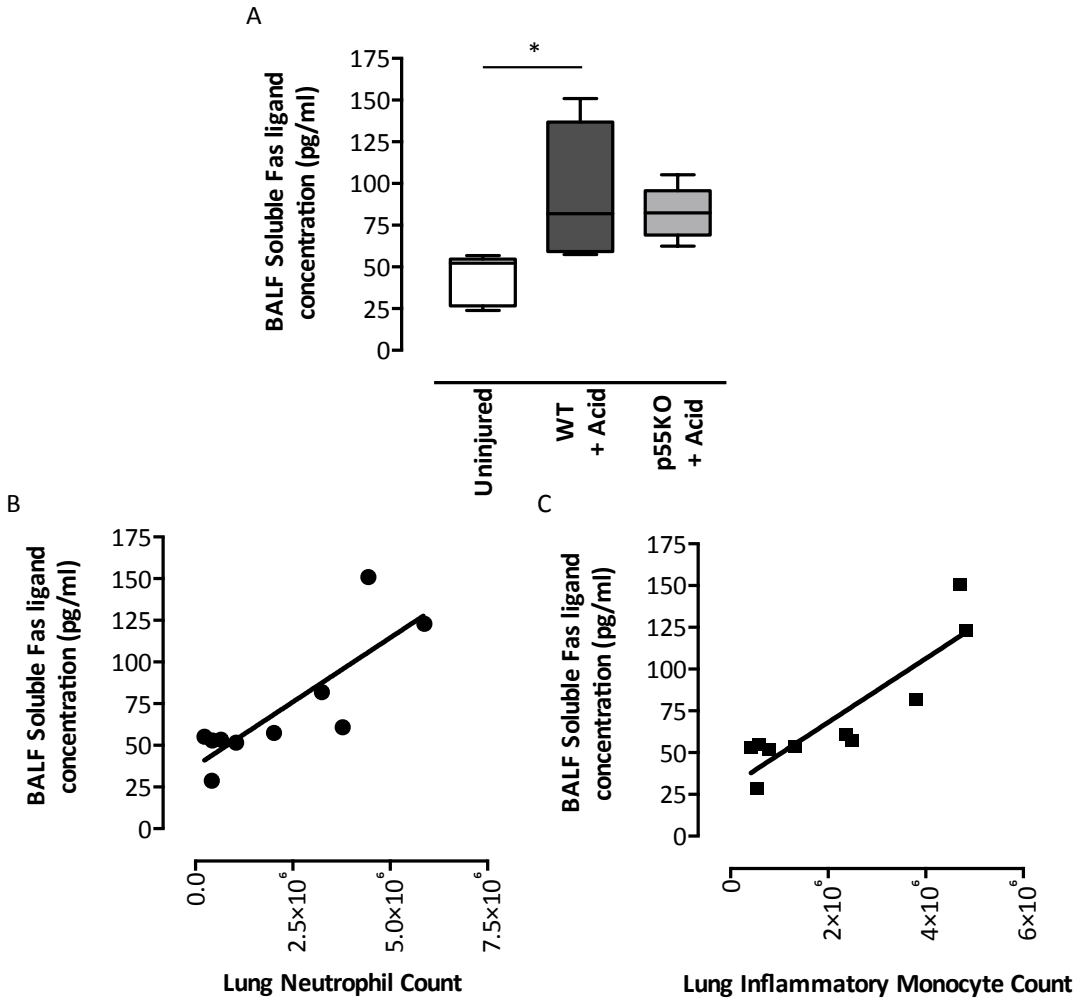

Figure 5.10. Correlations in alveolar FasL levels with leukocyte sequestration to the lung

Soluble Fas ligand was upregulated in the alveolar space at 3 hours after acid aspiration to a similar extent in both WT and p55KO animals (A). Levels of soluble BALF showed strong positive correlations to lung neutrophil (B – Pearson r = 0.83; P<0.01) and monocyte (C – Pearson r = 0.89; P<0.001) sequestration to the lung. N=5-8 per group; * P<0.05

5.5 Discussion

5.5.1 Alveolar fluid clearance – conceptual discussions

It is well established that a number of species, including bovid, canine, rodent and man, actively clear alveolar liquid through a process known as alveolar fluid clearance (69, 70, 242, 334-339) and that this is performed specifically by the alveolar epithelium. The majority of investigations have focussed on stimulating alveolar fluid clearance (AFC) through beta-adrenoceptor agonists that function to increase intracellular cAMP levels which in turn induce 1) an increased channel open probability and 2) an increased surface expression (from cytoplasmic stores within the endoplasmic reticulum) of ENaC, CFTR, and Na^+/K^+ ATPase ion channels (340). Whilst there has been extensive progress in the elucidation of mechanisms that enhance AFC through beta-agonists, the clinical translation has faltered through the failure of large clinical trials of intravenous and inhaled beta agonists (73, 75-77, 341, 342). A reason for this failure may be the fact that AFC can be enhanced in mild/moderate ARDS but deteriorates significantly in severe ARDS (340), and that the severity of ARDS was high in patients recruited to such trials. The rational explanation being that in mild/moderate ARDS there is sufficient functional epithelium remaining for intrinsic mechanisms to be enhanced whereas, in severe ARDS the severity of epithelial injury leads to the inability of exogenously administered agents to enhance AFC.

This measurement of AFC gives a specific indication into the state of the alveolar epithelium and no other parameter is as specific and so clinically relevant (46, 69). Measurements of basal AFC rate have varied significantly between investigators and may be due to a number of technical factors including the specific type of set-up (in situ flooded model (242), ex vivo isolated perfused model (217), in vivo ventilated model (333)) as well as the precise probes/instillate used for measurement. The in situ measurement of AFC using AlexaFluor594 in C57BL6 strain of mice showed a basal AFC rate of 11.7% over the first 30 minutes and 7.6% over the second 30 minutes confirming that the measurement over longer periods may be less accurate. Studies by Fukuda et al suggest that the fast accumulation of interstitial fluid volume

in such a non-perfused system limits AFC measurements in the in situ set-up, and furthermore may promote the re-flooding of the alveolar space leading to a plateau in AFC measurements (333).

5.5.2 RAGE, the epithelium, and apoptosis

After 90 minutes of acid aspiration there was a 50% reduction in AFC and this reduction correlated strongly with the upregulation of RAGE in the alveolar space. RAGE has been established as a marker of type 1 AEC injury (308, 343) and increased volumes and proton concentrations of acid aspiration lead to incremental increases in BALF soluble RAGE at 4 hours (308, 344). Su et al also showed that RAGE fails to be upregulated in indirect forms of lung injury implying that epithelial injury is an important determinant of RAGE release (344). This thesis also confirms that BALF RAGE levels (regardless of animal group) inversely correlate with AFC at 90 minutes providing strong evidence that the measured AFC is a robust marker of alveolar epithelial function during injury. Briot et al found a weaker but significant correlation between BALF RAGE and AFC in studies using isolated perfused human lungs, indicating its clinical relevance in this setting (345). RAGE is expressed as a transmembrane protein on the basal surface of epithelial cells and is thought to play a role in tethering the epithelium to the basement membrane (346). Work from our laboratory has shown a dramatic increase in alveolar RAGE only when oedema manifests in a model of VILI (239). Furthermore, Uchida showed that levels of RAGE are far greater in the BALF than plasma during pulmonary oedema suggesting a pulmonary source for this molecule (308). Hence, through as yet unknown mechanisms, in the presence of significant epithelial permeability, membrane bound RAGE is cleaved and its soluble form is released from the cell surface and accumulates in the alveolar space.

5.5.3 TNF, the epithelium and apoptosis

TNF has been shown to have opposing impacts upon AFC, with receptor-dependent pathways leading to a deterioration in AFC (216) and receptor-independent pathways inducing an augmentation (through the lectin-type domain of the TNF molecule (206)) (215, 218). Rezaiguia et al showed that upregulation of AFC in a model of pseudomonas *aeroginosa* pneumonia was TNF-dependant (193). Borjesson

et al also showed that an upregulation in AFC in a model of ischaemia-reperfusion of the gut was blocked by a monoclonal antibody to TNF (203). Braun and colleagues showed that the application of TNF into an in vivo ventilated system reduced AFC and that blockade of the receptor-binding domain of TNF (by soluble TNFR1) allowed TNF's lectin domain to augment AFC (216). This study concluded that the receptor dependant downregulation of AFC by TNF could partially be due to infiltrating neutrophils increasing inflammatory signalling of TNF through the p55 TNFR. However, no measurements of death signalling have ever been performed in all studies linking TNF with AFC.

The data presented in this chapter provides crucial evidence that p55 TNFR induced caspase-8 activation is a major determinant of the receptor dependant downregulation of AFC during injury. This is particularly evident given that p55 TNFR genetic depletion, caspase-8 inhibition and alveolar macrophage depletion studies all showed a significant correlation between AFC and the extent to which caspase-8 is activated (or inhibited) within the mouse lung. These data support a dominant in vivo role for TNF receptor dependent effects in reducing AFC during severe injury, and this outweighs the ligand's intrinsic ability to promote AFC.

The receptor independent mediated augmentation of AFC mediated through the lectin-like domain and the LTip peptide (a synthetic compound mimicking the lectin-like domain of TNF (218, 219, 347-349)) is thought to be due an upregulation of intrinsic epithelial ENaC activity/expression. Hence, in line with the previous discussions for the failure of beta-agonist treatments, the clinical application of the LTip peptide to promote fluid clearance during states of severe injury may be inappropriate given that the epithelium may not be in a state to increase AFC through the ENaC upregulation. In contrast, it may be more valuable to block caspase-8 activation and prevent deterioration in epithelial AFC machinery as opposed to apply futile therapeutic strategies akin to "flogging a dead horse".

Finally, although AFC is an important determinant within these data, the significant physiological protection observed in the p55KO animals from the beginning of the

acid aspiration protocol, may not be completely attributable to only a 2-fold improvement in AFC capacity. But, when this effect is synergistically combined with the 2-fold improvement in permeability; the 2.6 fold greater increase in extravascular lung water in WT animals as compared to p55KO animals can be more easily assimilated. This provides further argument against sole therapies (beta agonists and LTip) enhancing AFC given that these will have minimal impact upon permeability. Within this study AFC was used, as it is very specific to AECs and a provides an excellent representation of AEC function. However, it is crucial to appreciate that AEC function as a whole, not just AFC (figure 5.5 A) but also permeability (figure 3.5 C), is impaired by p55 TNFR induced death signalling in this model. Hence, targeting death receptor signalling, which impacts upon both permeability and lung liquid clearance, provides a compelling two-pronged approach to alveolar oedema formation and resolution. Furthermore, the application of beta-agonists/LTip peptide to enhance AFC in an alveolar epithelium already rescued from "apoptotic limbo" through the initial treatment with p55 TNF receptor DAb may be the ideal approach. However, the question as to how TNF-induced caspase-8 activation mediates this epithelial dysfunction (permeability and AFC) remains unanswered.

5.5.4 Caspase-8, the epithelium, and "apoptotic limbo"

The absence of significant cell death during the early phase of injury and the significant protection from caspase-8 inhibition suggests that physiological dysfunction can be attributed directly to death signalling per se. This is the first data linking the activation of proximal extrinsic death receptor signalling in alveolar epithelium, specifically caspase-8 activation, to its dysfunction. Although the apoptosis of alveolar epithelial cells has been implicated in a number of models of ARDS, definitive mechanisms as to how apoptosis affects the physiology of the lung have not been investigated. In addition, the majority of ARDS literature has assumed that alveolar cells simply die, creating 'cracks in the dam', which lead to alveolar flooding. Whilst permeability has been used as a global marker of endothelial/epithelial injury in lung apoptosis literature, this is the first study to implicate alveolar fluid clearance. At three hours less than 1% of cells are apoptotic

and, although TUNEL staining was not performed at 90 minutes, it is likely to be even lower. The caspase-8 inhibition studies show that even a 26% reduction in caspase-8 activation produces a significant improvement in AFC. The strong correlation between caspase-8 and AFC in both the pharmacological inhibition, as well as the macrophage depletion studies, suggests the downstream effects of caspase-8 directly influence AFC mechanisms, without progressing to cell death.

As introduced in the previous chapter, the impact of apoptotic intermediaries during "apoptosis interruptus" has received more attention in the field of heart failure, in particular in terminally differentiated cells such as cardiomyocytes. In the case of the heart, Communal et al showed that Caspase-3 activation is able to directly target alpha-actin, alpha-actinin and troponin T leading to a state of cardiomyocyte contractile dysfunction in the absence of nuclear fragmentation, the classic prequel to the final demise of a cell (350). Hence, despite the presence of nuclear integrity there is breakdown of cytosolic components leading to cellular dysfunction and organ failure. In this case, left ventricular systolic failure may be equivalent to AFC in the lung. We did not measure caspase-3 specifically, as a number of pathways can induce its activation including the intrinsic pathway. However, the measurement of caspase-8 shows that apoptotic signalling as a result of death receptor activation has occurred and the absence of TUNEL tells us that DNA fragmentation is low. However, alveolar fluid clearance (a functional correlate in the lung as is myocardial contractility within the heart) is impaired and can be rescued through caspase-8 inhibition. Hence, caspase-8 signalling itself leads to the downstream effects that induce deteriorations in epithelial function, namely permeability and alveolar fluid clearance. Although this requires further investigation, there is increasing literature potentially explaining how caspase activation can directly influence epithelial permeability and alveolar fluid clearance and these are now discussed.

5.5.5 Alveolar epithelial bioenergetics failure

The thin stretched position taken up by the type 1 alveolar cell producing the rounded shape of the alveolus, whilst aided by pulmonary surfactant, is likely to utilise significant amounts of ATP, whilst maintaining actin-myosin cytoskeletal

structure and tight junctional regulation (351). Loss of this shape and dysregulation leads to breaks within the barrier promoting permeability oedema. Furthermore, the active nature of alveolar fluid clearance is suggested by the Na^+/K^+ ATPase channel consuming nearly 40% of all ATP within cells (352). In fact, the Na^+/K^+ ATPase moves three Na+ ions out of the cell and two K+ ions into the cell per ATP molecule consumed. Islam et al recently showed that mitochondrial transfer occurred from mesenchymal stem cells to the alveolar epithelium restoring ATP levels in the lung and barrier function in an LPS model of lung injury (134). The presence of oxygen in the alveolar space and diffusion across the alveolar-capillary barrier provides a constant source of oxygen, which, unlike other tissue beds, is independent of blood flow but dependant on diffusion distance and FiO_2. Whilst there is significant knowledge on the impact of hypoxia on the pulmonary capillary endothelium and pulmonary circulation, e.g. hypoxic pulmonary vasoconstriction (352) and hypoxia-inducible factor mediated gene regulation (353), there is a paucity of data for the impact upon the alveolar epithelium, in particular, during times of increased demand such as when the alveolus is flooded. Indeed, high altitude pulmonary oedema (HAPE), a condition characterised by life-threatening pulmonary oedema on ascent impairs nasal ENaC activity, a surrogate for alveolar ENaC activity (354). Furthermore, salmeterol decreases the incidence of HAPE suggesting that alveolar fluid clearance mechanisms are impaired in hypoxic conditions.

Bioenergetics is intimately linked to apoptosis. Not only can apoptosis proceed through the intrinsic pathway and lead to mitochondrial/bioenergetic failure but paradoxically, ATP production is required for cell demise through apoptosis. Caspase-8 is a central controller between death receptor activation of the extrinsic pathway to the activation of the intrinsic pathway. If there is enough activation of caspase-3 by caspase-8 then there will be direct activation of effector caspases. This is known as type 1 extrinsic apoptosis. If there is slower assembly of the death inducing signalling complex (DISC) then the activation of caspase-8 is slower. Hence, in order to amplify the initial death signal caspase-8 localises to the outer mitochondrial membrane (355), leading to the formation of a complex with BID to induce mitochondrial outer membrane permeabilisation (MOMP) and the activation

of the intrinsic pathway, to aid in cellular demise through caspase-3 activation. Although we did not observe an increase in activation of caspase-9 between uninjured and acid injured animals, it is conceivable that caspase-8 activation was compartmentalised to the mitochondria leading to mitochondrial dysfunction and a low energy state, in the absence of caspase-9 activation. The disturbance in supply and demand of ATP may be the impediment to active sodium transport manifesting as reduced alveolar fluid clearance.

5.5.6 Alveolar epithelial cytoskeletal dysregulation

An alternative explanation could come from a number of studies that have investigated the impact of apoptosis on cytoskeletal regulation of the cell. Indeed, these downstream consequences, for example, the cleavage of the Rho GTPase effector, ROCK1, by caspase-3 induces the phosphorylation of myosin light chain kinase, which has been shown to induce dynamic cell membrane blebbing (356). Bouvry and colleagues found that hypoxia could induce alveolar epithelial cytoskeletal changes similar to those seen during apoptosis (357). These included a disruption of actin, and cleavage of alpha-spectrin, an anchor between cell surface proteins and the cytoskeleton. These effects subsequently reduced ENaC expression and transport. Most interestingly, these modifications in cytoskeletal and submembrane organisation recovered on application of a pan-caspase inhibitor. This suggests that the impact of death signalling on the intracellular cytoskeletal scaffold directly influences sodium transport through effects on ion channel expression. These effects may be secondary to reduced trafficking of channel subunits between cytoskeletal-localised and membrane-associated forms. Furthermore effects on tight junctional regulation as a result of intracellular cytoskeletal disruption could potentially account for the increased permeability associated with p55 TNFR mediated pulmonary oedema. These mechanisms require further exploration.

5.5.7 The epithelial death signal is initiated by alveolar macrophages…

The early events of acid aspiration are thought to be secondary to a physicochemical process (1-2 hours) and the later events (3-6 hours) to be partially mediated by neutrophils (88, 195, 196, 358). Undoubtedly, a chemical reaction may occur between acid and surfactant leading to oxidised phospholipids as has been shown in

a number of studies (359-361). However, it remains difficult to place a physicochemical disturbance as the main mechanism of oedema formation in this model, in particular, given that p55 TNF receptor deletion, caspase-8 inhibition and macrophage depletion, all abrogated injury with similar success. Indeed, such a reaction is likely to be much more upstream in this process occurring within minutes, before the upregulation of any inflammatory molecular mediator (such as TNF from macrophages).

Our data suggests that this physiological deterioration within 1-2 hours to be secondary to deteriorations in epithelial function as opposed to a direct consequence of a physicochemical reaction. Hence, it may be that given the importance of the epithelium in surfactant production (albeit type II cells, which are difficult to study in vivo) that TNF/p55/caspase-8 death signalling will also have downstream effects on surfactant production. One explanation may come from studies that have shown that TNF signalling reduces surfactant turnover and hence, p55 TNFR deletion may improve the recovery from early surfactant dysfunction (362-365). Furthermore, macrophage depletion with clodronate has also been shown to increase surfactant pool size in rats and hence, may confer some protection through this pathway (366).

The reduction in caspase-8 by macrophage depletion nearly approximates the reduction achieved through p55 TNFR deletion (68% versus 61%, respectively). This suggests that macrophage derived TNF mediates nearly all of this effect. Macrophage depletion studies may not have achieved complete reductions for several reasons that include incomplete depletion (i.e. 10% of macrophages remained intact in the lung); 2) an effect of clodronate pre-treatment (i.e. clodronate induces apoptosis in macrophages which may leave a residual signal within the lung). Beck-Schimmer and colleagues depleted macrophages using clodronate liposomes and found at 6 hours after acid aspiration there was attenuated upregulation of mRNA for a number of inflammatory mediators including TNF, ICAM-1, MCP-1, and MIP-2 (83). Our study found a reduction in soluble TNF, although we did not measure other inflammatory mediators, as they were not being

specifically studied. Beck-Schimmer et al also showed reductions in MPO activity and BALF cell number, however, our findings show no differences in the lung recruitment of neutrophils or inflammatory monocytes, despite the acute reduction in TNF production. Indeed, epithelial cells have been shown to produce a number of chemokines including MIP-2/KC and MCP-1 (265, 294, 367, 368). The clodronate treated group exposed to acid aspiration showed a tendency for increased lung neutrophil sequestration despite improved physiology and reduced epithelial injury. This increase may be accounted for by a mild alveolar neutrophilia induced by the instillation of clodronate liposomes, 48 hours earlier, as has been described by other investigators (293).

5.5.8 The epithelial death signal may be perpetuated by neutrophils…

Given that macrophage depletion and p55 TNFR deletion conveyed only a partial reduction in caspase-8 (60-70%), it was important to exclude if other death ligand/receptor interactions could account for the remaining 40%. In accordance with published literature we investigated FasL/Fas system that has been heavily implicated in ARDS. Alveolar soluble Fas ligand was only detected at 3 hours and not at 90 minutes, suggesting a minimal role for the soluble form at this early time-point. However, flow cytometry shows Fas ligand and TNF expression on the cell surface of alveolar macrophages, as well as blood derived monocytes and neutrophils. Hence, despite the significant reductions in soluble TNF and the absence of soluble FasL at 90 minutes, the incomplete attenuation of caspase-8 activation seen in clodronate treated animals could be explained through membrane expressed death ligands activating respective epithelial death receptors. Given that macrophage depletion showed a similar (and not significantly greater reduction) in caspase-8 activity (as compared to p55KO animals), this was unlikely to be a macrophage-derived source. Indeed, by 90 minutes there were significant numbers of neutrophils and monocytes sequestered within the lung parenchyma. Hence, it is possible that these interstitial and vascular adhered leukocytes could be promoting the remainder of the caspase activation through basal epithelial cell membrane interactions. Further analysis at three hours showed strong correlations between lung neutrophil/monocyte number and alveolar soluble Fas ligand concentrations in the BALF supporting the notion that

blood derived leukocytes could also determine the activation of caspase-8, taking the 'baton' from the alveolar macrophage.

With respect to the FasL/Fas axis most studies have investigated later time points (>4-6 hours), and a number of investigations have shown neutrophils and monocytes to be a source of soluble FasL (318, 369-372). Liles and colleagues were the first to show that neutrophils expressed FasL and Fas on their cell surface and this determined their short half-life through constitutive apoptosis (372). However, this study also concluded that neutrophils could release FasL from their cell surface. Serrao et al found that FasL from neutrophils undergoing apoptosis can also release FasL inducing caspase activation in primary alveolar epithelial cells (369). Mizuta found that monocytes could perform similar acts in vitro (371). Kitamura found that FasL expression was limited to macrophage like cells in the alveolar space and Fas was present on neutrophils and on alveolar cell walls, suggesting that FasL from macrophage-like cells induced activation of epithelial death signals in a model of endotoxin induced lung injury (318). Finally, Folkesson et al showed that lung injury after acid aspiration is mediated by IL-8 dependant neutrophil incursion into the alveolar space and that anti-IL-8 monoclonal antibody treatment given 5 minutes before or 1 hour after acid aspiration prevented lung injury and improved mortality (88). A follow-up study by Modelska and colleagues showed in the same model that pre-treatment with the same anti-IL-8 antibody also rescued fluid clearance at 4 hours after injury (255). These data in combination provide a strong rationale for the investigation of blood-derived leukocyte driving caspase-8 mediated derangements in AFC at later stages of lung injury. In particular, this suggests that there is a cellular handover for death receptor activation, with early signalling being dependant on alveolar macrophage derived TNF and later signalling possibly being dependant on additional neutrophil/monocyte derived death ligands. Indeed, the constant leukocyte infiltrate found in the alveolar space of non-resolving ARDS lungs suggests that they may have a role in a perpetuating state of death signalling, prolonging this "apoptotic limbo" within the alveolar epithelium.

Soon after the publication of our current work investigating the effect of early TNF death signalling on AFC (373), Herrero et al found similar effects induced by the instillation of human soluble FasL in mice (374). This study reports that alveolar fluid clearance is attenuated 16 hours after the instillation of human soluble FasL and that this effect was ameliorated through the administration of a pan-caspase inhibitor (Z-VAD-FMK). They also report a low frequency of TUNEL positive cell death and imply that Fas induced death signalling may also induce alveolar epithelial dysfunction. One limitation of many studies investigating the role of the FasL/Fas axis is that they utilise the instillation of either soluble Fas ligand or a Fas receptor activating antibody (anti-Jo2). Hence, the mechanisms focus specifically on lung injury induced by a specific receptor over-activation inherently producing biased conclusions. This is similar to injury induced by endotoxin, which investigates only TLR-4 mediated downstream events, which are predominantly inflammatory in nature. Whilst these models using single pathway overstimulation are useful, it is important to investigate the pathophysiological impact of death signalling initiated by a more clinically relevant insult that is also mediated through numerous pathways (TLR, death receptor, chemokine etc). Acid-induced lung injury remains such a model.

5.6 Concluding remarks

The data presented in the previous three chapters show that acid-induced lung injury is triggered by alveolar macrophage derived TNF which induces caspase-8 activation specifically in epithelial cells through its p55 TNFR. The activation of the death signalling, as opposed to TNF pro-inflammatory signalling, in the first two hours of aspiration, leads to a dysregulation in the ability of the endothelial/epithelial barrier to prevent oedema, as well as, the epithelium to resolve oedema through alveolar fluid clearance. The absence of cell death at early time points, and data showing that caspase-8 specific inhibition ameliorates lung injury, suggests that caspase-8 itself is a critical regulator of epithelial function. The precise mechanism through which caspase-8 mediates this impact remains unknown. Interestingly, at 3 hours FasL/Fas axis may also be activated in consequence to blood derived leukocytes.

The effect of both TNF and Fas mediated death signalling has now been shown to be an important determinant of epithelial function, both here and by a number of other laboratories (59, 65, 294, 374-379). However, it is also well established that the p55 TNFR and Fas receptors are also integral to leukocyte apoptosis and the timely removal of leukocytes through apoptosis is integral to the resolution of lung injury. In particular, the elucidation of death signalling and its effects on various cells is crucial to fully explore the potential benefits of anti-apoptotic therapies e.g. potentiating AFC; but also their potential harmful effects i.e. increasing leukocyte lifespan and preventing resolution of inflammation and injury. Hence, a future goal is to investigate the relevance and interactions of TNF, Fas and other death ligand induced activation of caspase-8 in a more clinically relevant longer-term model of lung injury.

Such a model should allow further mechanistic dissection of the consequences of death signalling, thereby improving translation and application of focussed therapies. However, no such ideal model exists and the remainder of the thesis discusses the development of a longer term resolving model of acid aspiration extending the investigation of death signalling to later, and arguably, more clinically relevant phases of lung injury.

6 Animal modelling of resolution in lung injury and inflammation

Abstract

The development of animal models to recapitulate clinically relevant pathophysiological processes that drive ARDS is crucial to find novel paradigms and targets, as well as testing potential therapies. The previous sections of the thesis have described the role of p55 TNFR mediated death signalling in the early phase of acid-induced lung injury. Most patients with ARDS, however, present at much later time points and therefore, any therapy against such a pleiotropic ligand/receptor interaction should be validated during later phases of injury progression. Most late-phase models of ARDS show minimal physiological injury with respect to clinical correlates of respiratory function such as oxygenation and respiratory mechanics.

To facilitate the investigation of TNF receptors and death signalling into the later phases of ARDS, my aim was to establish and characterise a model of acid-induced lung injury that produced significant physiological dysfunction whilst allowing investigation into the inflammatory, as well as, reparative/resolution phases of injury and inflammation. The model described within this chapter shows an injurious and pro-inflammatory phase over 2 days followed by a reparative and resolving phase over 7-8 days. The model encompasses all of the recommendations described in a recent American Thoracic Society workshop (192) detailing the requirements of an optimal model of ARDS. It shows significant deteriorations in lung physiology (respiratory mechanics and gas exchange), endothelial and epithelial injury (protein permeability and alveolar fluid clearance) and inflammation (soluble and cellular mediators). Most notably, there is resolution of all of these parameters enabling investigation into mechanisms that promote resolution of lung inflammation, as well as lung repair through fibrosis.

6.1 Introduction

The acute respiratory distress syndrome (ARDS) remains a major cause of morbidity and mortality in the intensive care unit. Despite decades of research there remains a significant deficit in the knowledge of mechanisms through which such severe lung failure manifests. The starkest evidence for this is the absence of biological treatments available to treat this devastating condition. This is partially due to the poor clinical translatability of pre-clinical models of ARDS, in that none truly recapitulate all of the complex pathophysiological features of this devastating clinical condition.

A number of recent publications have highlighted the importance of pre-clinical modelling of acute lung injury. In particular, an excellent and thorough review by Matute-Bello et al (37) describing the various animal models that are currently available. This review classified each model into those that impact upon the capillary endothelium, the alveolar epithelium, or both; and has contributed significantly to discussions as to how best to model and examine experimental lung injury. This was subsequently followed up by the publication of an American Thoracic Society (ATS) workshop report (192) produced by the ALI research community providing clear guidance as to what an animal model of ARDS should feature and measure, in particular, the limitations of some of the current models. Furthermore, these reports have highlighted the importance of understanding the setting in which a specific model is utilised and the cautious interpretation of data emanating from any model. An ideal animal model should produce all of the pathophysiological features of the human condition, which are listed in table 6.1 (adapted from Matute-Bello et al (37)). The acid aspiration model has been shown to replicate the entire range of features described and is regarded as the most clinically relevant model of direct ARDS in view of an immediate clinical correlate (253). Acid aspiration models have been well established to investigate the acute injurious responses i.e. less than 48 hours, however, their usefulness has been limited by either the need for mechanical ventilation (which limits the model to 4-6 hours) (259, 380), or a high mortality requiring the use of unilateral pulmonary instillation (381, 382). The former removes

the possibility for investigation into the later phases of experimental ALI (given difficulties in maintaining a stable experimental system for long term rodent mechanical ventilation), and the latter, arguably, does not fulfil the criteria for the clinical ARDS i.e. an acute onset of severe hypoxaemia, with bilateral alveolar infiltration. Hence, as a result of the high mortality, tight windows of acid dosing, and potential requirement of equipment for rodent ventilation, only 3% of the literature utilise this highly relevant model (37). There is no currently available acid aspiration model that truly recapitulates the later phases of ARDS. Hence, this chapter describes the development of an acid-induced lung injury model that captures all of the above pathophysiological features of clinical ALI, with respect to injury and inflammation, but also its temporal profile with repair and resolution. The model should allow investigation into the complex interactions between the various cellular and molecular mediators implicated in ARDS, as well as, produce changes to clinically relevant physiological indices of lung injury, such as respiratory mechanics, gas exchange, and alveolar fluid clearance.

Clinical features	Acute onset Diffuse bilateral alveolar injury Acute exudative phase Repair with fibrosis
Physiological changes	V/Q abnormalities Severe hypoxemia Decreased compliance/increased elastance Impaired alveolar fluid clearance
Biological changes	Increased endothelial and epithelial permeability Increased alveolar cytokine concentrations Intra-alveolar Coagulation abnormalities
Pathological changes	Neutrophilic alveolar infiltrate Intra-alveolar fibrin and hyaline membrane deposition Injury of the alveolar epithelium

Table 6.1. Pathophysiological features of human ALI
(adapted from Matute-Bello et al (37).

6.2 Aims

The specific aims of this chapter was to:

1. Develop a reproducible model of acid-induced lung injury to enable future investigation into the role of the death receptor signalling during later phases of injury, inflammation, and recovery in acid aspiration.
2. Characterise the model with respect to relevant features and measurements of lung injury, as suggested by the ATS workshop report (192).

6.3 Experimental Design

6.3.1 Intra-tracheal instillation technique

C57BL6 mice were anaesthetised and vertically suspended on a custom made stand as described previously. A non-thermal light source was used to transilluminate the

trachea. Subsequently, a blunt curved tooth forceps was used to displace the tongue out of the oral cavity. A second blunt tooth forceps was very gently introduced to retract the jaw posteriorly away from the upper palate. The tip of this second forceps was at the level of the epiglottis within the vallecula. The outward recoil of the forceps maintained an open oropharnyx enabling the tongue to be released and allowing the use of the other forceps to introduce a bevelled polyethylene catheter to 1 cm below the vocal cords. This ensured complete intra-tracheal instillation of any substance – hydrochloric acid in this case.

6.3.2 Provision of high dependency care

After instillation, mice were maintained in a vertical position for one minute. During preliminary experiments there was an unacceptably high immediate mortality (between 10 and 30 minutes after acid instillation). This was too soon to be a consequence of the development of ALI (as a result of acid instillation) but was a likely consequence from the significant respiratory depression/distress and laryngospasm induced by a combination of general anaesthesia and intratracheal fluid instillation. Occasionally, a low incidence is also observed during saline and endotoxin instillation. To facilitate the survival of mice for experimentation to later time-points and overcome this early mortality a high dependency recovery chamber was developed. This recovery unit (photo 2.3) provided warming, removal of carbon dioxide, and humidification. Mice were initially placed in an oxygen-enriched environment (FiO_2 1.0) with a gradual reduction in FiO_2 to 0.21 over 4 hours. This period ensured recovery from anaesthesia with spontaneous movement having been regained. On placement into this recovery chamber, mice were rotated from supine to left lateral to right lateral to prone, ensuring an even distribution of the instillate within the lungs. This protocol overcame the initial observed mortality and allowed all animals to survive and be investigated at later time points.

6.3.3 Measurement of physiology changes

At various hours/days after acid instillation, measurement of lung injury with respect to respiratory physiology and respiratory inflammation were made under terminal anaesthesia. Firstly, animals were weighed to obtain a generic estimation of injury severity. Anaesthetised mice underwent tracheostomy and insertion of carotid

arterial line as previously described. They were subsequently placed on a pulmonary ventilation system and ventilated with 8ml/kg tidal volume with a FiO_2 of 1.0 (as described in the acute model of acid aspiration). The original (pre-injury) weight was used for estimation of tidal volumes. Animals were placed on the system within 5 minutes of anaesthesia and a recruitment manoeuvre (30cmH_2O for 5 seconds) was performed in order to standardise the volume history of the lungs. After this initial recruitment manoeuvre, the animal was ventilated for a 30-minute period (tidal volume 8-9ml/kg, PEEP 2.5-3.0cmH_2O, RR 120bpm, FiO_2 1.0). Throughout these 30 minutes, respiratory mechanics were measured every 5 minutes. Arterial blood gas analysis was performed at the end of this 30-minute period of ventilation. Some animals underwent insertion of an external jugular vein (EJV) catheter through which AlexaFluor 594-conjugated albumin was injected (immediately after pulmonary recruitment) for calculation of permeability index as previously described.

6.3.4 Assessment of pulmonary inflammation

After the 30-minute ventilation period, mice were sacrificed and underwent bronchoalveolar lavage with 750μl of saline. Eppendorfs containing BAL samples were centrifuged at 1500rpm for 5 minutes. Levels of BALF cytokines and chemokines within the supernatant were quantified using ELISA kits (R&D Systems). BALF cell counts were obtained using haemocytometry and differential cytology.

6.3.5 Histological lung injury assessment

In a separate series of experiments, animals underwent acid aspiration for histopathological examination. Both lungs were examined macroscopically for bilateral injury. Left lungs of animals were also inflated at a transpulmonary pressure of 15cm height of 4% paraformaldehyde. Lungs were subsequently processed for paraffin embedding and sections attained for H&E staining. Furthermore, lung sections were stained with Masson's Trichrome stain for collagen deposition and identification of lung fibrosis.

6.3.6 Quantification of alveolar epithelial dysfunction

In a separate series of experiments, anaesthetised mice underwent tracheostomy and were ventilated for a short period. During this period animals underwent

cannulation of the EJV for administration of 20iu heparin. Mice were subsequently exsanguinated under terminal anaesthesia through ligation of the right and left internal carotid arteries, external jugular veins, as well as, the internal jugular vein/aorta at the level of the aortic bifurcation. Subsequently, the lungs underwent a standardised recruitment manoeuvre of 30cmH_2O and were instilled with 700µl of isoosmolar 5% BSA (Sigma-Aldrich) containing 50µg/ml of AlexaFluor 594-conjugated (AF594) BSA (Invitrogen), for measurement of alveolar fluid clearance over a 30-minute period using the in situ model previously described.

6.4 Results

6.4.1 Physiological injury induced by acid aspiration

Acid aspiration is a well-established paradigm for experimental lung injury, however, longer-term models have been limited by a high mortality, and hence, animals undergo unilateral instillation of acid (382, 383). Hence, the aim for the initial characterisation was to develop a model leading to severe injury but enabling animals to survive the immediate instillation period and be investigated at later stages of oedema progression and resolution, without the need for mechanical ventilation.

Similar to the acute model, there was a very narrow range for the development of significant injury in the absence of excessive mortality. Initial experiments to determine the severity of injury used instillate of various volumes and pH. Respiratory elastance (measured immediately after recruitment, hence, accounting for possible variations from the effects of general anaesthesia and surgical preparation) and BALF protein (to assess alveolar capillary permeability) were measured at 24 hours to ascertain the volume and pH required to attain a moderate physiological insult. A higher volume of instillate enabled better delivery of acid as assessed visually through Evans blue dye instillation. As can be seen in figure 6.1 A and B, 75µl 0.1M HCl induced significant increases in Ers and BALF protein at 24 hours. Interestingly, this instillate (75 µl of 0.1M) contained the same number of protons as the ventilated acute acid model (i.e. 50µl of 0.15M). It is likely that this

longer term model required a greater volume because acid was instilled through the orotracheal route followed by spontaneous ventilation, whereas the acute model involved acid delivery through a tracheotomy followed by positive pressure ventilation. The latter being more efficient and hence, explaining the requirement of a lower volume.

6.4.2 Weight loss.

Acid aspiration produced significant weight loss, proportional to the dose of acid instilled. Figure 6.1 C shows 75µl of 0.1M HCl produces a maximum reduction in body weight of 15%, as compared with 10% induced by the 50µl instillation. Additionally, this weight loss was more protracted in the 75µl as compared to the 50µl-instilled group. This most likely reflects a greater severity of illness in the higher volume group. Interestingly, after these adjustments to optimise the injury and recovery, animals survived despite significant injury, and between days 3 to 10 there was a weight gain back to baseline levels.

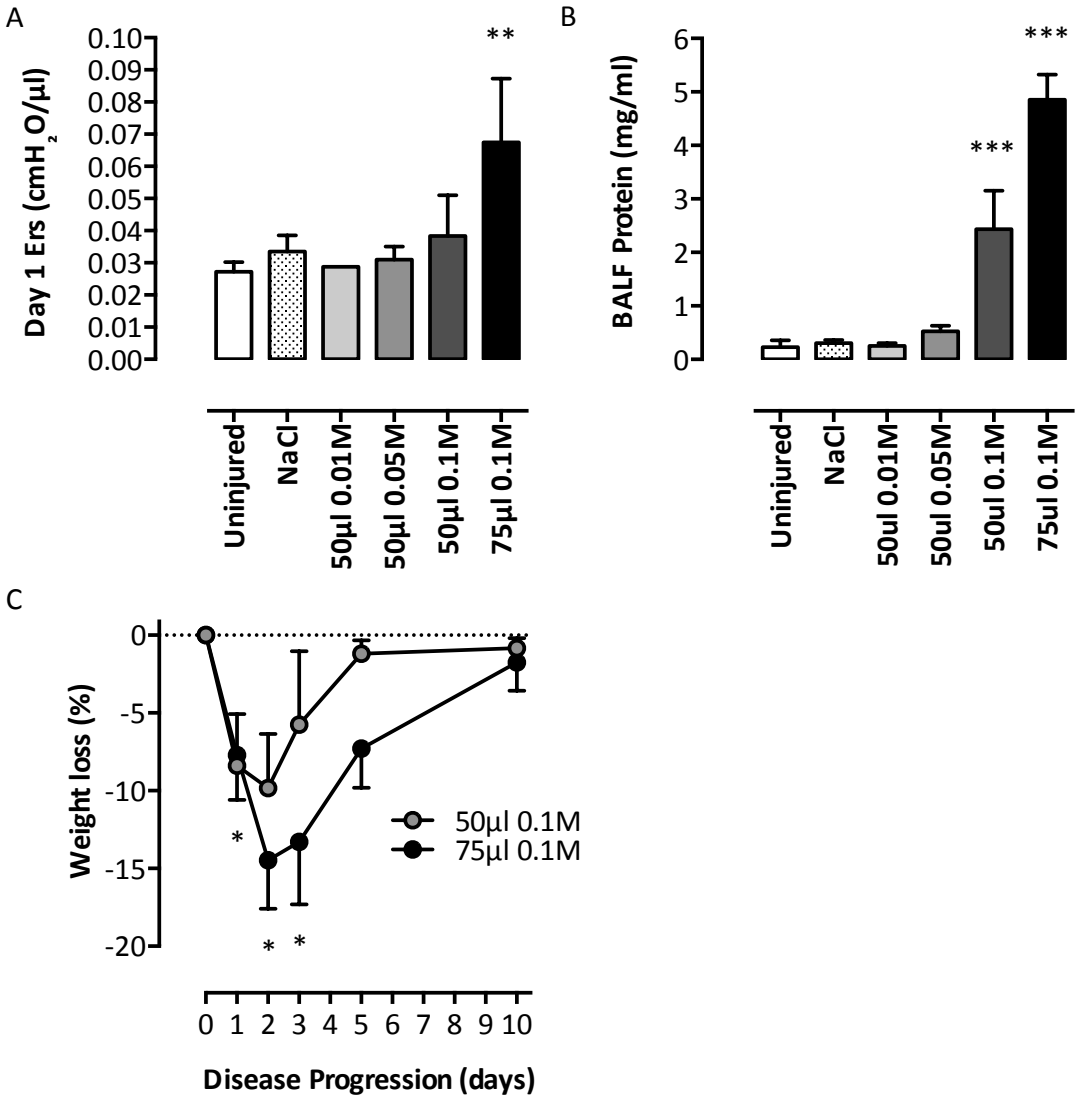

Figure 6.1. Development and refinement of the resolving model of acid aspiration
A dose titration performed by instillation of varying molarities of hydrochloric acid showed that 75µl of 0.1M produced a 2.5 fold increase in Ers (A) and a significant increase in alveolar capillary permeability as measured by BALF protein (B). Furthermore, this increased volume produced a significant 15% reduction in mouse body weight at 48 hours despite this group receiving an intraperitoneal 500µl fluid bolus. N=2-6/each time-point; *** P<0.001 ** P<0.01 * P<0.05 versus uninjured

6.4.3 Respiratory mechanics.

Lung mechanics were measured after rigorously standardising for the volume history of the lung through the application of a recruitment manoeuvre followed by a short period of anaesthesia. This was important as the impact of anaesthesia and surgery on mouse lungs (with and without injury) induces pulmonary atelectasis, which would effect any measurements of respiratory mechanics. Animals during days 1 and 2 of injury show an increase in Ers compared to non-injured animals and those at days 5 and 10 post-injury (figure 6.2 A and B). This could be explained by either the presence of pulmonary oedema as well as an increased propensity for atelectasis. The atelectasis component is represented by the significant increase in elastance between the initial recruitment (green line) and the end of the 30-minute period of ventilation. This atelectasis component was especially marked in first 2 days after acid aspiration.

6.4.4 Oxygenation.

Arterial blood gases were taken at the end of the 30-minute period of ventilation to obtain a true reflection of the impact of injury and not anaesthesia/recruitment. Similar to the ventilated model, there was an immediate deterioration in PaO_2/FiO_2 ratio at 3 hours post acid instillation in this longer-term model of acid aspiration. This remained below 200 in the first 24 hours (satisfying moderate ARDS criteria) with subsequent improvement to near normal levels over the following 9 days (Figure 6.2 C).

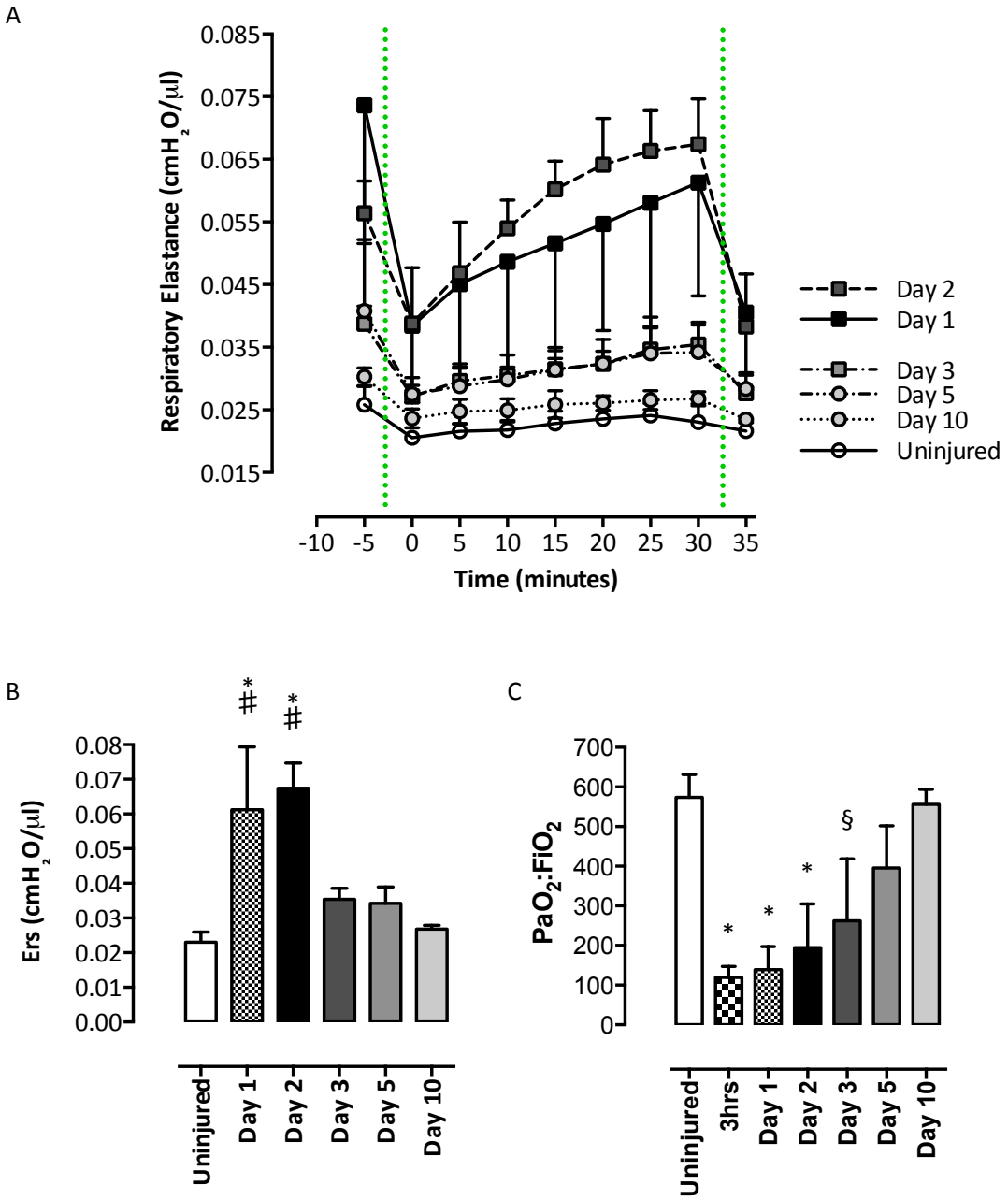

Figure 6.2. Changes in respiratory mechanics and oxygenation during resolving acid aspiration

(A) At 24 and 48 hours after acid instillation, mice show an increase propensity for alveolar collapse as demonstrated by the 30-minute ventilation time courses. Green lines represent recruitment manoeuvres. (B) Respiratory system elastance also peaks at days 1 and 2 with significant improvements by day 3. (C) Oxygenation deteriorates immediately at 3 hours and then recovers over 10 days. N=3-5/each time point. * P<0.001 versus uninjured; § P<0.05 versus uninjured; ♯P<0.001 versus Day 3.

6.4.5 Indices of lung oedema – permeability and clearance

These changes in oxygenation are most likely a consequence of 1) alveolar-capillary barrier dysfunction with ensuing pulmonary oedema; 2) ventilation/perfusion mismatch; and 3) alveolar atelectasis. Lavage protein concentration, a marker of alveolar capillary barrier permeability, showed a significant increase in the first 24 hours after injury followed by a gradual improvement to uninjured levels by day 10 (Figure 6.3 A). At later time-points the presence of BAL protein may not accurately represent alveolar-capillary barrier permeability given that the alveolar epithelium can also actively clear fluid as well as protein (384). Hence, we measured permeability index in animals at these time-points through the intravenous instillation of AF-594 labelled albumin during the 30-minute ventilation period. Interestingly during the first 48 hours, increases in permeability index matched BALF protein showing marked increases. However, unlike the BALF protein, permeability index did not return to baseline values by day 10 and remained elevated (non significant) from day 3 onwards (Figure 6.3 B). This confirmed the notion that BALF protein may not be a good reflection of alveolar capillary barrier permeability at later time points given that the majority of proteins likely translocate in the first 48 hours of injury and that the complete resolution of lavage protein levels likely reflects a combination of improved barrier permeability and increased clearance of protein from the alveolar space. Lung wet/dry weight ratios showed a near doubling of water content in the lungs (up to 7.2 g H_2O per gram of dry lung). This returned to baseline levels by day 10 (4.5 g H_2O per gram of dry lung) (Figure 6.3 C). Hence, despite a persistent derangement in permeability index, lung water had indeed returned to normal. Figure 6.4 shows the macroscopic appearance of uninjured lungs and lungs at day 2 and 10 after acid aspiration. Injured animals at day 2 show a bilateral injury with significant lung discolouration as a result of haemorrhage and oedema formation. The lungs of animals at day 10 after acid aspiration look similar to control lungs.

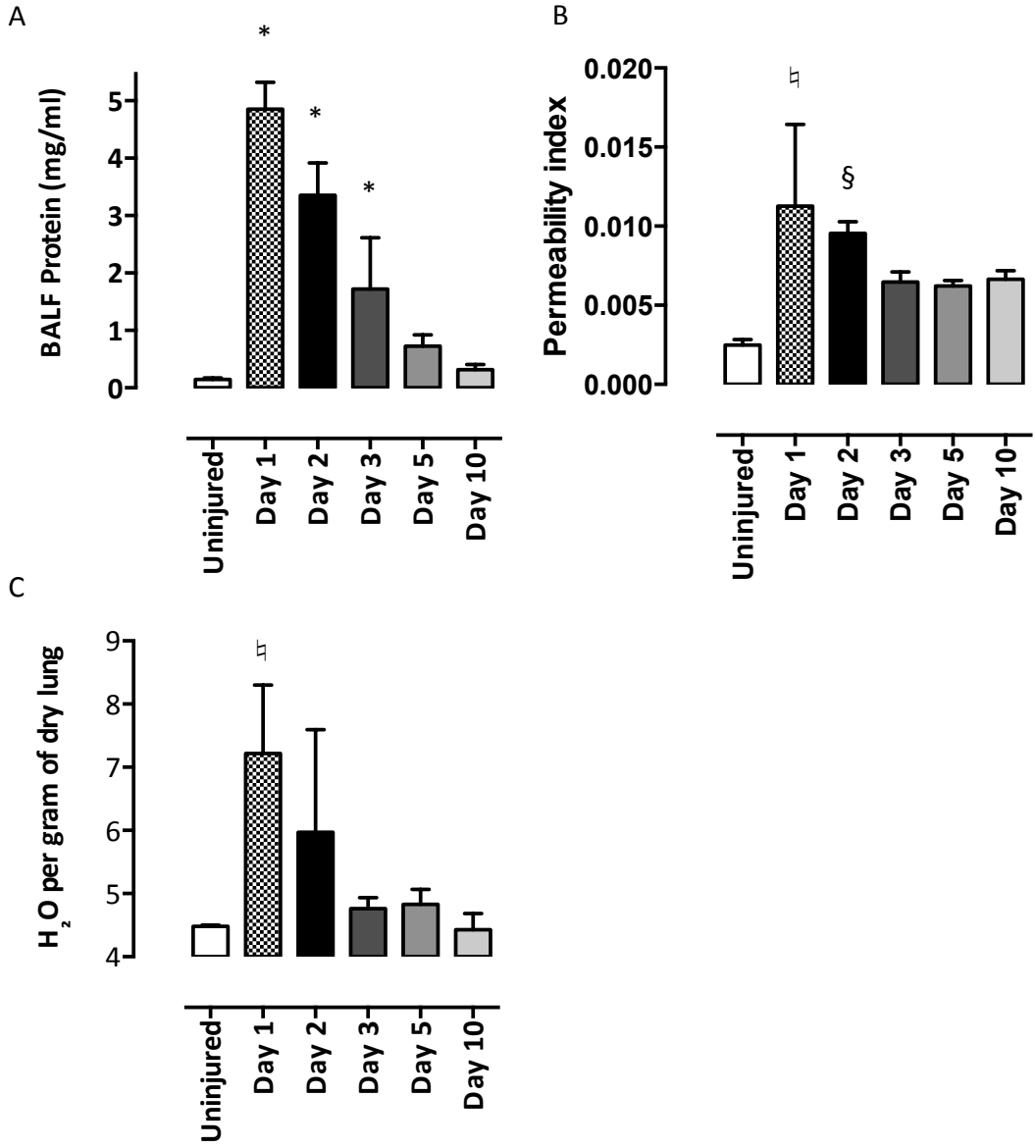

Figure 6.3. Changes in alveolar capillary barrier dysfunction during resolving acid aspiration

Mice show significant increases in epithelial and endothelial permeability as shown by increased BALF protein (A) and increased permeability index (B) at 24 hours. There is a doubling of lung water content at 24 hours with subsequent reduction (C). N=3-6/each time point. * P<0.001 ǂ P<0.01 § P<0.05 versus uninjured

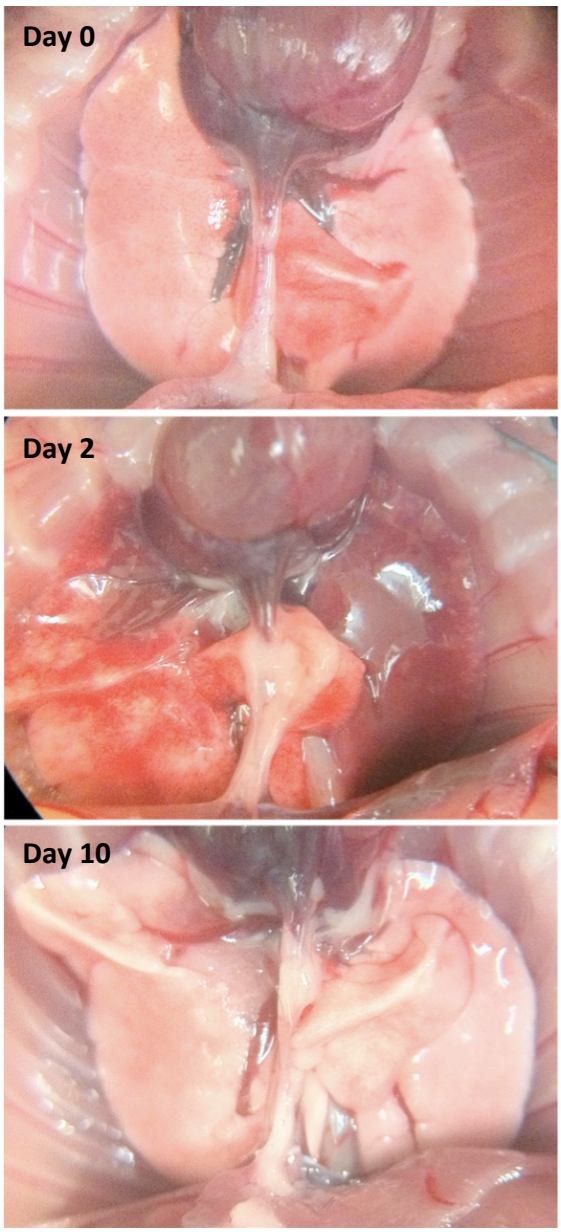

Figure 6.4. Changes in macroscopic appearance of lungs during resolving acid aspiration

Gross macroscopic appearance of normal uninjured mouse lungs (top) and lungs of mice after 2 (middle) and 10 days (bottom) after injury (the heart has been moved superiorly).

6.4.6 Epithelial injury and recovery.

The previous chapters have showed that early derangements in permeability and epithelial fluid clearance influenced the development of alveolar oedema over the first 3 hours of acid-induced lung injury. Alveolar fluid clearance rate was measured to ascertain if epithelial dysfunction was present during later stages of injury (i.e. 2-3 days), and whether resolution of epithelial injury was also apparent from day 3 onwards. In addition to alveolar fluid clearance being significantly reduced immediately after lung injury induction (within 90 minutes), there continues to be a 42% reduction on day 2, after which, the fluid clearance rate is re-established and recovers (figure 6.5 A). This recovery leads to a 15.5% increase in AFC rate on days 5 and 10 as compared to baseline. This may explain the normal wet/dry weight despite increased permeability index on day 10.

Soluble RAGE was detectable within 90 minutes of acid aspiration but reduce after this early peak (figure 6.5 B). RAGE levels follow a similar trend to other BALF soluble mediators and return to near baseline by day 5. There were strong correlations between RAGE, AFC, and PaO_2/FiO_2 ratio suggesting these parameters robustly represented measurements of epithelial function in this model (figure 6.5 C, D and E).

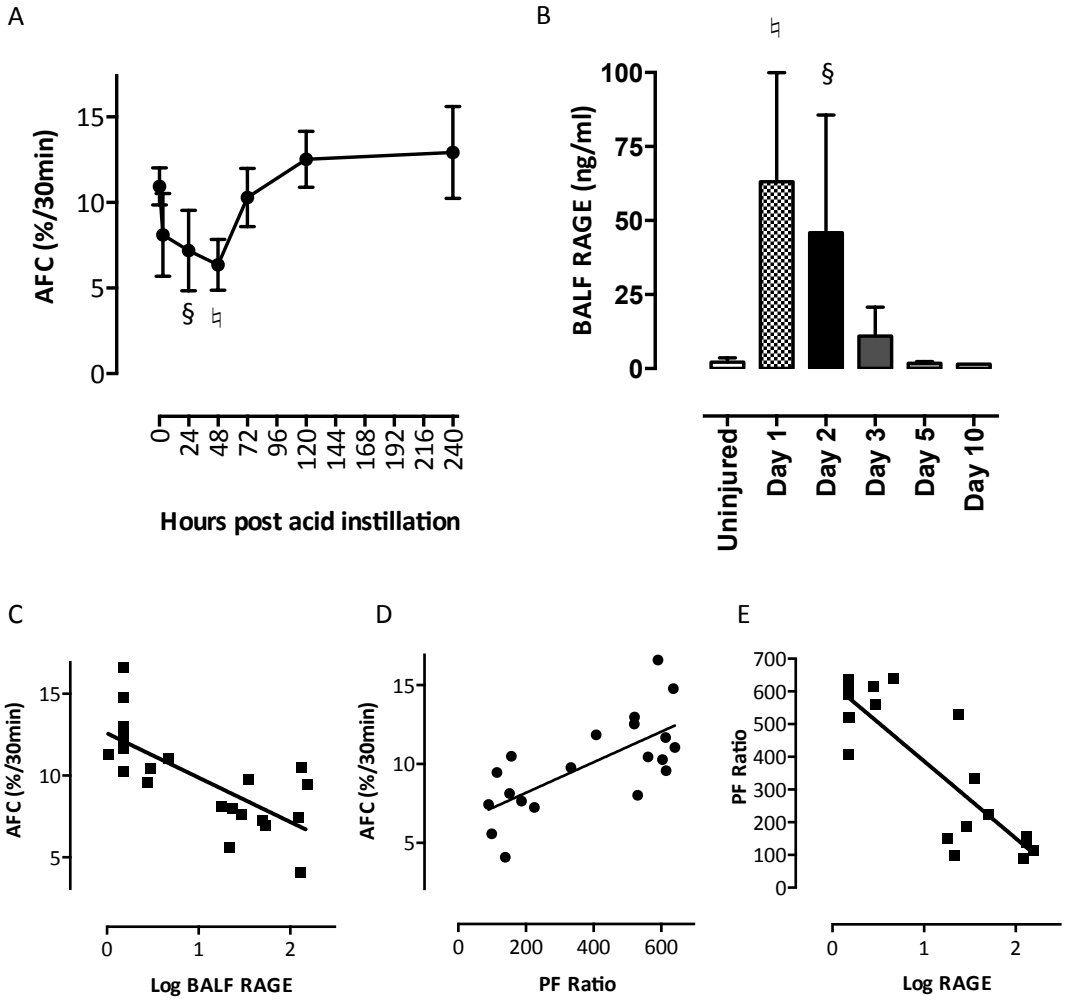

Figure 6.5. Changes in epithelial dysfunction and injury during resolving acid aspiration

AFC also deteriorates within 3 hours and remains low for the first 48 hours (A) and dramatically recovers on day 3. There is a significant upregulation of soluble RAGE in the alveolar space at 24 hours (B). There are strong relationships between markers of epithelial injury, epithelial dysfunction and arterial oxygenation. Levels of BALF RAGE inversely correlate with AFC (C - Pearson R = -0.7339; P<0.0001); AFC strongly correlates with oxygenation (D - Pearson R = 0.697; P<0.001); and PF ratio inversely correlates with BALF RAGE (E - Pearson R = -0.71; P<0.01). N=3-6/each time point. ǂP<0.01; § P<0.05 versus uninjured

6.4.7 Characterisation of alveolar inflammation and resolution

Differential cytology of BAL showed significant changes in the alveolar content of leukocytes (figure 6.6). Figure 6.7 also shows the representative photomicrographs of BAL cytology at various phases after acid aspiration. In uninjured animals, the major leukocyte population is the alveolar macrophage and constitutes over 95% of all alveolar cells. Acid aspiration induces a severe neutrophil alveolitis, peaking at day 2, and disappearing very rapidly by day 3. On day 3 there was a significant increase in the number of apoptotic neutrophils many of which were in the process of efferocytosis by macrophages (figure 6.7). Additionally, there is an increase in the myeloid cell population (macrophages and monocytes) at day 2 although relatively much lower and overshadowed by the neutrophil response. The increase in alveolar macrophage and monocyte populations likely reflects an exudative macrophage population with the total alveolar macrophage population being expanded through replenishment from blood monocyte populations. This recruited pool may be involved in the removal of apoptotic bodies and help clear the debris to facilitate resolution within the alveolar space. Furthermore, there were increases, from day 3 onwards, of a lymphocyte population that accounts for nearly 15% of all leukocytes by day 10. Lung homogenate myeloperoxidase activity (figure 6.6 C) shows a significant rise, as expected, at 24 hours with a subsequent decline at 48 hours. This initial peak corresponds well with the neutrophil influx into the alveolar space. However, MPO activity in this set of experiments continued to increase after this initial reduction at day 2 reaching significantly higher levels by day 10.

There was an increase in inflammatory cytokine production with day 2 showing the highest levels of TNF and IL-6. In addition, BALF levels of MIP-2 and KC (mouse IL-8 analogues), which drive neutrophil chemotaxis and infiltration into the alveolus also peak at day 2 but effectively, disappear by day 3. The cessation of pro-inflammatory mediator production and their catabolism is strongly suggestive of a shift in the alveolar milieu from a highly pro-inflammatory into an anti-inflammatory/pro-resolving state (figure 6.8).

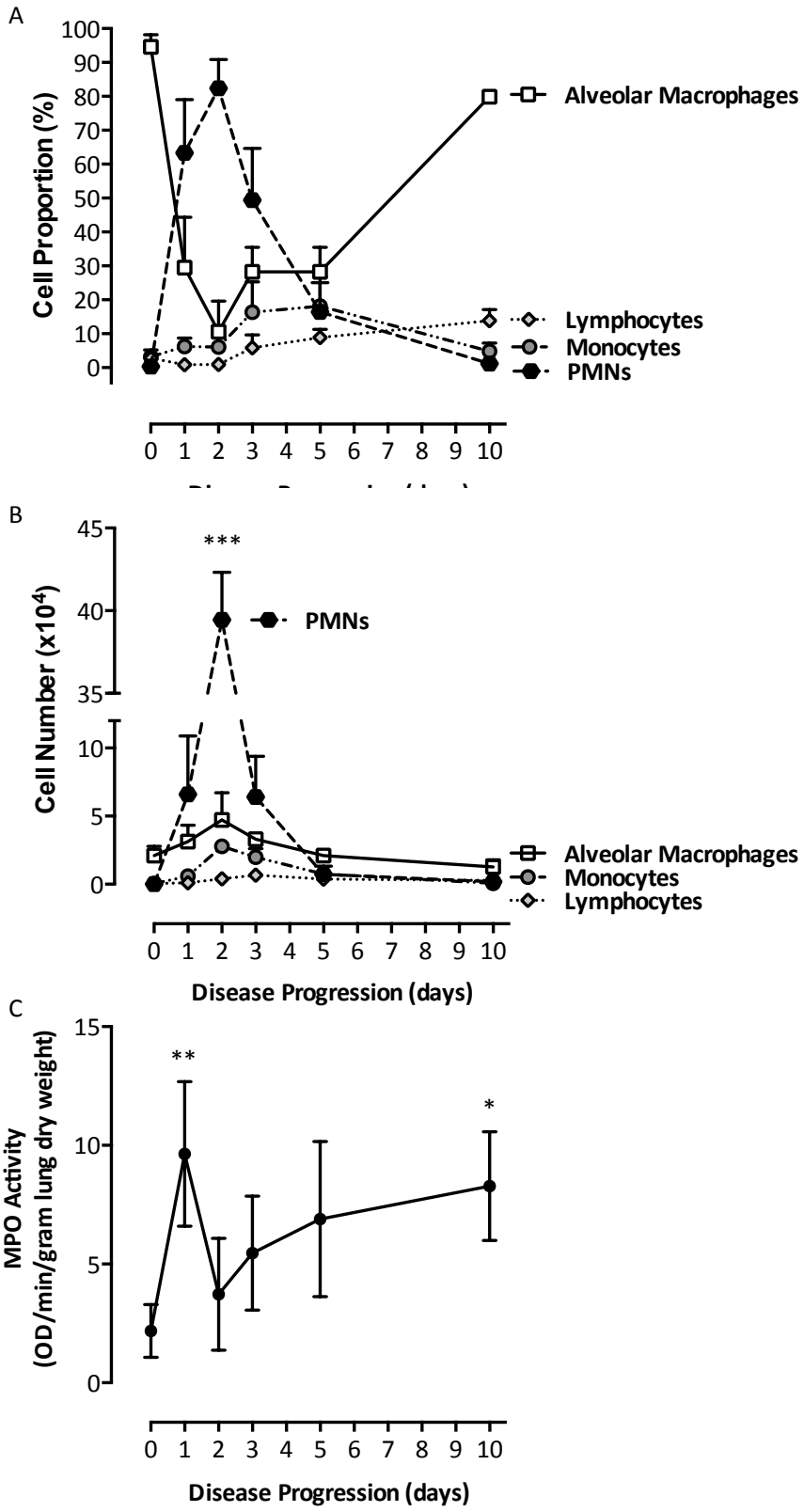

Figure 6.6. Changes in alveolar leukocyte types and numbers during resolving acid aspiration

Analysis of alveolar leukocyte proportion (A) and number (B) in the alveolar space showed significantly increased neutrophil influx peaking at 48 hours post acid

aspiration. Concomitantly there is an increase in monocyte/macrophage cell number in the alveolar space. Interestingly, myeloperoxidase (MPO) activity increases in the first 24 hours but then declines at day 2. It then continues to increase up to day 10. N=3-6/each time point. * P<0.001; ♮ P<0.01; § P<0.05 versus uninjured

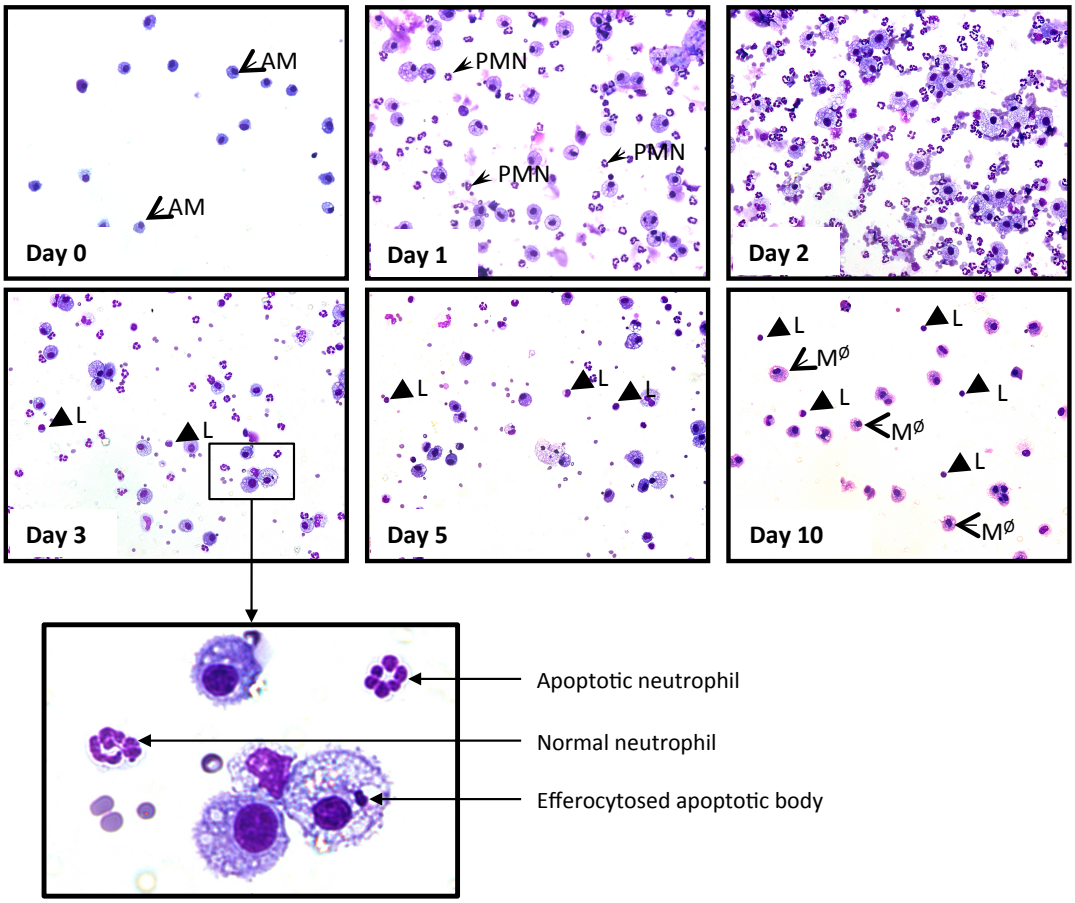

Figure 6.7. Changes in alveolar cytology during resolving acid aspiration
Photomicrographs show significant changes in alveolar cytology with increasing neutrophilia in the first 48 hours. By day 3 there is a dramatic reduction with increased number of apoptotic neutrophils (inset), many of which have been efferocytosed by alveolar macrophages. Over days 3 and 10 there is increasing proportion of lymphocytes and monocytic cells infiltrating into the alveolar space reaching a 15% lymphocytic infiltration by day 10.

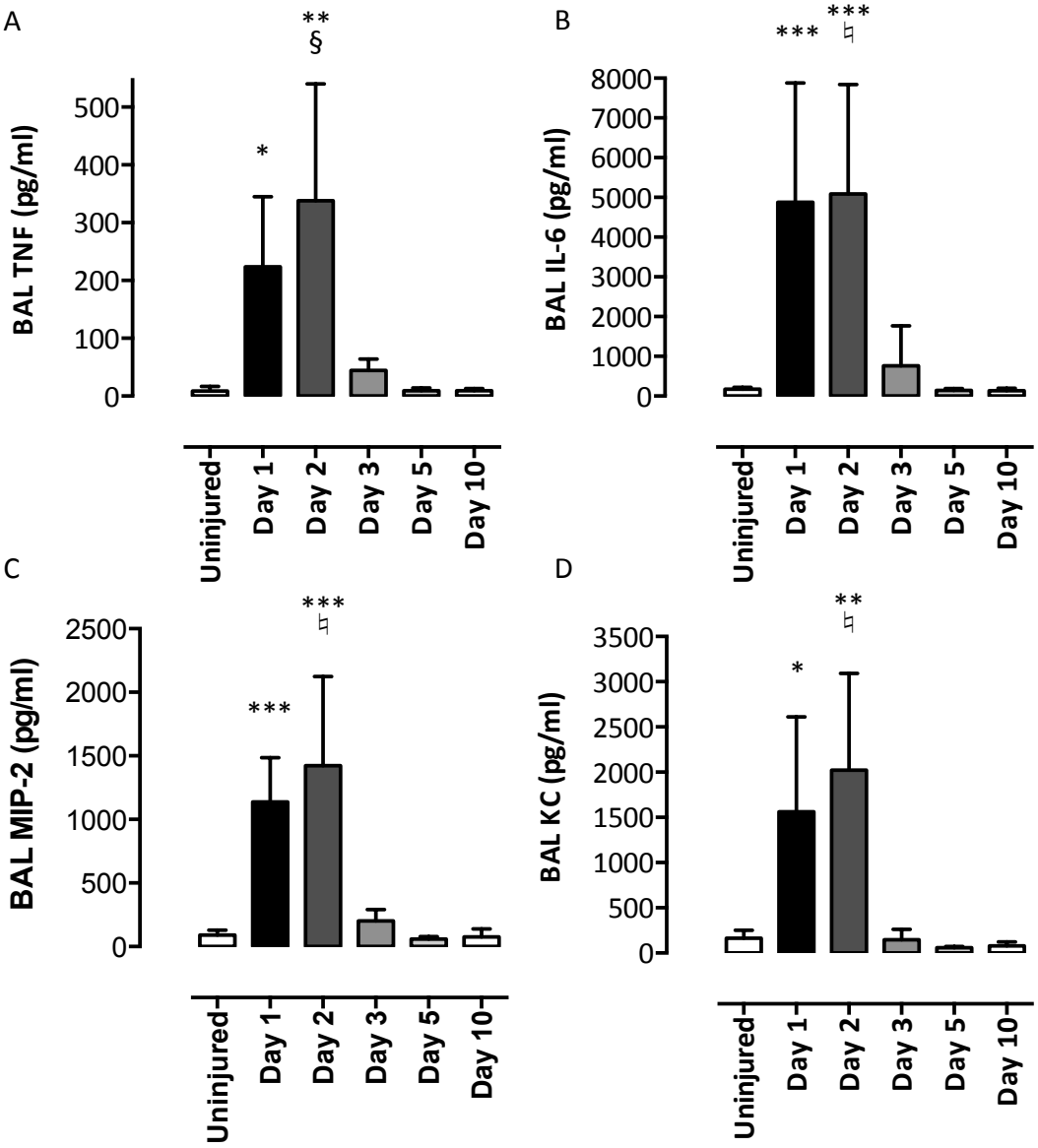

Figure 6.8. Changes in alveolar cytokines/chemokines during resolving acid aspiration

Analysis of alveolar cytokines - TNF (A) and IL-6 (B); and chemokines - MIP-2 (C) and KC (D) during the time course of injury shows significant increases in the first 48 hours which decline on day 3. N=3-6/each time point. *** P<0.001 ** P<0.01 * P<0.05 versus uninjured; ǂ P<0.01 § P<0.05 versus day 3

6.4.8 Lung injury scoring

We evaluated histological injury using recently published guidelines recommended by the ATS workshop report on animal modelling of ARDS (192). We found that there were significant changes to the lung parenchyma and cellular infiltration in the lung at various time-points after injury (figure 6.9). During the injurious phases there are significant increases in lung haemorrhage and fluid in the alveolar space (red arrows). There is significant disruption to the walls of the alveoli with thickening and multiple hyaline membranes being present on the inner surface (green arrows). As shown previously through lavage cytology there is a significant rise in alveolar neutrophils (white arrows). However, there are also significant numbers of interstitial neutrophils (yellow arrows). After this dramatic change in alveolar structure there appears to be resolution through the removal of neutrophil infiltrates as well as alveolar debris. This clearance process is associated with a steady increase (between days 2 and 5) in alveolar and interstitial mononuclear cells (blue arrows).

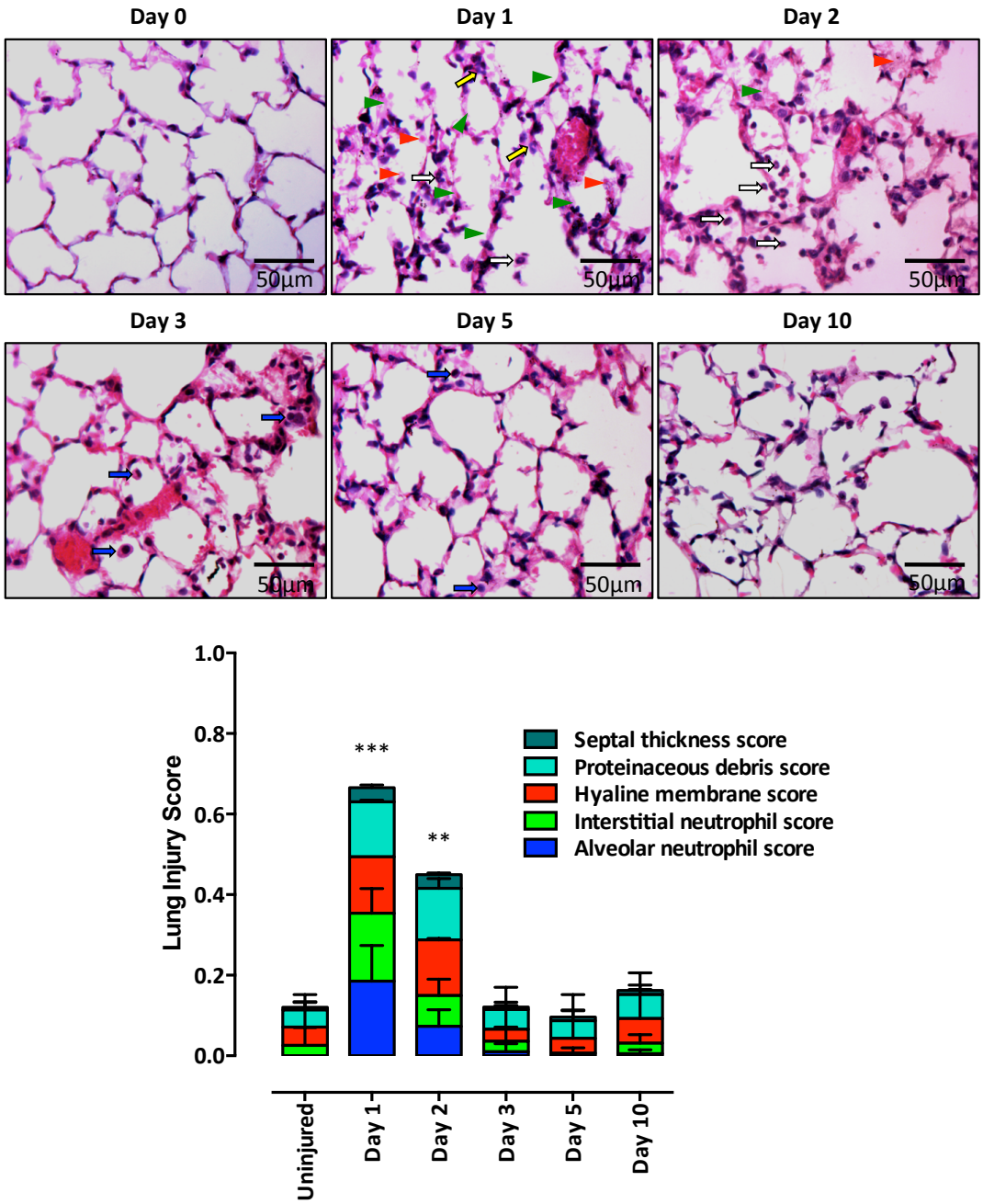

Figure 6.9. Histological analysis of resolving acid aspiration

Representative haematoxylin and eosin (H&E)-stained sections of uninjured and injured animals at all time-points after acid aspiration (A). There is greater cellularity consisting mainly of alveolar (white arrows) and interstitial (yellow arrows) neutrophils on days 1 and 2 with more areas of atelectasis as well as increased alveolar disruption with hyaline membranes (green arrowheads), proteinaceous debris and haemorrhage (red arrowheads). With increasing time there is a shift from a neutrophilic to a predominantly mononuclear infiltrate (blue arrows). Lung injury scoring shows a significant injury on days 1 and 2 with a reduction from day 3 onwards. Lung injury was assessed on a scale of 0–2 for each of the following criteria: i) neutrophils in the alveolar space, ii) neutrophils in the interstitial space, iii) number of hyaline membranes, iv) amount of proteinaceous debris, and v) extent of

alveolar septal thickening. N=3-4/each time point. *** P<0.001 ** P<0.01 versus uninjured

6.4.9 Resolution through fibrosis

To ascertain if the resolution of physiology manifest as complete histological recovery or through a fibrotic repair mechanism, lung sections were stained for collagen deposition with Masson's Trichrome stain. There was significantly increased collagen deposition (figure 6.10 - blue staining and blue arrows) as early as day 2 after acid aspiration. Sections showed a peri-bronchial cellular infiltration (red arrows) with marked thickening of bronchiolar walls (green arrows). There were multiple fibrotic foci (white arrows) visible by day 10 suggesting significant fibrosis that had also extended into neighbouring alveolar interstitium.

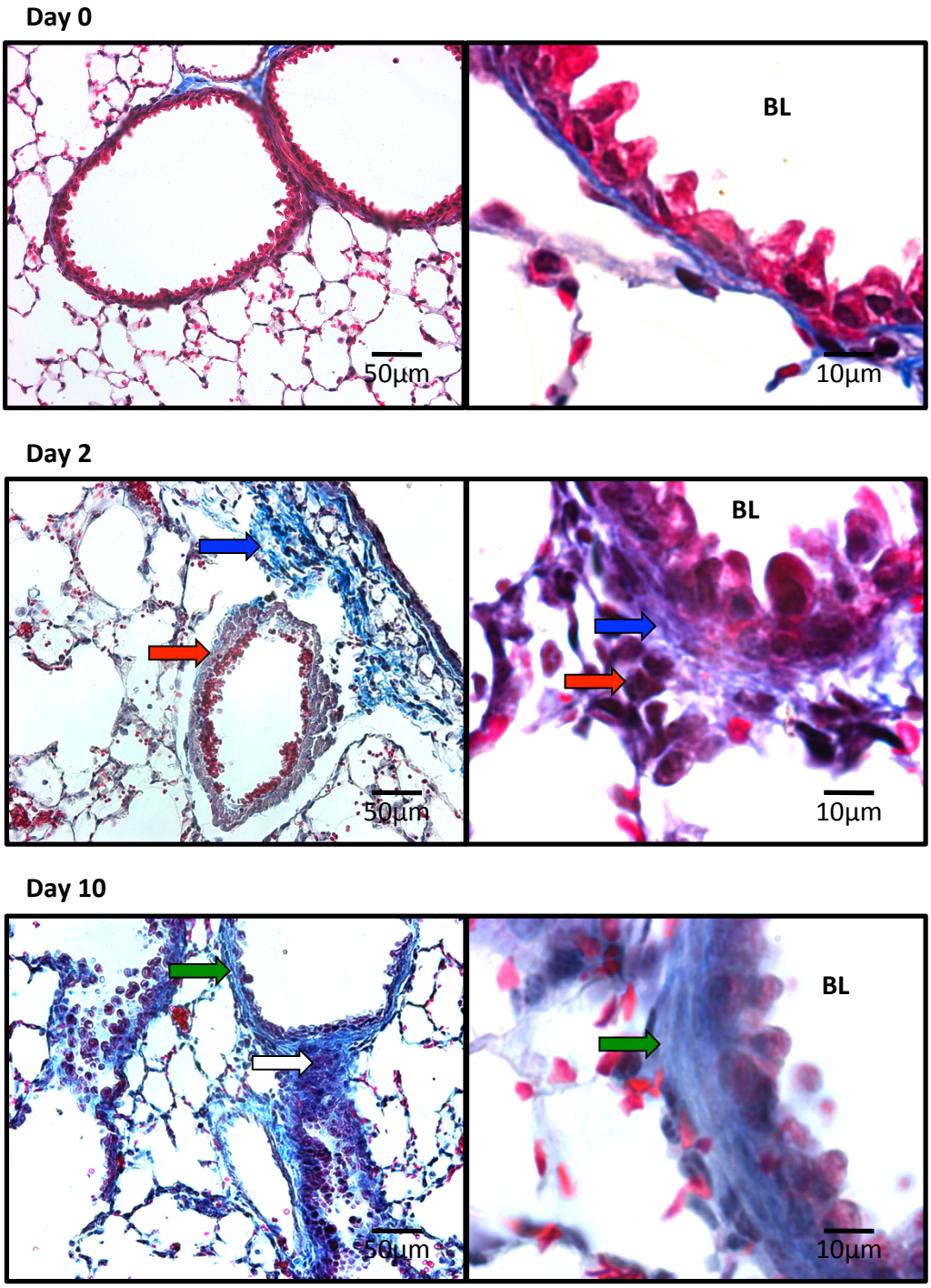

Figure 6.10. Analysis of fibrosis during resolution of acid aspiration
Representative Masson's trichrome stained sections in the absence of injury, during the peak of injury, and after the resolution of injury from acid aspiration. There is cellular infiltration focussed in the peribronchiolar regions (red arrows) with increasing thickness of bronchiolar walls (green arrows) as a result of increased collagen deposition (blue arrows), which is already apparent as early as day 2, and increases over the course of the injury. This is particularly apparent at day 10, which shows multiple fibrotic foci (white arrow). BL: bronchiolar lumen.

6.5 Discussion

Animal models of lung injury have significantly advanced our knowledge and understanding into the pathophysiology of ARDS. Furthermore, they test the application of preclinical therapeutics prior to application in humans. One of the major advantages of rodent models of disease is the potential application of genetically engineered knockout strains to elucidate the impact of specific proteins and signalling pathways in disease pathobiology, such as those used in previous chapters of this thesis. Furthermore, the abundance of experimental reagents (e.g. antibodies) in mouse species makes small animal modelling of disease essential in the translational pathway from target discovery to clinical application. Currently there are no targeted pharmacological treatments available for ARDS and all drugs that have been applied in the preclinical setting have failed in clinical trials. One of the reasons for this is the poor recapitulation of clinical entities such as ARDS, with respect to not only pathophysiology but also temporal profile, in the currently available preclinical animal models. This has been highlighted recently by two major publications in the lung injury literature. The first is a review by Matute-Bello et al (37) and the second, guidelines from an ATS workshop as to the features required to optimally model ARDS (192). Overall, no current clinical animal model replicates the complexities of ARDS in terms of severity, pathobiology, temporal profile and clinical relevance.

6.5.1 Pitfalls in animal models of ARDS

There are currently many models of ARDS that capture specific aspects of the clinical entity. For instance, endotoxin instillation produces significant inflammation as evidenced by a massive infiltration of neutrophils into the alveolar space. However, this is not preceded or followed by a significant increase in lung extravascular lung water (43). Bleomycin induced lung injury leads to increased inflammation but is followed by a massive fibrotic reaction and hence, it represents the major model used to investigate lung fibrosis (385). Other models such as intravenous oleic acid produce overwhelming injury but do not allow the investigation of later phases, in particular resolution. The aim of this chapter was to develop a model that allowed

the investigation of not only the injurious and inflammatory phases of ARDS, but also the resolution and recovery phases from a highly injured physiological baseline.

6.5.2 Acid aspiration – a truly translational model

The acid aspiration paradigm has been regarded as one of the most clinically relevant models of ARDS as it mimics aspiration pneumonitis in humans (also known as Mendelson's syndrome (194)). However, human aspiration consists of more than simply hydrochloric acid but also a variety of other insults including food and bacterial particulate matter. Each of these elements has been shown to enhance injury in rodents (197, 386-388). In spite of this, there is no other model that truly replicates a human cause and produces as many relevant features of human ARDS in mice.

The acid aspiration model has been mainly utilised in association with a period of mechanical ventilation as shown earlier in the acute 3-hour model. However, this does not allow for investigations into the later phases of illness due to limitations in providing prolonged mechanical ventilation in rodents. A major hurdle is the narrow window for dosing acid (37) – too much leading to overwhelming injury and unacceptably high mortality, and too little failing to produce sufficient injury for investigation. This is confirmed by the initial dose-titration experiments. Hence, those models that have used the acid aspiration paradigm to investigate later time-points of acute lung injury have compromised on mortality with a lower level of injury by using a smaller dose of acid (pH and volume) or through unilateral instillation (191, 381, 382). Arguably, these protocols do not reproduce the severity or the bilateral injury necessary for defining ARDS. The high mortality and need for techniques to provide mechanical ventilation may explain why the acid aspiration model is only utilised in 3% of ARDS literature (37) despite being cited as one of the most clinically relevant models (187, 253).

The model described in this chapter incorporates simple technical aspects of everyday clinical intensive care practice that cumulatively improve the recovery of animals during the immediate aspiration phase. This starts from the beginning of the

protocol where a fluid bolus is administered during anaesthesia to prevent excessive weight loss and haemodynamic compromise. Subsequently, careful airway manipulation enables a grade 2 “Levine and McCormack” view of the vocal cords allowing the careful insertion of a catheter to facilitate acid instillation (see photo 2.2). The subsequent care of animals in a custom made recovery box (see photo 2.3) providing humidification, warming, and oxygen therapy reduced the early immediate mortality to zero. This early mortality was likely secondary to severe bronchospasm and upper airway oedema given that sternal recession was visually apparent in those animals that died during model development. Despite the initial fluid resuscitation there was a significant reduction in weight over the first 2 days after acid aspiration. In previous studies within our group using a similar instillation technique, endotoxin (without the initial fluid bolus) produced only a 2% weight loss at 24 hours (389), in comparison to 8% in this model. The difference between 50ul and 75ul volumes of 0.1M acids likely represents different severities and progression of illness.

6.5.3 Respiratory physiology attains ARDS criteria

The current model achieves clinical ARDS criteria within 24 hours of insult. There is an acute onset of hypoxaemia (reaching a PaO_2/FiO_2 of 200), and as can be seen from the macroscopic lung images (figure 6.4) there is considerable bilateral lung oedema. Furthermore, there were significant deteriorations in respiratory mechanics and gas exchange. Many investigators ignore the need for robust standardisation of lung physiology, particularly in rodents. As a consequence of their high thoracic wall and respiratory compliance, anaesthesia and surgical preparation inevitably induces alveolar collapse. Hence, in the current experiments, respiratory mechanics and arterial oxygenation were measured after rigorous standardisation of the volume history of mouse lungs using a recruitment manoeuvre followed by a 30 minute period of low tidal volume ventilation. This enabled any confounding factors between animals (at different time-points and different severities of injury) to be standardised. We have recently shown that the measurement of lung mechanics in mice significantly depends on how they are manipulated during any mechanical ventilation protocol. For instance, mice ventilated at 10ml/kg without regular recruitment manoeuvres show a gradual decrease in lung compliance due to

atelectasis, as compared to mice ventilated at 10ml/kg but with regular 30 minutes recruitment manoeuvres (239). In this acid model, there is a tendency for alveolar collapse (as determined by substantial reduction in lung elastance after application of the first recruitment manoeuvre as seen in figure 6.2 A) especially on days 1 and 2. Hence, the changes in respiratory mechanics are a reflection of not only alveolar oedema formation but also alveolar atelectasis. The changes in BALF protein and lung wet/dry weight ratio confirm the significant increase in alveolar capillary barrier permeability and impact upon the alveolar epithelium.

6.5.4 Alveolar epithelial dysfunction and recovery in later phases of ARDS

The importance of the alveolar epithelium in lung injury pathogenesis has formed the basis of the thesis thus far. Even within this longer model we found that alveolar fluid clearance deteriorated within 3 hours of acid aspiration and showed a 42% reduction at 48 hours. In comparison with the 3-hour acute acid model, this reduction in AFC seemed less, potentially suggesting a lower severity of injury as a result of differences in the instillation technique (i.e. [orotracheal and spontaneous ventilation] versus [tracheostomy and mechanical ventilation]). Whilst acid aspiration models have been shown to induce deteriorations in AFC (71, 255), this model shows (for the first time) a recovery in AFC from day 3 onwards, suggesting that there is restoration and repair of the alveolar epithelium. This stark recovery in alveolar fluid clearance occurs between days 2 and 3 and coincides with a marked reduction in cytokines and neutrophil migration into the alveolar space. Hence, these data support the hypothesis that the later deteriorations in AFC may be secondary to signals (such as death ligands) emanating from recruited leukocytes (as discussed in section 5.5.8). Future investigation examining the relationship between caspase-8 activation and AFC at later time-points as well as other mediators maintaining the deterioration in AFC will provide interesting insights into this important pathophysiological phenomenon. Finally, AFC seems to increase up to day 10 achieving an 18% increase compared to baseline AFC using this system. This may account for the normal wet/dry weight ratio in the presence of increase permeability. The mechanisms that lead to this sudden improvement in AFC remain undetermined and remain the subject for future work.

6.5.5 DAMPen the RAGE

RAGE is a multi-ligand transmembrane protein that functions as a pattern recognition receptor. RAGE has been advocated as a specific biomarker for type 1 alveolar epithelial dysfunction in experimental and human models of disease (344, 345, 390). It is a member of the immunoglobulin superfamily and is highly expressed in lung tissue and is localised to the basal surface of type 1 alveolar epithelial cells. It recognises a large number of ligands including a number of damage-associated molecular patterns, ranging from advanced glycation end-products, amyloid beta-peptides, high-mobility group box-1 (HMGB-1) protein and S100 proteins. The activation of membrane bound RAGE leads to the activation of MAP kinase pathway leading to NFκB activation (391, 392). There is increasing recognition that RAGE is important in the detection of sterile damage by sensing danger signals (e.g. HMGB-1) released in response to cellular stress and cell death (12).

RAGE was utilised in this thesis as a marker of epithelial injury as has been shown by a number of investigators. Uchida et al (308) showed that as severity of acid-induced lung injury increased (increasing acid normality) the concentration of alveolar RAGE also increased in a dose-dependant manner. Furthermore, this effect was reproduced as the volume of acid was increased suggesting that the amount of protons instilled is the important determinant of injury in this model. No RAGE was detected in the serum (consistent with unreported findings from our group) of these animals suggesting a pulmonary source. In the same study, they also found that RAGE was increased during permeability pulmonary oedema with greater increases in those with ALI/ARDS as opposed to hydrostatic permeability oedema. Hence, these data suggest that the source of RAGE is indeed the lung and during injury it is released into the alveolar space. Although, there have been many studies examining the expression of membrane bound RAGE, the consensus at present is that it is expressed predominantly by type 1 AECs although expression may be inducible in primary human lung microvascular endothelial cells (393, 394).

The systemic administration of soluble RAGE significantly attenuated lung injury in a model of endotoxin induced lung injury and may contribute to the suppression of

excessive inflammatory responses (395). Briot et al utilised an isolated perfused human lung model to show that alveolar RAGE showed an inverse relationship to alveolar fluid clearance. In contrast, perfusate RAGE showed no significant association. In both our short (figure 5.3) and long-term model (figure 6.5) of acid aspiration used in this thesis there were significant inverse correlations between AFC and alveolar RAGE confirming that both were robust markers of epithelial dysfunction at all stages of lung injury.

However, the question remains in this longer-term model as to what soluble RAGE signifies at later time points. RAGE is shed within 90 minutes of acid instillation and hence, the pattern seen within this model suggests that RAGE could be an indicator for epithelial barrier permeability, whereas BAL protein is a marker of combined endothelial and epithelial permeability. This may hold true given that protein originates from the plasma compartment but RAGE is thought to be integral to the binding of the epithelium to the basement membrane of the lung (396) and hence any damage may promote disruption and facilitate alveolar flooding with the "washing in" of RAGE into the alveolar space. Furthermore, the proteolytic shedding of RAGE (by MMP-3 and -13) into its soluble form (397) may dampen inflammatory responses by acting as a decoy receptor reducing the extent to which damage associated molecular patterns (DAMPs - such as HMGB-1) can promote inflammation and the extent to which membrane RAGE can signal NFκB activation. The application of this resolving model of acid aspiration to investigate RAGE biology would potentially provide interesting avenues into the roles of this interesting molecule in acute sterile lung injury and inflammation.

It has recently been shown the down regulation of cellular expressed RAGE also promotes the development of fibrosis in patients with interstitial pulmonary fibrosis. This was also shown to be the case in mice injured with bleomycin and the authors suggested this to involve a mechanism involving a dysregulation in AEC cell adhesion, migration and proliferation (398). Given the substantial epithelial injury seen in the resolving acid model as well as the progression to fibrosis, this model may be ideal to investigate this association of RAGE with fibroproliferation.

6.5.6 Resolution of inflammation is integral to physiological resolution

The role of inflammation during various phases of ARDS is a relatively obscure entity. Whilst depletion of neutrophils and monocytes has attenuated ARDS in experimental models (89, 399-402), ARDS continues to occur during neutropenia in patients with haematological failure (91-94). Hence, rather than targeting these cells which have major roles in fighting bacterial infection, it may be more efficacious to target pro-resolving mechanisms to potentiate repair of the lung. Indeed, critical illness in its entirety may be seen primarily as a non-resolving state of inflammation. In the introduction, we discussed the mechanisms behind resolution and recovery in critical illness many of which are recapitulated within this model.

The first step towards resolution and recovery is the removal of any stimulus. An advantage of the instillation of acid is that it provides a defined time zero. The acid is likely to be buffered relatively quickly either within the alveolar space or in the blood. In contrast, the larger doses of endotoxin may remain within the respiratory system for longer and contribute to a sustained TLR-4 activation. Hence, although time zero is known, the activation kinetic in the endotoxin model is likely to be more prolonged. Furthermore, and most importantly, unlike any of the endotoxin models (intravenous or inhaled) there is significant physiological dysfunction recapitulating the picture of clinical ARDS. This facilitates much needed investigation into the mechanisms through which inflammation can promote and resolve physiological derangement (e.g. hypoxaemia, respiratory compliance, and AFC) during lung injury. In contrast, most investigators struggle to produce the same physiological dysfunction with other ARDS models, and hence, although resolution of lung inflammation can be investigated well, resolution of lung injury and physiology cannot. In fact, only models using extremely large doses of intravenous endotoxin, or oleic acid model produce any pulmonary oedema in mice (37). In general, the endothelial and epithelial surfaces of the lung are quite resistant to endotoxin (43). Indeed, the lack of mortality during days 1–2 (when injury peaked) may be specific to the acid model, which showed minimal haemodynamic compromise.

The lavage cellular profile shows a shift from a neutrophilic alveolitis to a more mononuclear alveolitis - another recommended workshop feature for an inflammatory response (192). The loss of neutrophils from day 2 onwards is a necessary feature for the resolution of inflammation. This reduction is likely to occur through apoptosis followed by subsequent efferocytosis by macrophages. Indeed, during day 3 there are an abundant number of apoptotic bodies visible within the cytoplasm of mononuclear cells on BAL cytology (figure 6.7). This apoptosis and efferocytosis of neutrophils is an integral step to signal the beginning of inflammatory resolution. The ingestion of apoptotic cell bodies by activated monocytes leads to a change in their phenotype and a reduced production of pro-inflammatory cytokines and an increased production of anti-inflammatory cytokines (129, 403).

It is interesting that the resolution of inflammation comprising the loss of neutrophils (likely through apoptosis); their ingestion by macrophages; the reduction in TNF/IL-6 production should coincide so well with the resolution of physiological injury (such as oxygenation and AFC). Indeed, this supports the notion that inflammatory leukocytes perpetuate lung injury but it is also evident that functionally pro-resolving leukocytes may be recruited to the lung. This switch between pro-inflammatory and pro-resolving phenotypes of leukocytes already within the lung is likely to be of paramount importance and one, which malfunctions in ARDS. Indeed, the BAL cytology shows increases in lymphocyte proportion accounting for up to 15% of all leukocytes in the alveolar space at 10 days. This is consistent with recent data from D'Alessio et al suggesting the importance of T-regulatory cell populations in the resolution of endotoxin mediated lung inflammation (98).

An interesting observation is that during the first 48 hours a significant number of neutrophils remain within the interstitial space (as assessed by the histological lung injury score). Indeed, this raise questions as to the robustness of using alveolar cytology counts to measure neutrophil influx. Of further interest is the increases in lung homogenate MPO activity after day 3 even after alveolar neutrophils have been

removed. This potentially suggests that interstitial populations or mononuclear cells may be contributing to this MPO activity. Hence, a technique to investigate the interstitial space of the lungs may be of significant interest. Such a technique would also be of significant value for other resident and itinerant cell populations (such as dendritic cells, interstitial macrophages, and lymphocytes) within the interstitial compartment. The functions and roles of these interstitial cell types have received little attention in ARDS research and will be the focus of chapter 7.

6.5.7 Resolution through pulmonary fibrosis

If patients survive the acute exudative phase of ARDS they either progress to repair normally or in a significant proportion proceed into the fibro-proliferative phase of the syndrome. In fact, Papazian et al performed open-lung biopsies on 100 patients after 7 days of fulfilling ARDS criteria and found 53% of patients had a significant fibrotic component (404). Whilst the fibroproliferative phase of ARDS has been predominantly discussed to occur after the exudative phase, in fact, a number of studies in man has shown the deposition of extracellular matrix during the early stages of ARDS, in particular, those caused by direct insults. Marshall et al showed that BAL from patients between 1 and 7 days of ARDS diagnosis was able to stimulate ex vivo lung fibroblast proliferation (405). Armstrong et al showed that markers of collagen turnover are elevated within 48 hours of ARDS suggesting that the fibroproliferative phases commences earlier than previously perceived (406). Pugin et al found collagen synthesis occurring on the first day of intubation in association with the production of pro-inflammatory cytokines (407). Indeed, type 1 collagen mRNA increases within 2 hours of cardiopulmonary bypass (a common cause of ARDS) and is dependant on resident fibroblasts (408). There are increased numbers of myofibroblasts and procollagen type 1 producing cells during the exudative phase of ARDS (409). Furthermore, TGF-beta, a mediator heavily implicated in various forms of lung fibrosis, is also upregulated on day 3 of ARDS (410-412).

The factors that determine the development of fibrosis in ARDS remain unknown and very few animal models allow investigation of this during a clinically relevant

interval (385, 413). Bleomycin is the most commonly used model to investigate mechanisms of fibrosis but fibrosis takes 3-4 weeks to develop, and the model is questioned for its clinical relevance. Within this acid model there is thickening of bronchioles through the deposition of peribronchial collagen as early as day 2, and this progresses to the development of alveolar fibrosis and peribronchial fibrotic foci by day 10. Indeed, the fibrotic component may explain why lung elastance had not normalised by day 10, continuing to show a significant 16% increase compared to normal. Hence, this model provides a temporal profile of ARDS fibroproliferation that is closer to the human condition. In addition, it will be interesting to investigate the impact of secondary insults on fibrosis, in particular, infectious and mechanical ventilatory insults both of which are pro-fibrotic in clinical and experimental ARDS (404, 414).

6.6 Concluding remarks

A model of experimental ARDS has been developed utilising the intratracheal instillation of hydrochloric acid. This model facilitates the investigation into the cellular and molecular factors that determine both early injurious and late resolving phases of lung injury. Unlike most models this resolving acid model recapitulates many of the physiological derangements found in ARDS including abnormalities in gas exchange, respiratory mechanics and alveolar fluid clearance. Hence, there is injury to the pulmonary capillary endothelium and alveolar epithelium, with subsequent repair through fibrosis. This model reproduces the temporal profile and illness severity found in clinical ARDS and combining it with other clinically relevant insults such as ventilation and infection will truly recapitulate the path followed by patients suffering with ARDS on the ICU.

7 Compartmental analysis of leukocytes in healthy and injured mouse lungs

Abstract

The analysis of leukocyte functions during the injurious and resolving phases of lung injury is crucial to gain further understanding of the roles for resident as well as itinerant cells during health and injury. Chapters 3,4 and 5 showed that resident alveolar macrophages trigger alveolar epithelial dysfunction through the elaboration of TNF. This occurs very early at 90 minutes after insult. The last chapter shows that neutrophils and monocytes migrate into the lung and remarkably that these migrated cells disappear between days 2 and 3. This disappearance coincides with a loss of inflammatory cytokines (including TNF) and also the improvement in lung oedema and physiology (respiratory mechanics, permeability and alveolar fluid clearance). Furthermore, histology shows a considerable number of neutrophils within the interstitial space. Hence, I developed and validated a technique to investigate the compartmental location of leukocytes within mouse lungs during health and after injury i.e. acid aspiration. Various leukocytes were characterised in the alveolar, interstitial and vascular spaces within the lung. Furthermore, during injury and resolution there were significant changes in leukocyte type and function in between compartments and time-points. This chapter points to the usefulness of this technique to examine the roles of each leukocyte depending on where it is located within the lung.

7.1 Introduction

Leukocytes have been consistently implicated in the pathogenesis of ALI/ARDS, however, there remains a gap in our understanding as to how they contribute to or are dysregulated in ALI/ARDS. Furthermore, the mechanisms linking leukocyte-mediated inflammation and alveolar-capillary barrier dysfunction in ARDS is far from clear. ARDS develops in patients with severe neutropenia and marrow failure (91-94) suggesting that other non-leukocyte mediated mechanisms also play a significant role, but recovery from neutropenia can also lead to ARDS in patients with haematological malignancy (95). Hence, the roles of leukocytes are likely to be dependant on the context to which they are recruited to the lung and influenced by extrinsic factors.

Although neutrophils are crucial in the first step against injury and infection, there is accumulating evidence that monocytic cell populations significantly influence the progression of injury, inflammation, as well as, resolution during experimental lung injury. For instance, work within our laboratory has shown that bone marrow derived inflammatory monocytes marginate to the lung microvasculature and promote pulmonary oedema and endothelial dysfunction within the hours of lung injury induction (241, 399, 415). Others have shown that monocytes promote on-going neutrophil recruitment to the lung (97) after endotoxin challenge. Finally, a number of investigators have shown that myeloid cells can also attenuate lung injury and promote its resolution (112, 246, 416). The early chapters of this thesis showed that resident alveolar macrophages play a significant role in promoting early epithelial dysfunction through death receptor activation. The prolonged model of experimental acid-induced lung injury described in the previous chapter enables investigation into later phases of injury, in particular, the determinants of resolution of this injury. Currently, intratracheal endotoxin is the most commonly used model to investigate pulmonary inflammation and its resolution, however as discussed previously, it does not induce sufficient amounts of alveolar oedema to allow investigation into how these inflammatory processes may promote alveolar-capillary barrier disruption. Interestingly, our acid model shows significant alveolar oedema

with a reduced alveolar fluid clearance in the first 2 days after acid instillation that dramatically improves once leukocytes (in particular, neutrophils) have disappeared. Furthermore, there is an increase in the number of exudative myeloid cells and lymphocytes over the course of injury and these cells may promote resolution, as has been shown in a number of other models (98, 100).

This chapter focuses on the development of a novel flow cytometry protocol to phenotype resident leukocyte subtypes during normal physiology, as well as, itinerant cells during injury and resolution within this model of lung injury. The techniques utilised thus far to investigate leukocyte infiltration into the lung have relied on histological examination and whole lung flow cytometry and hence, have been quite non-specific. For instance, histology may allow differentiation between interstitial and alveolar cells, but differences between vascular and interstitial components remains difficult, and artefacts during processing may influence the data obtained. Furthermore, different leukocyte subtypes can often be difficult to distinguish.

Flow cytometry is a powerful tool to elucidate the complex cellular and molecular phenotype as well as function of leukocytes within the lung. However, flow cytometric analyses are often based on comparisons between lavage versus lung homogenate. Unfortunately, it is likely that many intra-alveolar cells still remain within the lung after lavage, and hence, does not allow a complete and accurate assessment of cell localisation (intra-alveolar vs interstitial/intravascular) or quantification. Furthermore, flushing the vasculature of the lung leaves behind cells that are marginated to the endothelium of the lung (237), making the differentiation between interstitial and intravascular spaces very difficult by flow cytometry. Finally, it is likely that cells within the interstitium play a crucial role and hence have been ignored in the majority of literature often requiring expensive tools such as intravital microscopy to investigate them further (238, 417-420).

A major advantage with the lung, unlike solid organs, is the access to both sides of the endothelial-tissue interface. This enables the application of intratracheal and

intravenous labels to positively identify alveolar and intravenous cells and crucially identify (through negative gating) the interstitial cell population. With this in mind I set out to establish and validate a flow cytometry technique to enable the identification of the leukocyte subsets in the various lung compartments allowing investigation into their number, localisation, phenotype, and function in healthy and injured mouse lungs.

7.2 Aims

1) Develop a method to enable distinction between leukocytes in the three compartments within the lung – vascular, interstitial and alveolar.

2) Characterise the various leukocyte subsets within the lung compartments.

3) Attain a preliminary characterisation of the changes that occur during injury and resolution.

7.3 Experimental Design

7.3.1 In vivo protocols

Anaesthetised WT mice underwent instillation of hydrochloric acid as previously described in the resolution model. At various time-points after injury, animals underwent tracheostomy and right external jugular vein cannulation through which 2µg of a PE anti-CD45 antibody (diluted in 100µl sterile PBS) was injected. At the same time, animals underwent systemic anticoagulation and five minutes after injection of the antibody animals were exsanguinated under terminal anaesthesia. The thoracic cavity was exposed through a midline sternotomy and the lungs gently teased from their pleural adhesions. Subsequently, 5-0 silk sutures were placed carefully around the right and left main bronchi. One or both lungs underwent instillation with 0.5ml or 1ml sterile PBS containing 2µg of a PE-Cy7 anti-CD45 antibody, respectively. The bronchial ties were tightened and lungs were removed. Whole blood was also attained for analysis via the external jugular venous cannula and/or cardiac puncture. The PE- and PE-Cy7 anti-CD45 antibodies were of the same clone and hence, bound to the same epitope of the CD45 molecule.

7.3.2 Flow cytometric processing.

Each lung was placed in separate orange MACS tubes containing 2mls of IC fixation buffer. They then underwent standardised disruption using the MACS homogenisation. Ice-cold flow cytometry wash buffer (20ml) was added to the homogenate and the tube placed on ice. Subsequently, the homogenate was filtered through a 40µm filter and washed through with 20ml of ice-cold wash buffer. The single cell suspension was centrifuged at 2000rpm for 5 minutes at 4^{o}C. After discarding the supernatant the cell pellet was reconstituted in 500µl of FWB.

7.4 Results

7.4.1 Characterisation of myeloid populations in the uninjured mouse lung using standard in vitro antibody incubation

We used antibodies against CD45, CD11c, and CD11b to separate the various myeloid cell populations in lungs of uninjured mice. Gating on CD45 positive events (figure 7.1 A) found four distinct populations of leukocytes (R1 – R4; figure 7.1 B), as characterised by CD11c and CD11b.

CD11c+ alveolar macrophage and dendritic cell populations

The $CD11c^{+}$ population (R1+R2 in figure 7.1B) contained three populations of cells on the basis of their expression of CD11b and MHCII (figure 7.1 C). One population are CD11b and MHCII both negative (P1 in the dot plot), and considered to be resident alveolar macrophages. These cells are also CD103 negative, with strong expression of F4/80 and SiglecF (red line in the histogram), and are highly auto fluorescent. The next two groups of cells (P2 and P3) show high expression of MHCII and hence are most likely to be antigen presenting cells i.e. conventional dendritic cells (cDCs). Either CD11b or CD103 expression distinguishes between these two populations, i.e. $CD11b^{-}CD103^{+}$ DC (P2 and blue line) and $CD11b^{+}CD103^{-}$ DC (P3 and green line). CD103 is a receptor E-cadherin and is involved in the process through which DCs extend dendrites through the epithelial layer to sample the alveolus. Both cDC populations were negative expressers of F4/80 and SiglecF, which are both macrophage markers. These cDC phenotypes are consistent with data showing that the $CD11b^{-}CD103^{+}$ are localised under the alveolar and bronchial epithelium and

extrude dendrites into the alveolar space or bronchial lumen. These are called 'epithelial' cDCs. The $CD11b^{+}CD103^{-}$ have been localised to the walls of bronchioles and are called 'lamina propria' cDCs (421).

CD11b+CD11c- monocyte/neutrophil populations

The $CD11c^{-}$ population seems to have two cell populations, CD11b positive and negative (R3 and R4, respectively, in figure 7.1B). As CD11b is an integrin found predominantly on neutrophils and mononuclear cells, $CD11c^{-}CD11b^{+}$ cells (R3) are likely to be monocyte/neutrophil populations with CD11c-$CD11b^{-}$ cells (R4) likely to represent the non-myeloid cells e.g. lymphocytes. R3 was then analysed using Ly-6G and Ly-6C (figure 7.1D) – classic differentiation markers of neutrophil and monocyte subsets in mice (422). As mentioned previously the cell-fixation procedure used to prepare the lung cell suspension led to a denaturation of the Gr-1 epitope (which consists of Ly-6C/Ly-6G) on monocyte populations and the loss of recognition of the $Gr\text{-}1^{hi}$ monocyte populations (241). However, the use of a Ly-6C antibody enabled their identification with $Ly\text{-}6C^{hi}$ and $Ly\text{-}6C^{lo}$ being equivalent to classical/inflammatory and non-classical/resident subsets, respectively (422). When whole lung cell suspension was gated on $CD45^{+}CD11c^{-}CD11b^{+}$ population, and then analysed for Ly6G and Ly6C expression, there were five further populations distinguished (P4 to P8 in figure 7.1 D). P4 are neutrophils as they express high levels of Ly-6G. P5 are likely to be eosinophils as they are $Ly\text{-}6C^{inter}Ly\text{-}6G^{inter}$, and also founded to be, F4/80 positive with high side scatter (as a result of their granularity) (423). P6-8 are monocytes with two main subtypes – the non-classical/resident (P6) or classical/inflammatory (P8) subsets with low to high expression of Ly-6C, respectively. There is also an intermediate population (P7) likely to represent monocytes undergoing a stage of conversion between classical and non-classical forms.

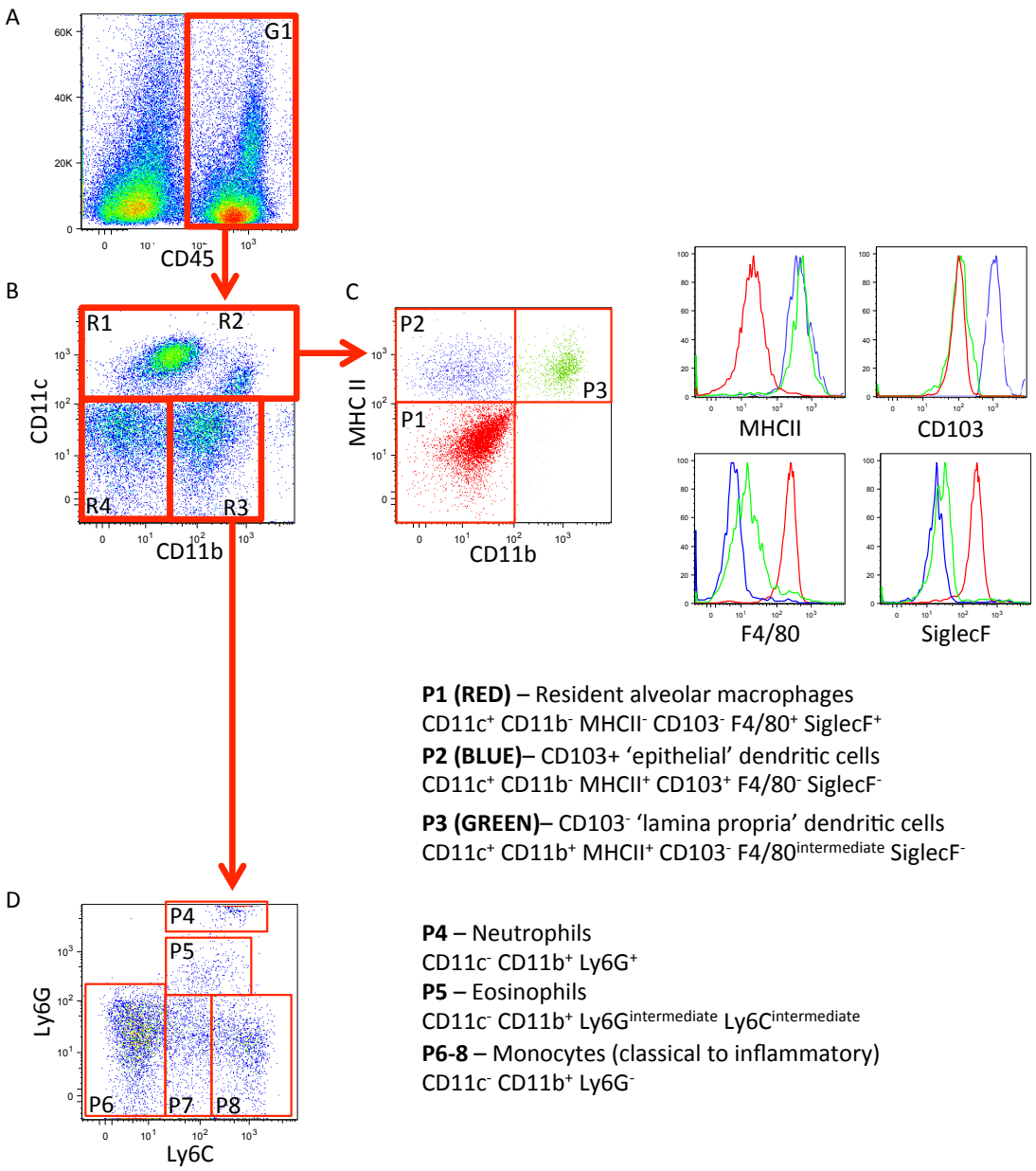

Figure 7.1. Flow cytometric analysis of naïve mouse lungs (without in vivo labelling)

Whole lung single cell suspension underwent in vitro incubation with relevant antibody combinations to determine the populations of myeloid cells present. **A)** The gating strategy defined all leukocytes, which were positively stained with CD45 antibody (G1). **B)** CD45 positive events were analysed with CD11c and CD11b and four distinct cell populations were defined (R1 – R4). **C)** Cells positive for CD11c (R1 and R2) were comprised of three populations – resident alveolar macrophages (P1), $CD103^{+}$ dendritic cells (P2), and $CD103^{-}$ dendritic cells (P3). Each of these also showed distinct cell surface markers with both dendritic cells being positive for MHCII and resident alveolar macrophages being positive for F4/80 and SiglecF. **D)** Events negative for CD11c and positive for CD11b (R3) were characterised using Ly-6C and Ly-6G. This R3 population was comprised of 3 main cell types - neutrophils (P4), eosinophils (P5), and monocyte subsets (P6-P8, depending on Ly-6C staining).

7.4.2 Validation of in vivo staining of alveolar and vascular compartments

The strategy described above only analyses whole lung homogenate using an in vitro incubation with the antibodies and hence, does not allow localisation of cell types to a particular compartment within the lung. To investigate the compartmental localisation of leukocytes, lungs were sequentially labelled 'in vivo' through administration of an intravenous (PE-conjugated) and intratracheal (PE-Cy7 conjugated) anti-CD45 antibody (figure 7.2). Firstly, in the absence of intravenous and intratracheal labelling of the lung, all events were negative in the PE and PE-Cy7 channels (Plot A – gate R1). The intravenous administration of a PE-conjugated anti-CD45 antibody produced a clearly separate population (Plot B – gate R3) of CD45 positive cells located in the vascular compartment leaving behind a population containing all of the unlabelled non-vascular events (Plot B – gate R2).

Subsequent 'in vitro' labelling (after intravenous injection) of the whole single cell suspension (to label all leukocytes) using a PE-Cy7-conjugated CD45 antibody (against the same epitope of the CD45 molecule as the intravenous antibody) leads to a clear shift upwards of all CD45 positive cells along the y-axis i.e. PE-Cy7 positive. Over 98% of the vascular labelled (intravenous PE CD45 positive events) (R3) also labelled positive to this in vitro PE-Cy7 CD45 antibody (R5), suggesting that despite the high dose, the intravenous antibody does not saturate the CD45 epitope. This co-labelling step with the in vitro PE-Cy7 anti-CD45 antibody, also brought out a population of leukocytes (R4) from the PE negative "non-vascular" gate (R2), consisting theoretically of all alveolar and interstitial leukocytes, not accessed by the intravenous CD45 antibody.

Instillation of a PE-Cy7 conjugated CD45 antibody into the airways showed that non-vascular cells can be further divided into two cell populations. Cells stained highly positive for intratracheal CD45 (R6) are likely to be mainly resident alveolar macrophages. The population remaining behind (R7) that has a relatively 'negative' MFI in intratracheal CD45 axis, is likely to contain interstitial leukocytes (as well as all other CD45 negative lung parenchymal cells). These populations were not accessible to either the intratracheal or intravenous administered CD45 antibodies. Of note,

the cells labelled positively with the PE-CD45 intravascular antibody (i.e. vascular leukocytes in R8) show a similar MFI to interstitial leukocytes (in R7) with respect to the intratracheal CD45 label.

The alveolar population (R6) shows an extremely high MFI in the intratracheal CD45 axis. Of note, the interstitial population (R7) shows a wide distribution in MFI in the PE-Cy7 channel (y-axis), although much lower than the alveolar R6 population. The R7 events with a relatively higher MFI cannot be explained by direct in vivo labelling (i.e. leak of the alveolar antibody into the interstitial compartment) given that they have the same MFI as vascular-labelled cells (R8). One would expect a higher staining of the interstitial population as compared to the vascular population by the intratracheal instilled antibody. However, one consideration should be the potential for indirect “in vitro” labelling by excess PE-Cy7 CD45 antibody during the lung homogenisation process prior to the first wash. This was minimised (as much as possible) by diluting the homogenised sample immediately in 20mls FWB during the first wash step. Despite this potential processing artefact, there remains a clear separation (in the order of one log fold) between the lowest MFI of the alveolar (R6) and highest MFI of the interstitial (R7) population allowing robust separation. R9 represents the theoretical population that would occur if bidirectional leak of antibody occurred. This was less than 0.3% of total lung events.

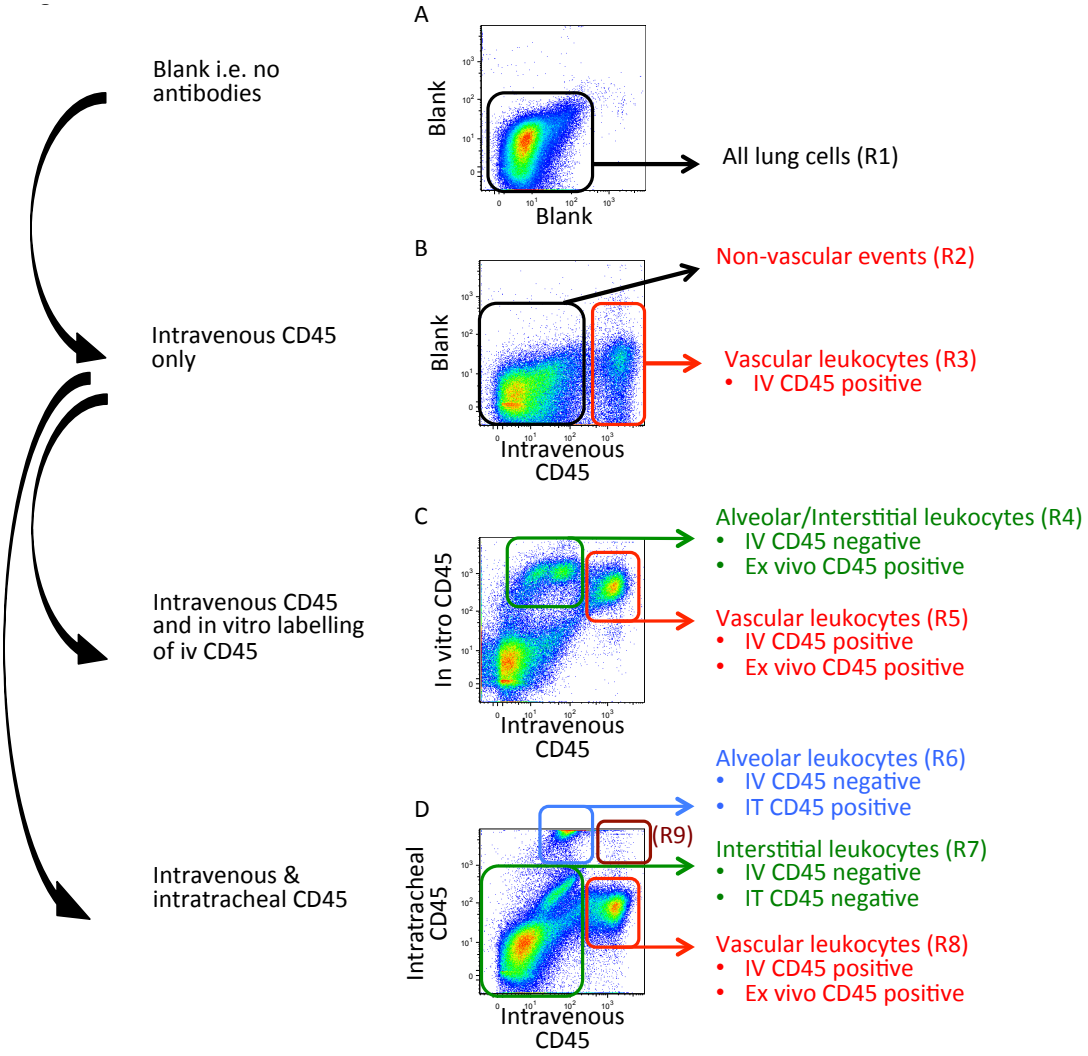

Figure 7.2. Development of in vivo labelling protocol

The absence of antibodies shows a clear negative population (R1) of cells when lung single cell suspension is analysed with the PE (x-axis) and PE-Cy7 (y-axis) channels. The in vivo injection of a PE conjugated CD45 antibody leads to a clear shift rightward of a population (R2) found in the vasculature of the lung leaving a region containing all non-vascular events (R3). The labelling of the lung suspension in vitro with a PE-Cy7 conjugated CD45 antibody leads to an upward shift of leukocyte populations. Of note nearly all of the intravenously labelled leukocytes (>98%) also stain positive for the in vitro CD45 antibody (R5). Additionally, two CD45 positive populations (R4) of cells emerge from the PE negative group (R2). These are likely to be the alveolar and interstitial populations. When the same PE-Cy7 conjugated CD45 antibody is instilled intratracheally one population is labelled strongly positive (R6) whereas the other remains relatively negative (R7). This positive population is likely to be alveolar leukocytes (R6) exposed to the inratracheal CD45 anitibody. The remaining dual negative region (i.e. R7 - negative for both iv and it labelling) contains all non-vascular and non-alveolar events and hence contains any interstitial leukocyte population (as well as other lung parenchymal cells) (R7). The vascular (R8) subset remains relatively negative for the intratracheal antibody compared to the R6 population. The number of events found in R9, representing the extent of bidirectional leak of antibody, is less than 0.3% of the total population. This confirms

that the in vivo labelling enables separation of events into alveolar, interstitial, and vascular compartments.

7.4.3 Resident alveolar macrophage and dendritic cell populations validate the distinction between the alveolar and interstitial compartments of the lung

This in vivo labelling strategy was further validated by confirming the presence of expected leukocyte phenotypes in the three compartments of the normal mouse lung:

1. PE-Cy7 CD45 positive alveolar compartment (R6) should contain predominantly resident alveolar macrophages.
2. Unlabelled interstitial compartment (R7) should harbour the dendritic cell populations.
3. PE CD45 positive vascular compartment (R8) should contain predominantly monocytes and neutrophils

Alveolar macrophages (P1 in figure 7.1 C), as their name suggests, have been established to be located predominantly in the alveolar space (424). The two dendritic cell populations (P2 and P3 in figure 7.1 C) have been previously characterised in mice and their predominant localisation is within the interstitial space (425, 426). Hence, the next step was to validate if this in vivo staining strategy could distinguish between cells located in the alveolar space (resident alveolar macrophage population - P1) and those located within the interstitium (dendritic cell populations - P2 and P3).

Analysis of the intratracheally labelled alveolar population (i.e. PE-Cy7 $CD45^+$ and PE-$CD45^-$; blue gate in Figure 7.3 A) revealed that $CD11c^+CD11b^-$ population accounted for over 95% of total alveolar events (A1 in figure 7.3 B). This population were also highly autofluorescent, $MHCII^-$ and $CD103^-$, and $F4/80^+$ and $SiglecF^+$, identifying them as resident alveolar macrophages, consistent with our previous experiments and previous literature (112, 423, 427, 428). The remaining 5% of leukocytes within the alveolar space consisted of $CD11c^+CD11b^-MHCII^+CD103^+$ (3%) and

$CD11c^+CD11b^+MHCII^+CD103^-$ (0.5%) likely to be conventional DC populations, and $CD11c^+CD11b^+Ly\text{-}6G^+$ neutrophils (1%). There were also events that were $CD11b^-$ $CD11c^-$ and these may represent a small lymphocyte population or plasmacytoid DCs (known to be low expressers of CD11c, $CD11b^-$ and $MHCII^+$ (425, 426, 429)) within the alveolar space.

Within the interstitial compartment (i.e. double negative for PE-CD45 and PECy7-CD45; green gate in figure 7.3 A) there were three populations of cells that could be characterised using CD11c and CD11b (figure 7.3 - I1, I2, and I3). $CD11c^+$ populations I1 and I2 are both interstitial dendritic cell populations given the extremely high expression of MHCII. Again, both DC populations could be distinguished by differences in the surface expression of CD11b and CD103. Population I1 are $CD11b^-$ $CD103^+$ whereas population I2 are $CD11b^+CD103^-$. Furthermore, these DC populations differ from resident alveolar macrophage populations with I1 and I2 being negative for F4/80 and SiglecF. The third population (I3), which are CD11c negative and CD11b positive, are discussed in the next section covering the distinction between interstitial and vascular compartments. Of note, in the uninjured mouse lung there were no CD11c positive cells in the vascular compartment (red gate in figure 7.3 A).

In summary, the intratracheal labelling strategy positively and specifically identifies alveolar macrophages whilst leaving interstitial cell populations (mainly comprising dendritic cells) unstained. Hence, allowing distinction between alveolar and interstitial cell types.

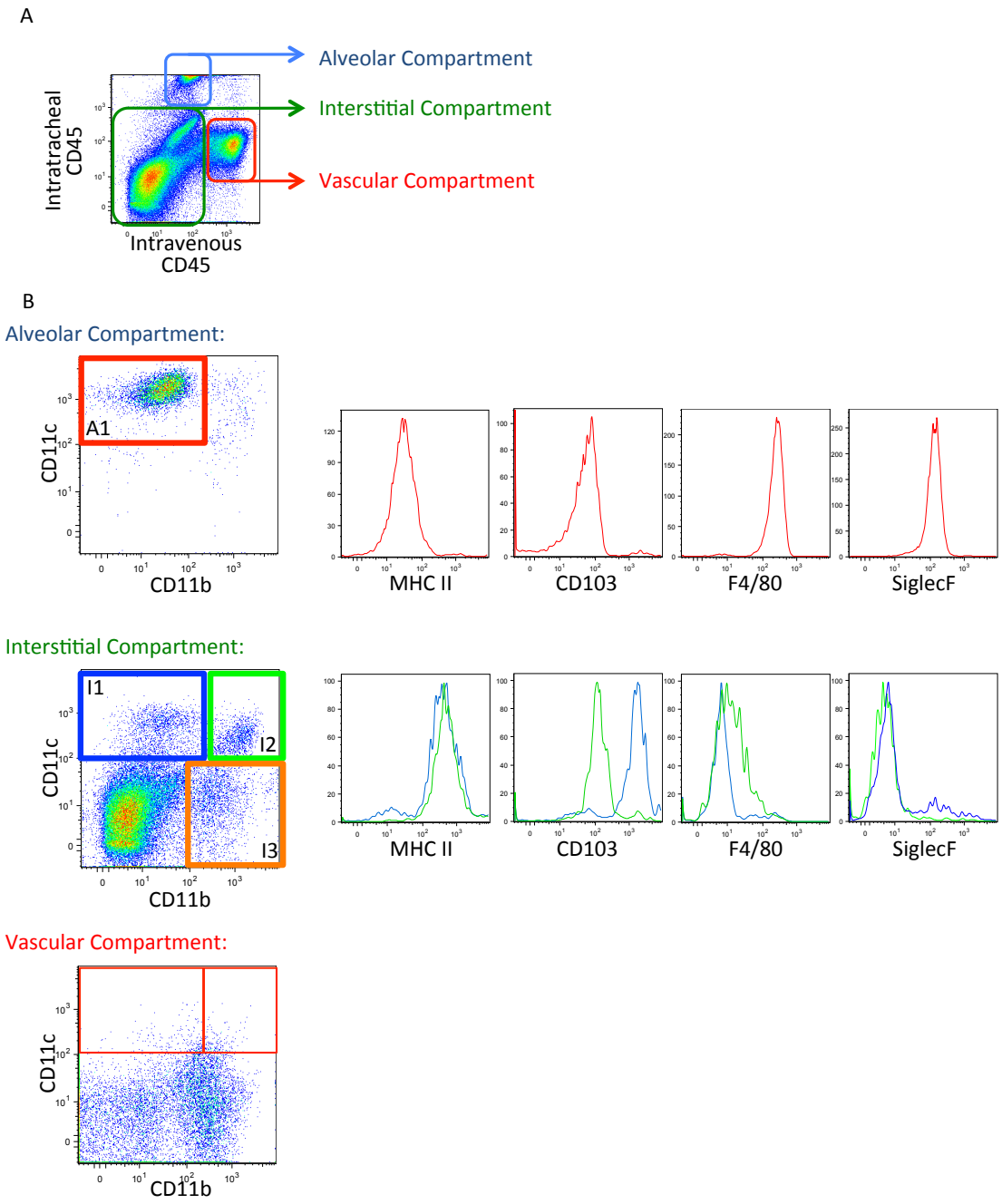

Figure 7.3. In vivo labelling protocol enables separation of alveolar and interstitial compartments of the naïve mouse lung

A) In vivo labelling and gating strategy to enable separation of the three compartments of the lung. B) The intratracheal CD45 antibody labels only the resident alveolar macrophage population (A1; red gate) that is MHCII$^-$, CD103$^-$, F4/80$^+$ and SiglecF$^+$. The interstitial compartment, as defined by those events not labelled by the intratracheal (PE-Cy7 CD45) and intravenous (PE CD45) antibody, shows two populations of dendritic cells that are CD11c$^+$ and MHCII$^+$. One population is CD11b$^-$CD103$^+$ (I1; blue gate) and the second CD11b$^+$CD103$^-$ (I2; green gate). The vascular compartment does not contain CD11c$^+$ events.

7.4.4 MHCII expression on interstitial and vascular monocyte populations validates the distinction between interstitial and vascular compartments of the lung

The in vivo labelling technique detected no $CD11c^{-}CD11b^{+}$ events within the alveolar space (figure 7.4 – Alveolar Compartment). All of $CD11c^{-}CD11b^{+}$ events (in the uninjured mouse lung) are in the interstitial or vascular compartments and these contain predominantly monocytes and neutrophils (figure 7.4).

Interestingly, within the interstitial compartment (figure 7.4), the $CD11c^{-}CD11b^{+}$ leukocytes (I3) consisted of a small proportion of neutrophils (approx. 5-10%; I3-1) and a predominant population of $Ly6C^{lo}$ monocytes (approx. 90-95%; I3-2). In contrast, the vascular compartment showed greater proportion of neutrophils (V1; 25%) as well as a more varied proportion of monocyte subsets: $Ly6C^{lo}$ (V3; 25%); $Ly6C^{inter}$ (V4; 15%); and $Ly6C^{hi}$ subset (V5; 30%). Additionally, there were a high proportion of eosinophils (V2; 5%), which were localised solely within the vascular compartment.

Most striking was the difference in MHCII expression of $Ly6C^{lo}$ monocyte populations between the interstitial and vascular compartments, with the interstitial $Ly6C^{lo}$ monocytes showing a 100-fold higher expression of MHCII compared to their vascular counterparts (figure 7.4). Hence, there are two different $Ly6C^{lo}$ monocyte populations within the mouse lung with distinct phenotypes separated by the capillary endothelium. These differences in MHCII expression suggest a functional diversity with different antigen presenting capabilities between these two monocyte populations. I have called this MHCII high population an interstitial 'monocyte' population, as opposed to a 'macrophage' population as it does not express CD11c. This clear separation in phenotype between interstitial and vascular $Ly6C^{lo}$ monocytes confirms minimal leak of intravenous antibody into the interstitial space in the uninjured lung, further supporting the case that the in vivo labelling protocol allows robust differentiation between cells within the vascular and interstitial compartments of the lung.

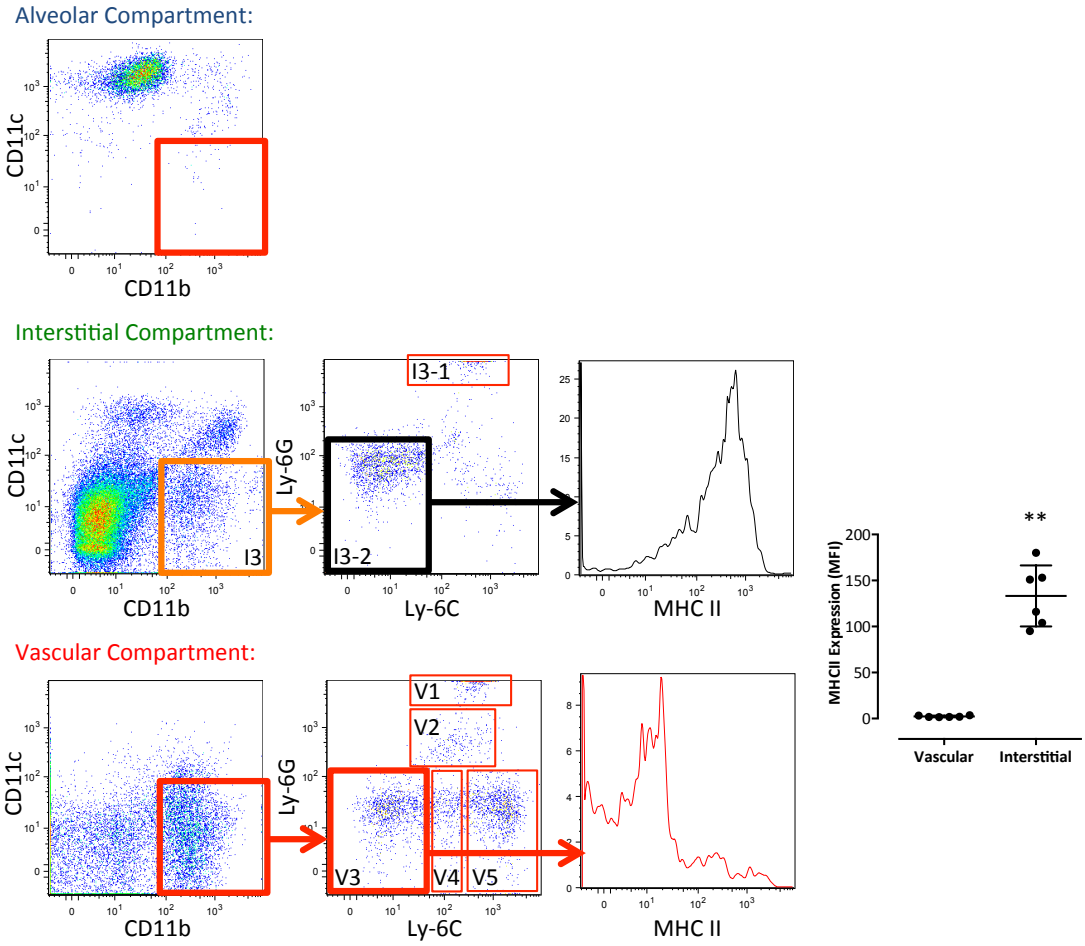

Figure 7.4. In vivo labelling enables separation of the interstitial and vascular compartments of the naïve mouse lung

There are no $CD11c^{-}CD11b^{+}$ events in the alveolar space. The interstitium has a $CD11c^{-}CD11b^{+}$ population and this consists of Ly-$6G^{hi}$ neutrophils (I1; 5-10%) and of Ly-$6C^{lo}$ monocytes (I2; 90-95%). The vascular space consists of a much larger population of $CD11c^{-}CD11b^{+}$ events that show a wider distribution in cell type: neutrophils (V1; 25%), eosinophils (V2; 5%), and Ly-$6C^{lo/inter/hi}$ monocytes (V3; 25% / V4; 15% / V5; 30%, respectively). The interstitial Ly-$6C^{lo}$ monocytes have a significantly higher MHCII expression compared to the vascular Ly-$6C^{lo}$ monocyte population. This confirms that the intravenous CD45 antibody allows separation between the vascular and interstitial spaces. **P<0.01; N=6

7.4.5 Phenotypic and compartmental characterisation of myeloid subsets in the naïve mouse lung

Overall the following table summarises the phenotypes of myeloid cells identified in the naive mouse lung during these experiments.

Cell Type	Location	CD11c	CD11b	MHCII	CD103	F4/80	SiglecF	Ly-6C	CD86	AF
Resident Alveolar Macrophage	Alveolar	+++	-	-	-	+++	+++	+++	+	+++
Epithelial cDC	Interstitium	+++	-	+++	+++	-	-	-	+++	-
Lamina Propria cDC	Interstitium	+++	+++	+++	-	+	-	-	+	-
Interstitial monocyte/macrophage	Interstitium	-	++	+++	-	+	-	-	+++	-
Classical 'inflammatory' Monocyte	Vascular	-	++	+/-	-	+	-	+++	?	-
Non-classical 'resident' monocyte	Vascular	-	++	-	-	+	-	-	?	-
Eosinophil	Vascular	-	++	-	-	+	?	++	?	+++
Neutrophil	Vascular	-	++	-	-	-	-	++	?	+

+++/++/+ high/intermediate/low; - negative; ? not tested; AF auto fluorescence
cDC – conventional dendritic cell

Table 7.1. The phenotypic characteristics of myeloid cell populations in the naïve mouse lung

7.4.6 A preliminary examination of leukocyte kinetics during experimental acid-induced lung injury

Observations into the flux of leukocytes through the various compartments of lungs at various stages of lung injury are crucial to gain a better understanding into their roles. The methods described above were applied to the acid aspiration model described in chapter 6 to gain a preliminary insight into the effectiveness of this labelling technique during injury. Animals underwent in vivo labelling on days 1, 2 and 4 after acid aspiration. These time-points were predicted to best show influx of leukocytes and efflux/loss of leukocytes during inflammation and resolution of

injury. Figure 7.5 A shows representative flow cytometry plots for the compartmental gating strategy as discussed previously in the uninjured mouse (figure 7.2 D). The numbers of dual positive (i.e. $PE^{+}PE\text{-}Cy7^{+}$) events, representing the extent of bidirectional leak of antibodies during the protocol across the alveolar capillary barrier, remain relatively unchanged (at <0.5%) between uninjured and injured animals even during significant barrier disruption on days 1 and 2. Hence, this allowed good separation and consistent gating of the three compartments between the various stages of injury.

Figure 7.5 B shows the CD11c and CD11b characteristics of CD45 positive cells in the various compartments of the lungs during injury. In the uninjured lung there are minimal numbers of $CD11c^{+}$ cells in the vascular space. There is an overall increase in $CD11b^{+}$ cells in the vascular compartment throughout the course of injury. In particular there is an increase on day 1 in $CD11c^{+}CD11b^{+}$ cells, representing neutrophils, as these events are also Ly-$6G^{hi}$. In contrast, there is a reduction in $CD11c^{-}CD11b^{+}$ cells on day 1 with substantial recovery from day 2 onwards. These events represent blood monocytes.

The interstitial and alveolar compartments also show an influx of CD11b positive cells from day 1 onwards, suggestive of the recruitment of these exudative leukocytes i.e. blood derived monocytes and neutrophils. Interestingly, monocytes seem to become increasingly CD11c positive as they transition from the vascular to interstitial to alveolar compartments. Further quantification of this is discussed in section 7.4.11.

The following sections shall now discuss, in more detail, the changes in kinetics and location of specific leukocyte subsets during acid-induced lung injury.

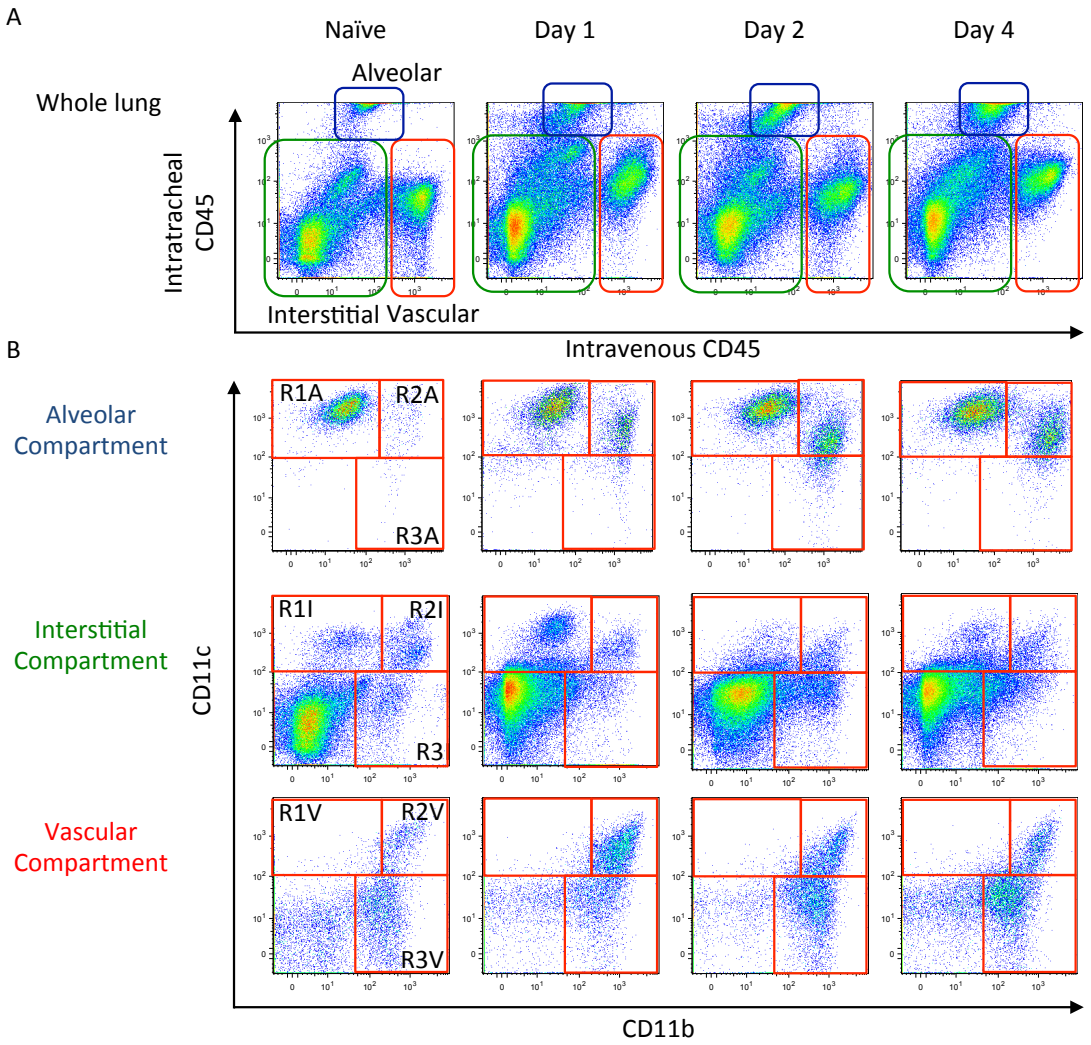

Figure 7.5. Changes in myeloid cell type in lung compartments after acid aspiration
A) In vivo labelling of lungs shows good separation between compartments during injury suggesting minimal leak of antibodies across the alveolar capillary barrier during the in vivo incubation period. B) Changes in CD11b and CD11c plots over injury (days 0-2) and resolution (day 4). There is an increase in CD11b positive event throughout the course of injury with these events being more CD11c+ in the alveolar space.

7.4.7 Changes in resident alveolar macrophages during the acute phase of lung injury

Resident alveolar macrophages are $CD45^{+}CD11c^{+}CD11b^{-}F4/80^{+}$ events. Using this gating strategy, we found approximately 1.5±0.3 million resident alveolar macrophages in the right lung of uninjured mice (figure 7.6 A). At 24 hours after acid aspiration there was a significant 3-fold decline in resident alveolar macrophage numbers within the alveolar space. This was restored to normal levels at day 2.

Interestingly, there was a significant rise of a cell population within the interstitial compartment showing essentially the same phenotype as resident alveolar macrophage (from 2.5% to 27.6% of total $CD45^+CD11c^+CD11b^-F4/80^+$ cells). These cells are also $SiglecF^+$, highly autofluorescent, with a low expression of MHCII (as compared to $CD11b^-$ dendritic cells which would have been the most likely potential contaminant), consistent with the phenotype of alveolar macrophages. This finding suggests that some alveolar macrophages may have moved into the space within the alveoli that is not easily accessible by the intratracheally administered antibody (e.g. embedded in cell clumps or debris), or that they have mobilised out of the alveolar space into the lung interstitium. If they are shown to move beyond the interstitium e.g. to nearby lymph nodes then this would potentially explain their disappearance at day 1.

A technical consideration for this interstitial localisation of alveolar macrophages on day 1 could also be due to a reduced labelling by the alveolar PE-Cy7 CD45 antibody from poor distribution or significant pulmonary oedema present at this 24-hour time point. However, this remains unlikely because levels of oedema between days 1 and 2 are comparable, but only animals on day 1 show this reduction in macrophage number and change to an interstitial distribution. Furthermore, there is a significant increase in MHCII expression of alveolar macrophages at day 1, suggesting an increased activation state (figure 7.6 B) and potential for antigen presentation.

7.4.8 Reductions in dendritic cell numbers from the onset of lung injury

The majority of $CD103^+$ cDCs in the uninjured mouse lung are predominantly interstitial in nature (over 90% in the uninjured mouse lung using this labelling strategy). Acid aspiration leads to a significant decline in this interstitial located $CD103^+$ cDC populations within 24 hours of injury (figure 7.6 C). Unlike the resident alveolar macrophage population, which is repopulated at day 2, this $CD103^+$ cDC population remains low in number even at 4 days after acid aspiration. Furthermore, this population already expresses a high level of MHCII and no significant changes were observed in their MHCII expression. Changes in $CD11c^+CD11b^+$ dendritic cells

remained difficult to investigate given the dramatic increase in other $CD11b^+$ cells during injury and hence, were hidden from potential analysis.

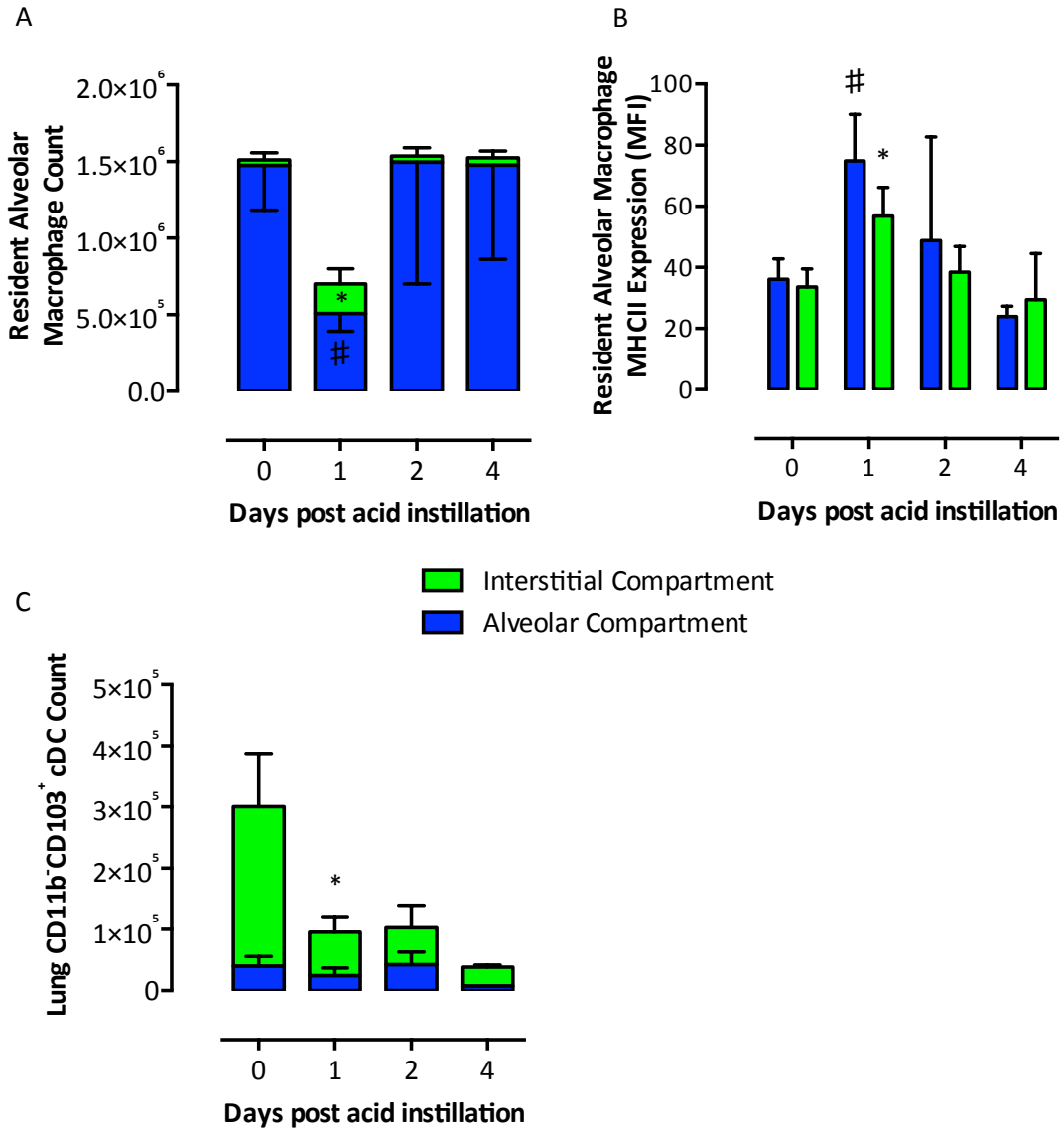

Figure 7.6. Changes in resident alveolar macrophage and dendritic cell numbers during lung injury

A) There is a marked reduction in the resident alveolar macrophage population (gated as $CD45^+CD11c^+CD11b^-F4/80^+$ events) on day 1 after injury. This is replenished on day 2 back to normal levels. There is also a significant increase in the number of interstitial macrophages on day 1 suggesting a possibility that they are capable of migration out of the alveolar space. B) There is an increased MHCII expression on both alveolar and interstitial macrophages on day 2 suggesting increased antigen presentation capability. C) There is a marked reduction in the interstitial $CD45^+CD11c^+CD11b^-CD103^+$ 'epithelial' dendritic cell population from day 1 after injury. This remains low even at day 4. N=3-5. ♯P<0.05 versus uninjured in alveolar compartment; *P<0.05 versus uninjured in interstitial compartment.

7.4.9 The pulmonary sequestration of blood derived myeloid cells

There are two phases of neutrophil and monocyte infiltration observed after acid aspiration. Flow cytometric quantification of whole lung homogenate during experiments using the acute ventilated model shows 4 million neutrophils and 6.5 million monocytes sequestered to the right lung during the first 3 hours after acid aspiration (figure 3.7). In vivo labelling experiments were not performed at this 3-hour time point and hence the precise localisation of leukocytes in the very early phase of acid-induced lung injury remains unknown. However, when total lung leukocytes are counted in this longer-term model this initial infiltration disappears by day 1 (the assumption being that a similar level of acute infiltration is also present in this longer-term model). This is followed by a second phase of neutrophil and monocyte sequestration on day 2 (figure 7.7 A). In vivo labelling shows a significant influx of neutrophils and monocytes into interstitial and alveolar spaces on day 2. This influx is also transient, declining in all compartments by day 4, and is consistent with the profile observed during BAL cytology in chapter 6 (figure 6.7).

The numbers of neutrophils and monocytes in the vascular space remains relatively constant but quantification of vascular compartment may be subject to variability. This variability is dependent on the consistency of exsanguination (i.e. anti-coagulation, transection of major vessels, and three recruitment manoeuvres) of the lungs between animals. The addition of a pulmonary vascular flushing step or an isolated perfused lung apparatus should enable more accurate determination of the vascular compartment i.e. leukocytes that are marginated and adhered to the lung endothelium. To gain some insight into the quantities of neutrophils and monocytes in the blood, whole blood was sampled and analysed. This showed a significant blood neutrophilia (increased neutrophil count) and conversely a monocytopenia (reduced monocyte count) on day 1 (figure 7.7 B and D, respectively).

Neutrophil kinetics during lung injury

There is an increase in blood neutrophils on day 1 (figure 7.7 B). The second influx of leukocytes into the right lung constitutes 3 million neutrophils (figure 7.7 C). Interestingly, there seems to be an equal distribution of neutrophils between the

alveolar and interstitial compartments. The increasing blood neutrophilia on day 1 could contribute to the significant rise in interstitial and alveolar neutrophils within the lung on day 2, although this requires further exploration. On day 2, preliminary data (N=2) suggests that over 25% of all alveolar located neutrophils stain positive for annexin V (figure 7.8), suggesting that apoptosis is the major mechanism for the decline in neutrophil numbers by day 4, by which time the distribution returns to a similar state as seen in naïve lungs. Many of these neutrophils are undergoing normal apoptosis given they are negative for propidium iodide (a marker of delayed apoptosis/necrosis).

Monocyte kinetics during lung injury

Interestingly, in contrast to neutrophil number at 24 hours after injury, there is a stark reduction in blood monocyte number (figure 7.7 D). However, similar to neutrophils, at 48 hours there is a pronounced expansion of monocyte numbers within the interstitial and alveolar spaces of lungs after acid aspiration (figure 7.7 E). This expansion disappears by day 4 and is associated with concomitant restoration of monocyte numbers within the blood. Interestingly, this influx of blood derived mononuclear cells coincides with the normalisation/replenishment of the alveolar macrophage populations (day 2 in figure 7.6 A).

Figure 7.9 shows representative flow plots for mononuclear and neutrophil infiltration into the three compartments of the lung. In the naïve uninjured mouse lung, the alveolar space shows no monocytes and minimal neutrophils (figure 7.9 B; orange arrow), and the interstitial space only contains the Ly-6C^{lo}MHCII^{+} subset of interstitial monocytes (figure 7.9 B; black arrow). However, as injury progresses, on day 1 there are the expected infiltrations of neutrophils (figure 7.9 B; red arrows) in the interstitial and alveolar spaces, as described. However, in addition on day 2 there is an expansion of the Ly-6C^{hi} "classical/inflammatory" subset of monocytes (figure 7.9 B; green arrow) that disappear by day 4. These likely derive from the blood, which shows a loss of this cell type on the previous day (figure 7.9 B; purple arrow). Additionally, on day 4 there is an increasing infiltration of Ly-6C^{intermediate} monocytes in the alveolar space (figure 7.9; blue arrow).

Overall, on day 2 there are over 3 million monocytes in each of the alveolar and interstitial spaces (accounting for 6 million infiltrated into the lung) (figure 7.10 A). In the interstitial space these consist of 40% Ly-6C^{lo}, 40% Ly-6c^{intermediate} and 20% Ly-6C^{hi}. The alveolar compartment contains mainly Ly-6c^{intermediate} (70%) with the remainder being Ly-6C^{lo}. Of note, resident alveolar macrophages also exhibit a Ly-6c^{intermediate} phenotype. Hence, these data support the notion that exudative monocytes could serve to replenish the resident alveolar macrophage population by taking on a Ly-6c^{intermediate} phenotype. All infiltrating monocyte populations (on day 2) also show increasing CD11c expression as they move into the alveolar space consistent with a change from a monocyte to a macrophage phenotype (figure 7.10 B). However, they do not express high levels of F4/80 or lose significant CD11b expression to completely adopt the resident alveolar macrophage phenotype.

On day 2 there is also a significant proportion of Ly-6C^{lo} monocytes in both alveolar and interstitial compartments of the lung (blue bars in figure 7.10 A). Interestingly, they show an increase in their MHCII expression from the vascular to the alveolar compartments (figure 7.10 C). The variations in MHCII expression suggest functional differences of these cells depending on the compartment in which they are localised, potentially, showing more antigen presenting capabilities/requirements in the alveolar space. Importantly, the infiltrating Ly-6C^{intermediate} and Ly-6C^{hi} monocytes show a much lower expression of MHCII (two log fold lower). Moreover, this CD11c and MHCII data also confirms that this technique is able to discern differences in cell surface marker expression within similar cells that are present in different compartments of the lung. The function and eventually fate of these exudative monocytes requires further elucidation using experimental protocols that may allow blood-derived monocytes to be tracked into the lung e.g. 5-bromo-2'-deoxyuridine (BrDU) pulse labelling of bone marrow progenitors as has been done in a number of recent publications (389, 430).

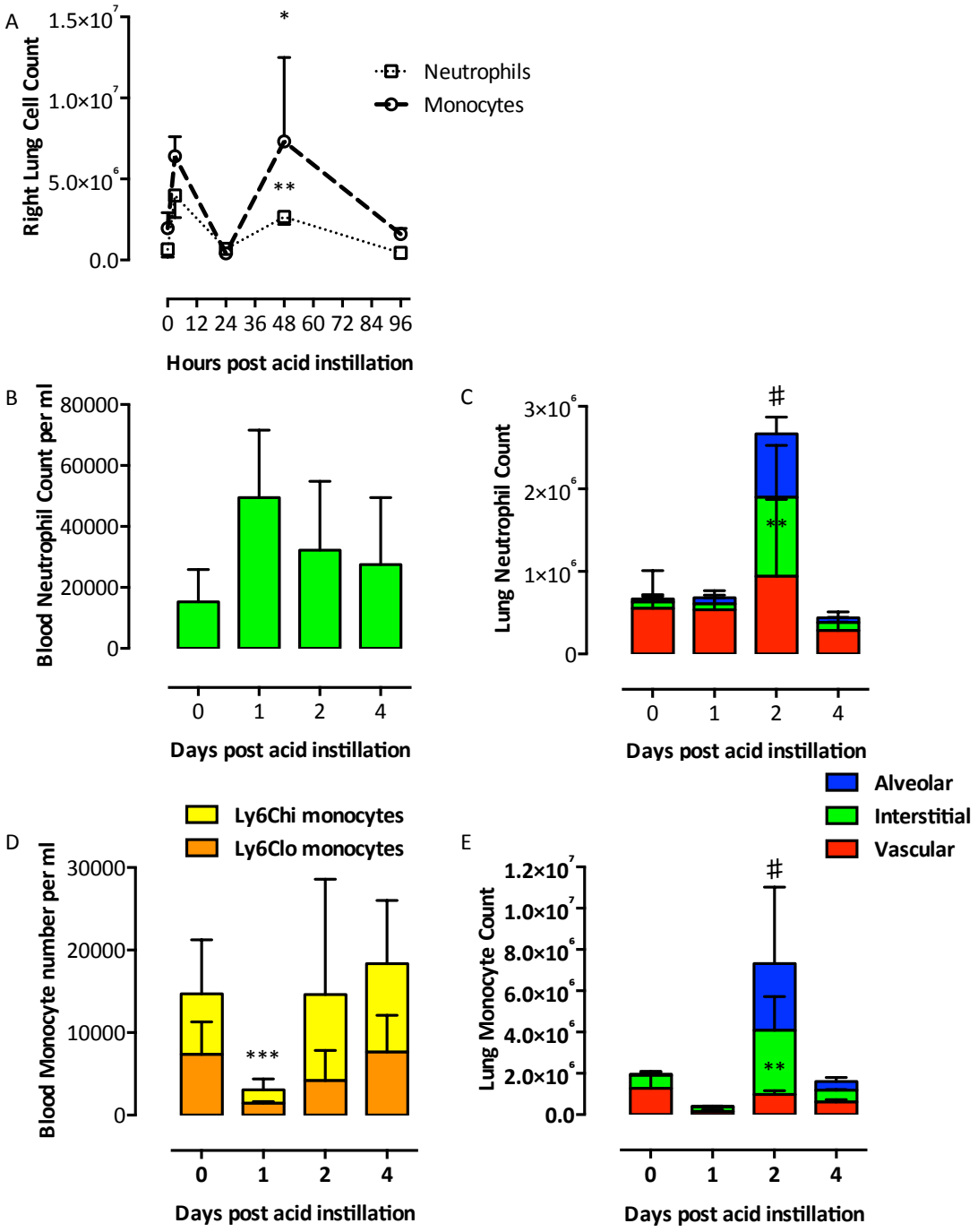

Figure 7.7. Changes in neutrophil and monocytes numbers in lung compartments and blood during lung injury

A) There are two phases of neutrophil/monocyte infiltration into the lungs after acid aspiration. The first occurs as early as 3 hours (as derived from the acute ventilated model) and the second at 2 days. (B) There is a blood neutrophilia on day 1 and (C) an increase in interstitial and alveolar infiltration on day 2. Over half of all infiltrated neutrophils remain in the interstitial compartment on day 2. (D) Blood monocyte levels reduce at day 1 but (E) their influx into the lungs shows a similar trend to neutrophils, increasing in the alveolar and interstitial compartments on day 2. However, there are double the number of monocytes as compared to neutrophils at

day 2. N=3-7; *P<0.05; ♯P<0.01 versus uninjured and day 1 in alveolar compartment; **P<0.01 versus uninjured and day 1 in interstitial compartment.

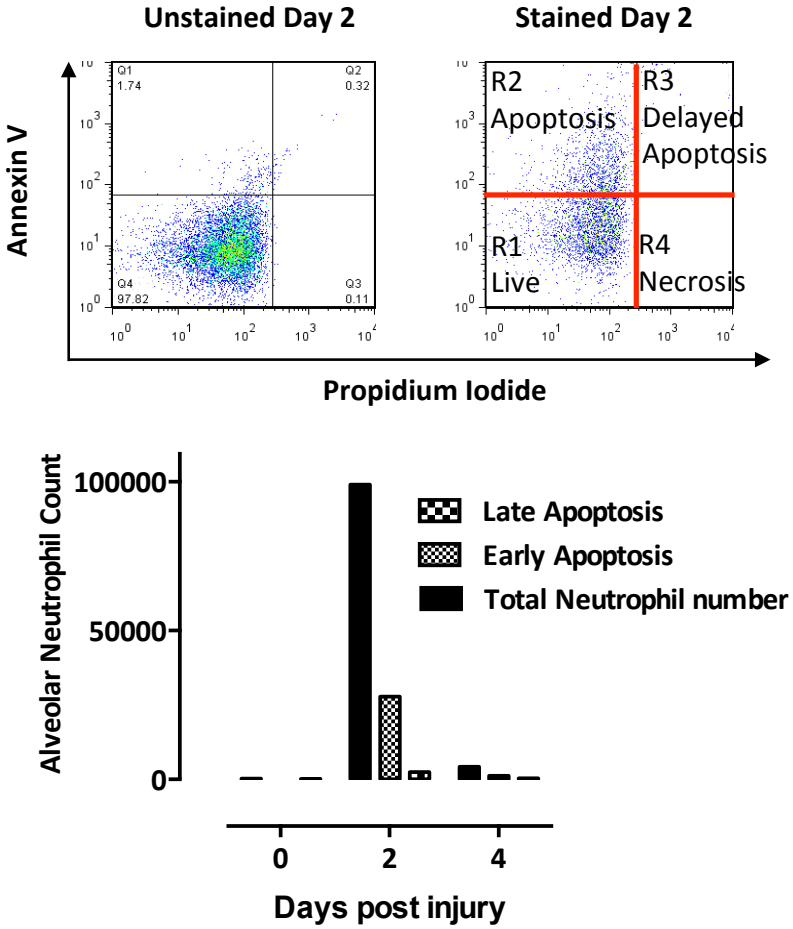

Figure 7.8. A preliminary analysis of neutrophil apoptosis during lung injury
A) Gating strategy for Annexin V and propidium iodide labelling of neutrophils obtained through alveolar lavage on on day 2 after acid aspiration. Plot on left side shows unstained control showing all events are in R1 quadrant. On labelling with Annexin V and propidium iodide there is an increase in the number of events in the R2 quadrant. These are events undergoing apoptosis and displaying phosphatydlserine on their outer surface for annexin V to bind. B) Over 25% of neutrophils are undergoing apoptosis on day 2 suggesting on-going resolution of inflammation. Of note there are no events showing delayed apoptosis (R3) or necrosis (R4). N=2 per time point.

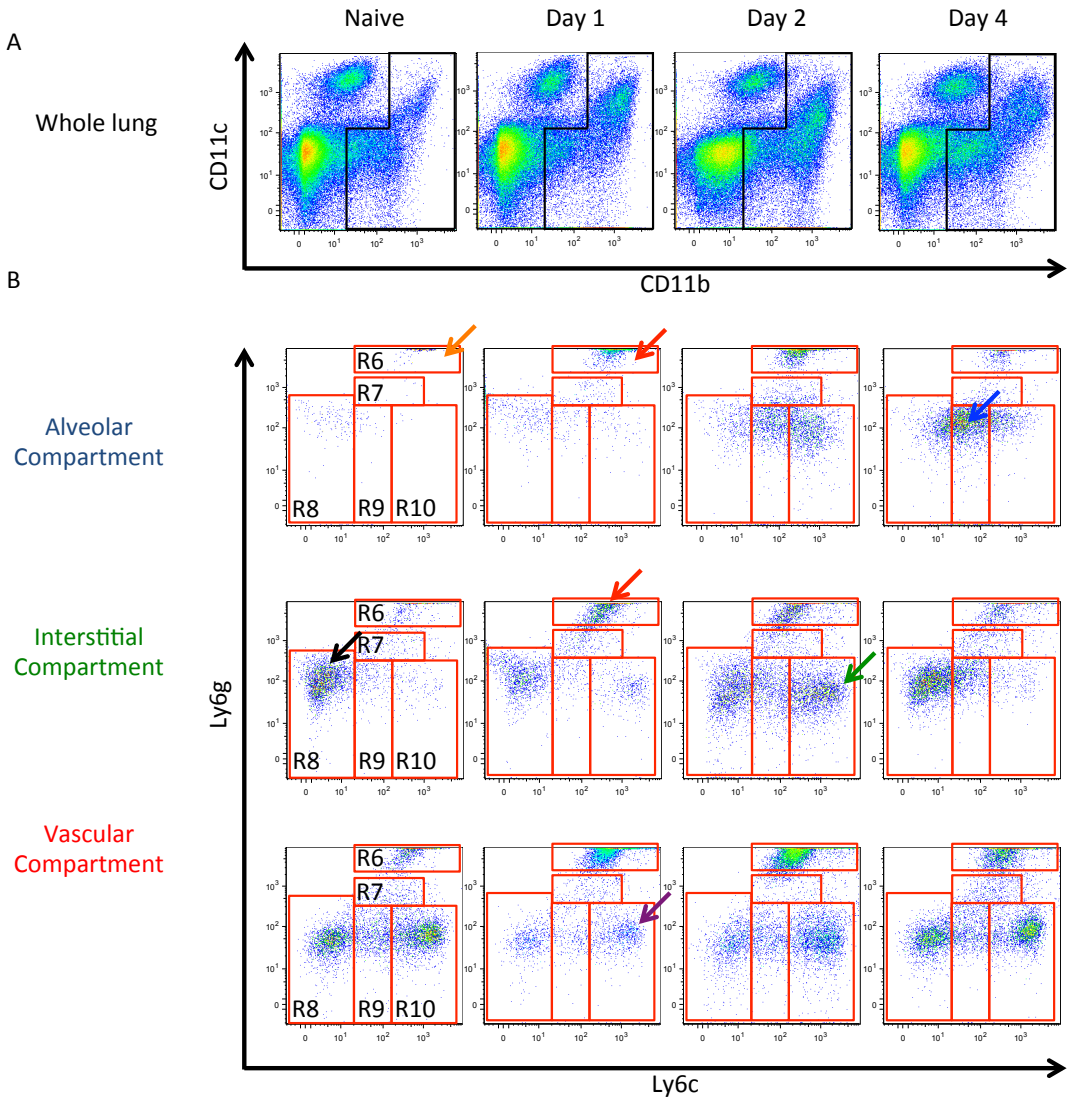

Figure 7.9. Kinetics of CD11b positive events during lung injury

A) There is an increase in the number of CD11b positive events (black gates) during the course of lung injury. B) The alveolar and interstitial compartments show an increase in neutrophils on day 1 (red arrows). The interstitial compartment shows infiltration of Ly-6C^{hi} monocytes on day 2 (green arrow). These are most likely derived from the blood, which shows a reduction in Ly-6C^{hi} monocytes on the preceding day 1 (purple arrow). The infiltration of Ly-6C^{hi} monocytes into the interstitial space is followed, on day 4, by a marked increase in Ly-6C^{intermediate} monocytes in the alveolar compartment (blue arrow). The vascular compartment only shows a monocytopenia on day 1, which recovers by day 2.

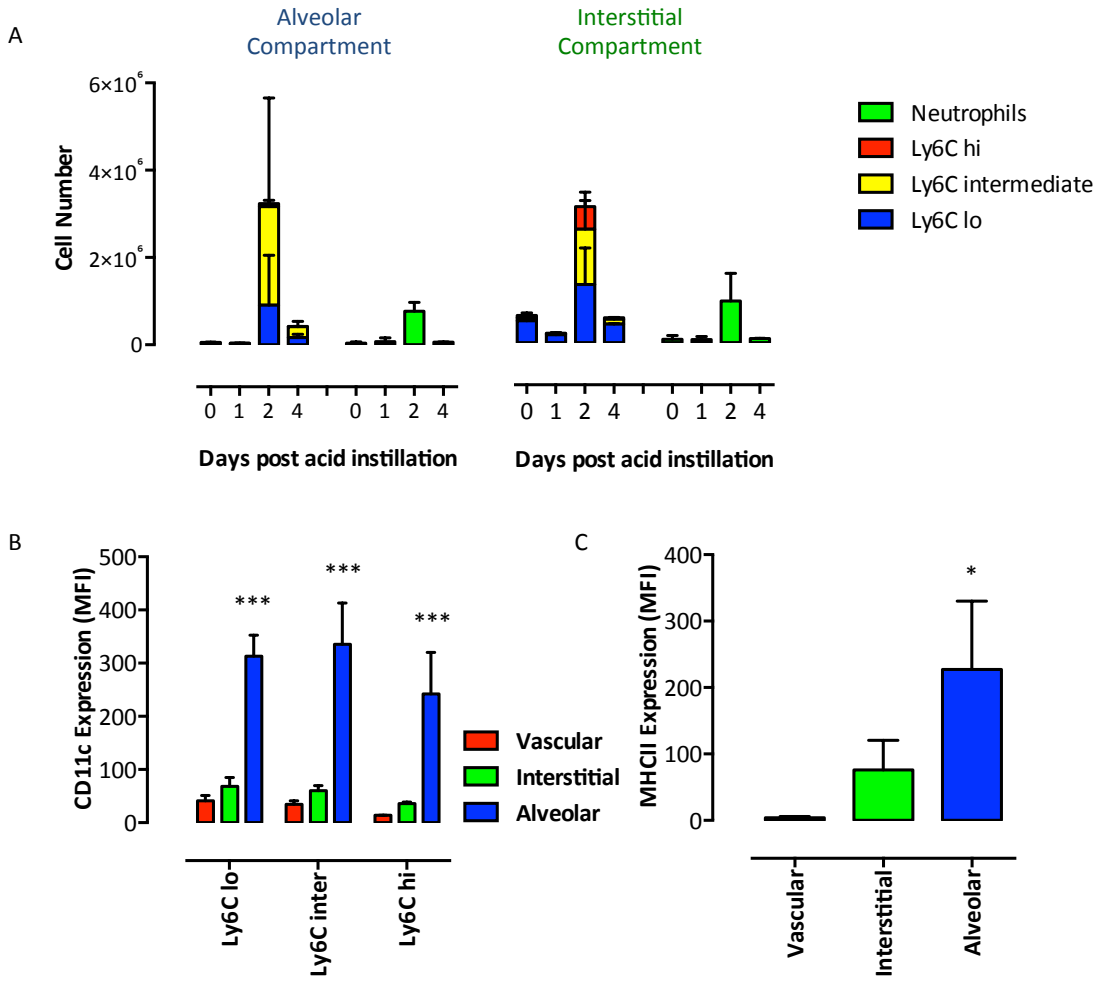

Figure 7.10. Increasing expression of cell surface CD11c and MHCII during monocyte transmigration

A) Monocyte influx on day 2 predominates over neutrophil influx in both the alveolar and interstitial compartments of the lungs. The interstitial compartment shows a increase in all monocyte subtypes on day 2. In contrast, the alveolar compartment consists predominantly of Ly-6C^{intermediate} monocytes. B) On day 2, all subsets of monocytes show an increase in CD11c expression as they traverse the endothelial and epithelial layers. The increase in Ly-6C^{intermediate} subpopulations and the increased CD11c expression suggests a conversion from a monocyte to a macrophage phenotype; N=3; P<0.001 by 2-way ANOVA (repeated measures) across compartments C) On day 2, there is an increasing expression of MHCII on Ly-6C^{lo} monocytes from the vascular to the alveolar compartment. N=3; P<0.05 across all groups by 1-way ANOVA; *P<0.05 versus vascular compartment.

7.4.10 CD4 T-cell infiltration during resolution of lung injury

The changes in MHCII expression in the various compartments imply a role for a T-cell response as a crucial component to inflammation in lung injury as has been suggested by a number of authors (98, 431). In view of this increasing expression of

MHCII on monocytes as they traverse from the vascular to interstitial to alveolar compartments (figure 7.10 C), and also the increased expression at 24 hours after injury on alveolar macrophages (figure 7.6 B), we sought to detect changes in CD4 helper T-cell infiltration into the lung, given that MHCII is the exclusive co-stimulatory molecule to CD4 T-cells (432). Hence, the numbers of $CD45^{+}CD11b^{-}CD4^{+}$ T-cells with low side scatter were quantified (figure 7.11 A). As expected there were minimal numbers of T-cells in the alveolar compartment in the naïve mouse lung, with over 90% of all $CD45^{+}CD11b^{-}CD4^{+}$ T-cells being present in the interstitial compartment at any time.

The response to injury showed a decline in the number of interstitial T-cells at day 1 (figure 7.11 B; green bars). At day 2 there is a marked increase in CD4 T-cells in both interstitial (green bars) and alveolar (blue bars) compartments. Over 20% of T-cells are present in the alveolar space during day 2. The overall number of T-cells decreases by day 4 in both alveolar and interstitial compartment (effectively back to naïve levels). The proportion of T-cells located in the alveolar versus the interstitial compartment also decreases at day 4 (with now only 13% in the alveolar space). It is important to note that lungs were harvested by transecting the bronchi distally to avoid T cell contamination in the sample from hilar lymph nodes. This was standardised in all animals. Even if this technical consideration could have influenced these data it would have done so only in the interstitial compartment (not exposed to the in vivo intratracheal PE-Cy7 CD45 antibody). Hence, the changes in the alveolar compartment truly reflect changes in CD4 T-cell numbers in response to acid aspiration. Of interest, the doubling in T-cell infiltration (within the alveolar and interstitial spaces) at day 2 occurs at the time when resolution of physiological injury and inflammation begins and at a point when the second phase of monocyte influx peaks in this model. The next step will be to examine the maximally suppressive anti-inflammatory/pro-resolution subset of these cells – the CD25+FoxP3+ population (280, 281, 433-435).

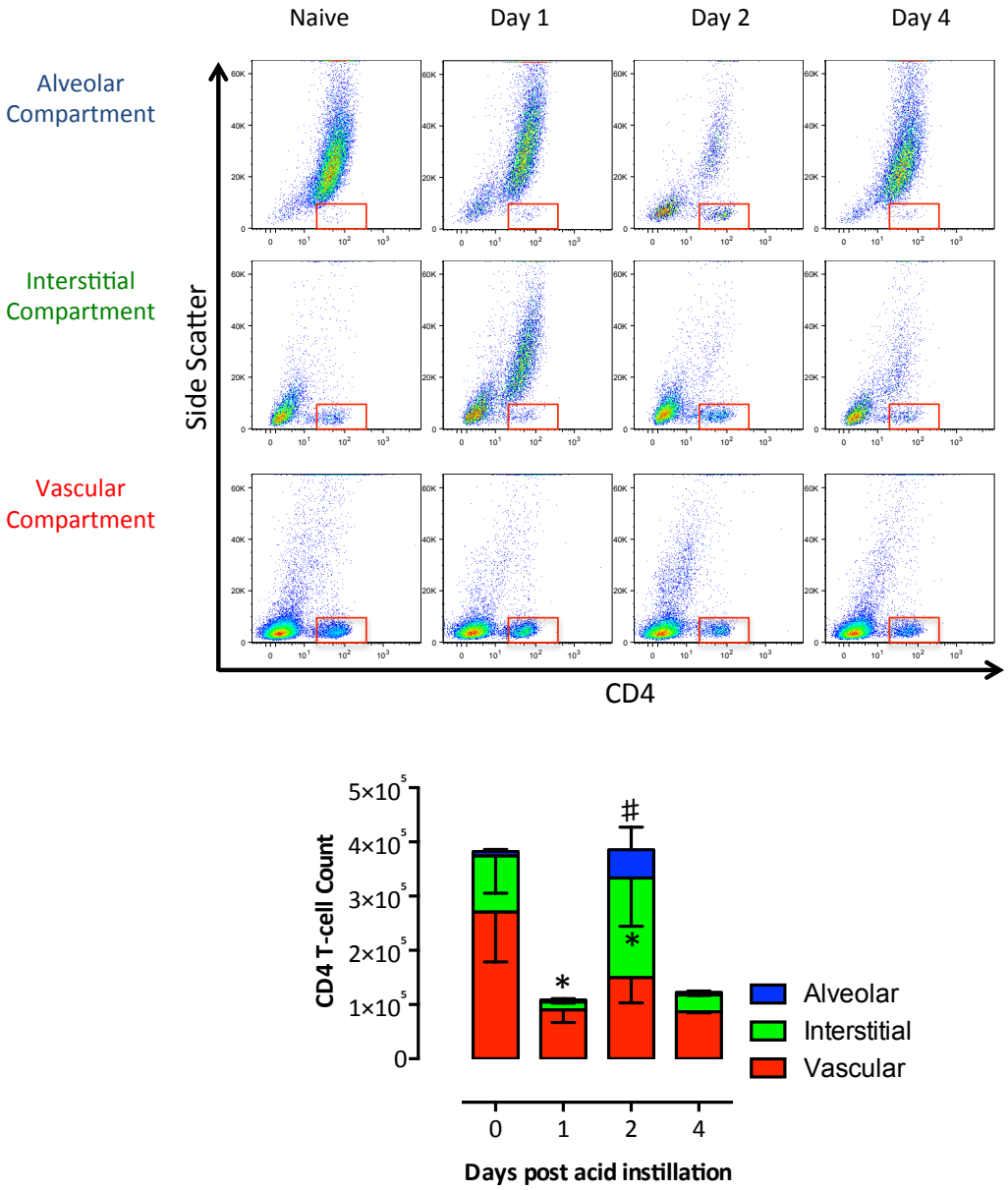

Figure 7.11. Interstitial T-cell infiltration during lung injury resolution
A) T-helper cells were gated as $CD45^{+}CD11b^{-}CD4^{+}$ events. B) In lung tissue from the uninjured mouse the majority of T cells are in the interstitial compartment (green bars). The alveolar space contains a negligible number. As injury progresses the interstitial population initially declines substantially on day 1 followed by a substantial increase on day 2. By day 4 there is a reduction in the populations suggesting a rapid fluctuations in CD4 positive T-cell responses during the injurious and reparative phases of lung injury. N=3-5; $^{\#}P<0.05$ Day 1 versus Day 2 alveolar compartment; *P<0.05 Day 0 vs Day 1; Day 1 versus Day 2 in interstitial compartment.

7.5 Discussion

This model of acid aspiration incorporates all of the important pathophysiological features of ARDS as suggested by the ATS workshop report in experimental modelling ARDS (192). Leukocytes have been implicated in the pathogenesis of acid aspiration since the first description of Mendelson's syndrome (194, 436). However, elucidating how leukocytes mediate the physiological dysfunction, in particular hypoxaemia that determines clinical management (e.g. intubation or implementation of extracorporeal oxygenation) remains unknown and ill defined. This is partly, as discussed previously, due to the lack of pre-clinical models that truly recapitulate the clinical picture.

In chapters 3, 4 and 5, I have described how the acute phase of acid-induced alveolar oedema formation is determined by the production of inflammatory mediators, in particular TNF, by alveolar macrophages which ultimately promotes epithelial barrier dysfunction and deteriorations in alveolar fluid clearance through the activation of p55 TNF receptor mediated caspase-8 signalling. This effect is seemingly independent of inflammatory mediators given that p55 TNFR deficient animals have similar lung leukocyte counts and that the physiological effects occur within 90 minutes of acid aspiration, far before substantial alveolar leukocyte infiltration.

However, given the extensive evidence for the involvement of leukocytes in acid aspiration and more broadly in ARDS it was important to establish the kinetics of leukocyte infiltration into the lungs within this model. In particular, the correlation between lung neutrophil/monocyte infiltration (at 3 hours) and Fas ligand levels in the alveolar space (figure 5.10) potentially suggests that the delivery of death ligands (by blood derived leukocytes) to the lung parenchyma could sustain the initial alveolar capillary barrier dysfunction and pulmonary oedema formation, initially triggered by alveolar macrophage derived TNF. Indeed, the continued increase in alveolar TNF levels up to day 2, in association with leukocyte infiltration, is consistent with this argument. The subsequent reduction at day 3 (of both cytokine levels and leukocyte numbers) and the recovery of alveolar epithelial function (as

determined by alveolar fluid clearance) suggest that molecular and cellular inflammatory mediators play a crucial role in the resolution and recovery of lung physiology. Investigations into the types and exact functions of itinerant leukocytes are lacking but crucial to understanding the reasons for and the consequences of such shifts in inflammatory responses. This chapter describes a technique to enable a more thorough evaluation into the types and location of leukocytes within the lung to help investigate their roles and function, but importantly, their interactions with parenchymal cells.

7.5.1 Rationale for compartmental evaluation

There are a vast variety of leukocytes within the lung with each having known or supposed roles during the various phases of lung injury. Flow cytometry provides a powerful tool to elucidate the phenotype and functions of these cells within the tissue. Although recent publications have presented data to analyse leukocyte subsets using flow cytometry (423, 437), they have not addressed the true localisation of leukocytes within the lung. Johnston et al performed cardiac perfusion and lavage procedures to determine which cells were present within the lung interstitium (437). However, lung lavage, in our hands, only removes approximately 10% of resident alveolar macrophages from the alveolar space in naïve animals. After the onset of injury the recoverability of alveolar macrophages is likely to worsen as a consequence of the macrophages becoming activated and more adherent to the underlying alveolar epithelium, a concept called ‘the macrophage disappearance reaction’ (82, 438, 439). Furthermore, it has been shown that cardiac perfusion does not remove all cells from the pulmonary vasculature and those that have marginated or adhered to the lung endothelium remain behind and play a substantial role in the propagation of lung injury (89, 237, 241, 399, 415). The in vivo labelling protocols described in this chapter enables the positive ‘real-time’ identification of leukocytes within the vascular and alveolar compartments of the lungs, and through negative gating strategies the identification of the interstitial compartment (as the unstained compartment). Investigation of the interstitial compartment of the lung has proven elusive. This is partly due to a limitation in histological techniques, which are limited to identifying only 2 or 3 cellular epitopes

(double or triple immunostaining). Hence, the full range of cells cannot be characterised. Furthermore, histology is subject to sectioning artefact and is only semi-quantitative. More recently, intravital microscopy has facilitated further investigation of this compartment but has limitations with respect to area of lungs that can be examined (sub-pleural) and the high costs (418-420). The advantage of the in vivo labelling technique presented here is that it offers all of the advantages of multi channel flow cytometry and allows the identification of numerous cell types using multiple markers within the three compartments of the mouse lung.

7.5.2 Confounding factors to in vivo labelling strategies

It is important at this stage to consider the potential confounding factors that would preclude the ideal separation of lung compartments e.g. the use of negative selection and potential for leak of antibodies between compartments. From this perspective, the use of negative selection in this technique would always more or less 'overestimate' the interstitial compartment especially when 100% labelling by intratracheal and intravascular antibody has not occurred. On the other hand, if intratracheal or intravenous antibodies leaked in vivo into other compartments, or they are not properly washed/removed before homogenisation and cell suspension making process, it would 'underestimate' the interstitial compartment.

The robust separation of alveolar and vascular compartments (figure 7.2) suggests a high proportion and intensity of labelling by the in vivo antibodies. However, any small amount of leak of these antibodies would also label interstitial events into either the alveolar or vascular compartments. If significant bidirectional leak were to occur then these interstitial events would be positively labelled by both antibodies and would be found in R9 (figure 7.2). This was found to be less than 0.3% of total lung events and this proportion remained unchanged throughout injury. Furthermore, this double positive population consisted mainly of $CD11b^{-}$ $CD11c^{+}F4/80^{+}$ events i.e. resident alveolar macrophages possibly due to their high autofluorescence. Another explanation could also be that despite optimal compensation of the flow cytometer, a small amount of the PE-Cy7 fluorescence may have drifted into the PE channel.

There are two further potential contaminants that could lead to the in vivo antibody labelling cells in different compartments. These are those that could occur during sample processing:

1. Intravascular antibody to sample
2. Intraalveolar antibody to sample

The first can be minimised by flushing the pulmonary vasculature. Although this was not performed it was felt that the following steps would have minimised the impact of this artefact:

1. The dilution of the intravenous administered antibody into the circulating volume.
2. Animals underwent systemic anticoagulation and exsanguination prior to processing, minimising the residual volume of blood left in the lung.

The second potential artefact could result from the excess intratracheally instilled PE-Cy7 antibody (present in the alveolar spaces and bronchial tree) binding to cells during lung homogenisation. This was possible due to the whole lung (tied with a suture at each respective bronchus) being placed in the homogenisation tubes. Hence, excess unbound intratracheal antibody, released during the lung homogenisation procedure, could have labelled interstitial or intravascular cells within the cell suspension, in particular prior to the first wash and centrifugation when the antibody has not yet been removed from the sample. This excess antibody was not allowed to drain out of the tracheobronchial tree because this would have allowed some alveolar localised cells to be lost from the sample. Hence, this protocol was pursued to allow the maximum retention of cells in the homogenate thereby enabling the most accurate determination of cell number. However, certain steps were taken to minimise this potential confounder. These included:

1. Ligation of the tracheobronchial tree as distal as possible to lung parenchyma.
2. Homogenisation of the lung in the largest possible fluid volume (2mls of ice-cold fixative solution added) with immediate dilution into 20mls of ice-

cold flow cytometry wash buffer. This would significantly dilute any residual excess antibody and the low temperature would minimise antibody-epitope reaction occurs. However, I believe that these potential 'in vivo leaks' or 'in vitro contamination' effects do not significantly influence these results given the fact that intratracheal (PE-Cy7) and intravenous (PE) CD45 double positive cells are indeed always <0.5% of total cells.

7.5.3 Resident alveolar macrophages populations during lung injury

Resident alveolar macrophages, as defined by a $CD45^{+}CD11c^{+}CD11b^{-}F4/80^{+}SiglecF^{+}$ phenotype, are the predominant cell type in the alveolar space. We found that there were 1.5 million alveolar macrophages in the right lungs of mice. Over 95% of these cells were labelled to be within the alveolar compartment and 5% were gated within the interstitial compartment. The total resident alveolar macrophage number significantly reduced after acid aspiration on day 1 to 50% of the original macrophage number. Most interestingly, nearly 25% of this population is present in the interstitial compartment. This differential dynamic location of the resident alveolar macrophages at different stages of injury suggests that some of these resident alveolar macrophages are indeed resident within the interstitial space. There are a number of reasons why there should be a decline in alveolar macrophage numbers.

Firstly, it is uncertain if alveolar macrophages are capable of migration away from the lung. Hence, the reduction in macrophage number could represent a trafficking to nearby lymph nodes. The increase in MHCII expression of this resident macrophage population at 24 hours suggests that they are functionally different on day 1 post-injury with a potential to present antigen to other cells. Kirby et al have shown, albeit in a mouse model of Streptococcus *pneumoniae* pneumonia, that resident alveolar macrophages are able to deliver bacteria and antigenic material to secondary lymphoid tissue (440). They found that this constitutive migration of alveolar macrophages precedes the migration of conventional dendritic cells, the classic route for antigenic delivery to draining lymphoid organs. Importantly, they

used a similar set of robust markers (F4/80, SiglecF and MHCII) to distinguish resident alveolar macrophages and dendritic cells.

The second potential cause of this loss is through apoptosis or necrosis of alveolar macrophages. Although at 90 minutes of acid aspiration death receptor activation of caspase-8 was not detectable in macrophages (figure 4.4), macrophages may die through alternative pathways including the intrinsic pathway (441) and autophagy (442, 443). Janssen et al showed that the basal turnover of the resident macrophage pool in uninjured C57BL6 mice was very slow having a half-life of greater than 12 months (112). On administration of a high dose of intratracheal endotoxin (200μg) they report a 40% decline in the resident macrophage population at the 72-hour time-point measured, but showed no recovery in macrophage number despite a significant increase in exudative macrophages. However, during the administration of a lower dose of endotoxin (20 μg) they found no decline in resident alveolar macrophage numbers. Hence, these data suggest contrasting effects in resident alveolar macrophage numbers depending potentially on the severity of the insult, or the degree of TLR-4 signalling.

The third explanation for a loss could be a change in epitopes expressed by alveolar macrophages (e.g. loss of CD11c expression) causing a proportion of them being outside the gating strategy used to detect them in uninjured animals. This is unlikely given that the days 2 and 4 show similar phenotypes and that other injury models show that these cells remain unchanged with respect to the markers used (437, 444). An intratracheal labelling strategy prior to injury (for instance, using PKH26-Phagocytic Cell Linker system as used by a number of investigators to distinguish resident from exudative macrophages (112, 445) may resolve this issue.

If we assume this loss of macrophages to be a real phenomenon, it is interesting that their number normalises by day 2. There may be a number of explanations for this. Firstly, an expansion of an interstitial progenitor population to replenish lost resident alveolar macrophages at day 1 could account for these results. Landsman and Jung showed that alveolar macrophages do indeed originate from blood monocytes but

have an indirect connection through an obligatory parenchymal lung intermediary phase (110).

In contrast, Yona et al have recently suggested that the resident population of macrophages located within the alveolar space are established in utero in mice, and remain on in adulthood (430). Their data also suggest that the replenishment of this established mature macrophage population does not seem to be influenced by the blood monocyte pool. Further flow cytometry based assays investigating the cell cycle of resident myeloid cells (cell death versus proliferation) may shed further light on this phenomenon of alveolar macrophage disappearance.

However, nearly all of these studies were performed under steady state naïve conditions and the influence of an injurious or inflammatory insult remains unclear. The replenishment of alveolar macrophages likely occurs through local as well as systemic replacement. The kinetics shown in figure 7.9 shows that Ly-6C^{hi} monocytes infiltrate the interstitial compartment of the lung (green arrow) on day 2. These cells reduce in number on day 4 but there is an increase in the Ly-6C^{intermediate} population in the alveolar space. This Ly-6C^{hi} population could be replenishing resident alveolar macrophage populations, which also show a Ly-6C^{intermediate} phenotype. This requires further investigation.

7.5.4 Resident interstitial monocyte populations

A number of groups have confirmed the presence of an interstitial monocyte/macrophage population that seems to be derived from circulating monocytes (110, 428). For the purposes of our work we have called these CD45^{+}CD11b^{+}Ly6C^{lo} cells, interstitial monocytes, given their relatively low expression of CD11c (a marker of mature macrophages (446, 447)). In the absence of this intravenous and intratracheal labelling methodology, their similarity to vascular monocytes produces significant difficulties in realising their existence and location. Misharin et al performed whole lung flow cytometry after perfusing the right heart with PBS (423). They described interstitial macrophages as CD11c^{+}CD11b^{+}MHCII^{+} cells, potentially confusing them with the CD11c^{+}CD11b^{+}CD103^{-}MHCII^{+} dendritic cell

population, and depending on the method and MFI of MHCII labelling, with vascular monocytes. Bedoret et al were the first to characterise a true interstitial monocyte population through flow cytometry and they ascribed a similar phenotype to that described in our experiments – $CD11b^{+}CD11c^{-}MHCII^{+}$. They confirmed that these were present only in the interstitial compartment through concurrent immunohistochemistry of lung sections (428).

7.5.5 Resident interstitial dendritic cell populations

Lung dendritic cells are divided into conventional (cDC) and plasmacytoid (pDC) cells. Lambrecht describes two main phenotypes of conventional cDCs within the lung (421, 448) (both expressing high levels of CD11c) and one pDC type (expressing low levels of CD11c). The two types of cDC are called epithelial (CD11b-CD103+) and lamina propria (CD11b+CD103-), in accordance to their location. The epithelial dendritic cell type samples the alveolar environment by extending dendrites between alveolar epithelial cells through interactions between CD103 and its only known ligand, E-cadherin (which is found in the tight junctions in between alveolar epithelial cells) (449). The predominant interstitial localisation of these CD11c positive cDC populations enabled robust confirmation that the exclusion of the vascular and alveolar compartments (vascular PE anti-CD45 labelled and intratracheal PECy7 anti-CD45 labelled, respectively) through negative gating strategies allowed a clear identification of the interstitial compartment. Over 95% of dendritic cells were located within the lung interstitium with 5% being labelled by the intratracheal PECy7 anti-CD45 antibody. However, it is important to appreciate that their apparent detection in the alveolar compartment may not necessarily be due to their actual localisation there but rather may inherently be an artefact of the intratracheal labelling technique given that a proportion of their surface dendrites sample the alveolar space and hence may well be exposed to intratracheal CD45 antibody. However, this is unlikely to be the case given a similar MFI (in PE-Cy7) between these alveolar localised cDCs and resident alveolar macrophages – suggesting an equivalent exposure to the intratracheal antibody. Hence, I feel that a proportion of the cDCs are likely localised in the alveolar compartment, consistent

with Vermaelen and Pauwels who also showed a similar distribution of DC populations (447).

The epithelial type ($CD11b^{-}CD103^{+}MHCII^{+}$) cDCs dramatically reduce in numbers and unlike resident alveolar macrophages remain lowered through out the 4-day period studied. This either represents a disappearance reaction (potentially to nearby lymph nodes) or a change in phenotype (similar to that discussed with the reduction in resident alveolar macrophages). The numbers of this DC subset in the alveolar compartment does not seem to be affected during injury, as seen in figure 7.6 C.

The lamina propria type ($CD11b^{+}CD11c^{+}MHCII^{+}$) cDCs are inherently difficult to distinguish during states of injury. As can be seen in figure 7.10 C, Ly-$6C^{lo}$ monocytes increase their MHCII and CD11c expression as they traverse into the interstitial compartment and hence, make it difficult for MHCII to be used as a reliable marker to distinguish CD11b+ monocyte and DC phenotypes. Indeed, DC populations have also been suggested to recover as a result of replenishment from blood-derived monocytes. Hence, the potential difficulties in finding distinguishing features between infiltrating Ly-$6C^{lo}$ monocytes and $CD11b^{+}CD103^{-}$ cDCs. Recently, the high affinity IgE α chain receptor (FcεRIα) has been proposed to distinguish between these cell types but only in models of virus-induced airway inflammation (448, 450). Preliminary experiments utilising the Mar-1 antibody against this epitope have failed potentially secondary to effects of the fixation protocol on the FcεRIα (possibly in a similar manner to its effect on the Ly-6G component of Gr-1).

7.5.6 Two phases of myeloid infiltration

The pulmonary capillary network can be as small as 2μm in diameter and hence, is able to trap many PMNs, slowing their transit time and providing an intimate contact with the capillary endothelium. The acute ventilated and resolution models seem comparable in terms of the proton dose (50μl of 0.15M for acute ventilated and 75μl of 0.1M for resolving non-ventilated model) and severity of lung protein permeability. The influence of mechanical ventilation in the acute model is unlikely to be injurious, given that we have previously shown that the surgical preparation

for ventilation at 10ml/kg in mice does not induce pro-inflammatory cytokine/chemokine upregulation in the alveolar space (239, 451). Furthermore, baseline neutrophil numbers are consistent between the acute ventilated and the non-ventilated resolution model implying robust and comparable flow cytometry counts. Hence, the kinetic gained on combining data from the acute ventilated 3-hour model and the longer-term resolution model shows that 4 million neutrophils and 6.5 million monocytes are recruited to the right lung at 3 hours after acid aspiration. This declines to 680,000 and 410,000, respectively, at 24 hours, and then subsequently rises to 2.7 and 7.3 million, respectively, on day 2 (figure 7.7 A). These data confirm two phases of neutrophil and monocyte sequestration to the lung as has been suggested by a number of investigators (97, 452).

Phase one

It is well established that neutrophils are sequestered to the lung at very early time points in a variety of models of lung injury including endotoxin (313, 401, 453-459), VILI (224, 225, 227, 228, 451, 460, 461), acid aspiration (88, 195, 257, 260, 261, 462), and oleic acid (463, 464). Reutershan et al found pronounced PMN recruitment between 2 and 4 hours in an LPS model of lung inflammation, which reached over 6 million at 4 hours, and steadily declined at 16 hours (458). Consistent with our model, Kennedy found an initial increase in PMN in the lungs at 4 hours that decreased by 15 hours in a rat model of acid aspiration (195).

An interesting observation is that both phases of neutrophil sequestration to the lung are associated with concomitant rises in monocyte numbers suggesting that the sequestration of these cell types share similar mechanisms and that one may be dependant on the other. The high number of Ly-6C^{hi} monocytes infiltrating the lung within 3 hours of insult has only recently been appreciated. Interestingly, our group was the first to show that these ‘inflammatory’ blood monocytes ‘marginate’ to the lung endothelium and promote alveolar capillary barrier dysfunction in a variety of experimental models of ARDS (89, 237, 241, 399, 415). The in vivo labelling technique has not as yet been applied at three hours and hence, the fate and exact location of these early cells during this first phase remains uncertain (i.e. whether

they transmigrate into the pulmonary interstitium, or continue to be recirculate after a period of attachment to the capillary endothelium). The source of the first monocyte sequestration phase (measured as early as 90 minutes) is most likely to be from monocytes already present in the vasculature. However, the number of lung sequestered monocytes far exceeds the circulating pool and hence, a large proportion are also likely to be derived from immature bone marrow precursors (415). Hence, the decline at 24 hours may suggest a relative depletion of bone marrow stores.

Phase Two

There is much less known about the second phase of neutrophil/monocyte infiltration. The kinetic of the acid model suggests that the first phase is over before the second phase even begins. Importantly, each is associated with quite different and distinct phases of lung injury. The first is associated with the initiation and amplification phase of lung injury whereas the second seems to be intimately linked to the recovery and resolution phase, given that lung physiology improves on the following day.

Numerous publications using depletion strategies have shown that a reduction in neutrophil and monocyte sequestration to the lung prior to injury leading to a reduction in the first phase of neutrophil/monocyte influx, seems to confer significant protection against oedema formation in experimental models of ARDS (237, 256, 400, 402, 465). However, depletion of the second phase has only been investigated more recently. Dhaliwal et al were the first to deplete monocytes after injury induction in an endotoxin induced lung injury model. This group of investigators showed that depletion of blood monocytes led to a reduction in second phase of neutrophil sequestration to the lung. Additionally, this led to significantly reduced protein permeability and improved oxygenation (97). In contrast, exudative monocytes have been shown to pro-resolving in nature by a number of other groups. Janssen shows exudative macrophages appearing in the airspaces on day 3 and disappear by day 6 through Fas mediated apoptosis and this coincides with resolution and repair. D'Allessio showed a similar profile but at day 4 (100).

Unfortunately, most studies have only examined the endotoxin model of lung injury and these studies have used different doses of endotoxin in different strains of mice (97, 100). Hence, the contrasting effects (injurious versus protective) may be secondary to the variability in type, preparation and instillation of endotoxin between investigators and the subsequent subtle differences in severity of illness and kinetics in leukocyte migration.

This acid-induced lung injury model shows a second phase of neutrophil/monocyte influx that occurs earlier (day 2) and seems to be associated with resolution. This may be due to endotoxin having potentially very different recruitment kinetics to the acid model. For instance, endotoxin could cause a more sustained TLR-4 activation leading to a protracted inflammatory response over days. In comparison, acid is likely buffered within 24 hours (466) and hence, a limited activation period may allow resolution mechanisms to occur earlier. Furthermore, the acid model shows a much greater disturbance to the endothelial and epithelial surfaces and hence, differences between sterile insults and endotoxin-based insults (mimicking "infection") may have different effects on leukocyte recruitment and different consequences.

Hence, the literature suggests quite conflicting roles for leukocytes and it is reasonable to suggest that neutrophils and monocytes can be directed to be injurious and protective depending on signalling from within the cell as well as communication with extrinsic mediators. Translating this "cellular language" that is used by different leukocytes will be an important step in the discovery of the mechanisms that promote resolution and repair and the development of strategies to promote the reestablishment of tissue homeostasis after severe injury. One such 'language' that research has made significant strides in deciphering is how neutrophil apoptosis and its recognition by macrophages can promote resolution of inflammation.

7.5.7 Neutrophil apoptosis may promote a resolving second phase

Controlled neutrophil elimination from tissues through apoptosis marks the beginning of resolution and promotes changes to macrophage phenotype (14). This constitutive apoptosis programme is delayed in clinical ARDS (103) through a variety of mechanisms (467, 468) including increased Granulocyte-Colony Stimulating factor (G-CSF) levels in the alveolar space (103). Indeed, it is G-CSF and GM-CSF that drives the maturation of neutrophils from the bone-marrow progenitors (469). This potential of the bone marrow to supply neutrophils is immense given the average half-life of a neutrophil being 6-8 hours (48).

The limited lifespan of 'first responder' neutrophils through constitutive apoptosis programmes likely accounts for the decline in lung neutrophil numbers from the first phase. Despite a relative abundance of blood neutrophils, a lower number were present in the lung during the second phase, as compared to the first phase (at 3 hours), suggesting a potential restriction to lung neutrophil sequestration during this second phase. In contrast, despite the significant monocytopenia observed, lung monocyte number tripled lung neutrophil number on day 2.

Overall, these observations suggest very different lifespan between these two myeloid cells with neutrophil turnover being quicker than that of monocytes. Indeed, preliminary data suggests that nearly 25% of all alveolar neutrophils on day 2 stain positive for Annexin V, a marker of apoptosis that is recognised by phagocytes enabling efferocytosis. Annexin V binds to phosphatidylserine (PS), a molecule usually found on the inner side of the cell membrane, which during the early stages of apoptosis, translocates to the outer surface (470). In addition, phosphatydylserine is a recognition marker for phagocytes to engulf apoptotic leukocytes, a process known as efferocytosis (130). This leads to a shift in the phenotype of such macrophages to a pro-resolution and healing phenotype (14, 15, 129, 403, 467, 471, 472).

There is significant evidence suggesting neutrophils to be instigators of resolution and repair, independent to apoptosis pathways. For instance, neutrophils have been

shown to release lipid mediators that also promote resolution of inflammation (104-106, 124, 473). More recently, neutrophils have been shown to promote repair of the lung epithelium during endotoxin induced lung inflammation (96). Such work suggesting that neutrophils may not always be injurious questions the simple measurement of neutrophil number and activity (myeloperoxidase assay) as monitors of proinflammatory and injurious responses.

7.5.8 Myeloid and T-cell interactions may enable healing and resolution

A major observation is the loss of $CD4^+$ T-cells on day 1 after injury. This potentially suggests that these lymphocytes migrate out of the lung into either nearby lymph nodes or the spleen to interact with macrophages or dendritic cells through MHCII-CD4 interactions. They then return to the lung interstitium and alveolar space on day 2 to direct the repair process within the lung. Indeed, the increasing MHCII expression of Ly-$6C^{lo}$ monocytes (on day 2) as they traverse from the vascular to the alveolar space also suggests important antigen presenting function to such a $CD4^+$ T-cell population. D'Alessio et al were the first to show such a relationship by elegantly showing that T-regulatory cells ($CD4^+CD25^+FoxP3^+$) interact with macrophages to produce TGF-beta, initiating the resolution of inflammation in endotoxin induced lung injury (98). Hence, interactions between myeloid cells and T-helper cells certainly promote repair and resolution of inflammation, and present an important potential for therapeutic intervention.

7.6 Concluding remarks

It is interesting that despite its significant severity of injury this model of acid aspiration shows spontaneous resolution. Ascertaining this trigger for repair and resolution and which factors delay resolution; how neutrophils, monocytes, dendritic cells may be influencing, interacting, and being influenced by other leukocytes; how the lung endothelium and epithelium fit into this cellular communication; and how other leukocyte stores, in particular, regional lymph nodes, bone marrow, and the spleen, influence cellular trafficking to the lung remain important areas that require investigation.

This model shows the potential to investigate this complex cellular and molecular matrix in a clinically relevant insult with significant disturbance to respiratory physiology. The model could be, in future combined with the application of bacterial/viral/fungal infection (mimicking nosocomial infection) to allow further characterisation of mediators that distract the respiratory system from normal resolution and repair. Importantly, this model may allow the link between cellular inflammation and clinically relevant physiological disturbances (such as hypoxaemia and alveolar fluid clearance) to be mechanistically investigated. This is an important relationship to investigate in the search for future therapeutics targeting leukocyte function in clinical ARDS.

8 Final thoughts – where to now in ARDS research…

8.1 The translation of p55 blockade to the ICU bedside

ARDS remains a major problem on the ICU and physiological consequences are currently only treated through therapies including mechanical ventilatory, extracorporeal, and multi-organ support. Despite improvements in general ICU care, the implementation of ultra-protective lung ventilation strategies, and the improvement in extracorporeal support technologies, mortality remains unacceptably high. TNF has been consistently implicated in ARDS and our findings suggest that total TNF blockade may be deleterious due to the receptors for TNF showing divergent roles in the formation of alveolar oedema, a cardinal feature of ARDS.

Chapter 3, 4 and 5 describe the divergent roles for the receptors in a model of acid-induced lung injury and puts forward a mechanism through which the p55 TNF receptor specifically mediates the formation of alveolar oedema by TNF. We also show that the injurious effect of p55 TNF receptor activation is likely to be due to the activation of death signalling as opposed to inflammatory signalling. Most interestingly, this death signalling is activated at a very early time point (within 90 minutes), well before inflammatory cells enter the lung from the circulation. Furthermore, this caspase-8 death signal, induced by the p55 TNF receptor, seems to be confined to the type 1 alveolar epithelium. This is also at a stage when there is minimal detectable completed cell death. Pharmacological blockade of caspase-8 activation suggest that the extent to which caspase-8 activity is upregulated determines the functional deficit seen within the alveolar epithelium (i.e. deteriorations in AFC) in injured mouse lungs. If cell death has not occurred then the consequent epithelial dysfunction may be reversible during this phase of “apoptotic limbo”. Hence, this work delivers a compelling rationale for the specific blockade of the p55 TNF receptor at the alveolar epithelial surface to rescue alveolar fluid clearance and reduce permeability.

8.2 The p55 DAb in acute ARDS

The potential for specific blockade of the p55 TNF receptor in ARDS has been opened by the development of a compound, p55 DAb (GSK1995057), by GlaxoSmithKline (GSK) (474). This compound is a novel IgG fragment called a domain antibody (figure 8.1). Advantages for its use as compared with conventional antibodies are the monovalent binding capacity to the p55 TNF receptor, small size (12kDa) and hence, potential for large quantities to be delivered with good tissue penetration and high local alveolar concentration (in particular, if delivered through the aerosolised route). Initial data suggests that intra-tracheal administration of the p55 DAb attenuates oedema formation and inflammatory activation (neutrophil recruitment, ICAM-1 upregulation on alveolar macrophages, and IL-6/MCP-1 levels in BAL) in a model of VILI (252).

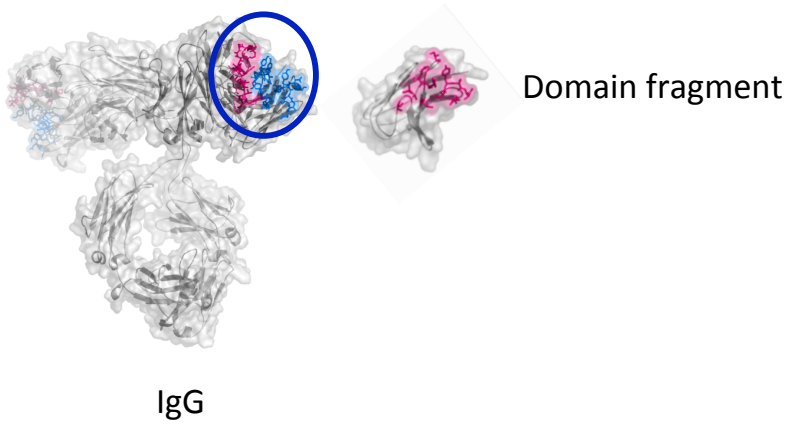

Figure 8.1. Domain antibody (DAb) fragment in comparison to an IgG molecule

Our laboratory has recently shown that that pre-treatment with the p55 DAb might be therapeutic at 3 hours in acid-induced lung injury (475). When the DAb is applied 1 hour prior to acid aspiration there is improved respiratory mechanics, oxygenation and alveolar protein at this time point. These all suggest improved alveolar-capillary barrier integrity. Interestingly, this pre-injury application also led to a reduced neutrophil and lavage cytokine level. This difference between the DAb treated WT animals and the p55 TNFR knockout animals after acid aspiration may be secondary to compensation in the p55 knockout animals (representing chronic inhibition).

Hence, acute inhibition of the p55 TNF receptor may also attenuate inflammatory events, for instance, through an inhibition of the p55 TNFR on alveolar macrophages leading to reduced activation and reduced cytokine storm. Consistent with this is the aforementioned reduction in ICAM-1 expression on alveolar macrophages by the p55 DAb in the VILI model (252). Levels of TNF were not measured in the BAL and hence, these studies did not exclude the potential for a reduced upregulation of TNF from alveolar macrophages in the protected groups.

Most recently, O'Kane et al applied the DAb in an in vivo human model of lung inflammation induced by inhaled endotoxin in healthy volunteers (476). This study pre-treated healthy volunteers (subsequently exposed to endotoxin) with inhaled p55 DAb versus placebo (in a randomised double blind manner) and found that the upregulation of pulmonary and systemic markers of inflammation (including BALF neutrophils and BALF chemokines (MIP-1α, MCP-1) and cytokines (IL-1β, IL-6, IL-8)) were significantly attenuated. Additionally there was reduced von Willebrand's factor (a marker of endothelial activation). However, BALF TNF levels were not measured and hence, it is not known if this anti-inflammatory effect manifest through reduced p55 TNFR activation on alveolar macrophages or was through a direct effect on the p55 TNFR on the alveolar epithelium. Indeed, as epithelial injury within this model is minimal, RAGE is not upregulated and hence, was not measured in this study.

A model in which epithelial injury does indeed occur is the one-lung ventilation model of lung injury. These include patients undergoing one-lung ventilation for thoracic surgical procedures, in which there is an incidence of ARDS of 2-4% post lobectomy, 8% post pneumonectomy, and 23% post-oesophagectomy (187). Application of the p55 DAb to these patients may help define the treatment in models with epithelial injury and RAGE upregulation. Importantly, these pre-injury treatment effects seen in the stretch and acid-induced mouse lung injury models as well as the human endotoxin model suggests that the p55 DAb could be prophylactically applied to patients with a high risk of developing ARDS.

8.3 The p55 DAb - epithelial rescue versus non-resolution of inflammation in ARDS

A further exciting direction that has been opened by the research presented in this thesis takes into account that alveolar cell death is minimal in early ARDS and accounts for less than 10% of all cells. It appears from our data that the epithelial cell enters a phase of 'apoptotic limbo' and lies in a state of dysfunction but does not actually die through completed apoptosis. Excitingly, this may present a therapeutic window in which the epithelium could be potentially rescued. Preliminary evidence suggests that there is minimal TUNEL staining at 24 hours after acid aspiration (resolution model) and hence, this window may be longer than the three hour time point investigated in chapter 4.

Application of intranasal DAb to WT animals, 4 hours prior to the instillation of acid in the resolving model of ARDS leads to a significant improvement in arterial oxygenation, respiratory mechanics, and lung water content (wet/dry weight) at 24 hours (data courtesy of Dr Kenji Wakabayashi). Similar to data presented in chapter 3 there is no attenuation in lung neutrophils, in fact, there was a tendency for an increased lung neutrophil count (475). Neutrophils have been shown to have p55 TNF receptor driven apoptosis (477-480) and hence, inhibition may prolong their lifespan and lead to increased injury. This makes it crucial to test any p55 DAb therapy targeting apoptosis pathways during the later phases of ARDS when neutrophils are abundant. Within the longer term model, the application of p55 DAb at stages where resolution of lung injury and improvement in AFC occurs (between day 2 and 3) may give valuable insight as to when not to apply the p55 DAb. These are on-going experiments within the lab and should further elucidate this double-edged sword of p55 TNFR blockade. Furthermore, the application of technologies presented in chapter 7 could enable the elucidation of p55 DAb effects on cells not only within the alveolar space, but also, within the interstitial compartment.

With respect to clinical application, the discovery of an epithelial biomarker may be valuable in stratifying which patients the p55 DAb will be beneficial. For instance, the

measurement of BALF RAGE or the measurement of AFC may allow the specific testing of the p55 DAb in those with epithelial dysfunction. Investigation in the one-lung ventilation model where RAGE is certainly raised may yield further insights.

8.4 Translating therapies to ARDS

A major hurdle to translation of therapies to ARDS is told through the story of TNF. Although implicated in ARDS pathogenesis over 3 decades ago, the rush to clinical trials of anti-TNF strategies, in the absence of mechanisms, has been detrimental in sepsis and ARDS. We show that TNF-induced death signalling is important in epithelial dysfunction during acid-induced lung injury. The protective effect of p55 TNF receptor blockade has now been proven in mouse models of stretch-induced oedema formation and acid-induced lung injury. Additionally, latest data suggest a beneficial effect in an in vivo human lung inflammation model. I consider the manner in which this DAb antibody has been investigated in the UK prior to its application in phase 2 studies a step change in drug testing in critical illness. In particular, current on-going investigation in a human ex vivo lung perfusion system may discover further insights into the application of this compound to clinical settings.

The lack of robust animal models of ARDS was highlighted in chapter 6. The resolution model described in this thesis will extend the impact of therapies such as this to more clinically relevant time-points, in particular, when severe injury is combined with severe inflammation. A clinically important investigation is the application of any therapeutic compound after the onset of lung injury especially with respect to effects on resolution, repair and fibrosis. Furthermore, the model allows investigation into the various pathophysiological features of clinical ARDS including alveolar-capillary barrier dysfunction, leukocyte mediated injury, and resolution of inflammation. Unlike other models of lung injury, this acid aspiration model also allows the measurement of robust physiological end-points including arterial oxygenation, respiratory mechanics, and alveolar fluid clearance. Furthermore, the application of the model to the ever-increasing variety of knockout strains may further elucidate the role of death signalling in lung injury. Finally, the

development of models using other clinically relevant insults such as those of bacterial and viral aetiologies will be of paramount importance. The greatest side effect of any therapy targeting inflammatory and apoptosis pathways is a potentially increased propensity to infection. Given that nosocomial infection such as ventilator-associated pneumonia is common in ICU, any such clinical risks need to be ascertained prior to phase 2 trials. An adaptation of such an acid-induced lung injury model with superadded infection will be of added value to investigate the underlying mechanisms of such risk.

8.5 Limitations of work in this thesis

There are a number of caveats that require discussion in order to move forward with translating the work described in this thesis. Firstly, the acid-induced lung injury model is although at present a very clinically translatable model, it only represents a single aetiology of lung injury. Further, the age of mice used was 20-30 weeks i.e. adolescent. As discussed, ARDS mortality increases with age and hence, using older mice may improve the translational relevance of this model. Mouse models remain the mainstay of pre-clinical experimental investigation in critical illness but the disparities between mice and men require appreciation given their genomic responses to stresses may well be different (481). The model certainly reproduces many aspects and features required of a model of ARDS but can only be proved to be the 'gold standard' if a therapy is translated from the bench to the bedside. This translational pathway for p55 receptor blockade is discussed further in the next sections.

The methods used to ascertain the importance of TNF-p55 TNFR-caspase-8 signalling on epithelial function also require discussion. The caspase-8 inhibitor and clodronate liposomes may also have off target effects. For instance, Z-VAD-IETD has been shown to interact with other caspase proteases (482). One method to explore these effects further is to compare the impact of various inhibitors against a variety of caspases. Conditional knockout of caspase-8 from the alveolar epithelium using a Cre-Lox system (as has been done in the gut epithelium (483)) may be a better alternative to

truly elucidate the role of caspase-8 in the epithelium. We have based many conclusions on the impact of caspase-8 on alveolar epithelial function through correlations with lung caspase-8 activity and AFC. However, these relationships include multiple groups rather than an intra-group analysis and hence, should be interpreted with caution. Although caspase-8 inhibition did indeed rescue alveolar fluid clearance, the inhibitor dose used produced a marginal reduction in lung caspase-8 activity, and hence, further measurements of AFC with increasing doses of caspase-8 inhibitor may provide more insights into this relationship. Furthermore, how caspase-8 induced the changes in fluid clearance observed remains to be investigated. Clodronate may also have cross target effects given that it was given 48 hours prior to acid instillation. Not only can it deplete alveolar macrophages but it can also influence effects through alternative pathways such as upregulation of matrix metalloproteinases and cytotoxic T-cell responses (484).

Finally, we measured alveolar fluid clearance with an aim to have a specific measure of epithelial function. Although clinically relevant, alveolar capillary permeability is a much more important determinant of lung injury given that if the dam had not been broken in the first instance then the pump would not have to work hard. However, measurement of permeability in experimental and clinical settings remains difficult and requires more robust investigation.

8.6 Future work

This thesis raises more questions than it answers and hence, a discussion of future investigations that may explore these further would seem appropriate.

1. How does apoptosis signaling promote epithelial injury?

- Investigation into the effects of caspase-8 inhibition (pharmacological) and lung specific genetic deletion through conditional alveolar epithelial knockouts (as has been developed in the gut) to ascertain the mechanisms

through which caspase-8 induces dysfunction. Plausible avenues include effects on :

- Epithelial actin-myosin cytoskeletal function
- Epithelial mitochondrial function
- Epithelial ion channel expression
- Epithelial tight junction protein expression e.g. claudins and occludins
- Anti-apoptotic pathways via NF-κB activation and transcription of anti-apoptotic factors.

- Investigate the role for leukocyte induced caspase-8 activation?
  - Adoptive transfer (into WT animals) of neutrophils/monocytes from Fas ligand deficient (*gld* strain) and Fas receptor deficient (*lpr* strain) mice.
  - Utilise isolated perfused lung apparatus (237).

- Investigation of the role of other caspases (inflammatory and apoptotic) in the development of alveolar epithelial dysfunction?

2. What is the role of the p75 TNF receptor?

Unfortunately, breeding difficulties prohibited the further investigation of the role of the p75 TNF receptor as an anti-inflammatory rheostat. However, further studies include:

- Flow cytometric assessment of resident alveolar macrophage activation during acid induced lung injury in p75KO versus WT animals. For instance, various phenotypes of macrophages have been described (figure 1.5) and measurement of such phenotypic markers may provide further insights.

- The impact of the p75 TNFR in the resolution of lung injury through T regulatory pathways requires study. Preliminary investigation into the

detection of Treg cells in spleens is positive and the FoxP3 subtype has a higher expression of the p75 TNFR.

3. What is the best model of ARDS and how does one compare against the other?

The impact of secondary insults and a study comparing between the kinetics of such a resolving acid model and a resolving endotoxin model (utilising similar phenotypic markers) may provide further insights into differences between models. Furthermore, we only had access to a seven-channel flow cytometer and hence, had to choose the markers carefully. Access to a flow cytometer with more channels may allow a more in depth analysis of a greater variety of cellular phenotypes especially if methods in chapter 7 are used.

4. What is the impact of co-morbidities in the pathobiology of ARDS?

As already discussed, the impact of co-morbidities such as age and other diseases may have more of an impact in ARDS than previously investigated. However, they remain under investigated. Indeed, we have used adolescent mice in our studies and their relevance may be questionable. Hence, investigation in older mice may be more appropriate.

The primary aim of such models is to increase our knowledge into the capabilities and side-effects of compounds prior to their use in a population of patients who are at the extremes of physiology, being supported by mechanical devices, and not easy to investigate given their high mortality. The development and application of such models that mimic patient pathways will be integral to future experiments that I carry out to bridge the gap between the bedside and the bench as I embark on a clinical academic career in perioperative and critical care medicine.

9 Publications and awards arising from work

9.1 Journal publications

Patel BV, Wilson MR, O'Dea KP, Takata M.
TNF-INDUCED DEATH SIGNALING TRIGGERS ALVEOLAR EPITHELIAL DYSFUNCTION IN ACUTE LUNG INJURY
Journal of Immunology. 190:4274-4282. PMID: 23487422

Patel BV, Wilson MR, Takata M.
RESOLUTION OF LUNG INJURY AND INFLAMMATION – A TRANSLATIONAL MOUSE MODEL.
European Respiratory Journal. 39:1162-1170 PMID: 22005920
Associated editorial:
Matthay, MA and Howard, JP
PROGRESS IN MODELLING ACUTE LUNG INJURY N A PRE-CLINICAL MOUSE MODEL
European Respiratory Journal. 39:1062-1063. PMID: 22547731

Patel, BV & Bellingan G.
REPAIR AND RECOVERY MECHANISMS FOLLOWING CRITICAL ILLNESS.
Oxford Textbook of Critical Care. 2nd Edition. In Press.

9.2 Abstract publications

Wakabayashi K, Wilson MR, Patel BV, Morley PJ, Bayliffe A, Takata M
INHIBITION OF TNF RECEPTOR P55 BY A DOMAIN ANTIBODY ATTENUATES ACID-INDUCED LUNG INJURY IN MICE.
Am J Respir Crit Care Med 187;2013:A5964

Patel BV, Wilson MR, Takata M.
MECHANISMS OF DIFFERENTIAL P55 AND P75 TNF RECEPTOR FUNCTIONS IN EXPERIMENTAL LUNG INJURY.
Am J Respir Crit Care Med 185;2012:A6744

Wilson MR, Patel BV, Takata M.
DO “CLINICALLY RELEVANT” TIDAL VOLUMES REALLY CAUSE VENTILATOR-INDUCED LUNG INJURY IN MICE?
Thorax 2011;66:A36-A37

Patel BV, Wilson MR, Takata M.
THE P55 TNF RECEPTOR PROMOTES ALVEOLAR EPITHELIAL DYSFUNCTION IN EXPERIMENTAL LUNG INJURY.
Intensive Care Medicine. 37:S205. (Sep 2011).

Patel BV, Wilson MR, Takata M.
PHYSIOLOGICAL CHARACTERISATION OF INJURY, INFLAMMATION AND RESOLUTION IN MURINE ASPIRATION PNEUMONITIS.
Thorax. 2010;65:A183.

Patel BV, Wilson MR, Takata M.
DIFFERENTIAL ROLES OF TUMOUR NECROSIS FACTOR RECEPTORS IN A MURINE MODEL OF ACID-INDUCED LUNG INJURY
European Respiratory Journal, 2008. 32 (Supplement 52): p. 280S.

9.3 Awards

The Intensive Care Society Core Topics for Training and Revalidation in ICM
Best trainee presentation – ESICM travel award
"Addressing the translational gap: Modeling resolution of lung injury and inflammation in mice"

The Intensive Care Society Research Gold Medal Award
State of the Art Meeting 2011
“TNF receptors in experimental lung injury – a double edged sword”

Best oral research presentation
Imperial College London Annual Clinical Academic Conference
“The critical roles of tumour necrosis factor receptors in experimental lung injury

10 References

1. Hamid Q, Shannon J, Martin J. Physiologic Basis of Respiratory Disease: PMPH-USA; 2005.

2. Voelkel N, Rounds S. The pulmonary endothelium: function in health and disease: Wiley; 2009.

3. Bhattacharya J, Matthay MA. Regulation and repair of the alveolar-capillary barrier in acute lung injury. Annu Rev Physiol. 2013: 75;593-615.

4. Doerschuk CM, Downey GP, Doherty DE, English D, Gie RP, Ohgami M, et al. Leukocyte and platelet margination within microvasculature of rabbit lungs. J Appl Physiol (1985). 1990: 68;1956-61.

5. Downey GP, Worthen GS, Henson PM, Hyde DM. Neutrophil sequestration and migration in localized pulmonary inflammation. Capillary localization and migration across the interalveolar septum. Am Rev Respir Dis. 1993: 147;168-76.

6. Panes J, Perry MA, Anderson DC, Manning A, Leone B, Cepinskas G, et al. Regional differences in constitutive and induced ICAM-1 expression in vivo. Am J Physiol. 1995: 269;H1955-64.

7. Matthay MA, Robriquet L, Fang X. Alveolar epithelium: role in lung fluid balance and acute lung injury. Proc Am Thorac Soc. 2005: 2;206-13.

8. Wright JR. Immunoregulatory functions of surfactant proteins. Nat Rev Immunol. 2005: 5;58-68.

9. Taylor PR, Martinez-Pomares L, Stacey M, Lin HH, Brown GD, Gordon S. Macrophage receptors and immune recognition. Annu Rev Immunol. 2005: 23;901-44.

10. Medzhitov R. Approaching the asymptote: 20 years later. Immunity. 2009: 30;766-75.

11. Rock KL, Kono H. The inflammatory response to cell death. Annu Rev Pathol. 2008: 3;99-126.

12. Chen GY, Nunez G. Sterile inflammation: sensing and reacting to damage. Nat Rev Immunol. 2010: 10;826-37.

13. Menezes GB, Mansur DS, McDonald B, Kubes P, Teixeira MM. Sensing sterile injury: opportunities for pharmacological control. Pharmacol Ther. 2011: 132;204-14.

14. Savill JS, Wyllie AH, Henson JE, Walport MJ, Henson PM, Haslett C. Macrophage phagocytosis of aging neutrophils in inflammation. Programmed cell death in the neutrophil leads to its recognition by macrophages. J Clin Invest. 1989: 83;865-75.

15. Cox G, Crossley J, Xing Z. Macrophage engulfment of apoptotic neutrophils contributes to the resolution of acute pulmonary inflammation in vivo. Am J Respir Cell Mol Biol. 1995: 12;232-7.

16. Ashbaugh DG, Bigelow DB, Petty TL, Levine BE. Acute respiratory distress in adults. Lancet. 1967: 2;319-23.

17. Bernard GR, Artigas A, Brigham KL, Carlet J, Falke K, Hudson L, et al. The American-European Consensus Conference on ARDS. Definitions, mechanisms, relevant outcomes, and clinical trial coordination. Am J Respir Crit Care Med. 1994: 149;818-24.

18. Ferguson ND, Fan E, Camporota L, Antonelli M, Anzueto A, Beale R, et al. The Berlin definition of ARDS: an expanded rationale, justification, and supplementary material. Intensive Care Med. 2012: 38;1573-82.

19. Ranieri VM, Rubenfeld GD, Thompson BT, Ferguson ND, Caldwell E, Fan E, et al. Acute respiratory distress syndrome: the Berlin Definition. JAMA. 2012: 307;2526-33.

20. Thille AW, Esteban A, Fernandez-Segoviano P, Rodriguez JM, Aramburu JA, Penuelas O, et al. Comparison of the Berlin definition for acute respiratory distress syndrome with autopsy. Am J Respir Crit Care Med. 2013: 187;761-7.

21. Rubenfeld GD, Caldwell E, Peabody E, Weaver J, Martin DP, Neff M, et al. Incidence and outcomes of acute lung injury. N Engl J Med. 2005: 353;1685-93.

22. Bersten AD, Edibam C, Hunt T, Moran J, Australian NZICSCT, Group. Incidence and mortality of acute lung injury and the acute respiratory distress syndrome in three Australian States. Am J Respir Crit Care Med. 2002: 165;443-8.

23. Vincent JL, Sakr Y, Ranieri VM. Epidemiology and outcome of acute respiratory failure in intensive care unit patients. Crit Care Med. 2003: 31;S296-9.

24. Montgomery AB, Stager MA, Carrico CJ, Hudson LD. Causes of mortality in patients with the adult respiratory distress syndrome. 1985: 132;485-9.

25. Phua J, Badia JR, Adhikari NK, Friedrich JO, Fowler RA, Singh JM, et al. Has mortality from acute respiratory distress syndrome decreased over time?: A systematic review. Am J Respir Crit Care Med. 2009: 179;220-7.

26. Ventilation with lower tidal volumes as compared with traditional tidal volumes for acute lung injury and the acute respiratory distress syndrome. The Acute Respiratory Distress Syndrome Network. N Engl J Med. 2000: 342;1301-8.

27. Peek GJ, Mugford M, Tiruvoipati R, Wilson A, Allen E, Thalanany MM, et al. Efficacy and economic assessment of conventional ventilatory support versus extracorporeal membrane oxygenation for severe adult respiratory failure (CESAR): a multicentre randomised controlled trial. Lancet. 2009: 374;1351-63.

28. Australia, New Zealand Extracorporeal Membrane Oxygenation Influenza I, Davies A, Jones D, Bailey M, Beca J, et al. Extracorporeal Membrane Oxygenation for 2009 Influenza A(H1N1) Acute Respiratory Distress Syndrome. JAMA. 2009: 302;1888-95.

29. Suchyta MR, Clemmer TP, Elliott CG, Orme JF, Jr., Morris AH, Jacobson J, et al. Increased mortality of older patients with acute respiratory distress syndrome. Chest. 1997: 111;1334-9.

30. Johnston CJ, Rubenfeld GD, Hudson LD. Effect of age on the development of ARDS in trauma patients. 2003: 124;653-9.

31. Ely EW, Wheeler AP, Thompson BT, Ancukiewicz M, Steinberg KP, Bernard GR. Recovery rate and prognosis in older persons who develop acute lung injury and the acute respiratory distress syndrome. Annals of internal medicine. 2002: 136;25-36.

32. Hamman L, Rich A. Acute diffuse interstitial fibrosis of the lungs. Bull Johns Hopkins Hosp. 1944: 74;177–212.

33. Katzenstein AL, Bloor CM, Leibow AA. Diffuse alveolar damage--the role of oxygen, shock, and related factors. A review. Am J Pathol. 1976: 85;209-28.

34. Zapol WM, Trelstad RL, Coffey JW, Tsai I, Salvador RA. Pulmonary fibrosis in severe acute respiratory failure. Am Rev Respir Dis. 1979: 119;547-54.

35. Landesberg G, Gilon D, Meroz Y, Georgieva M, Levin PD, Goodman S, et al. Diastolic dysfunction and mortality in severe sepsis and septic shock. European heart journal. 2012: 33;895-903.

36. Ware LB, Calfee CS, Janz DR, Bernard GR, May AK, Matthay MA. Plasma Biomarkers Of Lung Epithelial Versus Endothelial Injury Differentiate Direct From Indirect Acute Lung Injury. American Thoracic Society; 2013. p. A2220-A.

37. Matute-Bello G, Frevert CW, Martin TR. Animal models of acute lung injury. Am J Physiol Lung Cell Mol Physiol. 2008: 295;L379-99.

38. Gorin AB, Stewart PA. Differential permeability of endothelial and epithelial barriers to albumin flux. J Appl Physiol Respir Environ Exerc Physiol. 1979: 47;1315-24.

39. Kuebler WM, Parthasarathi K, Wang PM, Bhattacharya J. A novel signaling mechanism between gas and blood compartments of the lung. J Clin Invest. 2000: 106;607.

40. Chatterjee S, Baeter S, Bhattacharya J. Endothelial and epithelial signaling in the lung. Am J Physiol Lung Cell Mol Physiol. 2007: 293;L517-9.

41. Parthasarathi K, Bhattacharya J. Localized acid instillation by a wedged-catheter method reveals a role for vascular gap junctions in spatial expansion of acid injury. Anat Rec (Hoboken). 2011: 294;1585-91.

42. Westphalen K, Monma E, Islam MN, Bhattacharya J. Acid contact in the rodent pulmonary alveolus causes proinflammatory signaling by membrane pore formation. Am J Physiol Lung Cell Mol Physiol. 2012: 303;L107-16.

43. Wiener-Kronish JP, Albertine KH, Matthay MA. Differential responses of the endothelial and epithelial barriers of the lung in sheep to Escherichia coli endotoxin. J Clin Invest. 1991: 88;864-75.

44. Pittet JF, Wiener-Kronish JP, Serikov V, Matthay MA. Resistance of the alveolar epithelium to injury from septic shock in sheep. Am J Respir Crit Care Med. 1995: 151;1093-100.

45. Holter JF, Weiland JE, Pacht ER, Gadek JE, Davis WB. Protein permeability in the adult respiratory distress syndrome. Loss of size selectivity of the alveolar epithelium. J Clin Invest. 1986: 78;1513-22.

46. Matthay MA, Wiener-Kronish JP. Intact epithelial barrier function is critical for the resolution of alveolar edema in humans. Am Rev Respir Dis. 1990: 142;1250-7.

47. Perl M, Lomas-Neira J, Venet F, Chung CS, Ayala A. Pathogenesis of indirect (secondary) acute lung injury. Expert review of respiratory medicine. 2011: 5;115-26.

48. Summers C, Rankin SM, Condliffe AM, Singh N, Peters AM, Chilvers ER. Neutrophil kinetics in health and disease. Trends Immunol. 2010: 31;318-24.

49. Schmidt EP, Yang Y, Janssen WJ, Gandjeva A, Perez MJ, Barthel L, et al. The pulmonary endothelial glycocalyx regulates neutrophil adhesion and lung injury during experimental sepsis. Nat Med. 2012: 18;1217-23.

50. Petrache I, Birukova A, Ramirez SI, Garcia JG, Verin AD. The role of the microtubules in tumor necrosis factor-alpha-induced endothelial cell permeability. Am J Respir Cell Mol Biol. 2003: 28;574-81.

51. Vandenbroucke E, Mehta D, Minshall R, Malik AB. Regulation of endothelial junctional permeability. Annals of the New York Academy of Sciences. 2008: 1123;134-45.

52. Frank JA, Gutierrez JA, Jones KD, Allen L, Dobbs L, Matthay MA. Low tidal volume reduces epithelial and endothelial injury in acid-injured rat lungs. Am J Respir Crit Care Med. 2002: 165;242-9.

53. Imai Y, Parodo J, Kajikawa O, de Perrot M, Fischer S, Edwards V, et al. Injurious mechanical ventilation and end-organ epithelial cell apoptosis and organ dysfunction in an experimental model of acute respiratory distress syndrome. JAMA. 2003: 289;2104-12.

54. Fine A, Anderson NL, Rothstein TL, Williams MC, Gochuico BR. Fas expression in pulmonary alveolar type II cells. Am J Physiol. 1997: 273;L64-71.

55. Hagimoto N, Kuwano K, Nomoto Y, Kunitake R, Hara N. Apoptosis and expression of Fas/Fas ligand mRNA in bleomycin-induced pulmonary fibrosis in mice. Am J Respir Cell Mol Biol. 1997: 16;91-101.

56. Matute-Bello G, Liles WC, Steinberg KP, Kiener PA, Mongovin S, Chi EY, et al. Soluble Fas ligand induces epithelial cell apoptosis in humans with acute lung injury (ARDS). Journal of immunology. 1999: 163;2217-25.

57. Matute-Bello G, Liles WC, Frevert CW, Nakamura M, Ballman K, Vathanaprida C, et al. Recombinant human Fas ligand induces alveolar epithelial cell apoptosis and lung injury in rabbits. Am J Physiol Lung Cell Mol Physiol. 2001: 281;L328-35.

58. Albertine KH, Soulier MF, Wang Z, Ishizaka A, Hashimoto S, Zimmerman GA, et al. Fas and fas ligand are up-regulated in pulmonary edema fluid and lung tissue of patients with acute lung injury and the acute respiratory distress syndrome. Am J Pathol. 2002: 161;1783-96.

59. Herrero R, Kajikawa O, Matute-Bello G, Wang Y, Hagimoto N, Mongovin S, et al. The biological activity of FasL in human and mouse lungs is determined by the structure of its stalk region. J Clin Invest. 2011: 121;1174-90.

60. Guthmann F, Wissel H, Schachtrup C, Tolle A, Rudiger M, Spener F, et al. Inhibition of TNFalpha in vivo prevents hyperoxia-mediated activation of caspase 3 in type II cells. Respir Res. 2005: 6;10.

61. An S, Hishikawa Y, Liu J, Koji T. Lung injury after ischemia-reperfusion of small intestine in rats involves apoptosis of type II alveolar epithelial cells mediated by TNF-alpha and activation of Bid pathway. Apoptosis. 2007: 12;1989-2001.

62. Zhang M, Qian J, Xing X, Kong FM, Zhao L, Chen M, et al. Inhibition of the tumor necrosis factor-alpha pathway is radioprotective for the lung. Clinical cancer research : an official journal of the American Association for Cancer Research. 2008: 14;1868-76.

63. Lipke AB, Matute-Bello G, Herrero R, Kurahashi K, Wong VA, Mongovin SM, et al. Febrile-range hyperthermia augments lipopolysaccharide-induced lung injury by a mechanism of enhanced alveolar epithelial apoptosis. Journal of immunology. 2010: 184;3801-13.

64. White LE, Santora RJ, Cui Y, Moore FA, Hassoun HT. TNFR1-dependent pulmonary apoptosis during ischemic acute kidney injury. Am J Physiol Lung Cell Mol Physiol. 2012: 303;L449-59.

65. Weckbach S, Hohmann C, Denk S, Kellermann P, Huber-Lang MS, Baumann B, et al. Apoptotic and inflammatory signaling via Fas and tumor necrosis factor receptor I contribute to the development of chest trauma-induced septic acute lung injury. J Trauma Acute Care Surg. 2013: 74;792-800.

66. Herold S, Steinmueller M, von Wulffen W, Cakarova L, Pinto R, Pleschka S, et al. Lung epithelial apoptosis in influenza virus pneumonia: the role of macrophage-expressed TNF-related apoptosis-inducing ligand. J Exp Med. 2008: 205;3065-77.

67. McGrath EE, Lawrie A, Marriott HM, Mercer P, Cross SS, Arnold N, et al. Deficiency of tumour necrosis factor-related apoptosis-inducing ligand exacerbates lung injury and fibrosis. Thorax. 2012: 67;796-803.

68. Budinger GR, Mutlu GM, Urich D, Soberanes S, Buccellato LJ, Hawkins K, et al. Epithelial cell death is an important contributor to oxidant-mediated acute lung injury. Am J Respir Crit Care Med. 2011: 183;1043-54.

69. Ware LB, Matthay MA. Alveolar fluid clearance is impaired in the majority of patients with acute lung injury and the acute respiratory distress syndrome. Am J Respir Crit Care Med. 2001: 163;1376-83.

70. Berthiaume Y, Staub NC, Matthay MA. Beta-adrenergic agonists increase lung liquid clearance in anesthetized sheep. J Clin Invest. 1987: 79;335-43.

71. McAuley DF, Frank JA, Fang X, Matthay MA. Clinically relevant concentrations of beta2-adrenergic agonists stimulate maximal cyclic adenosine monophosphate-dependent airspace fluid clearance and decrease pulmonary edema in experimental acid-induced lung injury. Crit Care Med. 2004: 32;1470-6.

72. Pawlik MT, Schubert T, Hopf S, Lubnow M, Gruber M, Selig C, et al. The effects of fenoterol inhalation after acid aspiration-induced lung injury. Anesth Analg. 2009: 109;143-50.

73. Matthay MA, Abraham E. Beta-adrenergic agonist therapy as a potential treatment for acute lung injury. Am J Respir Crit Care Med. 2006: 173;254-5.

74. Frank JA, Briot R, Lee JW, Ishizaka A, Uchida T, Matthay MA. Physiological and biochemical markers of alveolar epithelial barrier dysfunction in perfused human lungs. Am J Physiol Lung Cell Mol Physiol. 2007: 293;L52-9.

75. Perkins GD, McAuley DF, Thickett DR, Gao F. The beta-agonist lung injury trial (BALTI): a randomized placebo-controlled clinical trial. Am J Respir Crit Care Med. 2006: 173;281-7.

76. Gao Smith F, Perkins GD, Gates S, Young D, McAuley DF, Tunnicliffe W, et al. Effect of intravenous beta-2 agonist treatment on clinical outcomes in acute

respiratory distress syndrome (BALTI-2): a multicentre, randomised controlled trial. Lancet. 2012: 379;229-35.

77. National Heart L, Blood Institute Acute Respiratory Distress Syndrome Clinical Trials Network, Matthay MA, Brower RG, Carson S, Douglas IS, Eisner M, et al. Randomized, placebo-controlled clinical trial of an aerosolized beta(2)-agonist for treatment of acute lung injury. Am J Respir Crit Care Med. 2011: 184;561-8.

78. McGuire WW, Spragg RG, Cohen AB, Cochrane CG. Studies on the pathogenesis of the adult respiratory distress syndrome. J Clin Invest. 1982: 69;543-53.

79. Cochrane CG, Spragg R, Revak SD. Pathogenesis of the adult respiratory distress syndrome. Evidence of oxidant activity in bronchoalveolar lavage fluid. J Clin Invest. 1983: 71;754-61.

80. Cochrane CG, Spragg RG, Revak SD, Cohen AB, McGuire WW. The presence of neutrophil elastase and evidence of oxidation activity in bronchoalveolar lavage fluid of patients with adult respiratory distress syndrome. Am Rev Respir Dis. 1983: 127;S25-7.

81. Beck-Schimmer B, Schwendener R, Pasch T, Reyes L, Booy C, Schimmer RC. Alveolar macrophages regulate neutrophil recruitment in endotoxin-induced lung injury. Respir Res. 2005: 6;61.

82. Frank JA, Wray CM, McAuley DF, Schwendener R, Matthay MA. Alveolar macrophages contribute to alveolar barrier dysfunction in ventilator-induced lung injury. Am J Physiol Lung Cell Mol Physiol. 2006: 291;L1191-8.

83. Beck-Schimmer B, Rosenberger DS, Neff SB, Jamnicki M, Suter D, Fuhrer T, et al. Pulmonary aspiration: new therapeutic approaches in the experimental model. Anesthesiology. 2005: 103;556-66.

84. Bevilacqua MP, Pober JS, Wheeler ME, Cotran RS, Gimbrone MA, Jr. Interleukin 1 acts on cultured human vascular endothelium to increase the adhesion of polymorphonuclear leukocytes, monocytes, and related leukocyte cell lines. J Clin Invest. 1985: 76;2003-11.

85. Rowlands DJ, Islam MN, Das SR, Huertas A, Quadri SK, Horiuchi K, et al. Activation of TNFR1 ectodomain shedding by mitochondrial Ca2+ determines the

severity of inflammation in mouse lung microvessels. J Clin Invest. 2011: 121;1986-99.

86. Meduri GU, Kohler G, Headley S, Tolley E, Stentz F, Postlethwaite A. Inflammatory cytokines in the BAL of patients with ARDS. Persistent elevation over time predicts poor outcome. Chest. 1995: 108;1303-14.

87. Hammerschmidt DE, Weaver LJ, Hudson LD, Craddock PR, Jacob HS. Association of complement activation and elevated plasma-C5a with adult respiratory distress syndrome. Pathophysiological relevance and possible prognostic value. Lancet. 1980: 1;947-9.

88. Folkesson HG, Matthay MA, Hebert CA, Broaddus VC. Acid aspiration-induced lung injury in rabbits is mediated by interleukin-8-dependent mechanisms. J Clin Invest. 1995: 96;107-16.

89. Wilson MR, O'Dea KP, Zhang D, Shearman AD, van Rooijen N, Takata M. Role of lung-marginated monocytes in an in vivo mouse model of ventilator-induced lung injury. Am J Respir Crit Care Med. 2009: 179;914-22.

90. Martin TR, Pistorese BP, Chi EY, Goodman RB, Matthay MA. Effects of leukotriene B4 in the human lung. Recruitment of neutrophils into the alveolar spaces without a change in protein permeability. J Clin Invest. 1989: 84;1609-19.

91. Ognibene FP, Martin SE, Parker MM, Schlesinger T, Roach P, Burch C, et al. Adult respiratory distress syndrome in patients with severe neutropenia. N Engl J Med. 1986: 315;547-51.

92. Vansteenkiste JF, Boogaerts MA. Adult respiratory distress syndrome in neutropenic leukemia patients. Blut. 1989: 58;287-90.

93. Sivan Y, Mor C, al-Jundi S, Newth CJ. Adult respiratory distress syndrome in severely neutropenic children. Pediatric pulmonology. 1990: 8;104-8.

94. Mokart D, van Craenenbroeck T, Lambert J, Textoris J, Brun JP, Sannini A, et al. Prognosis of acute respiratory distress syndrome in neutropenic cancer patients. The European respiratory journal. 2012: 40;169-76.

95. Rhee CK, Kang JY, Kim YH, Kim JW, Yoon HK, Kim SC, et al. Risk factors for acute respiratory distress syndrome during neutropenia recovery in patients with hematologic malignancies. Critical care. 2009: 13;R173.

96. Zemans RL, Briones N, Campbell M, McClendon J, Young SK, Suzuki T, et al. Neutrophil transmigration triggers repair of the lung epithelium via beta-catenin signaling. Proc Natl Acad Sci U S A. 2011: 108;15990-5.

97. Dhaliwal K, Scholefield E, Ferenbach D, Gibbons M, Duffin R, Dorward DA, et al. Monocytes control second-phase neutrophil emigration in established lipopolysaccharide-induced murine lung injury. Am J Respir Crit Care Med. 2012: 186;514-24.

98. D'Alessio FR, Tsushima K, Aggarwal NR, West EE, Willett MH, Britos MF, et al. CD4+CD25+Foxp3+ Tregs resolve experimental lung injury in mice and are present in humans with acute lung injury. J Clin Invest. 2009: 119;2898-913.

99. Aggarwal NR, D'Alessio FR, Tsushima K, Sidhaye VK, Cheadle C, Grigoryev DN, et al. Regulatory T cell-mediated resolution of lung injury: identification of potential target genes via expression profiling. Physiol Genomics. 2010: 41;109-19.

100. D'Alessio FR, Tsushima K, Aggarwal NR, Mock JR, Eto Y, Garibaldi BT, et al. Resolution of experimental lung injury by monocyte-derived inducible nitric oxide synthase. Journal of immunology. 2012: 189;2234-45.

101. Gibbons MA, MacKinnon AC, Ramachandran P, Dhaliwal K, Duffin R, Phythian-Adams AT, et al. Ly6Chi monocytes direct alternatively activated profibrotic macrophage regulation of lung fibrosis. Am J Respir Crit Care Med. 2011: 184;569-81.

102. Kotecha S, Mildner RJ, Prince LR, Vyas JR, Currie AE, Lawson RA, et al. The role of neutrophil apoptosis in the resolution of acute lung injury in newborn infants. Thorax. 2003: 58;961-7.

103. Matute-Bello G, Liles WC, Radella F, 2nd, Steinberg KP, Ruzinski JT, Jonas M, et al. Neutrophil apoptosis in the acute respiratory distress syndrome. Am J Respir Crit Care Med. 1997: 156;1969-77.

104. Serhan CN, Savill J. Resolution of inflammation: the beginning programs the end. Nat Immunol. 2005: 6;1191-7.

105. Fiore S, Serhan CN. Formation of lipoxins and leukotrienes during receptor-mediated interactions of human platelets and recombinant human granulocyte/macrophage colony-stimulating factor-primed neutrophils. J Exp Med. 1990: 172;1451-7.

106. Levy BD, Clish CB, Schmidt B, Gronert K, Serhan CN. Lipid mediator class switching during acute inflammation: signals in resolution. Nat Immunol. 2001: 2;612-9.

107. Norling LV, Perretti M. Control of myeloid cell trafficking in resolution. J Innate Immun. 2013: 5;367-76.

108. Mosser DM, Edwards JP. Exploring the full spectrum of macrophage activation. Nat Rev Immunol. 2008: 8;958-69.

109. Landsman L, Varol C, Jung S. Distinct differentiation potential of blood monocyte subsets in the lung. Journal of immunology. 2007: 178;2000-7.

110. Landsman L, Jung S. Lung macrophages serve as obligatory intermediate between blood monocytes and alveolar macrophages. Journal of immunology. 2007: 179;3488-94.

111. Santos FB, Nagato LK, Boechem NM, Negri EM, Guimaraes A, Capelozzi VL, et al. Time course of lung parenchyma remodeling in pulmonary and extrapulmonary acute lung injury. J Appl Physiol (1985). 2006: 100;98-106.

112. Janssen WJ, Barthel L, Muldrow A, Oberley-Deegan RE, Kearns MT, Jakubzick C, et al. Fas determines differential fates of resident and recruited macrophages during resolution of acute lung injury. Am J Respir Crit Care Med. 2011: 184;547-60.

113. Bellingan GJ, Caldwell H, Howie SE, Dransfield I, Haslett C. In vivo fate of the inflammatory macrophage during the resolution of inflammation: inflammatory macrophages do not die locally, but emigrate to the draining lymph nodes. Journal of immunology. 1996: 157;2577-85.

114. Uhal BD. The role of apoptosis in pulmonary fibrosis. Eur resp rev. 2008: 17;138-44.

115. Sisson TH, Mendez M, Choi K, Subbotina N, Courey A, Cunningham A, et al. Targeted injury of type II alveolar epithelial cells induces pulmonary fibrosis. Am J Respir Crit Care Med. 2010: 181;254-63.

116. Goldstein RH, Polgar P. The effect and interaction of bradykinin and prostaglandins on protein and collagen production by lung fibroblasts. The Journal of biological chemistry. 1982: 257;8630-3.

117. Fielding CA, McLoughlin RM, McLeod L, Colmont CS, Najdovska M, Grail D, et al. IL-6 regulates neutrophil trafficking during acute inflammation via STAT3. Journal of immunology. 2008: 181;2189-95.

118. Hurst SM, Wilkinson TS, McLoughlin RM, Jones S, Horiuchi S, Yamamoto N, et al. Il-6 and its soluble receptor orchestrate a temporal switch in the pattern of leukocyte recruitment seen during acute inflammation. Immunity. 2001: 14;705-14.

119. Solito E, Kamal A, Russo-Marie F, Buckingham JC, Marullo S, Perretti M. A novel calcium-dependent proapoptotic effect of annexin 1 on human neutrophils. FASEB J. 2003: 17;1544-6.

120. Liles WC, Dale DC, Klebanoff SJ. Glucocorticoids inhibit apoptosis of human neutrophils. Blood. 1995: 86;3181-8.

121. Ruiz LM, Bedoya G, Salazar J, Garcia de OD, Patino PJ. Dexamethasone inhibits apoptosis of human neutrophils induced by reactive oxygen species. Inflammation. 2002: 26;215-22.

122. Vago JP, Nogueira CR, Tavares LP, Soriani FM, Lopes F, Russo RC, et al. Annexin A1 modulates natural and glucocorticoid-induced resolution of inflammation by enhancing neutrophil apoptosis. J Leukoc Biol. 2012: 92;249-58.

123. Giles KM, Ross K, Rossi AG, Hotchin NA, Haslett C, Dransfield I. Glucocorticoid augmentation of macrophage capacity for phagocytosis of apoptotic cells is associated with reduced p130Cas expression, loss of paxillin/pyk2 phosphorylation, and high levels of active Rac. Journal of immunology. 2001: 167;976-86.

124. Serhan CN, Chiang N. Endogenous pro-resolving and anti-inflammatory lipid mediators: a new pharmacologic genus. Br J Pharmacol. 2008: 153 Suppl 1;S200-15.

125. Serhan CN, Chiang N, Van Dyke TE. Resolving inflammation: dual anti-inflammatory and pro-resolution lipid mediators. Nat Rev Immunol. 2008: 8;349-61.

126. Bonnans C, Levy BD. Lipid mediators as agonists for the resolution of acute lung inflammation and injury. Am J Respir Cell Mol Biol. 2007: 36;201-5.

127. Spite M, Norling LV, Summers L, Yang R, Cooper D, Petasis NA, et al. Resolvin D2 is a potent regulator of leukocytes and controls microbial sepsis. Nature. 2009: 461;1287-91.

128. Paul-Clark MJ, Van Cao T, Moradi-Bidhendi N, Cooper D, Gilroy DW. 15-epi-lipoxin A4-mediated induction of nitric oxide explains how aspirin inhibits acute inflammation. J Exp Med. 2004: 200;69-78.

129. Fadok VA, Bratton DL, Konowal A, Freed PW, Westcott JY, Henson PM. Macrophages that have ingested apoptotic cells in vitro inhibit proinflammatory cytokine production through autocrine/paracrine mechanisms involving TGF-beta, PGE2, and PAF. J Clin Invest. 1998: 101;890-8.

130. Huynh ML, Fadok VA, Henson PM. Phosphatidylserine-dependent ingestion of apoptotic cells promotes TGF-beta1 secretion and the resolution of inflammation. J Clin Invest. 2002: 109;41-50.

131. Matthay MA, Goolaerts A, Howard JP, Lee JW. Mesenchymal stem cells for acute lung injury: preclinical evidence. Crit Care Med. 2010: 38;S569-73.

132. Tran M, Tam D, Bardia A, Bhasin M, Rowe GC, Kher A, et al. PGC-1alpha promotes recovery after acute kidney injury during systemic inflammation in mice. J Clin Invest. 2011: 121;4003-14.

133. Protti A, Singer M. Bench-to-bedside review: potential strategies to protect or reverse mitochondrial dysfunction in sepsis-induced organ failure. Critical care. 2006: 10;228.

134. Islam MN, Das SR, Emin MT, Wei M, Sun L, Westphalen K, et al. Mitochondrial transfer from bone-marrow-derived stromal cells to pulmonary alveoli protects against acute lung injury. Nat Med. 2012: 18;759-65.

135. Coley WB. II. Contribution to the Knowledge of Sarcoma. Annals of surgery. 1891: 14;199-220.

136. Shear MJ, Turner FC, Perrault A, Shovelton T. Chemical Treatment of Tumors. V. Isolation of the Hemorrhage-Producing Fraction from Serratia marcescens (Bacillus prodigiosus) Culture Filtrate. J Natl Cancer Inst. 1943: 4;81-97.

137. Algire GH, Legallais FY, Anderson BF. Vascular reactions of normal and malignant tissues in vivo. V. The role of hypotension in the action of a bacterial polysaccharide on tumors. J Natl Cancer Inst. 1952: 12;1279-95.

138. Carswell EA, Old LJ, Kassel RL, Green S, Fiore N, Williamson B. An endotoxin-induced serum factor that causes necrosis of tumors. Proc Natl Acad Sci U S A. 1975: 72;3666-70.

139. Beutler B, Cerami A. Cachectin and tumour necrosis factor as two sides of the same biological coin. Nature. 1986: 320;584-8.

140. Beutler B, Greenwald D, Hulmes JD, Chang M, Pan YC, Mathison J, et al. Identity of tumour necrosis factor and the macrophage-secreted factor cachectin. Nature. 1985: 316;552-4.

141. Aggarwal BB. Signalling pathways of the TNF superfamily: a double-edged sword. Nat Rev Immunol. 2003: 3;745-56.

142. Old LJ. Tumour necrosis factor. Another chapter in the long history of endotoxin. Nature. 1987: 330;602-3.

143. Granger GA, Shacks SJ, Williams TW, Kolb WP. Lymphocyte in vitro cytotoxicity: specific release of lymphotoxin-like materials from tuberculin-sensitive lymphoid cells. Nature. 1969: 221;1155-7.

144. Black RA, Rauch CT, Kozlosky CJ, Peschon JJ, Slack JL, Wolfson MF, et al. A metalloproteinase disintegrin that releases tumour-necrosis factor-alpha from cells. Nature. 1997: 385;729-33.

145. Brockhaus M, Schoenfeld HJ, Schlaeger EJ, Hunziker W, Lesslauer W, Loetscher H. Identification of two types of tumor necrosis factor receptors on human cell lines by monoclonal antibodies. Proc Natl Acad Sci U S A. 1990: 87;3127-31.

146. Hohmann HP, Remy R, Brockhaus M, van Loon AP. Two different cell types have different major receptors for human tumor necrosis factor (TNF alpha). The Journal of biological chemistry. 1989: 264;14927-34.

147. Grell M, Douni E, Wajant H, Lohden M, Clauss M, Maxeiner B, et al. The transmembrane form of tumor necrosis factor is the prime activating ligand of the 80 kDa tumor necrosis factor receptor. Cell. 1995: 83;793-802.

148. Grell M, Wajant H, Zimmermann G, Scheurich P. The type 1 receptor (CD120a) is the high-affinity receptor for soluble tumor necrosis factor. Proc Natl Acad Sci U S A. 1998: 95;570-5.

149. Peschon JJ, Slack JL, Reddy P, Stocking KL, Sunnarborg SW, Lee DC, et al. An essential role for ectodomain shedding in mammalian development. Science. 1998: 282;1281-4.

150. Pinckard JK, Sheehan KC, Arthur CD, Schreiber RD. Constitutive shedding of both p55 and p75 murine TNF receptors in vivo. Journal of immunology. 1997: 158;3869-73.

151. Reddy P, Slack JL, Davis R, Cerretti DP, Kozlosky CJ, Blanton RA, et al. Functional analysis of the domain structure of tumor necrosis factor-alpha converting enzyme. The Journal of biological chemistry. 2000: 275;14608-14.

152. Tartaglia LA, Pennica D, Goeddel DV. Ligand passing: the 75-kDa tumor necrosis factor (TNF) receptor recruits TNF for signaling by the 55-kDa TNF receptor. The Journal of biological chemistry. 1993: 268;18542-8.

153. Wajant H, Pfizenmaier K, Scheurich P. Tumor necrosis factor signaling. Cell Death Differ. 2003: 10;45-65.

154. Beg AA, Baltimore D. An essential role for NF-kappaB in preventing TNF-alpha-induced cell death. Science. 1996: 274;782-4.

155. Liu ZG, Hsu H, Goeddel DV, Karin M. Dissection of TNF receptor 1 effector functions: JNK activation is not linked to apoptosis while NF-kappaB activation prevents cell death. Cell. 1996: 87;565-76.

156. Van Antwerp DJ, Martin SJ, Kafri T, Green DR, Verma IM. Suppression of TNF-alpha-induced apoptosis by NF-kappaB. Science. 1996: 274;787-9.

157. Wertz IE, Dixit VM. Regulation of death receptor signaling by the ubiquitin system. Cell Death Differ. 2010: 17;14-24.

158. Walczak H. TNF and ubiquitin at the crossroads of gene activation, cell death, inflammation, and cancer. Immunol Rev. 2011: 244;9-28.

159. O'Donnell MA, Ting AT. Chronicles of a death foretold: dual sequential cell death checkpoints in TNF signaling. Cell Cycle. 2010: 9;1065-71.

160. Karin M, Gallagher E. TNFR signaling: ubiquitin-conjugated TRAFfic signals control stop-and-go for MAPK signaling complexes. Immunol Rev. 2009: 228;225-40.

161. Faustman D, Davis M. TNF receptor 2 pathway: drug target for autoimmune diseases. 2010: 9;482-93.

162. Fontaine V, Mohand-Said S, Hanoteau N, Fuchs C, Pfizenmaier K, Eisel U. Neurodegenerative and neuroprotective effects of tumor Necrosis factor (TNF) in retinal ischemia: opposite roles of TNF receptor 1 and TNF receptor 2. J Neurosci. 2002: 22;RC216.

163. Rodriguez M, Cabal-Hierro L, Carcedo MT, Iglesias JM, Artime N, Darnay BG, et al. NF-kappaB signal triggering and termination by tumor necrosis factor receptor 2. The Journal of biological chemistry. 2011: 286;22814-24.

164. Pan S, An P, Zhang R, He X, Yin G, Min W. Etk/Bmx as a tumor necrosis factor receptor type 2-specific kinase: role in endothelial cell migration and angiogenesis. Molecular and cellular biology. 2002: 22;7512-23.

165. Millar AB, Foley NM, Singer M, Johnson NM, Meager A, Rook GA. Tumour necrosis factor in bronchopulmonary secretions of patients with adult respiratory distress syndrome. Lancet. 1989: 2;712-4.

166. Marks JD, Marks CB, Luce JM, Montgomery AB, Turner J, Metz CA, et al. Plasma tumor necrosis factor in patients with septic shock. Mortality rate, incidence of adult respiratory distress syndrome, and effects of methylprednisolone administration. Am Rev Respir Dis. 1990: 141;94-7.

167. Hyers TM, Tricomi SM, Dettenmeier PA, Fowler AA. Tumor necrosis factor levels in serum and bronchoalveolar lavage fluid of patients with the adult respiratory distress syndrome. Am Rev Respir Dis. 1991: 144;268-71.

168. Simpson SQ, Modi HN, Balk RA, Bone RC, Casey LC. Reduced alveolar macrophage production of tumor necrosis factor during sepsis in mice and men. 1991: 19;1060-6.

169. Parsons PE, Moore FA, Moore EE, Iklé DN, Henson PM, Worthen GS. Studies on the role of tumor necrosis factor in adult respiratory distress syndrome. 1992: 146;694-700.

170. Armstrong L, Thickett DR, Christie SJ, Kendall H, Millar AB. Increased expression of functionally active membrane-associated tumor necrosis factor in acute respiratory distress syndrome. Am J Respir Cell Mol Biol. 2000: 22;68-74.

171. Fisher CJ, Jr., Opal SM, Dhainaut JF, Stephens S, Zimmerman JL, Nightingale P, et al. Influence of an anti-tumor necrosis factor monoclonal antibody on cytokine levels in patients with sepsis. The CB0006 Sepsis Syndrome Study Group. Crit Care Med. 1993: 21;318-27.

172. Abraham E, Wunderink R, Silverman H, Perl TM, Nasraway S, Levy H, et al. Efficacy and safety of monoclonal antibody to human tumor necrosis factor alpha in

patients with sepsis syndrome. A randomized, controlled, double-blind, multicenter clinical trial. TNF-alpha MAb Sepsis Study Group. JAMA. 1995: 273;934-41.

173. Abraham E, Glauser MP, Butler T, Garbino J, Gelmont D, Laterre PF, et al. p55 Tumor necrosis factor receptor fusion protein in the treatment of patients with severe sepsis and septic shock. A randomized controlled multicenter trial. Ro 45-2081 Study Group. JAMA. 1997: 277;1531-8.

174. Fisher CJ, Jr., Agosti JM, Opal SM, Lowry SF, Balk RA, Sadoff JC, et al. Treatment of septic shock with the tumor necrosis factor receptor:Fc fusion protein. The Soluble TNF Receptor Sepsis Study Group. N Engl J Med. 1996: 334;1697-702.

175. Opal SM, Laterre PF, Francois B, LaRosa SP, Angus DC, Mira JP, et al. Effect of eritoran, an antagonist of MD2-TLR4, on mortality in patients with severe sepsis: the ACCESS randomized trial. JAMA. 2013: 309;1154-62.

176. Poltorak A, He X, Smirnova I, Liu MY, Van Huffel C, Du X, et al. Defective LPS signaling in C3H/HeJ and C57BL/10ScCr mice: mutations in Tlr4 gene. Science. 1998: 282;2085-8.

177. Schroder NW, Morath S, Alexander C, Hamann L, Hartung T, Zahringer U, et al. Lipoteichoic acid (LTA) of Streptococcus pneumoniae and Staphylococcus aureus activates immune cells via Toll-like receptor (TLR)-2, lipopolysaccharide-binding protein (LBP), and CD14, whereas TLR-4 and MD-2 are not involved. The Journal of biological chemistry. 2003: 278;15587-94.

178. Han SH, Kim JH, Martin M, Michalek SM, Nahm MH. Pneumococcal lipoteichoic acid (LTA) is not as potent as staphylococcal LTA in stimulating Toll-like receptor 2. Infect Immun. 2003: 71;5541-8.

179. Tse MT. Trial watch: Sepsis study failure highlights need for trial design rethink. Nature reviews Drug discovery. 2013: 12;334.

180. Raven K. Rodent models of sepsis found shockingly lacking. Nat Med. 2012: 18;998.

181. Ranieri VM, Thompson BT, Barie PS, Dhainaut JF, Douglas IS, Finfer S, et al. Drotrecogin alfa (activated) in adults with septic shock. N Engl J Med. 2012: 366;2055-64.

182. Williams SC. After Xigris, researchers look to new targets to combat sepsis. Nat Med. 2012: 18;1001.

183. Bastarache JA, Blackwell TS. Development of animal models for the acute respiratory distress syndrome. Dis Model Mech. 2009: 2;218-23.

184. Luna CM, Sibila O, Agusti C, Torres A. Animal models of ventilator-associated pneumonia. The European respiratory journal. 2009: 33;182-8.

185. Haouzi P. Murine models in critical care research. Crit Care Med. 2011: 39;2290-3.

186. Henzler D, Hochhausen N, Chankalal R, Xu Z, Whynot SC, Slutsky AS, et al. Physiologic and biologic characteristics of three experimental models of acute lung injury in rats. Anesth Analg. 2011: 112;1139-46.

187. Proudfoot AG, McAuley DF, Griffiths MJ, Hind M. Human models of acute lung injury. Dis Model Mech. 2011: 4;145-53.

188. Reiss LK, Uhlig U, Uhlig S. Models and mechanisms of acute lung injury caused by direct insults. Eur J Cell Biol. 2012: 91;590-601.

189. Clerici C. The challenge of modeling human acute respiratory distress syndrome: a new model of lung injury due to sepsis with impaired alveolar edema fluid removal. Am J Physiol Lung Cell Mol Physiol. 2011: 301;L20-2.

190. Shaffer TH, Wolfson MR. Translational research: matching experimental models with therapeutic interventions. Pediatr Crit Care Med. 2012: 13;369-70.

191. Zambelli V, Di Grigoli G, Scanziani M, Valtorta S, Amigoni M, Belloli S, et al. Time course of metabolic activity and cellular infiltration in a murine model of acid-induced lung injury. Intensive Care Med. 2012: 38;694-701.

192. Matute-Bello G, Downey G, Moore BB, Groshong SD, Matthay MA, Slutsky AS, et al. An official American Thoracic Society workshop report: features and measurements of experimental acute lung injury in animals. Am J Respir Cell Mol Biol. 2011: 44;725-38.

193. Rezaiguia S, Garat C, Delclaux C, Meignan M, Fleury J, Legrand P, et al. Acute bacterial pneumonia in rats increases alveolar epithelial fluid clearance by a tumor necrosis factor-alpha-dependent mechanism. J Clin Invest. 1997: 99;325-35.

194. Mendelson CL. The aspiration of stomach contents into the lungs during obstetric anesthesia. American journal of obstetrics and gynecology. 1946: 52;191-205.

195. Kennedy TP, Johnson KJ, Kunkel RG, Ward PA, Knight PR, Finch JS. Acute acid aspiration lung injury in the rat: biphasic pathogenesis. Anesth Analg. 1989: 69;87-92.

196. Goldman G, Welbourn R, Kobzik L, Valeri CR, Shepro D, Hechtman HB. Tumor necrosis factor-alpha mediates acid aspiration-induced systemic organ injury. Annals of surgery. 1990: 212;513-9; discussion 9-20.

197. Davidson BA, Knight PR, Helinski JD, Nader ND, Shanley TP, Johnson KJ. The role of tumor necrosis factor-alpha in the pathogenesis of aspiration pneumonitis in rats. Anesthesiology. 1999: 91;486-99.

198. Stephens KE, Ishizaka A, Larrick JW, Raffin TA. Tumor necrosis factor causes increased pulmonary permeability and edema. Comparison to septic acute lung injury. Am Rev Respir Dis. 1988: 137;1364-70.

199. Horvath CJ, Ferro TJ, Jesmok G, Malik AB. Recombinant tumor necrosis factor increases pulmonary vascular permeability independent of neutrophils. Proc Natl Acad Sci U S A. 1988: 85;9219-23.

200. Goldblum SE, Hennig B, Jay M, Yoneda K, McClain CJ. Tumor necrosis factor alpha-induced pulmonary vascular endothelial injury. Infect Immun. 1989: 57;1218-26.

201. Bertok S, Wilson MR, Dorr AD, Dokpesi JO, O'Dea KP, Marczin N, et al. Characterization of TNF receptor subtype expression and signaling on pulmonary endothelial cells in mice. Am J Physiol Lung Cell Mol Physiol. 2011: 300;L781-9.

202. Li XY, Donaldson K, Brown D, MacNee W. The role of tumor necrosis factor in increased airspace epithelial permeability in acute lung inflammation. Am J Respir Cell Mol Biol. 1995: 13;185-95.

203. Borjesson A, Norlin A, Wang X, Andersson R, Folkesson HG. TNF-alpha stimulates alveolar liquid clearance during intestinal ischemia-reperfusion in rats. Am J Physiol Lung Cell Mol Physiol. 2000: 278;L3-12.

204. Tillie-Leblond I, Guery BP, Janin A, Leberre R, Just N, Pittet JF, et al. Chronic bronchial allergic inflammation increases alveolar liquid clearance by TNF-alpha -dependent mechanism. Am J Physiol Lung Cell Mol Physiol. 2002: 283;L1303-9.

205. Garat C, Rezaiguia S, Meignan M, D'Ortho MP, Harf A, Matthay MA, et al. Alveolar endotoxin increases alveolar liquid clearance in rats. J Appl Physiol (1985). 1995: 79;2021-8.

206. Lucas R, Magez S, De Leys R, Fransen L, Scheerlinck JP, Rampelberg M, et al. Mapping the lectin-like activity of tumor necrosis factor. Science. 1994: 263;814-7.

207. Lucas R, Magez S, Songa B, Darji A, Hamers R, de Baetselier P. A role for TNF during African trypanosomiasis: involvement in parasite control, immunosuppression and pathology. Res Immunol. 1993: 144;370-6.

208. Magez S, Lucas R, Darji A, Songa EB, Hamers R, De Baetselier P. Murine tumour necrosis factor plays a protective role during the initial phase of the experimental infection with Trypanosoma brucei brucei. Parasite Immunol. 1993: 15;635-41.

209. Magez S, Geuskens M, Beschin A, del Favero H, Verschueren H, Lucas R, et al. Specific uptake of tumor necrosis factor-alpha is involved in growth control of Trypanosoma brucei. J Cell Biol. 1997: 137;715-27.

210. Baldwin RL, Chang MP, Bramhall J, Graves S, Bonavida B, Wisnieski BJ. Capacity of tumor necrosis factor to bind and penetrate membranes is pH-dependent. Journal of immunology. 1988: 141;2352-7.

211. Kagan BL, Baldwin RL, Munoz D, Wisnieski BJ. Formation of ion-permeable channels by tumor necrosis factor-alpha. Science. 1992: 255;1427-30.

212. Hribar M, Bloc A, van der Goot FG, Fransen L, De Baetselier P, Grau GE, et al. The lectin-like domain of tumor necrosis factor-alpha increases membrane conductance in microvascular endothelial cells and peritoneal macrophages. European journal of immunology. 1999: 29;3105-11.

213. van der Goot FG, Pugin J, Hribar M, Fransen L, Dunant Y, De Baetselier P, et al. Membrane interaction of TNF is not sufficient to trigger increase in membrane conductance in mammalian cells. FEBS Lett. 1999: 460;107-11.

214. Fukuda N, Jayr C, Lazrak A, Wang Y, Lucas R, Matalon S, et al. Mechanisms of TNF-alpha stimulation of amiloride-sensitive sodium transport across alveolar epithelium. Am J Physiol Lung Cell Mol Physiol. 2001: 280;L1258-65.

215. Elia N, Tapponnier M, Matthay MA, Hamacher J, Pache JC, Brundler MA, et al. Functional identification of the alveolar edema reabsorption activity of murine tumor necrosis factor-alpha. Am J Respir Crit Care Med. 2003: 168;1043-50.

216. Braun C, Hamacher J, Morel DR, Wendel A, Lucas R. Dichotomal role of TNF in experimental pulmonary edema reabsorption. Journal of immunology. 2005: 175;3402-8.

217. Vadasz I, Schermuly RT, Ghofrani HA, Rummel S, Wehner S, Muhldorfer I, et al. The lectin-like domain of tumor necrosis factor-alpha improves alveolar fluid balance in injured isolated rabbit lungs. Crit Care Med. 2008: 36;1543-50.

218. Hamacher J, Stammberger U, Roux J, Kumar S, Yang G, Xiong C, et al. The lectin-like domain of tumor necrosis factor improves lung function after rat lung transplantation--potential role for a reduction in reactive oxygen species generation. Crit Care Med. 2010: 38;871-8.

219. Hartmann EK, Boehme S, Duenges B, Bentley A, Klein KU, Kwiecien R, et al. An inhaled tumor necrosis factor-alpha-derived TIP peptide improves the pulmonary function in experimental lung injury. Acta Anaesthesiol Scand. 2013: 57;334-41.

220. Peschon JJ, Torrance DS, Stocking KL, Glaccum MB, Otten C, Willis CR, et al. TNF receptor-deficient mice reveal divergent roles for p55 and p75 in several models of inflammation. Journal of immunology. 1998: 160;943-52.

221. Ebach DR, Riehl TE, Stenson WF. Opposing effects of tumor necrosis factor receptor 1 and 2 in sepsis due to cecal ligation and puncture. Shock. 2005: 23;311-8.

222. Al-Lamki RS, Brookes AP, Wang J, Reid MJ, Parameshwar J, Goddard MJ, et al. TNF receptors differentially signal and are differentially expressed and regulated in the human heart. Am J Transplant. 2009: 9;2679-96.

223. Monden Y, Kubota T, Inoue T, Tsutsumi T, Kawano S, Ide T, et al. Tumor necrosis factor-alpha is toxic via receptor 1 and protective via receptor 2 in a murine model of myocardial infarction. American journal of physiology Heart and circulatory physiology. 2007: 293;H743-53.

224. Wilson MR, Goddard ME, O'Dea KP, Choudhury S, Takata M. Differential roles of p55 and p75 tumor necrosis factor receptors on stretch-induced pulmonary edema in mice. Am J Physiol Lung Cell Mol Physiol. 2007: 293;L60-8.

225. Takata M, Abe J, Tanaka H, Kitano Y, Doi S, Kohsaka T, et al. Intraalveolar expression of tumor necrosis factor-alpha gene during conventional and high-frequency ventilation. Am J Respir Crit Care Med. 1997: 156;272-9.

226. Imai Y, Kawano T, Iwamoto S, Nakagawa S, Takata M, Miyasaka K. Intratracheal anti-tumor necrosis factor-alpha antibody attenuates ventilator-induced lung injury in rabbits. J Appl Physiol (1985). 1999: 87;510-5.

227. Wilson MR, Choudhury S, Goddard ME, O'Dea KP, Nicholson AG, Takata M. High tidal volume upregulates intrapulmonary cytokines in an in vivo mouse model of ventilator-induced lung injury. J Appl Physiol (1985). 2003: 95;1385-93.

228. Wilson MR, Choudhury S, Takata M. Pulmonary inflammation induced by high-stretch ventilation is mediated by tumor necrosis factor signaling in mice. Am J Physiol Lung Cell Mol Physiol. 2005: 288;L599-607.

229. Ghosh S, Wilson MR, Choudhury S, Yamamoto H, Goddard ME, Falusi B, et al. Effects of inhaled carbon monoxide on acute lung injury in mice. Am J Physiol Lung Cell Mol Physiol. 2005: 288;L1003-9.

230. Mizgerd JP, Skerrett SJ. Animal models of human pneumonia. Am J Physiol Lung Cell Mol Physiol. 2008: 294;L387-98.

231. Chiavolini D, Pozzi G, Ricci S. Animal models of Streptococcus pneumoniae disease. Clin Microbiol Rev. 2008: 21;666-85.

232. Scotton CJ, Chambers RC. Bleomycin revisited: towards a more representative model of IPF? Am J Physiol Lung Cell Mol Physiol. 2010: 299;L439-41.

233. Yoshikawa S, King JA, Lausch RN, Penton AM, Eyal FG, Parker JC. Acute ventilator-induced vascular permeability and cytokine responses in isolated and in situ mouse lungs. J Appl Physiol (1985). 2004: 97;2190-9.

234. Zhao M, Fernandez LG, Doctor A, Sharma AK, Zarbock A, Tribble CG, et al. Alveolar macrophage activation is a key initiation signal for acute lung ischemia-reperfusion injury. Am J Physiol Lung Cell Mol Physiol. 2006: 291;L1018-26.

235. Miyahara T, Hamanaka K, Weber DS, Anghelescu M, Frost JR, King JA, et al. Cytosolic phospholipase A2 and arachidonic acid metabolites modulate ventilator-induced permeability increases in isolated mouse lungs. J Appl Physiol (1985). 2008: 104;354-62.

236. Walker MG, Yao LJ, Patterson EK, Joseph MG, Cepinskas G, Veldhuizen RA, et al. The effect of tidal volume on systemic inflammation in Acid-induced lung injury. Respiration. 2011: 81;333-42.

237. Wakabayashi K, Wilson MR, Tatham KC, O'Dea KP, Takata M. Volutrauma, but not Atelectrauma, Induces Systemic Cytokine Production by Lung-Marginated Monocytes*. Crit Care Med. 2014: 42;e49-e57.

238. Hickey MJ, Westhorpe CL. Imaging inflammatory leukocyte recruitment in kidney, lung and liver--challenges to the multi-step paradigm. Immunol Cell Biol. 2013: 91;281-9.

239. Wilson MR, Patel BV, Takata M. Ventilation with "clinically relevant" high tidal volumes does not promote stretch-induced injury in the lungs of healthy mice. Crit Care Med. 2012: 40;2850-7.

240. Ewart S, Levitt R, Mitzner W. Respiratory system mechanics in mice measured by end-inflation occlusion. J Appl Physiol (1985). 1995: 79;560-6.

241. O'Dea KP, Dokpesi JO, Tatham KC, Wilson MR, Takata M. Regulation of monocyte subset proinflammatory responses within the lung microvasculature by the p38 MAPK/MK2 pathway. Am J Physiol Lung Cell Mol Physiol. 2011: 301;L812-21.

242. Garat C, Carter EP, Matthay MA. New in situ mouse model to quantify alveolar epithelial fluid clearance. J Appl Physiol (1985). 1998: 84;1763-7.

243. Gavrieli Y, Sherman Y, Ben-Sasson SA. Identification of programmed cell death in situ via specific labeling of nuclear DNA fragmentation. J Cell Biol. 1992: 119;493-501.

244. Lockshin RA, Zakeri Z. When cells die two: Wiley-Blackwell; 2004. 549 p.

245. Kroemer G, Galluzzi L, Vandenabeele P, Abrams J, Alnemri ES, Baehrecke EH, et al. Classification of cell death: recommendations of the Nomenclature Committee on Cell Death 2009. Cell Death Differ. 2009: 16;3-11.

246. Herold S, Tabar TS, Janssen H, Hoegner K, Cabanski M, Lewe-Schlosser P, et al. Exudate macrophages attenuate lung injury by the release of IL-1 receptor antagonist in gram-negative pneumonia. Am J Respir Crit Care Med. 2011: 183;1380-90.

247. Unkel B, Hoegner K, Clausen BE, Lewe-Schlosser P, Bodner J, Gattenloehner S, et al. Alveolar epithelial cells orchestrate DC function in murine viral pneumonia. J Clin Invest. 2012: 122;3652-64.

248. Dorr AD, Wilson MR, Wakabayashi K, Waite AC, Patel BV, van Rooijen N, et al. Sources of alveolar soluble TNF receptors during acute lung injury of different etiologies. J Appl Physiol (1985). 2011: 111;177-84.

249. Evans TJ, Moyes D, Carpenter A, Martin R, Loetscher H, Lesslauer W, et al. Protective effect of 55- but not 75-kD soluble tumor necrosis factor receptor-immunoglobulin G fusion proteins in an animal model of gram-negative sepsis. J Exp Med. 1994: 180;2173-9.

250. Pittet D, Harbarth S, Suter PM, Reinhart K, Leighton A, Barker C, et al. Impact of immunomodulating therapy on morbidity in patients with severe sepsis. Am J Respir Crit Care Med. 1999: 160;852-7.

251. Abraham E, Laterre PF, Garbino J, Pingleton S, Butler T, Dugernier T, et al. Lenercept (p55 tumor necrosis factor receptor fusion protein) in severe sepsis and early septic shock: a randomized, double-blind, placebo-controlled, multicenter phase III trial with 1,342 patients. Crit Care Med. 2001: 29;503-10.

252. Bertok S, Wilson MR, Morley PJ, de Wildt R, Bayliffe A, Takata M. Selective inhibition of intra-alveolar p55 TNF receptor attenuates ventilator-induced lung injury. Thorax. 2012: 67;244-51.

253. Ware LB. Modeling human lung disease in animals. Am J Physiol Lung Cell Mol Physiol. 2008: 294;L149-50.

254. Imai Y, Kuba K, Neely GG, Yaghubian-Malhami R, Perkmann T, van Loo G, et al. Identification of oxidative stress and Toll-like receptor 4 signaling as a key pathway of acute lung injury. Cell. 2008: 133;235-49.

255. Modelska K, Pittet JF, Folkesson HG, Courtney Broaddus V, Matthay MA. Acid-induced lung injury. Protective effect of anti-interleukin-8 pretreatment on alveolar epithelial barrier function in rabbits. Am J Respir Crit Care Med. 1999: 160;1450-6.

256. Weiser MR, Pechet TT, Williams JP, Ma M, Frenette PS, Moore FD, et al. Experimental murine acid aspiration injury is mediated by neutrophils and the alternative complement pathway. J Appl Physiol (1985). 1997: 83;1090-5.

257. Goldman G, Welbourn R, Kobzik L, Valeri CR, Shepro D, Hechtman HB. Reactive oxygen species and elastase mediate lung permeability after acid aspiration. J Appl Physiol (1985). 1992: 73;571-5.

258. Nader-Djalal N, Knight PR, 3rd, Thusu K, Davidson BA, Holm BA, Johnson KJ, et al. Reactive oxygen species contribute to oxygen-related lung injury after acid aspiration. Anesth Analg. 1998: 87;127-33.

259. Imai Y, Kuba K, Rao S, Huan Y, Guo F, Guan B, et al. Angiotensin-converting enzyme 2 protects from severe acute lung failure. Nature. 2005: 436;112-6.

260. Zarbock A, Singbartl K, Ley K. Complete reversal of acid-induced acute lung injury by blocking of platelet-neutrophil aggregation. J Clin Invest. 2006: 116;3211-9.

261. Ichikawa A, Kuba K, Morita M, Chida S, Tezuka H, Hara H, et al. CXCL10-CXCR3 enhances the development of neutrophil-mediated fulminant lung injury of viral and nonviral origin. Am J Respir Crit Care Med. 2013: 187;65-77.

262. Allen GB, Pavone LA, DiRocco JD, Bates JH, Nieman GF. Pulmonary impedance and alveolar instability during injurious ventilation in rats. J Appl Physiol (1985). 2005: 99;723-30.

263. Allen GB, Suratt BT, Rinaldi L, Petty JM, Bates JH. Choosing the frequency of deep inflation in mice: balancing recruitment against ventilator-induced lung injury. Am J Physiol Lung Cell Mol Physiol. 2006: 291;L710-7.

264. Allen GB, Leclair T, Cloutier M, Thompson-Figueroa J, Bates JH. The response to recruitment worsens with progression of lung injury and fibrin accumulation in a mouse model of acid aspiration. Am J Physiol Lung Cell Mol Physiol. 2007: 292;L1580-9.

265. Cornell TT, Hinkovska-Galcheva V, Sun L, Cai Q, Hershenson MB, Vanway S, et al. Ceramide-dependent PP2A regulation of TNFalpha-induced IL-8 production in respiratory epithelial cells. Am J Physiol Lung Cell Mol Physiol. 2009: 296;L849-56.

266. Mitzner W, Blosser S, Yager D, Wagner E. Effect of bronchial smooth muscle contraction on lung compliance. J Appl Physiol (1985). 1992: 72;158-67.

267. Mohler KM, Torrance DS, Smith CA, Goodwin RG, Stremler KE, Fung VP, et al. Soluble tumor necrosis factor (TNF) receptors are effective therapeutic agents in lethal endotoxemia and function simultaneously as both TNF carriers and TNF antagonists. Journal of immunology. 1993: 151;1548-61.

268. Al-Lamki RS, Wang J, Vandenabeele P, Bradley JA, Thiru S, Luo D, et al. TNFR1- and TNFR2-mediated signaling pathways in human kidney are cell type-specific and differentially contribute to renal injury. FASEB J. 2005: 19;1637-45.

269. Liu J, Zhao MQ, Xu L, Ramana CV, Declercq W, Vandenabeele P, et al. Requirement for tumor necrosis factor-receptor 2 in alveolar chemokine expression depends upon the form of the ligand. Am J Respir Cell Mol Biol. 2005: 33;463-9.

270. Ermert M, Pantazis C, Duncker HR, Grimminger F, Seeger W, Ermert L. In situ localization of TNFalpha/beta, TACE and TNF receptors TNF-R1 and TNF-R2 in control and LPS-treated lung tissue. Cytokine. 2003: 22;89-100.

271. MacEwan DJ. TNF ligands and receptors--a matter of life and death. Br J Pharmacol. 2002: 135;855-75.

272. MacEwan DJ. TNF receptor subtype signalling: differences and cellular consequences. Cell Signal. 2002: 14;477-92.

273. Zarbock A, Polanowska-Grabowska RK, Ley K. Platelet-neutrophil-interactions: linking hemostasis and inflammation. Blood Rev. 2007: 21;99-111.

274. Matt U, Warszawska JM, Bauer M, Dietl W, Mesteri I, Doninger B, et al. Bbeta(15-42) protects against acid-induced acute lung injury and secondary pseudomonas pneumonia in vivo. Am J Respir Crit Care Med. 2009: 180;1208-17.

275. Azoulay E, Mokart D, Rabbat A, Pene F, Kouatchet A, Bruneel F, et al. Diagnostic bronchoscopy in hematology and oncology patients with acute respiratory failure: prospective multicenter data. Crit Care Med. 2008: 36;100-7.

276. Lentsch AB, Czermak BJ, Bless NM, Van Rooijen N, Ward PA. Essential role of alveolar macrophages in intrapulmonary activation of NF-kappaB. Am J Respir Cell Mol Biol. 1999: 20;692-8.

277. Shanley TP, Davidson BA, Nader ND, Bless N, Vasi N, Ward PA, et al. Role of macrophage inflammatory protein-2 in aspiration-induced lung injury. Crit Care Med. 2000: 28;2437-44.

278. Dai H, Guzman J, Chen B, Costabel U. Production of soluble tumor necrosis factor receptors and tumor necrosis factor-alpha by alveolar macrophages in sarcoidosis and extrinsic allergic alveolitis. Chest. 2005: 127;251-6.

279. Masli S, Turpie B. Anti-inflammatory effects of tumour necrosis factor (TNF)-alpha are mediated via TNF-R2 (p75) in tolerogenic transforming growth factor-beta-treated antigen-presenting cells. Immunology. 2009: 127;62-72.

280. Chen X, Baumel M, Mannel DN, Howard OM, Oppenheim JJ. Interaction of TNF with TNF receptor type 2 promotes expansion and function of mouse CD4+CD25+ T regulatory cells. Journal of immunology. 2007: 179;154-61.

281. Chen X, Subleski JJ, Kopf H, Howard OM, Mannel DN, Oppenheim JJ. Cutting edge: expression of TNFR2 defines a maximally suppressive subset of mouse CD4+CD25+FoxP3+ T regulatory cells: applicability to tumor-infiltrating T regulatory cells. Journal of immunology. 2008: 180;6467-71.

282. Veroni C, Gabriele L, Canini I, Castiello L, Coccia E, Remoli ME, et al. Activation of TNF receptor 2 in microglia promotes induction of anti-inflammatory pathways. Mol Cell Neurosci. 2010: 45;234-44.

283. Kanehiro A, Lahn M, Makela MJ, Dakhama A, Joetham A, Rha YH, et al. Requirement for the p75 TNF-alpha receptor 2 in the regulation of airway hyperresponsiveness by gamma delta T cells. Journal of immunology. 2002: 169;4190-7.

284. Schneeberger-Keeley EE, Karnovsky MJ. The ultrastructural basis of alveolar-capillary membrane permeability to peroxidase used as a tracer. J Cell Biol. 1968: 37;781-93.

285. Schneeberger EE, Karnovsky MJ. The influence of intravascular fluid volume on the permeability of newborn and adult mouse lungs to ultrastructural protein tracers. J Cell Biol. 1971: 49;319-34.

286. Schneeberger EE. The permeability of the alveolar-capillary membrane to ultrastructural protein tracers. Annals of the New York Academy of Sciences. 1974: 221;238-43.

287. Gropper MA, Wiener-Kronish J. The epithelium in acute lung injury/acute respiratory distress syndrome. Curr Opin Crit Care. 2008: 14;11-5.

288. Martin TR, Hagimoto N, Nakamura M, Matute-Bello G. Apoptosis and epithelial injury in the lungs. Proc Am Thorac Soc. 2005: 2;214-20.

289. Matute-Bello G, Frevert CW, Liles WC, Nakamura M, Ruzinski JT, Ballman K, et al. Fas/Fas ligand system mediates epithelial injury, but not pulmonary host defenses, in response to inhaled bacteria. Infect Immun. 2001: 69;5768-76.

290. Matute-Bello G, Winn RK, Jonas M, Chi EY, Martin TR, Liles WC. Fas (CD95) induces alveolar epithelial cell apoptosis in vivo: implications for acute pulmonary inflammation. Am J Pathol. 2001: 158;153-61.

291. Nakamura M, Matute-Bello G, Liles WC, Hayashi S, Kajikawa O, Lin SM, et al. Differential response of human lung epithelial cells to fas-induced apoptosis. Am J Pathol. 2004: 164;1949-58.

292. Matute-Bello G, Lee JS, Liles WC, Frevert CW, Mongovin S, Wong V, et al. Fas-mediated acute lung injury requires fas expression on nonmyeloid cells of the lung. Journal of immunology. 2005: 175;4069-75.

293. Bem RA, Farnand AW, Wong V, Koski A, Rosenfeld ME, van Rooijen N, et al. Depletion of resident alveolar macrophages does not prevent Fas-mediated lung injury in mice. Am J Physiol Lung Cell Mol Physiol. 2008: 295;L314-25.

294. Farnand AW, Eastman AJ, Herrero R, Hanson JF, Mongovin S, Altemeier WA, et al. Fas activation in alveolar epithelial cells induces KC (CXCL1) release by a MyD88-dependent mechanism. Am J Respir Cell Mol Biol. 2011: 45;650-8.

295. Uhal BD. Fas and apoptosis in the alveolar epithelium: holes in the dike? Am J Physiol Lung Cell Mol Physiol. 2001: 281;L326-7.

296. Perkowski SZ, Sloane PJ, Spath JA, Jr., Elsasser TH, Fisher JK, Gee MH. TNF-alpha and the pathophysiology of endotoxin-induced acute respiratory failure in sheep. J Appl Physiol (1985). 1996: 80;564-73.

297. Calkins CM, Heimbach JK, Bensard DD, Song Y, Raeburn CD, Meng X, et al. TNF receptor I mediates chemokine production and neutrophil accumulation in the lung following systemic lipopolysaccharide. The Journal of surgical research. 2001: 101;232-7.

298. Song Y, Ao L, Raeburn CD, Calkins CM, Abraham E, Harken AH, et al. A low level of TNF-alpha mediates hemorrhage-induced acute lung injury via p55 TNF receptor. Am J Physiol Lung Cell Mol Physiol. 2001: 281;L677-84.

299. Parsons PE, Matthay MA, Ware LB, Eisner MD, National Heart L, Blood Institute Acute Respiratory Distress Syndrome Clinical Trials Network. Elevated

plasma levels of soluble TNF receptors are associated with morbidity and mortality in patients with acute lung injury. Am J Physiol Lung Cell Mol Physiol. 2005: 288;L426-31.

300. Shah NG, Tulapurkar ME, Damarla M, Singh IS, Goldblum SE, Shapiro P, et al. Febrile-range hyperthermia augments reversible TNF-alpha-induced hyperpermeability in human microvascular lung endothelial cells. Int J Hyperthermia. 2012: 28;627-35.

301. Lucas R, Lou J, Morel DR, Ricou B, Suter PM, Grau GE. TNF receptors in the microvascular pathology of acute respiratory distress syndrome and cerebral malaria. J Leukoc Biol. 1997: 61;551-8.

302. Kambas K, Markiewski MM, Pneumatikos IA, Rafail SS, Theodorou V, Konstantonis D, et al. C5a and TNF-alpha up-regulate the expression of tissue factor in intra-alveolar neutrophils of patients with the acute respiratory distress syndrome. Journal of immunology. 2008: 180;7368-75.

303. Gibbs LS, Lai L, Malik AB. Tumor necrosis factor enhances the neutrophil-dependent increase in endothelial permeability. J Cell Physiol. 1990: 145;496-500.

304. Lipke AB, Matute-Bello G, Herrero R, Wong VA, Mongovin SM, Martin TR. Death receptors mediate the adverse effects of febrile-range hyperthermia on the outcome of lipopolysaccharide-induced lung injury. Am J Physiol Lung Cell Mol Physiol. 2011: 301;L60-70.

305. Maniatis NA, Sfika A, Nikitopoulou I, Vassiliou AG, Magkou C, Armaganidis A, et al. Acid-induced acute lung injury in mice is associated with P44/42 and c-Jun N-terminal kinase activation and requires the function of tumor necrosis factor alpha receptor I. Shock. 2012: 38;381-6.

306. Kudoh I, Ohtake M, Nishizawa H, Kurahashi K, Hattori S, Okumura F, et al. The effect of pentoxifylline on acid-induced alveolar epithelial injury. Anesthesiology. 1995: 82;531-41.

307. Dodd DC, Marshall BE, Soma LR, Leatherman J. Experimental acid-aspiration pneumonia in the rabbit. A pathologic and morphometric study. Vet Pathol. 1976: 13;436-48.

308. Uchida T, Shirasawa M, Ware LB, Kojima K, Hata Y, Makita K, et al. Receptor for advanced glycation end-products is a marker of type I cell injury in acute lung injury. Am J Respir Crit Care Med. 2006: 173;1008-15.

309. Scherpereel A, Depontieu F, Grigoriu B, Cavestri B, Tsicopoulos A, Gentina T, et al. Endocan, a new endothelial marker in human sepsis. Critical care medicine. 2006: 34;532-7.

310. Kasahara Y, Tuder RM, Taraseviciene-Stewart L, Le Cras TD, Abman S, Hirth PK, et al. Inhibition of VEGF receptors causes lung cell apoptosis and emphysema. J Clin Invest. 2000: 106;1311-9.

311. Schneider-Brachert W, Tchikov V, Neumeyer J, Jakob M, Winoto-Morbach S, Held-Feindt J, et al. Compartmentalization of TNF receptor 1 signaling: internalized TNF receptosomes as death signaling vesicles. Immunity. 2004: 21;415-28.

312. Chollet-Martin S, Jourdain B, Gibert C, Elbim C, Chastre J, Gougerot-Pocidalo MA. Interactions between neutrophils and cytokines in blood and alveolar spaces during ARDS. Am J Respir Crit Care Med. 1996: 154;594-601.

313. Smedly LA, Tonnesen MG, Sandhaus RA, Haslett C, Guthrie LA, Johnston RB, Jr., et al. Neutrophil-mediated injury to endothelial cells. Enhancement by endotoxin and essential role of neutrophil elastase. J Clin Invest. 1986: 77;1233-43.

314. Sudo E, Fukuchi Y, Ishida K, Matsuse T, Nagase T, Teramoto S, et al. [An aspiration pneumonia in acute airway damage model induced by HCl and/or LPS]. Nihon Ronen Igakkai Zasshi. 1993: 30;1032-8.

315. Moraes TJ, Chow CW, Downey GP. Proteases and lung injury. Crit Care Med. 2003: 31;S189-94.

316. Mantell LL, Kazzaz JA, Xu J, Palaia TA, Piedboeuf B, Hall S, et al. Unscheduled apoptosis during acute inflammatory lung injury. Cell Death Differ. 1997: 4;600-7.

317. Kawasaki M, Kuwano K, Hagimoto N, Matsuba T, Kunitake R, Tanaka T, et al. Protection from lethal apoptosis in lipopolysaccharide-induced acute lung injury in mice by a caspase inhibitor. Am J Pathol. 2000: 157;597-603.

318. Kitamura Y, Hashimoto S, Mizuta N, Kobayashi A, Kooguchi K, Fujiwara I, et al. Fas/FasL-dependent apoptosis of alveolar cells after lipopolysaccharide-induced lung injury in mice. Am J Respir Crit Care Med. 2001: 163;762-9.

319. Bachofen M, Weibel ER. Alterations of the gas exchange apparatus in adult respiratory insufficiency associated with septicemia. Am Rev Respir Dis. 1977: 116;589-615.

320. White LE, Cui Y, Shelak CM, Lie ML, Hassoun HT. Lung endothelial cell apoptosis during ischemic acute kidney injury. Shock. 2012: 38;320-7.

321. Corti M, Brody AR, Harrison JH. Isolation and primary culture of murine alveolar type II cells. Am J Respir Cell Mol Biol. 1996: 14;309-15.

322. Shi Y. Caspase activation: revisiting the induced proximity model. Cell. 2004: 117;855-8.

323. Hornsby PJ, Didenko VV. In situ ligation: a decade and a half of experience. Methods Mol Biol. 2011: 682;49-63.

324. Henson PM, Tuder RM. Apoptosis in the lung: induction, clearance and detection. Am J Physiol Lung Cell Mol Physiol. 2008: 294;L601-11.

325. Friggeri A, Banerjee S, Biswas S, de Freitas A, Liu G, Bierhaus A, et al. Participation of the receptor for advanced glycation end products in efferocytosis. Journal of immunology. 2011: 186;6191-8.

326. Micheau O, Tschopp J. Induction of TNF receptor I-mediated apoptosis via two sequential signaling complexes. Cell. 2003: 114;181-90.

327. Varfolomeev EE, Ashkenazi A. Tumor necrosis factor: an apoptosis JuNKie? Cell. 2004: 116;491-7.

328. Madjdpour L, Kneller S, Booy C, Pasch T, Schimmer RC, Beck-Schimmer B. Acid-induced lung injury: role of nuclear factor-kappaB. Anesthesiology. 2003: 99;1323-32.

329. Haider N, Arbustini E, Gupta S, Liu H, Narula N, Hajjar R, et al. Concurrent upregulation of endogenous proapoptotic and antiapoptotic factors in failing human hearts. Nat Clin Pract Cardiovasc Med. 2009: 6;250-61.

330. Haider N, Narula N, Narula J. Apoptosis in heart failure represents programmed cell survival, not death, of cardiomyocytes and likelihood of reverse remodeling. J Card Fail. 2002: 8;S512-7.

331. Narula J, Haider N, Arbustini E, Chandrashekhar Y. Mechanisms of disease: apoptosis in heart failure--seeing hope in death. Nat Clin Pract Cardiovasc Med. 2006: 3;681-8.

332. Meneton P, Ichikawa I, Inagami T, Schnermann J. Renal physiology of the mouse. American journal of physiology Renal physiology. 2000: 278;F339-51.

333. Fukuda N, Folkesson HG, Matthay MA. Relationship of interstitial fluid volume to alveolar fluid clearance in mice: ventilated vs. in situ studies. J Appl Physiol (1985). 2000: 89;672-9.

334. Berthiaume Y, Broaddus VC, Gropper MA, Tanita T, Matthay MA. Alveolar liquid and protein clearance from normal dog lungs. J Appl Physiol (1985). 1988: 65;585-93.

335. Serikov VB, Grady M, Matthay MA. Effect of temperature on alveolar liquid and protein clearance in an in situ perfused goat lung. J Appl Physiol (1985). 1993: 75;940-7.

336. Jayr C, Garat C, Meignan M, Pittet JF, Zelter M, Matthay MA. Alveolar liquid and protein clearance in anesthetized ventilated rats. J Appl Physiol (1985). 1994: 76;2636-42.

337. Verghese GM, Ware LB, Matthay BA, Matthay MA. Alveolar epithelial fluid transport and the resolution of clinically severe hydrostatic pulmonary edema. J Appl Physiol (1985). 1999: 87;1301-12.

338. Ware LB, Golden JA, Finkbeiner WE, Matthay MA. Alveolar epithelial fluid transport capacity in reperfusion lung injury after lung transplantation. Am J Respir Crit Care Med. 1999: 159;980-8.

339. Song Y, Fukuda N, Bai C, Ma T, Matthay MA, Verkman AS. Role of aquaporins in alveolar fluid clearance in neonatal and adult lung, and in oedema formation following acute lung injury: studies in transgenic aquaporin null mice. J Physiol. 2000: 525 Pt 3;771-9.

340. Berthiaume Y, Matthay MA. Alveolar edema fluid clearance and acute lung injury. Respir Physiol Neurobiol. 2007: 159;350-9.

341. Perkins GD, McAuley DF. Pro: beta-agonists in acute lung injury--the end of the story? Am J Respir Crit Care Med. 2011: 184;503-4.

342. Papazian L. Con: beta2-adrenergic agonists in ALI/ARDS--not recommended or potentially harmful? Am J Respir Crit Care Med. 2011: 184;504-6.

343. McElroy MC, Kasper M. The use of alveolar epithelial type I cell-selective markers to investigate lung injury and repair. The European respiratory journal. 2004: 24;664-73.

344. Su X, Looney MR, Gupta N, Matthay MA. Receptor for advanced glycation end-products (RAGE) is an indicator of direct lung injury in models of experimental lung injury. Am J Physiol Lung Cell Mol Physiol. 2009: 297;L1-5.

345. Briot R, Frank JA, Uchida T, Lee JW, Calfee CS, Matthay MA. Elevated levels of the receptor for advanced glycation end products, a marker of alveolar epithelial type I cell injury, predict impaired alveolar fluid clearance in isolated perfused human lungs. Chest. 2009: 135;269-75.

346. Buckley ST, Ehrhardt C. The receptor for advanced glycation end products (RAGE) and the lung. J Biomed Biotechnol. 2010: 2010;917108.

347. Marquardt A, Bernevic B, Przybylski M. Identification, affinity characterisation and biological interactions of lectin-like peptide-carbohydrate complexes derived from human TNF-alpha using high-resolution mass spectrometry. J Pept Sci. 2007: 13;803-10.

348. Hazemi P, Tzotzos SJ, Fischer B, Andavan GS, Fischer H, Pietschmann H, et al. Essential structural features of TNF-alpha lectin-like domain derived peptides for activation of amiloride-sensitive sodium current in A549 cells. J Med Chem. 2010: 53;8021-9.

349. Xiong C, Yang G, Kumar S, Aggarwal S, Leustik M, Snead C, et al. The lectin-like domain of TNF protects from listeriolysin-induced hyperpermeability in human pulmonary microvascular endothelial cells - a crucial role for protein kinase C-alpha inhibition. Vascul Pharmacol. 2010: 52;207-13.

350. Communal C, Sumandea M, de Tombe P, Narula J, Solaro RJ, Hajjar RJ. Functional consequences of caspase activation in cardiac myocytes. Proc Natl Acad Sci U S A. 2002: 99;6252-6.

351. Marchiando AM, Graham WV, Turner JR. Epithelial barriers in homeostasis and disease. Annu Rev Pathol. 2010: 5;119-44.

352. Jain M, Sznajder JI. Effects of hypoxia on the alveolar epithelium. Proc Am Thorac Soc. 2005: 2;202-5.

353. Clerici C, Planes C. Gene regulation in the adaptive process to hypoxia in lung epithelial cells. Am J Physiol Lung Cell Mol Physiol. 2009: 296;L267-74.

354. Sartori C, Duplain H, Lepori M, Egli M, Maggiorini M, Nicod P, et al. High altitude impairs nasal transepithelial sodium transport in HAPE-prone subjects. The European respiratory journal. 2004: 23;916-20.

355. Schug ZT, Gonzalvez F, Houtkooper RH, Vaz FM, Gottlieb E. BID is cleaved by caspase-8 within a native complex on the mitochondrial membrane. Cell Death Differ. 2011: 18;538-48.

356. Ndozangue-Touriguine O, Hamelin J, Breard J. Cytoskeleton and apoptosis. Biochem Pharmacol. 2008: 76;11-8.

357. Bouvry D, Planes C, Malbert-Colas L, Escabasse V, Clerici C. Hypoxia-induced cytoskeleton disruption in alveolar epithelial cells. Am J Respir Cell Mol Biol. 2006: 35;519-27.

358. Goldman G, Welbourn R, Klausner JM, Kobzik L, Valeri CR, Shepro D, et al. Leukocytes mediate acid aspiration-induced multiorgan edema. Surgery. 1993: 114;13-20.

359. Eijking EP, Gommers D, So KL, de Maat MP, Mouton JW, Lachmann B. Prevention of respiratory failure after hydrochloric acid aspiration by intratracheal surfactant instillation in rats. Anesth Analg. 1993: 76;472-7.

360. Eijking EP, Gommers D, So KL, Vergeer M, Lachmann B. Surfactant treatment of respiratory failure induced by hydrochloric acid aspiration in rats. Anesthesiology. 1993: 78;1145-51.

361. Davidson BA, Knight PR, Wang Z, Chess PR, Holm BA, Russo TA, et al. Surfactant alterations in acute inflammatory lung injury from aspiration of acid and gastric particulates. Am J Physiol Lung Cell Mol Physiol. 2005: 288;L699-708.

362. Ryan AJ, McCoy DM, McGowan SE, Salome RG, Mallampalli RK. Alveolar sphingolipids generated in response to TNF-alpha modifies surfactant biophysical activity. J Appl Physiol (1985). 2003: 94;253-8.

363. Balibrea-Cantero JL, Arias-Diaz J, Garcia C, Torres-Melero J, Simon C, Rodriguez JM, et al. Effect of pentoxifylline on the inhibition of surfactant synthesis induced by TNF-alpha in human type II pneumocytes. Am J Respir Crit Care Med. 1994: 149;699-706.

364. Salome RG, McCoy DM, Ryan AJ, Mallampalli RK. Effects of intratracheal instillation of TNF-alpha on surfactant metabolism. J Appl Physiol (1985). 2000: 88;10-6.

365. Carroll JL, Jr., McCoy DM, McGowan SE, Salome RG, Ryan AJ, Mallampalli RK. Pulmonary-specific expression of tumor necrosis factor-alpha alters surfactant lipid metabolism. Am J Physiol Lung Cell Mol Physiol. 2002: 282;L735-42.

366. Forbes A, Pickell M, Foroughian M, Yao LJ, Lewis J, Veldhuizen R. Alveolar macrophage depletion is associated with increased surfactant pool sizes in adult rats. J Appl Physiol (1985). 2007: 103;637-45.

367. Barrett EG, Johnston C, Oberdorster G, Finkelstein JN. Silica-induced chemokine expression in alveolar type II cells is mediated by TNF-alpha. Am J Physiol. 1998: 275;L1110-9.

368. Cerri C, Chimenti D, Conti I, Neri T, Paggiaro P, Celi A. Monocyte/macrophage-derived microparticles up-regulate inflammatory mediator synthesis by human airway epithelial cells. Journal of immunology. 2006: 177;1975-80.

369. Serrao KL, Fortenberry JD, Owens ML, Harris FL, Brown LA. Neutrophils induce apoptosis of lung epithelial cells via release of soluble Fas ligand. Am J Physiol Lung Cell Mol Physiol. 2001: 280;L298-305.

370. Kiener PA, Davis PM, Rankin BM, Klebanoff SJ, Ledbetter JA, Starling GC, et al. Human monocytic cells contain high levels of intracellular Fas ligand: rapid release following cellular activation. Journal of immunology. 1997: 159;1594-8.

371. Mizuta M, Nakajima H, Mizuta N, Kitamura Y, Nakajima Y, Hashimoto S, et al. Fas ligand released by activated monocytes causes apoptosis of lung epithelial cells in human acute lung injury model in vitro. Biological & pharmaceutical bulletin. 2008: 31;386-90.

372. Liles WC, Kiener PA, Ledbetter JA, Aruffo A, Klebanoff SJ. Differential expression of Fas (CD95) and Fas ligand on normal human phagocytes: implications for the regulation of apoptosis in neutrophils. J Exp Med. 1996: 184;429-40.

373. Patel BV, Wilson MR, O'Dea KP, Takata M. TNF-induced death signaling triggers alveolar epithelial dysfunction in acute lung injury. Journal of immunology. 2013: 190;4274-82.

374. Herrero R, Tanino M, Smith LS, Kajikawa O, Wong VA, Mongovin S, et al. The Fas/FasL pathway impairs the alveolar fluid clearance in mouse lungs. Am J Physiol Lung Cell Mol Physiol. 2013: 305;L377-88.

375. Perl M, Chung CS, Lomas-Neira J, Rachel TM, Biffl WL, Cioffi WG, et al. Silencing of Fas, but not caspase-8, in lung epithelial cells ameliorates pulmonary apoptosis, inflammation, and neutrophil influx after hemorrhagic shock and sepsis. Am J Pathol. 2005: 167;1545-59.

376. Perl M, Chung CS, Perl U, Lomas-Neira J, de Paepe M, Cioffi WG, et al. Fas-induced pulmonary apoptosis and inflammation during indirect acute lung injury. Am J Respir Crit Care Med. 2007: 176;591-601.

377. Perl M, Lomas-Neira J, Chung CS, Ayala A. Epithelial cell apoptosis and neutrophil recruitment in acute lung injury-a unifying hypothesis? What we have learned from small interfering RNAs. Mol Med. 2008: 14;465-75.

378. Lomas-Neira J, Perl M, Venet F, Chung CS, Ayala A. The role and source of tumor necrosis factor-alpha in hemorrhage-induced priming for septic lung injury. Shock. 2012: 37;611-20.

379. Messer MP, Kellermann P, Weber SJ, Hohmann C, Denk S, Klohs B, et al. Silencing of fas, fas-associated via death domain, or caspase 3 differentially affects lung inflammation, apoptosis, and development of trauma-induced septic acute lung injury. Shock. 2013: 39;19-27.

380. Imai Y, Kuba K, Neely GG, Yaghubian-Malhami R, Perkmann T, van Loo G, et al. Identification of oxidative stress and Toll-like receptor 4 signaling as a key pathway of acute lung injury. 2008: 133;235-49.

381. Fukunaga K, Kohli P, Bonnans C, Fredenburgh LE, Levy BD. Cyclooxygenase 2 plays a pivotal role in the resolution of acute lung injury. Journal of immunology. 2005: 174;5033-9.

382. Amigoni M, Bellani G, Scanziani M, Masson S, Bertoli E, Radaelli E, et al. Lung injury and recovery in a murine model of unilateral acid aspiration: functional, biochemical, and morphologic characterization. Anesthesiology. 2008: 108;1037-46.

383. Bonnans C, Fukunaga K, Levy MA, Levy BD. Lipoxin A(4) regulates bronchial epithelial cell responses to acid injury. Am J Pathol. 2006: 168;1064-72.

384. Hastings RH, Folkesson HG, Matthay MA. Mechanisms of alveolar protein clearance in the intact lung. Am J Physiol Lung Cell Mol Physiol. 2004: 286;L679-89.

385. B BM, Lawson WE, Oury TD, Sisson TH, Raghavendran K, Hogaboam CM. Animal models of fibrotic lung disease. Am J Respir Cell Mol Biol. 2013: 49;167-79.

386. Knight PR, Davidson BA, Nader ND, Helinski JD, Marschke CJ, Russo TA, et al. Progressive, severe lung injury secondary to the interaction of insults in gastric aspiration. Exp Lung Res. 2004: 30;535-57.

387. Hutson AD, Davidson BA, Raghavendran K, Chess PR, Tait AR, Holm BA, et al. Statistical prediction of the type of gastric aspiration lung injury based on early cytokine/chemokine profiles. Anesthesiology. 2006: 104;73-9.

388. van Westerloo DJ, Knapp S, van't Veer C, Buurman WA, de Vos AF, Florquin S, et al. Aspiration pneumonitis primes the host for an exaggerated inflammatory response during pneumonia. Crit Care Med. 2005: 33;1770-8.

389. Wilson MR, O'Dea KP, Dorr AD, Yamamoto H, Goddard ME, Takata M. Efficacy and safety of inhaled carbon monoxide during pulmonary inflammation in mice. PLoS One. 2010: 5;e11565.

390. Griffiths MJ, McAuley DF. RAGE: a biomarker for acute lung injury. Thorax. 2008: 63;1034-6.

391. Lander HM, Tauras JM, Ogiste JS, Hori O, Moss RA, Schmidt AM. Activation of the receptor for advanced glycation end products triggers a p21(ras)-dependent mitogen-activated protein kinase pathway regulated by oxidant stress. The Journal of biological chemistry. 1997: 272;17810-4.

392. Bierhaus A, Schiekofer S, Schwaninger M, Andrassy M, Humpert PM, Chen J, et al. Diabetes-associated sustained activation of the transcription factor nuclear factor-kappaB. Diabetes. 2001: 50;2792-808.

393. Mangalmurti NS, Friedman JL, Wang LC, Stolz D, Muthukumaran G, Siegel DL, et al. The receptor for advanced glycation end products mediates lung endothelial activation by RBCs. Am J Physiol Lung Cell Mol Physiol. 2013: 304;L250-63.

394. Meloche J, Courchesne A, Barrier M, Carter S, Bisserier M, Paulin R, et al. Critical role for the advanced glycation end-products receptor in pulmonary arterial hypertension etiology. J Am Heart Assoc. 2013: 2;e005157.

395. Zhang H, Tasaka S, Shiraishi Y, Fukunaga K, Yamada W, Seki H, et al. Role of soluble receptor for advanced glycation end products on endotoxin-induced lung injury. Am J Respir Crit Care Med. 2008: 178;356-62.

396. Hergrueter AH, Nguyen K, Owen CA. Matrix metalloproteinases: all the RAGE in the acute respiratory distress syndrome. Am J Physiol Lung Cell Mol Physiol. 2011: 300;L512-5.

397. Yamakawa N, Uchida T, Matthay MA, Makita K. Proteolytic release of the receptor for advanced glycation end products from in vitro and in situ alveolar epithelial cells. Am J Physiol Lung Cell Mol Physiol. 2011: 300;L516-25.

398. Queisser MA, Kouri FM, Konigshoff M, Wygrecka M, Schubert U, Eickelberg O, et al. Loss of RAGE in pulmonary fibrosis: molecular relations to functional changes in pulmonary cell types. Am J Respir Cell Mol Biol. 2008: 39;337-45.

399. O'Dea KP, Young AJ, Yamamoto H, Robotham JL, Brennan FM, Takata M. Lung-marginated monocytes modulate pulmonary microvascular injury during early endotoxemia. Am J Respir Crit Care Med. 2005: 172;1119-27.

400. Looney MR, Su X, Van Ziffle JA, Lowell CA, Matthay MA. Neutrophils and their Fc gamma receptors are essential in a mouse model of transfusion-related acute lung injury. J Clin Invest. 2006: 116;1615-23.

401. Worthen GS, Haslett C, Rees AJ, Gumbay RS, Henson JE, Henson PM. Neutrophil-mediated pulmonary vascular injury. Synergistic effect of trace amounts of lipopolysaccharide and neutrophil stimuli on vascular permeability and neutrophil sequestration in the lung. Am Rev Respir Dis. 1987: 136;19-28.

402. Wolters PJ, Wray C, Sutherland RE, Kim SS, Koff J, Mao Y, et al. Neutrophil-derived IL-6 limits alveolar barrier disruption in experimental ventilator-induced lung injury. Journal of immunology. 2009: 182;8056-62.

403. Voll RE, Herrmann M, Roth EA, Stach C, Kalden JR, Girkontaite I. Immunosuppressive effects of apoptotic cells. Nature. 1997: 390;350-1.

404. Papazian L, Doddoli C, Chetaille B, Gernez Y, Thirion X, Roch A, et al. A contributive result of open-lung biopsy improves survival in acute respiratory distress syndrome patients. Crit Care Med. 2007: 35;755-62.

405. Marshall RP, Bellingan G, Webb S, Puddicombe A, Goldsack N, McAnulty RJ, et al. Fibroproliferation occurs early in the acute respiratory distress syndrome and impacts on outcome. Am J Respir Crit Care Med. 2000: 162;1783-8.

406. Armstrong L, Thickett DR, Mansell JP, Ionescu M, Hoyle E, Billinghurst RC, et al. Changes in collagen turnover in early acute respiratory distress syndrome. Am J Respir Crit Care Med. 1999: 160;1910-5.

407. Pugin J, Verghese G, Widmer MC, Matthay MA. The alveolar space is the site of intense inflammatory and profibrotic reactions in the early phase of acute respiratory distress syndrome. Crit Care Med. 1999: 27;304-12.

408. Deheinzelin D, Jatene FB, Saldiva PH, Brentani RR. Upregulation of collagen messenger RNA expression occurs immediately after lung damage. Chest. 1997: 112;1184-8.

409. Liebler JM, Qu Z, Buckner B, Powers MR, Rosenbaum JT. Fibroproliferation and mast cells in the acute respiratory distress syndrome. Thorax. 1998: 53;823-9.

410. Madtes DK, Rubenfeld G, Klima LD, Milberg JA, Steinberg KP, Martin TR, et al. Elevated transforming growth factor-alpha levels in bronchoalveolar lavage fluid of patients with acute respiratory distress syndrome. Am J Respir Crit Care Med. 1998: 158;424-30.

411. Fahy RJ, Lichtenberger F, McKeegan CB, Nuovo GJ, Marsh CB, Wewers MD. The acute respiratory distress syndrome: a role for transforming growth factor-beta 1. Am J Respir Cell Mol Biol. 2003: 28;499-503.

412. Budinger GR, Chandel NS, Donnelly HK, Eisenbart J, Oberoi M, Jain M. Active transforming growth factor-beta1 activates the procollagen I promoter in patients with acute lung injury. Intensive Care Med. 2005: 31;121-8.

413. Moore BB, Hogaboam CM. Murine models of pulmonary fibrosis. Am J Physiol Lung Cell Mol Physiol. 2008: 294;L152-60.

414. Curley GF, Contreras M, Higgins B, O'Kane C, McAuley DF, O'Toole D, et al. Evolution of the inflammatory and fibroproliferative responses during resolution and repair after ventilator-induced lung injury in the rat. Anesthesiology. 2011: 115;1022-32.

415. O'Dea KP, Wilson MR, Dokpesi JO, Wakabayashi K, Tatton L, van Rooijen N, et al. Mobilization and margination of bone marrow Gr-1high monocytes during

subclinical endotoxemia predisposes the lungs toward acute injury. Journal of immunology. 2009: 182;1155-66.

416. Amano H, Morimoto K, Senba M, Wang H, Ishida Y, Kumatori A, et al. Essential contribution of monocyte chemoattractant protein-1/C-C chemokine ligand-2 to resolution and repair processes in acute bacterial pneumonia. Journal of immunology. 2004: 172;398-409.

417. Sikora L, Johansson AC, Rao SP, Hughes GK, Broide DH, Sriramarao P. A murine model to study leukocyte rolling and intravascular trafficking in lung microvessels. Am J Pathol. 2003: 162;2019-28.

418. Kuebler WM, Parthasarathi K, Lindert J, Bhattacharya J. Real-time lung microscopy. J Appl Physiol (1985). 2007: 102;1255-64.

419. Tabuchi A, Mertens M, Kuppe H, Pries AR, Kuebler WM. Intravital microscopy of the murine pulmonary microcirculation. J Appl Physiol (1985). 2008: 104;338-46.

420. Chagnon F, Fournier C, Charette PG, Moleski L, Payet MD, Dobbs LG, et al. In vivo intravital endoscopic confocal fluorescence microscopy of normal and acutely injured rat lungs. Lab Invest. 2010: 90;824-34.

421. Lambrecht BN, Hammad H. Lung dendritic cells in respiratory viral infection and asthma: from protection to immunopathology. Annu Rev Immunol. 2012: 30;243-70.

422. Auffray C, Sieweke MH, Geissmann F. Blood monocytes: development, heterogeneity, and relationship with dendritic cells. Annu Rev Immunol. 2009: 27;669-92.

423. Misharin AV, Morales-Nebreda L, Mutlu GM, Budinger GR, Perlman H. Flow cytometric analysis of macrophages and dendritic cell subsets in the mouse lung. Am J Respir Cell Mol Biol. 2013: 49;503-10.

424. Lambrecht BN. Alveolar macrophage in the driver's seat. Immunity. 2006: 24;366-8.

425. GeurtsvanKessel CH, Lambrecht BN. Division of labor between dendritic cell subsets of the lung. Mucosal Immunol. 2008: 1;442-50.

426. Guilliams M, Lambrecht BN, Hammad H. Division of labor between lung dendritic cells and macrophages in the defense against pulmonary infections. Mucosal Immunol. 2013: 6;464-73.

427. Maus UA, Janzen S, Wall G, Srivastava M, Blackwell TS, Christman JW, et al. Resident alveolar macrophages are replaced by recruited monocytes in response to endotoxin-induced lung inflammation. Am J Respir Cell Mol Biol. 2006: 35;227-35.

428. Bedoret D, Wallemacq H, Marichal T, Desmet C, Quesada Calvo F, Henry E, et al. Lung interstitial macrophages alter dendritic cell functions to prevent airway allergy in mice. J Clin Invest. 2009: 119;3723-38.

429. Colonna M, Trinchieri G, Liu YJ. Plasmacytoid dendritic cells in immunity. Nat Immunol. 2004: 5;1219-26.

430. Yona S, Kim KW, Wolf Y, Mildner A, Varol D, Breker M, et al. Fate mapping reveals origins and dynamics of monocytes and tissue macrophages under homeostasis. Immunity. 2013: 38;79-91.

431. Garibaldi BT, D'Alessio FR, Mock JR, Files DC, Chau E, Eto Y, et al. Regulatory T cells reduce acute lung injury fibroproliferation by decreasing fibrocyte recruitment. Am J Respir Cell Mol Biol. 2013: 48;35-43.

432. Konig R, Huang LY, Germain RN. MHC class II interaction with CD4 mediated by a region analogous to the MHC class I binding site for CD8. Nature. 1992: 356;796-8.

433. Chen X, Oppenheim JJ. Resolving the identity myth: key markers of functional CD4+FoxP3+ regulatory T cells. Int Immunopharmacol. 2011: 11;1489-96.

434. Fontenot JD, Gavin MA, Rudensky AY. Foxp3 programs the development and function of CD4+CD25+ regulatory T cells. Nat Immunol. 2003: 4;330-6.

435. Fontenot JD, Rudensky AY. A well adapted regulatory contrivance: regulatory T cell development and the forkhead family transcription factor Foxp3. Nat Immunol. 2005: 6;331-7.

436. Greenfield LJ, Singleton RP, McCaffree DR, Coalson JJ. Pulmonary effects of experimental graded aspiration of hydrochloric acid. Annals of surgery. 1969: 170;74-86.

437. Johnston LK, Rims CR, Gill SE, McGuire JK, Manicone AM. Pulmonary macrophage subpopulations in the induction and resolution of acute lung injury. Am J Respir Cell Mol Biol. 2012: 47;417-26.

438. Nelson DS, Boyden SV. The loss of macrophages from peritoneal exudates following the injection of antigens into guinea-pigs with delayed-type hypersensitivity. Immunology. 1963: 6;264-75.

439. Bozinovski S, Jones J, Beavitt SJ, Cook AD, Hamilton JA, Anderson GP. Innate immune responses to LPS in mouse lung are suppressed and reversed by neutralization of GM-CSF via repression of TLR-4. Am J Physiol Lung Cell Mol Physiol. 2004: 286;L877-85.

440. Kirby AC, Coles MC, Kaye PM. Alveolar macrophages transport pathogens to lung draining lymph nodes. Journal of immunology. 2009: 183;1983-9.

441. Lasbury ME, Durant PJ, Ray CA, Tschang D, Schwendener R, Lee CH. Suppression of alveolar macrophage apoptosis prolongs survival of rats and mice with pneumocystis pneumonia. Journal of immunology. 2006: 176;6443-53.

442. Monick MM, Powers LS, Walters K, Lovan N, Zhang M, Gerke A, et al. Identification of an autophagy defect in smokers' alveolar macrophages. Journal of immunology. 2010: 185;5425-35.

443. Patel AS, Morse D, Choi AM. Regulation and functional significance of autophagy in respiratory cell biology and disease. Am J Respir Cell Mol Biol. 2013: 48;1-9.

444. Barletta KE, Cagnina RE, Wallace KL, Ramos SI, Mehrad B, Linden J. Leukocyte compartments in the mouse lung: distinguishing between marginated, interstitial, and alveolar cells in response to injury. J Immunol Methods. 2012: 375;100-10.

445. Maus U, Herold S, Muth H, Maus R, Ermert L, Ermert M, et al. Monocytes recruited into the alveolar air space of mice show a monocytic phenotype but upregulate CD14. Am J Physiol Lung Cell Mol Physiol. 2001: 280;L58-68.

446. Nakstad B, Haugen T, Skjonsberg OH, Lyberg T. Expression of leukocyte integrins and tissue factor in mononuclear phagocytes. The European respiratory journal. 1998: 12;601-6.

447. Vermaelen K, Pauwels R. Accurate and simple discrimination of mouse pulmonary dendritic cell and macrophage populations by flow cytometry: methodology and new insights. Cytometry A. 2004: 61;170-77.

448. Lambrecht BN, Hammad H. Biology of lung dendritic cells at the origin of asthma. Immunity. 2009: 31;412-24.

449. Manicone AM, Huizar I, McGuire JK. Matrilysin (Matrix Metalloproteinase-7) regulates anti-inflammatory and antifibrotic pulmonary dendritic cells that express CD103 (alpha(E)beta(7)-integrin). Am J Pathol. 2009: 175;2319-31.

450. Grayson MH, Cheung D, Rohlfing MM, Kitchens R, Spiegel DE, Tucker J, et al. Induction of high-affinity IgE receptor on lung dendritic cells during viral infection leads to mucous cell metaplasia. J Exp Med. 2007: 204;2759-69.

451. Choudhury S, Wilson MR, Goddard ME, O'Dea KP, Takata M. Mechanisms of early pulmonary neutrophil sequestration in ventilator-induced lung injury in mice. Am J Physiol Lung Cell Mol Physiol. 2004: 287;L902-10.

452. Petty JM, Sueblinvong V, Lenox CC, Jones CC, Cosgrove GP, Cool CD, et al. Pulmonary stromal-derived factor-1 expression and effect on neutrophil recruitment during acute lung injury. Journal of immunology. 2007: 178;8148-57.

453. Haslett C, Worthen GS, Giclas PC, Morrison DC, Henson JE, Henson PM. The pulmonary vascular sequestration of neutrophils in endotoxemia is initiated by an effect of endotoxin on the neutrophil in the rabbit. Am Rev Respir Dis. 1987: 136;9-18.

454. Young SK, Worthen GS, Haslett C, Tonnesen MG, Henson PM. Interaction between chemoattractants and bacterial lipopolysaccharide in the induction and enhancement of neutrophil adhesion. Am J Respir Cell Mol Biol. 1990: 2;523-32.

455. Horgan MJ, Palace GP, Everitt JE, Malik AB. TNF-alpha release in endotoxemia contributes to neutrophil-dependent pulmonary edema. Am J Physiol. 1993: 264;H1161-5.

456. Chignard M, Balloy V. Neutrophil recruitment and increased permeability during acute lung injury induced by lipopolysaccharide. Am J Physiol Lung Cell Mol Physiol. 2000: 279;L1083-90.

457. Thorn J. The inflammatory response in humans after inhalation of bacterial endotoxin: a review. Inflamm Res. 2001: 50;254-61.

458. Reutershan J, Basit A, Galkina EV, Ley K. Sequential recruitment of neutrophils into lung and bronchoalveolar lavage fluid in LPS-induced acute lung injury. Am J Physiol Lung Cell Mol Physiol. 2005: 289;L807-15.

459. Reutershan J, Morris MA, Burcin TL, Smith DF, Chang D, Saprito MS, et al. Critical role of endothelial CXCR2 in LPS-induced neutrophil migration into the lung. J Clin Invest. 2006: 116;695-702.

460. Imanaka H, Shimaoka M, Matsuura N, Nishimura M, Ohta N, Kiyono H. Ventilator-induced lung injury is associated with neutrophil infiltration, macrophage activation, and TGF-beta 1 mRNA upregulation in rat lungs. Anesth Analg. 2001: 92;428-36.

461. Belperio JA, Keane MP, Burdick MD, Londhe V, Xue YY, Li K, et al. Critical role for CXCR2 and CXCR2 ligands during the pathogenesis of ventilator-induced lung injury. J Clin Invest. 2002: 110;1703-16.

462. Knight PR, Druskovich G, Tait AR, Johnson KJ. The role of neutrophils, oxidants, and proteases in the pathogenesis of acid pulmonary injury. Anesthesiology. 1992: 77;772-8.

463. Hussain N, Wu F, Zhu L, Thrall RS, Kresch MJ. Neutrophil apoptosis during the development and resolution of oleic acid-induced acute lung injury in the rat. Am J Respir Cell Mol Biol. 1998: 19;867-74.

464. Zhou Z, Kozlowski J, Schuster DP. Physiologic, biochemical, and imaging characterization of acute lung injury in mice. Am J Respir Crit Care Med. 2005: 172;344-51.

465. Daley JM, Thomay AA, Connolly MD, Reichner JS, Albina JE. Use of Ly6G-specific monoclonal antibody to deplete neutrophils in mice. J Leukoc Biol. 2008: 83;64-70.

466. James CF, Modell JH, Gibbs CP, Kuck EJ, Ruiz BC. Pulmonary aspiration--effects of volume and pH in the rat. Anesth Analg. 1984: 63;665-8.

467. Haslett C, Lee A, Savill JS, Meagher L, Whyte MK. Apoptosis (programmed cell death) and functional changes in aging neutrophils. Modulation by inflammatory mediators. Chest. 1991: 99;6S.

468. Haslett C, Savill JS, Whyte MK, Stern M, Dransfield I, Meagher LC. Granulocyte apoptosis and the control of inflammation. Philosophical transactions of the Royal Society of London Series B, Biological sciences. 1994: 345;327-33.

469. Gasson JC, Weisbart RH, Kaufman SE, Clark SC, Hewick RM, Wong GG, et al. Purified human granulocyte-macrophage colony-stimulating factor: direct action on neutrophils. Science. 1984: 226;1339-42.

470. Vermes I, Haanen C, Steffens-Nakken H, Reutelingsperger C. A novel assay for apoptosis. Flow cytometric detection of phosphatidylserine expression on early apoptotic cells using fluorescein labelled Annexin V. J Immunol Methods. 1995: 184;39-51.

471. Peiser L, Gordon S. The function of scavenger receptors expressed by macrophages and their role in the regulation of inflammation. Microbes Infect. 2001: 3;149-59.

472. Lawrence T, Willoughby DA, Gilroy DW. Anti-inflammatory lipid mediators and insights into the resolution of inflammation. Nat Rev Immunol. 2002: 2;787-95.

473. Serhan CN. Resolution phase of inflammation: novel endogenous anti-inflammatory and proresolving lipid mediators and pathways. Annu Rev Immunol. 2007: 25;101-37.

474. Holland MC, Wurthner JU, Morley PJ, Birchler MA, Lambert J, Albayaty M, et al. Autoantibodies to variable heavy (VH) chain Ig sequences in humans impact the safety and clinical pharmacology of a VH domain antibody antagonist of TNF-alpha receptor 1. Journal of clinical immunology. 2013: 33;1192-203.

475. Wakabayashi K, Wilson MR, Patel BV, Morley PJ, Bayliffe A, Takata M. Inhibition Of TNF Receptor P55 By A Domain Antibody Attenuates Acid-induced Lung Injury In Mice. American Thoracic Society; 2013. p. A5964-A.

476. O'Kane CM, Bayliffe A, Serone A, Bareille P, Smith S, Hamid U, et al. Tumour Necrosis Factor receptor 1 inhibition using a novel inhaled human antibody reduces inflammation in a human model of lung injury induced by inhaled lipopolysaccharide; a randomized placebo-controlled clinical trial. Thorax. 2013: 68;A50.

477. Maianski NA, Maianski AN, Kuijpers TW, Roos D. Apoptosis of neutrophils. Acta haematologica. 2004: 111;56-66.

478. Maianski NA, Roos D, Kuijpers TW. Tumor necrosis factor alpha induces a caspase-independent death pathway in human neutrophils. Blood. 2003: 101;1987-95.

479. Chen HC, Wang CJ, Chou CL, Lin SM, Huang CD, Lin TY, et al. Tumor necrosis factor-alpha induces caspase-independent cell death in human neutrophils via reactive oxidants and associated with calpain activity. Journal of biomedical science. 2006: 13;261-73.

480. Akgul C, Edwards SW. Regulation of neutrophil apoptosis via death receptors. Cell Mol Life Sci. 2003: 60;2402-8.

481. Seok J, Warren HS, Cuenca AG, Mindrinos MN, Baker HV, Xu W, et al. Genomic responses in mouse models poorly mimic human inflammatory diseases. Proceedings of the National Academy of Sciences. 2013: 110;3507-12.

482. Berger AB, Sexton KB, Bogyo M. Commonly used caspase inhibitors designed based on substrate specificity profiles lack selectivity. Cell research. 2006: 16;961-3.

483. Günther C, Martini E, Wittkopf N, Amann K, Weigmann B, Neumann H, et al. Caspase-8 regulates TNF-α-induced epithelial necroptosis and terminal ileitis. 2011: 477;335-9.

484. van Rooijen N, van Kesteren-Hendrikx E. Clodronate liposomes: perspectives in research and therapeutics. 2002: 12;81-94.